FRANKFORD ARSENAL

REPORT No. R-1425
Copy No. 18

FEASIBILITY STUDY OF AN ADVANCED RECOILLESS RIFLE WEAPON SYSTEM UTILIZING A TERMINALLY GUIDED PROJECTILE (U)

S. J. FENTON
Bulova Research and Development Laboratories, Inc.

December 1957

Contract No. DA-30-069-ORD-1766

OCO Project No. TS4-4024
DA Project No. 5S02-01-008

Pitman-Dunn Laboratories Group
FRANKFORD ARSENAL
Philadelphia 37, Pa.

Initial distribution of this report has been made in accordance with the distribution list contained herein.

Ordnance Corps installations will make requests for copies direct to Armed Services Technical Information Agency (ASTIA), Document Service Center, Arlington Hall Station, Arlington 12, Virginia.

Department of Defense agencies other than Ordnance Corps, as well as government agencies outside the Department of Defense, and Ordnance Corps and other Department of Defense Agency Contractors having approved Field of Interest Registers on file with ASTIA, will make requests for copies to ASTIA through the Commanding Officer, Diamond Ordnance Fuze Laboratories, Washington 25, D. C., Attn: Technical Reference Section.

If no approved Field of Interest Register is on file with ASTIA, Department of Defense agency contractors will transmit requests for copies through the appropriate screening point for certification of "need-to-know," to the Commanding Officer, Diamond Ordnance Fuze Laboratories, Attn: Technical Reference Section.

```
--    1   OF     1
-- 1 -  AD NUMBER: 153886
-- 2 -  FIELDS AND GROUPS: 16/4, 16/1, 17/7, 19/1
--        19/6
-- 3 -  ENTRY CLASSIFICATION:    UNCLASSIFIED
-- 5 -  CORPORATE AUTHOR: BULOVA RESEARCH AND DEVELOPMENT LABS INC WOODSIDE
--        N Y
-- 6 -  UNCLASSIFIED TITLE:      FEASIBILITY STUDY OF AN ADVANCED RECOILLESS
--        RIFLE WEAPON SYSTEM UTILIZING A TERMINALLY GUIDED PROJECTILE.
-- 8 -  TITLE CLASSIFICATION:    UNCLASSIFIED
.;                                                  --10 -  PERSONAL AUTHORS: FENTON, S. J
--11 -  REPORT DATE:        DEC    , 1957
--12 -  PAGINATION:      227P
--14 -  REPORT NUMBER:      R-1425
--15 -  CONTRACT NUMBER:   DA30 0690RD1766
--16 -  PROJECT NUMBER:     TS4-4024
--20 -  REPORT CLASSIFICATION:  UNCLASSIFIED
--23 -  DESCRIPTORS:          *GUIDED MISSILE LAUNCHERS, *GUIDED MISSILES,
--        *RECOILLESS GUNS, *TANKS (COMBAT VEHICLES), COUNTERMEASURES, DESIGN,
--        SURFACE TO SURFACE
--24 -  DESCRIPTOR CLASSIFICATION:    UNCLASSIFIED
--25 -  IDENTIFIERS:         POLCAT WEAPON SYSTEM
--          <<P FOR NEXT PAGE>> OR <<ENTER NEXT COMMAND>>

--26 -  IDENTIFIER CLASSIFICATION:    UNCLASSIFIED

--35 -  SOURCE CODE:        066750
--36 -  DOCUMENT LOCATION:        NTIS
--40 -  GEOPOLITICAL CODE:       3609
--41 -  TYPE CODE:   4
--49 -  AUTHORITY FOR CHANGE:    C TO U + ST-A, USAARRADCOM LTR, 23 SEP 81
```

[redacted]

AD No. Accession No.
Pitman-Dunn Laboratories Group, Frankford Arsenal
Philadelphia 37, Pa.

FEASIBILITY STUDY OF AN ADVANCED RECOILLESS RIFLE WEAPON SYSTEM UTILIZING A TERMINALLY GUIDED PROJECTILE (U) - S. J. Fenton, Bulova Research and Development Laboratories, Inc.

Classification: Title - Uncl; Report - Confidential
Report No. R-1425, Dec 1957; 227 pages; 80 illus; 18 tables
Contract DA-30-069-ORD-1766 DA Project No. 5S02-01-008
Ordnance Project TS4-4024

Presented is a summary of the feasibility study of adapting post firing trajectory correction techniques to operational recoilless antitank weapons.

The study, informally designated Project POLCAT, contributes a solution to the problem in the form of a specific weapon system. The recommended system minimizes miss distance by combining conventional fire control methods with relatively simple post firing correction techniques. Post firing correction is achieved by using a frame fixed infrared seeker for guidance and impulse sterring for control. Based on the technical analyses and the experimental testing as reported, it is concluded that the recommended advanced weapon system is entirely feasible and warrants serious consideration for weapon engineering design and development.

[redacted]

1. GUIDANCE, Recoilless, Projectile
2. WEAPON SYSTEM, Recoilless with post launching trajectory correction
3. INFRA-RED
4. PROJECTILES, Terminal Guidance
5. TRAJECTORY, In-flight Correction

Copy No.______

CONFIDENTIAL

AD No. Accession No.
Pitman-Dunn Laboratories Group, Frankford Arsenal
Philadelphia 37, Pa.

FEASIBILITY STUDY OF AN ADVANCED RECOILLESS RIFLE WEAPON SYSTEM UTILIZING A TERMINALLY GUIDED PROJECTILE (U) - S. J. Fenton, Bulova Research and Development Laboratories, Inc.

Classification: Title - Uncl; Report - Confidential
Report No. R-1425, Dec 1957; 227 pages; 80 illus; 18 tables
Contract DA-30-069-ORD-1766 DA Project No. 5S02-01-008
Ordnance Project TS4-4024

Presented is a summary of the feasibility study of adapting post firing trajectory correction techniques to operational recoilless antitank weapons.

The study, informally designated Project POLCAT, contributes a solution to the problem in the form of a specific weapon system. The recommended system minimizes miss distance by combining conventional fire control methods with relatively simple post firing correction techniques. Post firing correction is achieved by using a frame fixed infrared seeker for guidance and impulse sterring for control. Based on the technical analyses and the experimental testing as reported, it is concluded that the recommended advanced weapon system is entirely feasible and warrants serious consideration for weapon engineering design and development.

[redacted] A L

1. GUIDANCE, Recoilless, Projectile
2. WEAPON SYSTEM, Recoilless with post launching trajectory correction
3. INFRA-RED
4. PROJECTILES, Terminal Guidance
5. TRAJECTORY, In-flight Correction

Copy No.______

[redacted] N T I A L

AD No. Accession No.
Pitman-Dunn Laboratories Group, Frankford Arsenal
Philadelphia 37, Pa.

FEASIBILITY STUDY OF AN ADVANCED RECOILLESS RIFLE WEAPON SYSTEM UTILIZING A TERMINALLY GUIDED PROJECTILE (U) - S. J. Fenton, Bulova Research and Development Laboratories, Inc.

Classification: Title - Uncl; Report - Confidential
Report No. R-1425, Dec 1957; 227 pages; 80 illus; 18 tables
Contract DA-30-069-ORD-1766 DA Project No. 5S02-01-008
Ordnance Project TS4-4024

Presented is a summary of the feasibility study of adapting post firing trajectory correction techniques to operational recoilless antitank weapons.

The study, informally designated Project POLCAT, contributes a solution to the problem in the form of a specific weapon system. The recommended system minimizes miss distance by combining conventional fire control methods with relatively simple post firing correction techniques. Post firing correction is achieved by using a frame fixed infrared seeker for guidance and impulse sterring for control. Based on the technical analyses and the experimental testing as reported, it is concluded that the recommended advanced weapon system is entirely feasible and warrants serious consideration for weapon engineering design and development.

[redacted] L

1. GUIDANCE, Recoilless, Projectile
2. WEAPON SYSTEM, Recoilless with post launching trajectory correction
3. INFRA-RED
4. PROJECTILES, Terminal Guidance
5. TRAJECTORY, In-flight Correction

Copy No.______

[redacted]

AD No. Accession No.
Pitman-Dunn Laboratories Group, Frankford Arsenal
Philadelphia 37, Pa.

FEASIBILITY STUDY OF AN ADVANCED RECOILLESS RIFLE WEAPON SYSTEM UTILIZING A TERMINALLY GUIDED PROJECTILE (U) - S. J. Fenton, Bulova Research and Development Laboratories, Inc.

Classification: Title - Uncl; Report - Confidential
Report No. R-1425, Dec 1957; 227 pages; 80 illus; 18 tables
Contract DA-30-069-ORD-1766 DA Project No. 5S02-01-008
Ordnance Project TS4-4024

Presented is a summary of the feasibility study of adapting post firing trajectory correction techniques to operational recoilless antitank weapons.

The study, informally designated Project POLCAT, contributes a solution to the problem in the form of a specific weapon system. The recommended system minimizes miss distance by combining conventional fire control methods with relatively simple post firing correction techniques. Post firing correction is achieved by using a frame fixed infrared seeker for guidance and impulse sterring for control. Based on the technical analyses and the experimental testing as reported, it is concluded that the recommended advanced weapon system is entirely feasible and warrants serious consideration for weapon engineering design and development.

[redacted]

1. GUIDANCE, Recoilless, Projectile
2. WEAPON SYSTEM, Recoilless with post launching trajectory correction
3. INFRA-RED
4. PROJECTILES, Terminal Guidance
5. TRAJECTORY, In-flight Correction

Copy No.______

[redacted]

AD No. Accession No.
Pitman-Dunn Laboratories Group, Frankford Arsenal
Philadelphia 37, Pa.

FEASIBILITY STUDY OF AN ADVANCED RECOILLESS RIFLE WEAPON SYSTEM UTILIZING A TERMINALLY GUIDED PROJECTILE (U) -
S. J. Fenton, Bulova Research and Development Laboratories, Inc.

Classification: Title - Uncl; Report - Confidential
Report No. R-1425, Dec 1957; 227 pages; 80 illus; 18 tables
Contract DA-30-069-ORD-1766 DA Project No. 5S02-01-008
Ordnance Project TS4-4024

Presented is a summary of the feasibility study of adapting post firing trajectory correction techniques to operational recoilless antitank weapons.

The study, informally designated Project POLCAT, contributes a solution to the problem in the form of a specific weapon system. The recommended system minimizes miss distance by combining conventional fire control methods with relatively simple post firing correction techniques. Post firing correction is achieved by using a frame fixed infrared seeker for guidance and impulse sterring for control. Based on the technical analyses and the experimental testing as reported, it is concluded that the recommended advanced weapon system is entirely feasible and warrants serious consideration for weapon engineering design and development.

[redacted]

1. GUIDANCE, Recoilless, Projectile
2. WEAPON SYSTEM, Recoilless with post launching trajectory correction
3. INFRA-RED
4. PROJECTILES, Terminal Guidance
5. TRAJECTORY, In-flight Correction

Copy No.________

[redacted]

AD No. Accession No.
Pitman-Dunn Laboratories Group, Frankford Arsenal
Philadelphia 37, Pa.

FEASIBILITY STUDY OF AN ADVANCED RECOILLESS RIFLE WEAPON SYSTEM UTILIZING A TERMINALLY GUIDED PROJECTILE (U) -
S. J. Fenton, Bulova Research and Development Laboratories, Inc.

Classification: Title - Uncl; Report - Confidential
Report No. R-1425, Dec 1957; 227 pages; 80 illus; 18 tables
Contract DA-30-069-ORD-1766 DA Project No. 5S02-01-008
Ordnance Project TS4-4024

Presented is a summary of the feasibility study of adapting post firing trajectory correction techniques to operational recoilless antitank weapons.

The study, informally designated Project POLCAT, contributes a solution to the problem in the form of a specific weapon system. The recommended system minimizes miss distance by combining conventional fire control methods with relatively simple post firing correction techniques. Post firing correction is achieved by using a frame fixed infrared seeker for guidance and impulse sterring for control. Based on the technical analyses and the experimental testing as reported, it is concluded that the recommended advanced weapon system is entirely feasible and warrants serious consideration for weapon engineering design and development.

[redacted]

1. GUIDANCE, Recoilless, Projectile
2. WEAPON SYSTEM, Recoilless with post launching trajectory correction
3. INFRA-RED
4. PROJECTILES, Terminal Guidance
5. TRAJECTORY, In-flight Correction

Copy No.________

[redacted]

AD No. Accession No.
Pitman-Dunn Laboratories Group, Frankford Arsenal
Philadelphia 37, Pa.

FEASIBILITY STUDY OF AN ADVANCED RECOILLESS RIFLE WEAPON SYSTEM UTILIZING A TERMINALLY GUIDED PROJECTILE (U) -
S. J. Fenton, Bulova Research and Development Laboratories, Inc.

Classification: Title - Uncl; Report - Confidential
Report No. R-1425, Dec 1957; 227 pages; 80 illus; 18 tables
Contract DA-30-069-ORD-1766 DA Project No. 5S02-01-008
Ordnance Project TS4-4024

Presented is a summary of the feasibility study of adapting post firing trajectory correction techniques to operational recoilless antitank weapons.

The study, informally designated Project POLCAT, contributes a solution to the problem in the form of a specific weapon system. The recommended system minimizes miss distance by combining conventional fire control methods with relatively simple post firing correction techniques. Post firing correction is achieved by using a frame fixed infrared seeker for guidance and impulse sterring for control. Based on the technical analyses and the experimental testing as reported, it is concluded that the recommended advanced weapon system is entirely feasible and warrants serious consideration for weapon engineering design and development.

[redacted]

1. GUIDANCE, Recoilless, Projectile
2. WEAPON SYSTEM, Recoilless with post launching trajectory correction
3. INFRA-RED
4. PROJECTILES, Terminal Guidance
5. TRAJECTORY, In-flight Correction

Copy No.________

[redacted]

AD No. Accession No.
Pitman-Dunn Laboratories Group, Frankford Arsenal
Philadelphia 37, Pa.

FEASIBILITY STUDY OF AN ADVANCED RECOILLESS RIFLE WEAPON SYSTEM UTILIZING A TERMINALLY GUIDED PROJECTILE (U) -
S. J. Fenton, Bulova Research and Development Laboratories, Inc.

Classification: Title - Uncl; Report - Confidential
Report No. R-1425, Dec 1957; 227 pages; 80 illus; 18 tables
Contract DA-30-069-ORD-1766 DA Project No. 5S02-01-008
Ordnance Project TS4-4024

Presented is a summary of the feasibility study of adapting post firing trajectory correction techniques to operational recoilless antitank weapons.

The study, informally designated Project POLCAT, contributes a solution to the problem in the form of a specific weapon system. The recommended system minimizes miss distance by combining conventional fire control methods with relatively simple post firing correction techniques. Post firing correction is achieved by using a frame fixed infrared seeker for guidance and impulse sterring for control. Based on the technical analyses and the experimental testing as reported, it is concluded that the recommended advanced weapon system is entirely feasible and warrants serious consideration for weapon engineering design and development.

[redacted]

1. GUIDANCE, Recoilless, Projectile
2. WEAPON SYSTEM, Recoilless with post launching trajectory correction
3. INFRA-RED
4. PROJECTILES, Terminal Guidance
5. TRAJECTORY, In-flight Correction

Copy No.________

~~CONFIDENTIAL~~

REPORT No. R-1425
COPY No. 18

FRANKFORD ARSENAL
PITMAN-DUNN LABORATORIES GROUP
Philadelphia 37, Pa.

FEASIBILITY STUDY OF AN ADVANCED RECOILLESS RIFLE WEAPON SYSTEM UTILIZING A TERMINALLY GUIDED PROJECTILE (U)

December 1957

Contract No. DA-30-069-ORD-1766

OCO Project No. TS4-4024
DA Project No. 5S02-01-008

Prepared by

S. J. FENTON
Project Engineer
Bulova Research and Development
Laboratories, Inc.

Reviewed by

T. PETRIDES
Department Head
Bulova Research and Development
Laboratories, Inc.

E. M. PATTERSON
President
Bulova Research and Development
Laboratories, Inc.

S. ROSS
Project Leader

E. R. THILO
Director
Physics Research Laboratory

W. J. KROEGER
Senior Scientist

Approved by

C. C. FAWCETT
Director
Pitman-Dunn Laboratories Group

For

JAMES A. RICHARDSON, III
Brigadier General, USA
Commanding

~~CONFIDENTIAL~~

ACKNOWLEDGMENT

This is the final report covering the work performed by Bulova Research and Development Laboratories, Inc., under Contract DA-30-069-ORD-1766.

The following personnel made material technical contributions to the phase of the program reported herein.

Bulova Research and Development Laboratories, Inc.

O. B. Brockmeyer
H. Kamenetsky
M. Kaswen
J. Korman
T. Petrides
H. Reismann
W. P. Stapelfeld
L. Tuckerman
A. M. Winzemer

Pitman-Dunn Laboratories Group

A. Cianciosi
C. W. Fleischer
C. Fulton
H. Sokolowski
J. Wilson

Recognition is extended to Mr. Sidney Ross, Project Supervisor, whose efforts in guiding the overall technical effort were particularly vital to the execution of the contract.

FOREWORD

This report contains the results of an advanced weapons systems study whose objective was to establish the most effective means for killing heavy armor in forward combat areas. This program was originated at Pitman-Dunn Laboratories Group, Frankford Arsenal, by Mr. Sidney Ross, who initiated the concept of post firing correction for anti-tank recoilless rifle-launched missiles. Although this concept has been evaluated within a single, well defined area of application, the principles of post firing correction presented herein can be readily applied to numerous weapons systems of varying range and warhead delivery requirements.

TABLE of CONTENTS

OBJECT

To conduct a feasibility study of the application of terminal guidance to operational recoilless antitank weapons systems

SUMMARY

Presented is a summary of the feasibility study of adapting post firing trajectory correction techniques to operational recoilless antitank weapons.

The study, informally designated Project POLCAT, contributes a solution to the problem in the form of a specific weapon system. The recommended system minimizes miss distance by combining conventional fire control methods with relatively simple post firing correction techniques. Post firing correction is achieved by using a frame fixed infrared seeker for guidance and impulse steering for control. Based on the technical analyses and the experimental testing as reported, it is concluded that the recommended advanced weapon system is entirely feasible and warrants serious consideration for weapon engineering design and development.

AUTHORIZATION

OCTM No. 36146, 29 March 1956

1.0 INTRODUCTION

Project POLCAT was initiated as a weapon system feasibility study to establish a means for increasing the long range hit probability of recoilless antitank weapons. The material presented herein constitutes the final report on this effort and, as such, contains a proposed weapon system that is judged to be the most promising method for fulfilling the requirements of the study program.

Since the POLCAT system represents a solution to a problem which has received extensive examination in the past and since the specific weapon system described herein is the result of a considerable effort currently being conducted by the Pitman-Dunn Laboratories, Frankford Arsenal, and the Bulova Research and Development Laboratories, the subject material is introduced by discussing (1) the historical background from which the weapon system concept was generated and (2) the status of the effort that has been conducted up to this time wherein a specific weapon system was developed and, then, examined in many areas to establish feasibility.

1.1 HISTORICAL BACKGROUND

During World War II, the Army initiated a phase of weapon development with the objective of providing infantrymen with lightweight, direct fire, artillery caliber weapons. The subsequent program produced a family of recoilless rifles that supplied infantry units with a destructive capability that could not be attained with conventional weapons. The earlier recoilless rifles, 57 mm and 75 mm, could be deployed against light vehicles, crew-served weapons, and pillboxes. These were not considered as primarily antitank weapons, but were used as such when required. The relative effectiveness of these rifles as antitank weapons has decreased with increased tank armor development since World War II, and they are no longer considered as antitank weapons. However, the continuing development of the recoilless rifle over the years has yielded notable increases in overall weapon effectiveness by increasing warhead size and effectiveness, by increasing accuracy and range, and by decreasing rifle weight. As a result, the primary mission of the more current recoilless rifles is antitank support for the infantry unit, battalion, and platoon. The modern, more powerful recoilless rifle can destroy heavy enemy armor forward of the battle position and still be transported by hand for short distances. Concurrent with the most recent advances in the technology of recoilless rifles, Pitman-Dunn Laboratories has realized that the current estimates and appraisals of future weapon performance require that a constant search and examination be made for a means to increase the destruction capability and the range effectiveness of such weapons.

An early study (ref.43) of the effect on hit probability of increased

velocity attained with rocket assist indicated that little could be gained by the "flat trajectory" attained. It was apparent that an order of magnitude advance was required.

In response to this need, Bulova Research and Development Laboratories, Inc., were requested by Frankford Arsenal to investigate the problem of increasing the long range hit probability of recoilless rifles by considering the application of several guidance and control techniques utilized in guided missile systems. On 30 March 1956, the Bulova Research and Development Laboratories, Inc., were awarded a study contract by Frankford Arsenal to investigate the feasibility of adapting post-firing correction technique to recoilless rifle systems. At the outset it was recognized that much of the current guided missile technology was not directly applicable to this specific problem due to the severe conditions imposed by rifle launching and the relatively short time of flight. Further, it was realized that any proposed weapons system would have to retain, insofar as possible, the basic characteristics of infantry type antitank weapons, viz., simplicity, ruggedness, mobility, and relative immunity to detection. The prevailing determination was, and still is, to generate ideas that do the Army's job and live in the field.

The study contract was initiated by examining several likely guidance and control techniques to establish whether any of the subsequently evolved systems appeared sufficiently promising to warrant detailed consideration. From this effort a system was conceived which, by virtue of its obviously uniqueness and apparent compatibility, was outstanding and deemed most capable of fulfilling the specified requirements. It is this weapon system that is described in detail in the following sections of the report.

1.2 STATUS of PROJECT POLCAT

The Project POLCAT effort has consisted of two general areas of examination;

1) analyzing general weapon system requirements based on immediate and future needs of the Army and

2) substantiating the feasibility of a weapon system that fulfills specific performance requirements.

To evolve valid and definitive weapon requirements an effort was made to obtain and study the judgment of the most competent and knowledgable personnel in the Army. This was accomplished during the initial phases of the program by conducting a literature survey and through direct contact with those personnel responsible for field evaluation, planning, weapon development, research, weapon assessment, etc. From these contacts the specific weapon system requirements discussed in Section 2.1 were established. Further, general conclusions were obtained regarding the deployment of weapons in the future. It appears that for a wide cross-section of weapon types and for varying mission requirements, mobility is a prime attribute. The demands of modern weapon system planning, as exemplified by the operational requirements of the "brush-fire" war or the atomic environment, place a new definition on weapon mobility. In this respect merely putting a weapon on wheels is no longer sufficient. Mobility is determined by such capabilities as self-propelled, air droppable weapons, but also includes logistic requirements, minimal crew considerations, and combat readiness as established by weapon maintenance and crew training requirements. These factors combined with the other major system requirements are reflected in proposed antitank weapon since all the considered weapon system approaches were evaluated on the basis of fulfilling the broad requirements of the Army as well as specific performance requirements.

With a well founded background for evolving a tactically useful antitank weapon, the technical effort of Project POLCAT proceeded to solve the specific engineering problems associated with the weapon system itself. The initial task consisted of analyzing likely guidance and control technique for incorporation within an antitank projectile. The results are summarized in Reference 1 wherein it was recommended that an impulse controlled, infrared seeking projectile be given serious consideration as a post firing correction technique. Following this recommendation, an analytical program was conducted in order to more carefully examine the dynamic and kinematic characteristics of this type of guidance and control. The results obtained by two-dimensional and three-dimensional simulation served to verify the compatibility of the proposed guidance and control technique as applied to the antitank weapon system. (See Reference 2). At this point a field test program was initiated to substantiate the apparent benefits of impulse control by flight test. A detailed description of the test program is presented in Reference 3. Briefly, the program required no special instrumentation or equipment. The test vehicle shown in Figure 1.1 was an existing projectile modified to permit installation of a control unit. The tests were notably successful, unquestionably demonstrating the effectiveness and reliability of impulse control. The results of the firings are presented in the Technical Discussion, Section 3.3. Presently, the Bulova Research and Development Laboratories are investigating the problems of semi-active illumination of targets.

This study program awarded by Frankford Arsenal requires the construction of a lamp capable of fulfilling target illumination requirements, similar to those of the proposed weapon system.

While the status of the Project POLCAT accomplishments are limited in terms of the overall engineering effort required for weapon development, the achievements to date do represent solutions to some of the more critical problems. Project POLCAT has undoubtedly served to generate a new weapon system concept and in addition to qualify to some extent the proposed antitank weapon.

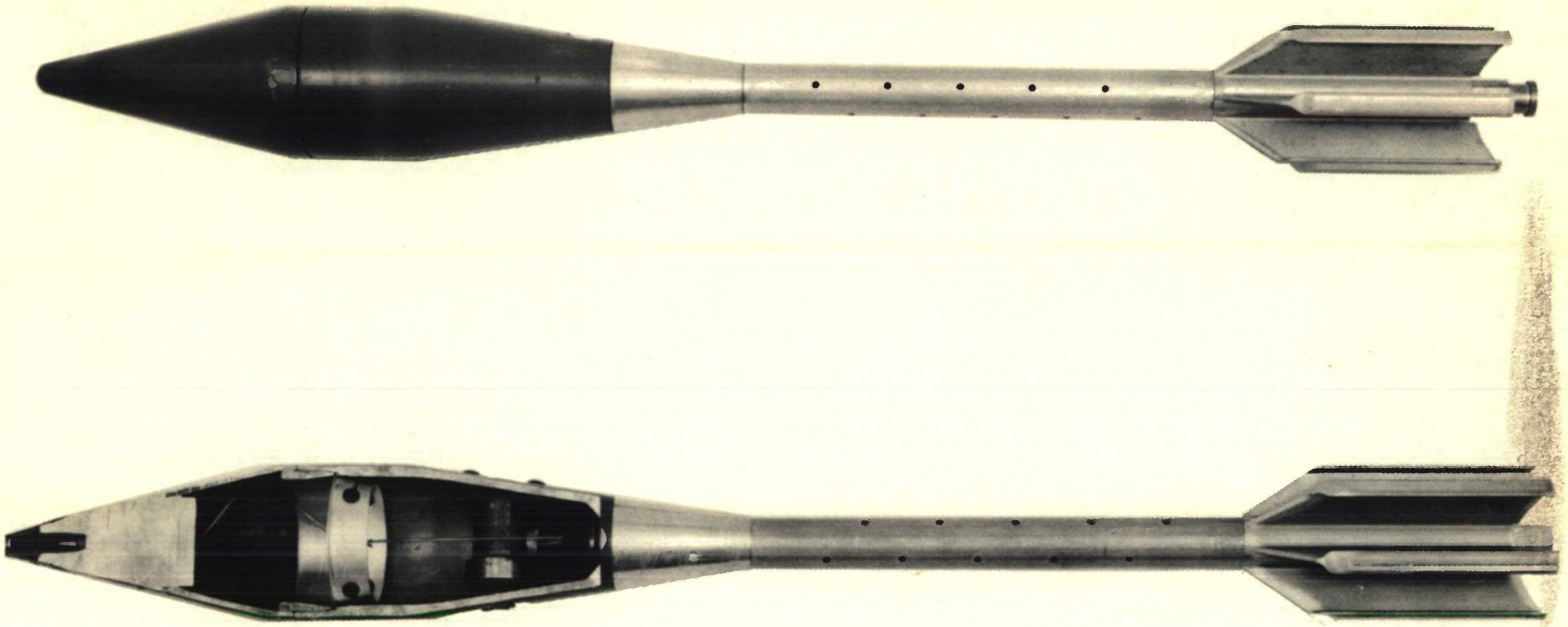

Figure 1.1 STANDARD T184 PROJECTILE (top) and TEST PROJECTILE (bottom, cutaway)
BULOVA RESEARCH AND DEVELOPMENT LABORATORIES, INC.

2.0 GENERAL DISCUSSION

The characteristics of the POLCAT weapon are presented in the following manner:

(1) The operational requirements as derived from the nature of the antitank mission and guided by general weapon system requirements are stated in Section 2.1.

(2) The weapon system concept which provides the means for fulfilling the specified requirements is described in Section 2.2.

(3) The application of the system concept to the POLCAT weapon is given in Section 2.3 which contains the functional description of the antitank system.

(4) An estimate of the physical characteristics and the required performance characteristics of the system components is given in Section 2.4.

2.1 OPERATIONAL REQUIREMENTS

The basic objective of the POLCAT program is the eventual development of an antitank weapon system that is capable of attacking and destroying enemy armor deployed in forward combat areas.

By possessing an extraordinarily high hit probability and a high degree of mobility, the more advanced antitank weapon can provide ground units, infantry or mobile, with an effective means for combatting

tanks despite any advantages afforded the target by heavier armor or superior firepower.

To perform this task the antitank weapon must be provided with the following operational capabilities:

(1) First round probability of hit shall be greater than .80 at maximum target range.

(2) Effective combat range shall be at least 2000 yards. There shall be no limitation within the weapon system that establishes a minimum engagement range.

(3) The weapon system weight (less ammunition) shall not exceed 600 pounds. This permits the weapon system to be hand carried for short distances, mounted on light vehicles or helicopters, etc., thereby assuring the eventual fulfillment of any self-propelled and/or air drop requirements.

(4) The weapon shall deliver a warhead of such size and effectiveness to defeat heavy armor.

(5) The weapon system combat readiness shall be equivalent to conventional ordnance systems. Once the weapon system is deployed in the field there shall be no need for special maintenance or check-out.

(6) The weapon system shall require a crew of three men. The operation of the weapon shall not require any of the crew to qualify as technicians or specialists.

2.2 WEAPON SYSTEM CONCEPT

The outstanding capability of the proposed weapon results from a well-considered integration of fire control methods and guidance and control techniques. The unique quality of the weapon system lies with this concept of obtaining more advanced weapon effectiveness by dividing the responsibility for system accuracy between fire control and post firing correction and by relying on simple, rugged components to effect system simplicity and mobility. The basis, then, of the system concept is the establishment of a compatible combination of fire control equipment and guidance and control components. A significant aspect of this approach is the breadth of the area of possible application. Any weapon that depends on a pre-firing estimate for target impact can be examined in terms of augmenting its existing hit capability with post firing correction. Current efforts to increase weapon effectiveness have considered two distinct approaches, by improving the fire control of conventional ordnance systems or by developing guided missile systems to replace gun systems. The long established trend in the development of fire control has indicated that, presently, a small improvement in the accuracy of the fire control equipment is accompanied by a substantial increase in complexity and weight, thereby reducing reliability and mobility. Even if the penalties of improved fire control accuracy could be sustained, the gains in overall weapon effectiveness are limited to an absolute maximum since the random errors of projectile flight still remain. These inherent limitations of the conventional ordnance system have supported the potential changeover to guided missile systems. While the missile system presents a direct solution to the accuracy problem, it does not always fulfill all the requirements that establish overall weapon effectiveness. Where it is essential that

weapons be deployed in forward combat areas, the complexity of the equipment, the difficulty of transport, and the crew requirements of the pure missile system severely limit the utility of this type of weapon, hence, degrading its overall effectiveness.

The POLCAT concept relies on conventional fire control equipment and gun launching to establish near accurate initial conditions for projectile flight. The resulting deviations of the projectile from the desired trajectory are small compared to the excursions of low acceleration launching systems (rocket boost). While the launching loads of the POLCAT technique are extremely high, the requirement on the magnitude of subsequent in-flight correction is low. This permits consideration of simple, almost crude guidance and control techniques, which inherently are capable of sustaining the loads at launch. For the application examined in the POLCAT effort, the system concept proved to be fundamental to the generation of a weapon system that fulfilled the desired requirements.

2.3 DESCRIPTION of WEAPON SYSTEM

The proposed weapon system represents an integration of (1) a recoilless rifle for launching (2) optical fire control equipment for initial gun pointing (3) a projectile containing the required guidance and control components for post-firing correction, and (4) a lamp for target illumination. The unique characteristics and capabilities of this antitank weapon that differentiate it from existing recoilless rifle systems can be attributed to the projectile which incorporates an impulse type control system and a frame fixed infrared seeker for guidance. The projectile is similar to existing rounds in that it is fin stabilized, fired from a 106mm recoilless rifle, and contains a shaped charge warhead. However, the overall projectile design is distinctive by nature of the requirements for guidance and control as illustrated in Figure 2.1. The infrared sensing elements with the associated electronic equipment are located in the projectile nose which is constructed to fulfill the requirements for satisfactory seeker operation. Since the seeker system is fixed to the projectile body its capability is limited to measuring the angle between the projectile longitudinal axis and the target line-of-sight. Thus, the seeker cannot detect nor separate false inputs (resulting from projectile pitching motion or flight path curvature) from actual flight path error. However, by filtering the seeker output and by a judicious selection of a steering law, the required relationship between the actual and the measured flight path error angle is maintained. The steering law is simple requiring a single application of control during flight. The magnitude of the flight path correction which is induced instantaneously by the firing of the impulse cartridge, is equal to a predetermined, seeker measured, flight path error angle. This reference angle for control is selected to provide the highest probability of hit over

the design range for the one-shot steering technique. In addition to the hit probability requirement, the accuracy of the fire control system has a significant influence on the choice of seeker threshold angle for control. However, once the optimum threshold is chosen, the impulse requirements for control are established. Essential to the functioning of the proposed guidance and control technique is projectile roll rate. The spin of the projectile provides the means for seeker scanning and establishes the rate of detecting the target signal. Further, projectile spin introduces continuous and rapid orientation of the control cartridge thereby reducing time delays in the control functioning cycle, and affecting near optimum conditions for polar steering.

To attain high hit probabilities with single shot control, flight path correction must occur relatively close to the target. For the maximum expected trajectory errors, the distance from the target at which control is applied will not exceed 600 feet. In committing the system to single shot control the benefits of any type of fire control are fully exploited since post-firing correction is utilized only when the projectile is destined to miss the target.

In operation, the projectile is fired at the target based on the available pre-firing estimate of range to obtain a hit. With the target illuminated by the lamp, the launched projectile continually obtains a homing signal which, by design of the lamp, is of sufficient intensity and is of discrete nature to prevent jamming or confusion. When the target line of sight angle exceeds the pre-selected threshold angle for control the seeker fires the cartridge. If at launch the projectile is destined to hit the target, the line of sight angle will not exceed the threshold angle in which case the projectile will remain on its established ballistic trajectory.

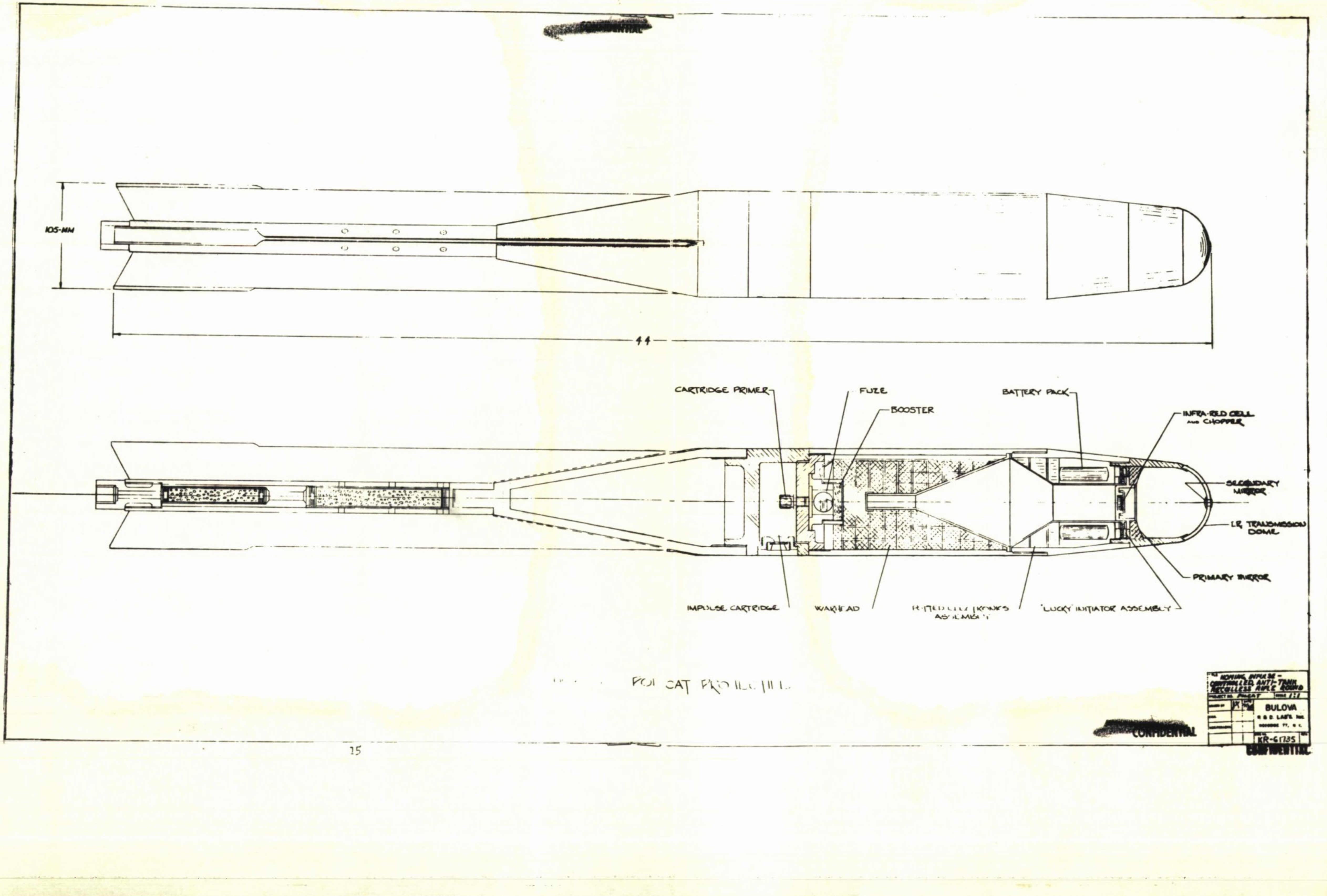

POLCAT PROJECTILE

The proposed technique for post firing correction requires a new and in many respects a unique projectile design whereas the recoilless rifle and fire control system are fundamentally unchanged. This does not imply that an eventual development program will not require redesign of the recoilless rifle or consider the use of various fire control techniques. The system requirements, however, regarding the gun or the fire control equipment are reasonable within the state of the art, and not subject to questions of feasibility. The same philosophy applies to handling and transporting the proposed weapons system. The system can be mounted and carried in a similar manner that is used in the deployment of, existing or projected, conventional recoilless rifle systems. Thus, the weapons system does not present special problems in logistics or personnel training.

The mechanism of post-firing correction is self-contained with the responsibility of the gun crew limited to initially pointing the gun and, then, keeping the beam of the illuminator on the target during the flight time of the projectile. The overall effort that will be required to place the weapon in the field might be summarized as the adaptation of the specified guidance and control concept to existing recoilless rifles.

2.4 DESIGN REQUIREMENTS

To provide a brief, yet distinct, representation of the antitank weapon, preliminary design requirements for the system components and for component performance are described. These specifications represent what is presently considered essential to successful weapon system operation. The analytical work that established the specified characteristics is presented in the following section, Technical Discussion.

The POLCAT weapon system is considered to be constituted of the sub-systems presented herein and illustrated below in a functional block diagram.

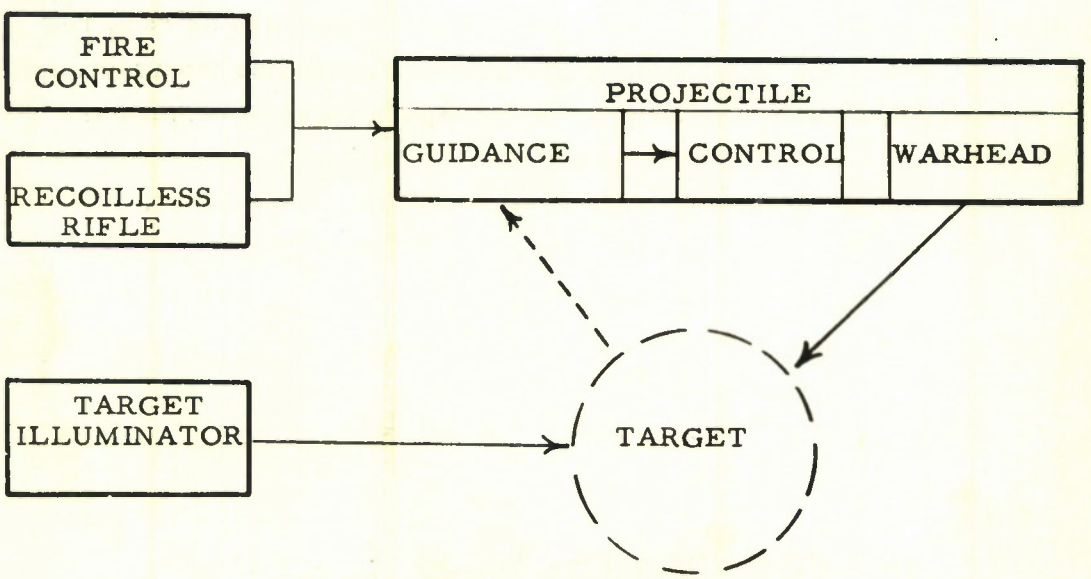

2.4.1 PROJECTILE

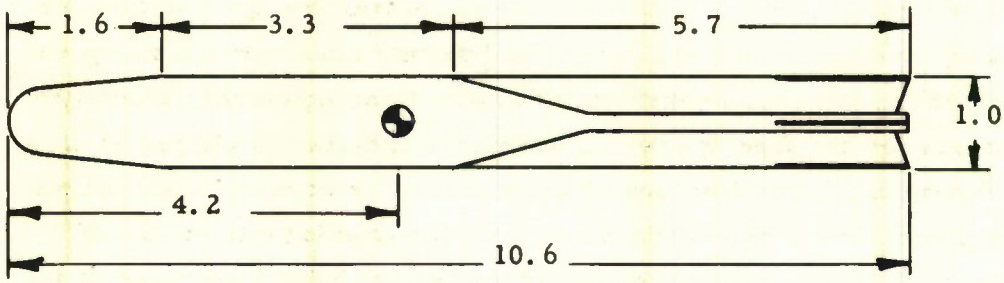

All dimensions in calibers

Weight	23.4 lbs
Diameter	105 mm
Length	44.0 in
Center-of-Gravity from Nose	17.4 in
Moment of Inertia in Pitch	2350 lb-in^2
Moment of Inertia in Roll	43 lb-in^2

The projectile design provides for the incorporation of the frame fixed infrared seeker, the impulse control cartridge, and the shaped charge within an airframe that fulfills the basic aerodynamic requirements for satisfactory flight and, in addition, fully reflects the requirements for gun launching. Accordingly, the component and airframe design is predicated on the extremely high axial accelerations imposed at launch. The size and arrangement of the components are dictated by the physical restriction of the gun tube diameter and the requirements for effective and reliable performance of the target seeker, control

cartridge and the warhead. The projectile nose is shaped to assure efficient collection and transmission of radiant energy. Within the forward section of the projectile the internal arrangement and packaging of the infrared seeker and its associated electronic equipment accounts for the free space requirements peculiar to shaped charge performance. The location of the warhead relative to its initiation mechanism in the projectile nose provides an adequate stand-off distance. The control cartridge is placed behind the warhead at the projectile center-of-gravity thereby fulfilling the primary requirement for the effective utilization of impulse-type control.

By gun launching the projectile and by incorporating an infrared seeker, obvious compromises are reflected in the aerodynamic design of the projectile. Despite the rigorous design restrictions the proposed airframe possesses the desired flight characteristics. Although the seeker is housed in a hemispherical nose the total projectile drag is not inordinately high. Adequate projectile stability is obtained from the short span, dorsal like, tail which is fixed and does not extend beyond the limits of the gun tube diameter. Every consideration has been given toward evolving the lightest possible airframe whereby it will be possible to use existing guns for launching.

2.4.2 GUIDANCE PACKAGE

The target seeker is an infrared sensing device that provides homing information to the control system by measuring the angle between the projectile longitudinal axis and the line of sight to the target. Utilizing reflective optics, the target line of sight angle is detected within the seeker in the form of a polar angle. The seeker always provides the orientation of trajectory error and when the magnitude of line of sight angle equals the specified angular control capability of the system, control is initiated. Since the target seeker is fixed to the projectile airframe, the measured line of sight angle includes projectile angle of attack. To provide the required accuracy, the seeker output is filtered whereby the influence of spurious airframe motion is effectively reduced.

As in any infrared homing system the selection of the type of sensing element is based on the target radiation characteristics. Since the proposed weapon system provides for illuminating the target rather than depending on its inherent radiant energy to provide a signal of sufficient intensity, the problem of evolving a target seeker is considerably less complex. The resulting seeker design is relatively simple consistent with the need for rugged, highly reliable equipment.

Sensing Element	PbS
Spectral Range	1.0 to 3.0 microns
Field of View	10 degrees
Accuracy of LOS Angle Measurement	2 mils
Power Required	28 volts, 5 watts

2.4.3 CONTROL PACKAGE

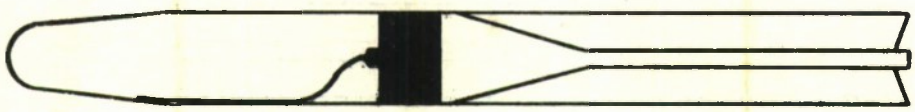

Flight path correction is introduced by a single impulsive force applied at the projectile center-of-gravity normal to the projectile body axis. The impulse delivered to the airframe is generated by a rapid burning propellant contained in the cartridge located aft of the projectile warhead. In-flight control is initiated by the target seeker which functions the electrical primer. The primer has been selected to provide reliable and efficient ignition of the propellant. Working within practical limits of maximum chamber pressure, the primer and propellant combination initiate and deliver the required impulse with minimum time delay. This assures that control is obtained with the desired orientation for the anticipated projectile roll rates.

Impulse Control	35 lb-sec
Duration	003 sec
Chamber Volume	10 cu. in.
Propellant	M2
Primer	M 52
Maximum Correction to Flight Path	50 mils
Minimum Correction to Flight Path	33 mils

2.4.4 WARHEAD AND FUZING

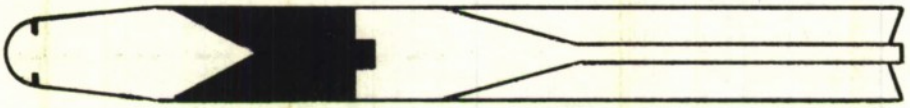

The projectile contains a shaped charge warhead whose size is comparable to existing 105 mm HEAT rounds. Although the warhead is placed behind the target seeker, the latter is packaged in such a manner that the zone within the warhead cone and forward along the warhead axis is free of any equipment or structure that could conceivably prevent the formation of a continuous and effective jet upon target impact. The armor penetration performance of the shaped charge is enhanced by maintaining a relatively large distance between the warhead liner and the projectile nose. Stand-off distance of the homing projectile is greater than that of most existing uncontrolled HEAT rounds. In addition, by including several warhead initiators in the fuzing system, the warhead can function effectively at higher angles of obliquity.

While the shaped charge is detonated electrically, the warhead is armed at setback mechanically. A delay of 33 milliseconds is incorporated in the arming mechanism to provide crew safety.

Weight of Charge	3.5 lbs.
Type of Charge	Comp. B or better
Stand-off Distance	2.0 cal.
Shaped Charge Liner	copper
Arming Delay	50 ft.

2.4.5 TARGET ILLUMINATOR

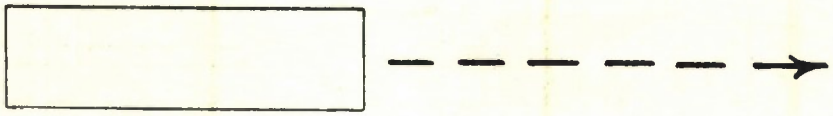

Target illumination for the projectile homing seeker is provided by narrow beam, arc-type lamp. Complete security against counter-measures is assured by suppressing the visible light and pulsing the infrared energy at a discrete frequency. The aiming of the beam is accomplished by boresighting the axis of the lamp with a fixed focus telescope similar to the instrument used for fire control. The narrow beam width is obtained from a folded, reflective optical system. Modulation of the beam is performed by a mechanical chopper. The overall design of the lamp is oriented toward achieving lightweight, thereby affording portability in the field.

Type	carbon arc
Power Output	46×10^6 candlepower
Beam Width	1 mil
Diameter	18 inches

2.4.6 FIRE CONTROL

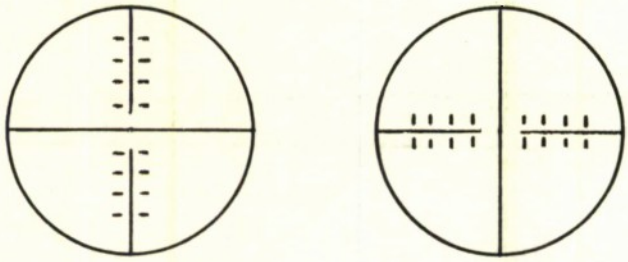

The overall system requirements on fire control accuracy are predicated on the use of the simplest of existing equipments, namely, a fixed focus telescope and a coincident type range finder. The telescope mount is secured to the recoilless rifle so that it moves in azimuth and elevation with the rifle. The gunner aims with that part of the reticle so as to obtain the desired deflection and range. The reticle is illuminated for night operation. The range finder provides range estimation by depressing or elevating the finder until the erect and inverted target images meet at the halving line. The telescope determines the angle of site whereas the range finder determines super elevation.

Telescope	M85C
Magnification	3X
Field of View	12 degrees
Range Finder	M 7 or M9A1
Magnification	14X
Base Length	1 meter
Field of View	3 degrees

2.4.7 RECOILLESS RIFLE

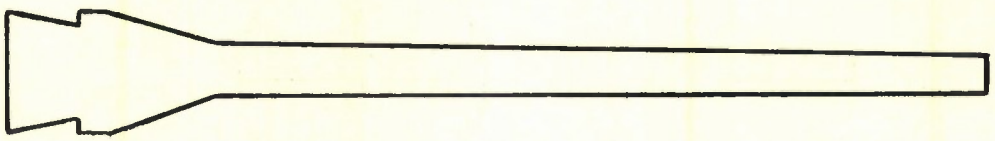

The controlled projectile is fired from a recoilless, portable weapon. The outstanding feature of the recoilless rifle is its light weight permitting transport by hand for short distances or mounting on relatively light vehicles. While the mobility of the recoilless rifle is an unquestionable advantage, its rearward blast must be considered in all cases of its deployment. In addition to the danger to personnel within a considerable zone to the rear and sides of the rifle, the problem of security after firing exists.

The recoilless rifle is single loaded with a manually operated breech. Within the present application it is used in direct fire only.

Rifle .....M40 (modified)
Caliber .....106 mm
Length ..... 134 inches
Weight .....250 lbs
Ammunition ..... Controlled, HEAT round
Muzzle Velocity .. 1650 ft/sec
Powder Charge .. 10.0 lbs

3.0 TECHNICAL DISCUSSION

A complete and detailed summary of the analytical and experimental work conducted for Project POLCAT is presented in the following sections. In addition to describing the efforts of the Bulova Research and Development Laboratories in executing its contractual commitments, the subsequent discussion also includes the substantial contribution of the Pitman-Dunn Laboratories, Frankford Arsenal, to the overall POLCAT effort.

3.1 AERODYNAMICS

It is the purpose of this section to present the estimated aerodynamic characteristics of the POLCAT projectile and based on these predictions to perform an approximate aerodynamic analysis. The immediate discussion describes the manner in which theoretical methods and experimental data were used to determine drag, lift, moment, and damping of the projectile. The estimates of these coefficients are summarized in Figure 3.1-1. In the subsequent sections the trajectory characteristics, the projectile dynamic behavior, and the aerodynamic loads are presented.

Throughout the analysis, the aerodynamic notation given below is used.

AR	aspect ratio (b^2/S_f)
b	exposed fin span, ft.
C_D	drag coefficient, $\frac{\text{Drag}}{qS}$
C_L	lift coefficient, $\frac{\text{Lift}}{qS}$
C_{L_α}	lift curve slope, per deg.
C_M	pitching moment coefficient, $\frac{\text{Moment}}{qSd}$

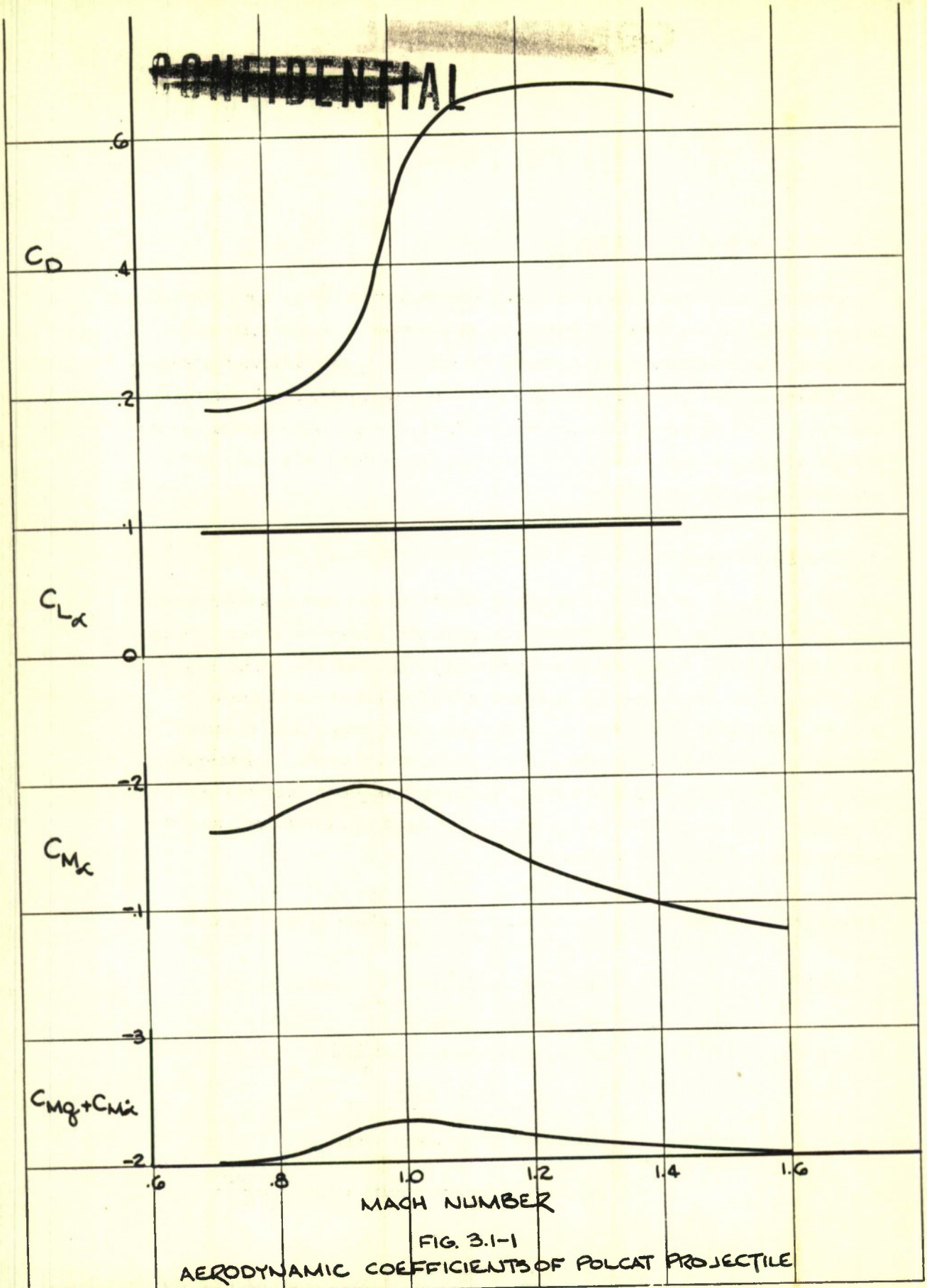

FIG. 3.1-1
AERODYNAMIC COEFFICIENTS OF POLCAT PROJECTILE

C_P	pressure coefficient, $\frac{\Delta P}{q}$
d	maximum projectile diameter, (.344 ft.)
I_x	moment of inertia in roll, (.0093 slug-ft^2)
I_y	moment of inertia in pitch, (.507 slug-ft^2)
M	Mach number
m	mass (.726 slugs)
q	dynamic pressure
R_T	target range, yds.
S	maximum projectile frontal area, (.0935 sq. ft.)
S_f	exposed plan area of two fins, (.30 ft.)
V	velocity, ft/sec
α	projectile angle of attack
θ	projectile pitch angle
γ	projectile flight path angle
ϕ	projectile roll angle
w_θ	frequency in pitch
λ	target line-of-sight angle
ϕ_T	target polar angle

3.1.1 Estimation of Aerodynamic Coefficients

The drag estimate of the POLCAT projectile is based entirely on experimental data obtained from wind tunnel and free flight tests of References 4 to 12. The drag penalties of various missile nose shape for infrared seeking are given in Reference 9 from which it can be concluded that over the expected Mach number range of POLCAT

projectile flight the use of a hemispherical nose appears reasonable. At these speeds this nose shape does not incur unduly high drags whereas significant advantages are derived in terms of more efficient collection and transmission of radiant energy. The effect of nose bluntness on drag is illustrated in Figure 3.1-2 which indicates a substantial reduction in drag by utilizing a nose radius less than the body radius. The difference in drag between parabolic and round nose shapes is shown in Figure 3.1-3. The drag variation specified for the POLCAT projectile is faired between the test data to account for the minor differences in nose shape. With this increment of drag due to the blunt nose, the total projectile drag is estimated from the test results given in Reference 4 for a missile configuration that closely resembles the POLCAT projectile except for nose shape. The similarity between the test model and the POLCAT projectile, the drag build-up, and the variation of projectile drag coefficient with Mach number are illustrated in Figure 3.1-4.

The lift characteristics of the projectile are determined by combining theoretical estimation techniques and experimental data. In the absence of test data, projectile lift is usually obtained analytically using such procedures as presented in Reference 13 and 14. The value of these methods is based primarily on the ability to estimate wing-body interference effects. The POLCAT configuration with a blunt nose and dorsal-like tail fins does not lend itself to direct treatment by either of the analytical methods whereby the interference effects can be determined. However, the procedure of determining total lift from component lift is used to establish Mach number effects whereas experimental data are used to establish the magnitude of total projectile lift. Initially, it is shown that slender body theory provides a reasonable estimate of body-alone lift curve slope for

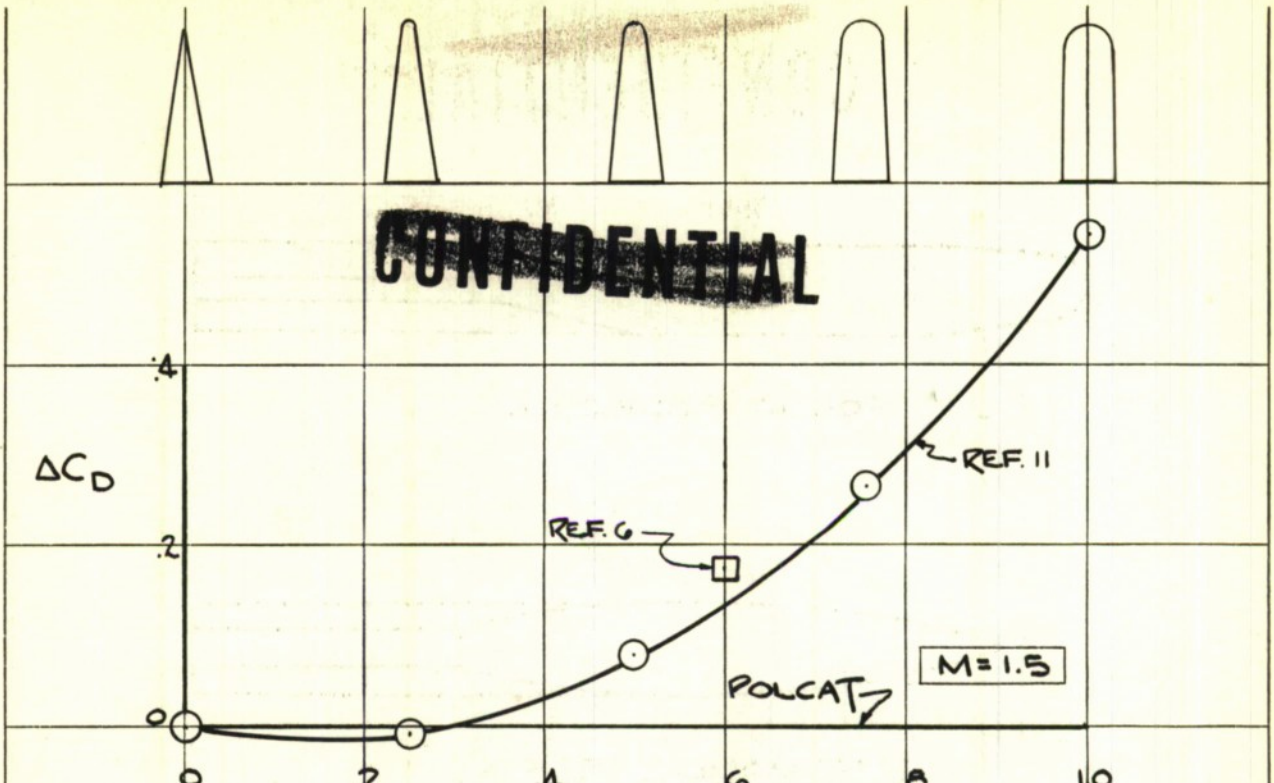

FIG. 3.1-2
EFFECT OF BLUNTNESS ON DRAG COEFFICIENT (M=1.5)

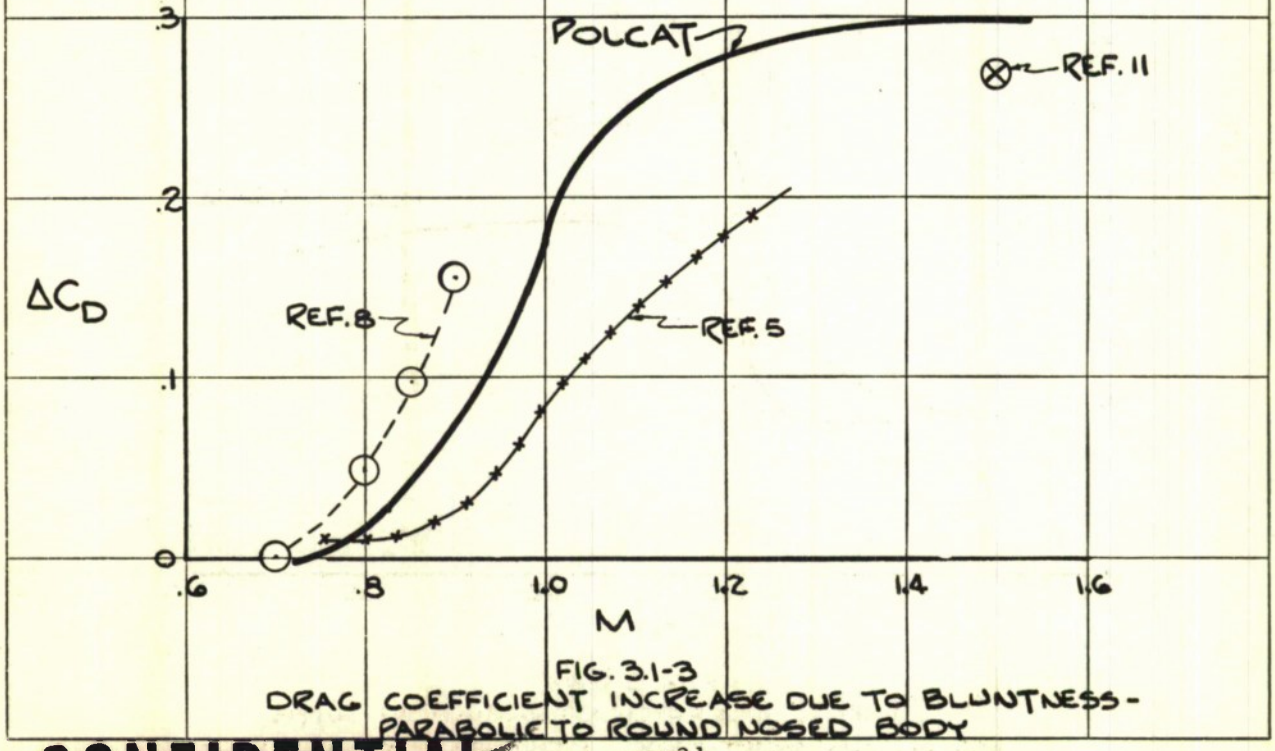

FIG. 3.1-3
DRAG COEFFICIENT INCREASE DUE TO BLUNTNESS - PARABOLIC TO ROUND NOSED BODY

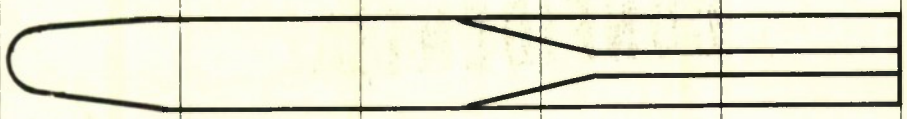

POLCAT PROJECTILE

TEST MODEL (REF. 4)

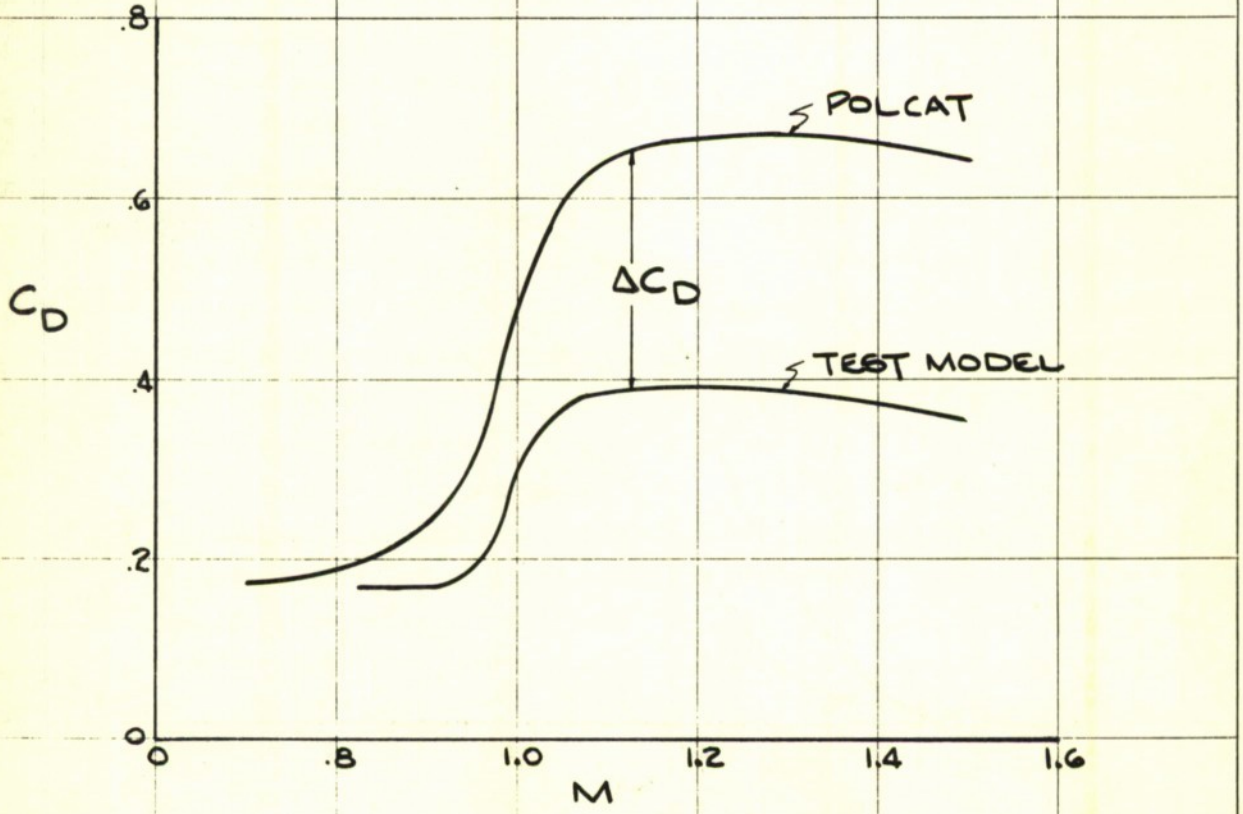

FIG. 3.1-4
DRAG COEFFICIENT VARIATION WITH MACH NUMBER FOR POLCAT PROJECTILE

all body shapes at low angles of attack. A correlation of experimental lift curve slopes at subsonic and supersonic speed is shown in Figure 3.1-5 for round, conical, and parabolic nosed bodies of varying fineness ratios; the change in lift curve slope with Mach number is not substantial. The effect of angle of attack is given in Figure 3.1-6 where it is shown that the slender body value is applicable for angles as high as 5 degrees. With regard to the lift curve slope of lifting surfaces, the various low aspect ratio theories establish that for aspect ratios less than 1.0 the value of lift curve slope at low angles of attack is independent of Mach number and planform. In Figure 3.1-7 two theoretical variations of lift curve slope with aspect ratio are shown. The results from Reference 19 (Jones) treats low aspect ratio delta wings and indicates a linear relationship between lift and aspect ratio. Reference 20 contains the analysis by Krienes of low aspect ratio elliptical wings. Despite the difference in planform both theories agree at the lower aspect ratios. Thus, with regard to body-alone and wing-alone lift it is concluded that neither varies with Mach number for the conditions established by the POLCAT configuration. Further it is assumed that the wing-body inference effects are also independent of Mach number. The latter assumption is substantiated by the experimental data plotted in Figure 3.1-8. The test results from Reference 21 and 22 were obtained for wing-body combinations with very low aspect ratio wings. It is apparent there is no substantial variation of lift curve slope with Mach number of these configurations. The usual lift curve slope variation is shown by the test results from Reference 23 with the expected transonic rise of lift. However, these data were obtained with a configuration that possessed an aspect ratio 3 wing. Having established that lift curve slope of the POLCAT can reasonably be assumed to be constant with Mach number, the value of lift curve slope is determined from a correlation of

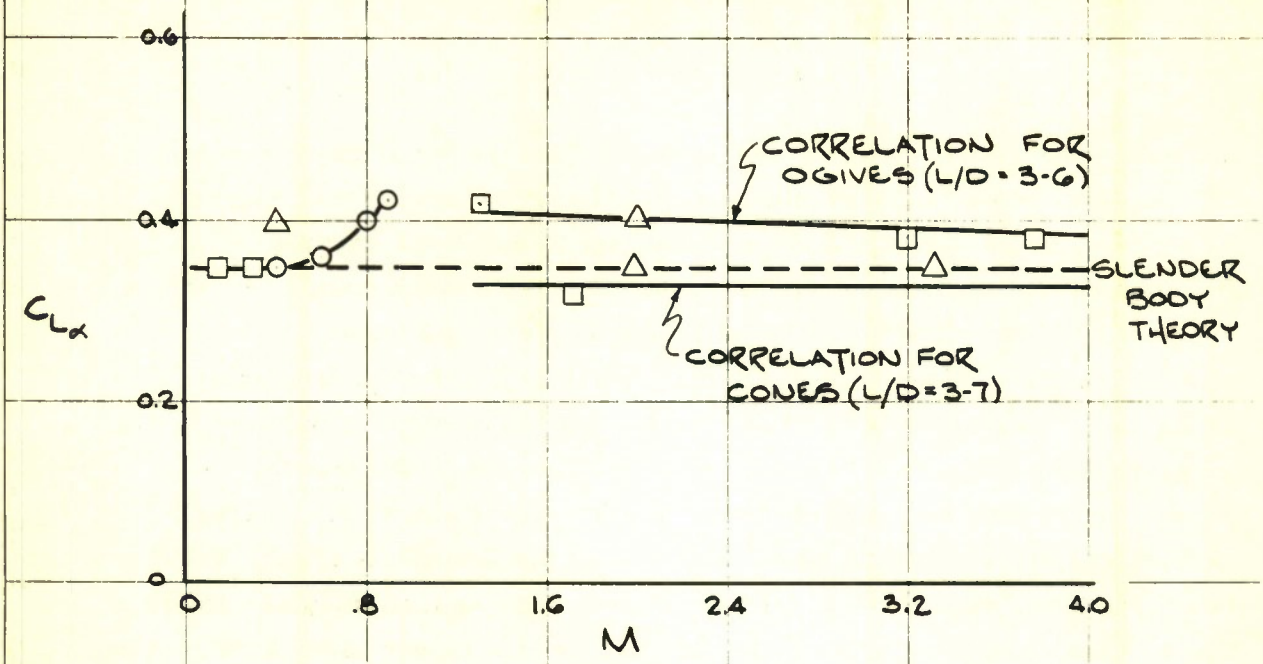

FIG. 3.1-5
BODY ALONE LIFT CURVE SLOPE VARIATION WITH MACH NUMBER

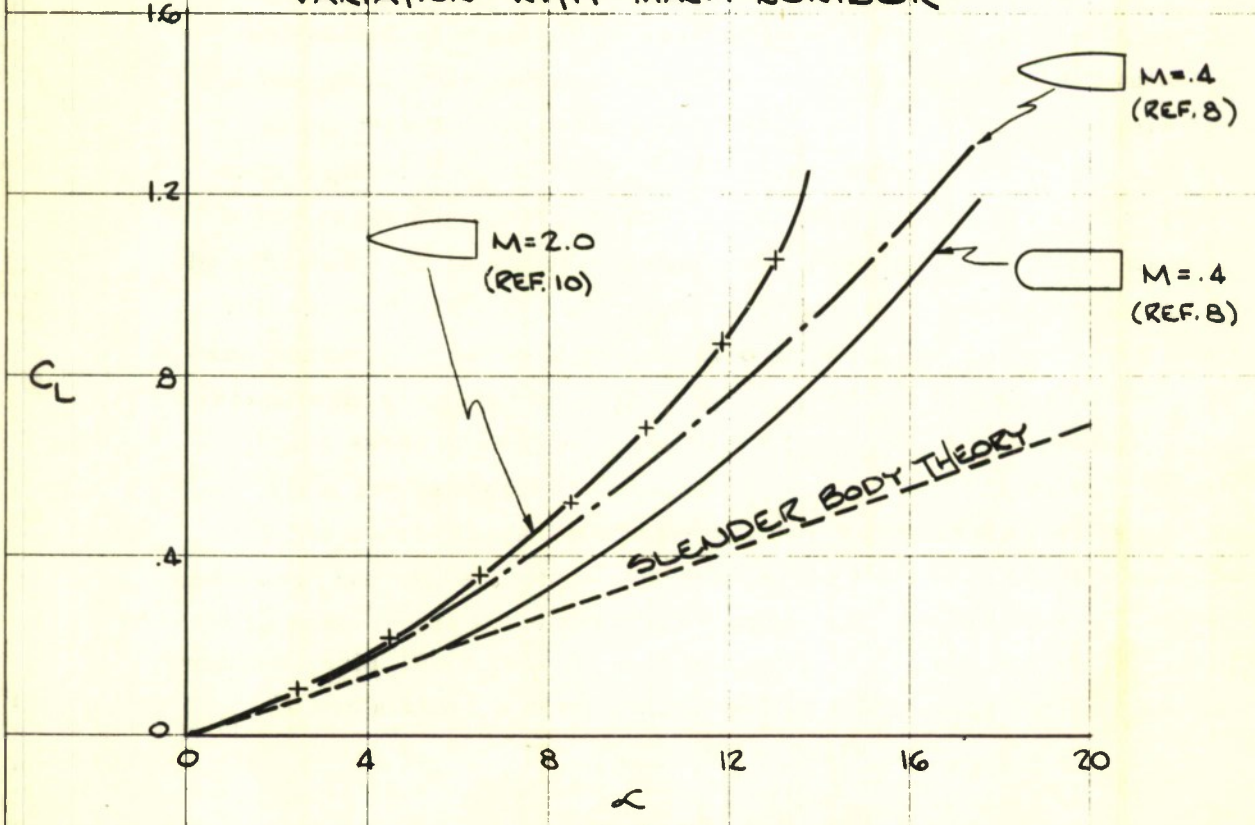

FIG. 3.1-6
BODY ALONE LIFT FOR PARABOLIC AND ROUND NOSES

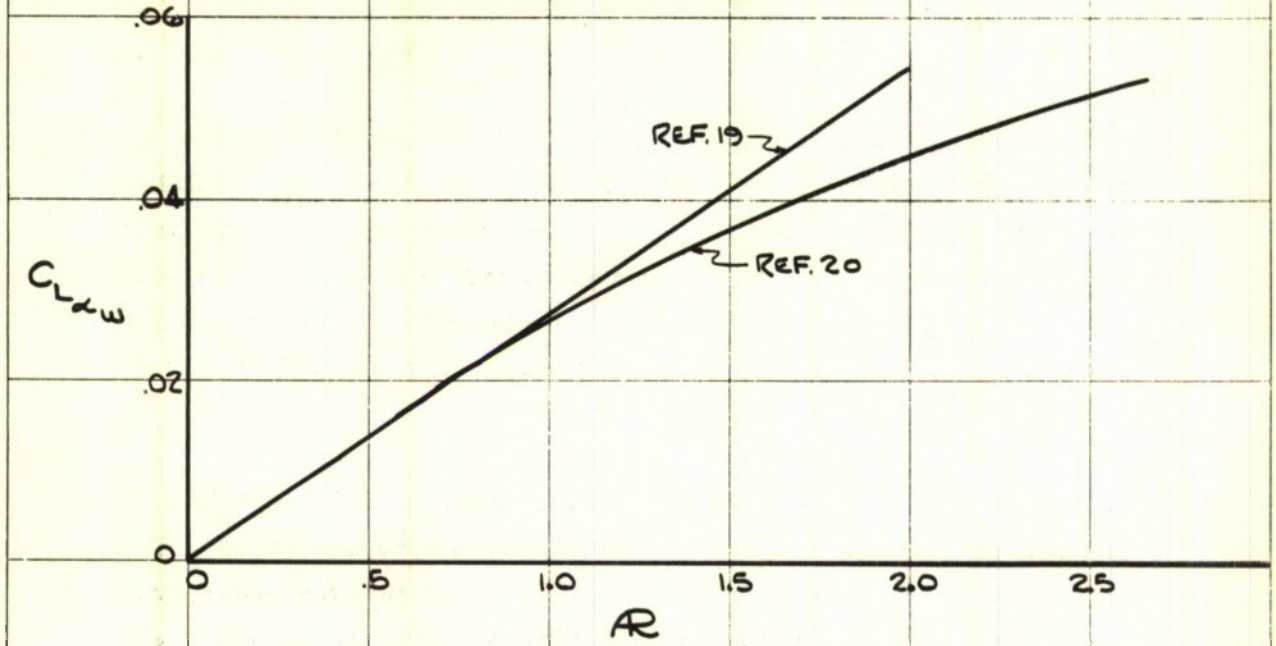

FIG. 3.1-7
THEORETICAL LIFT CURVE SLOPE
FOR LOW ASPECT RATIO WINGS

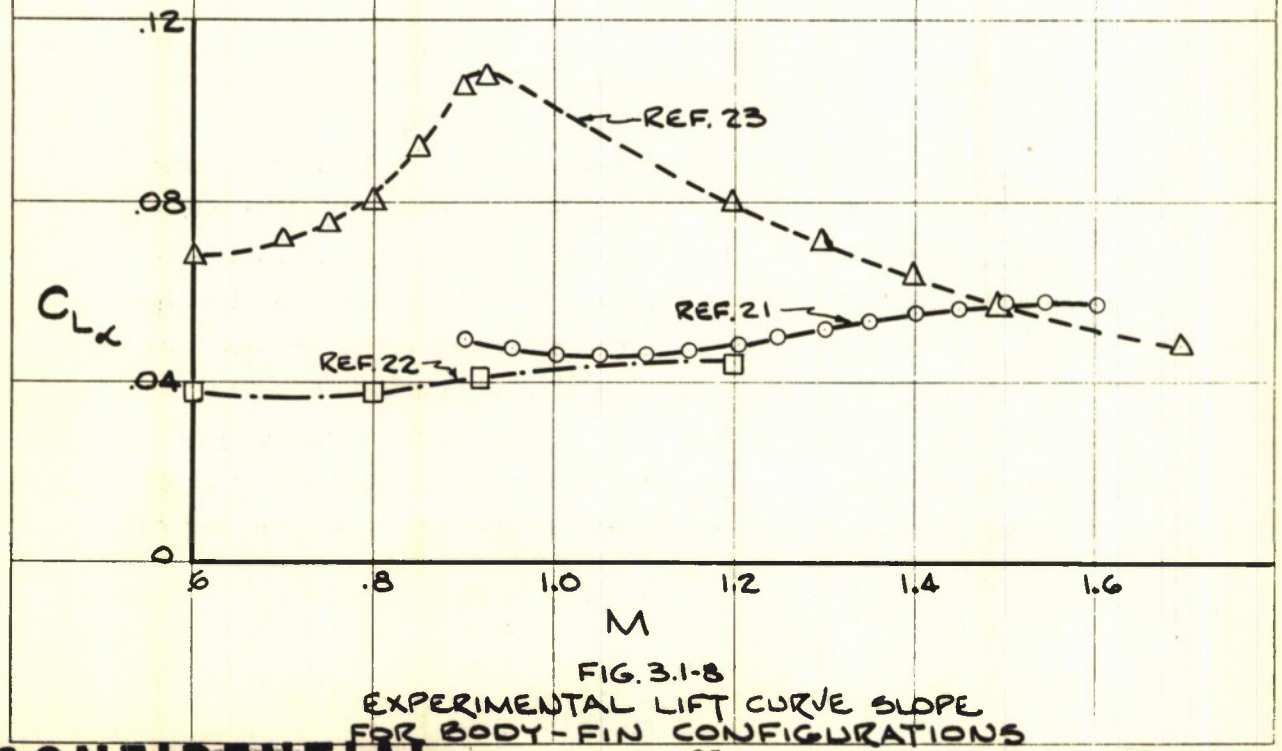

FIG. 3.1-8
EXPERIMENTAL LIFT CURVE SLOPE
FOR BODY-FIN CONFIGURATIONS

experimental data given in References 10, 24, and 25. Figures 3.1-9 and 3.1-10 illustrate the results of correlating the lift data obtained for a series of short span, wing-body combinations whose tail area and planform characteristics can be classed with the POLCAT projectile. The tail aspect ratio and the tail exposed area-to-body frontal area ratio of the POLCAT are applied to the two correlation curves to obtain the estimated lift curve slope.

While it can be assumed that the lift curve slope of the POLCAT is constant with Mach number, this assumption cannot reasonably be applied to pitching moment since it is known that the pressure distributions on the body and lifting surfaces undergo considerable change with Mach number. As previously noted in Figure 3.1-8 this distribution change does not necessarily reflect in the lift curve slope although distinct shifts in center-of-pressure are known to occur. The pitching moment coefficient of the POLCAT projectile is estimated by the relationship

$$x_{cg} - x_{cp} = \frac{C_{M_\alpha}}{C_{L_\alpha}}$$

where x_{cp} and x_{cg} are measured from the nose in calibers. Since center-of-gravity location and lift curve slope have been predicted, pitching moment coefficient slope is determined when center-of-pressure location is known. Figure 3.1-11 illustrates the in-flight stability of a rocket test model for various center-of-gravity locations. These data obtained from Reference 4 have been corrected for projectile fineness ratio and shown relative to the POLCAT projectile. The center-of-pressure movement as obtained from Reference 21 is used to guide the fairing of a curve between the subsonic neutral

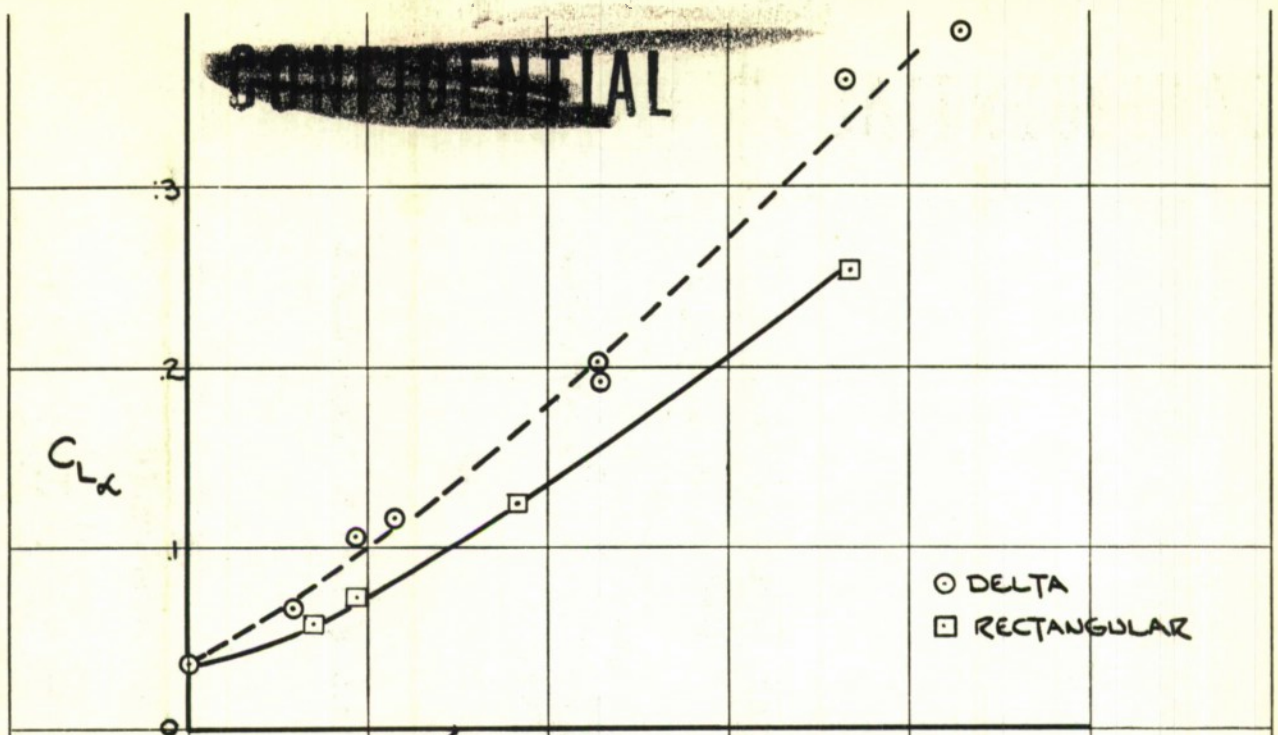

FIG. 3.1-9
LIFT CURVE SLOPE VARIATION WITH EXPOSED FIN AREA

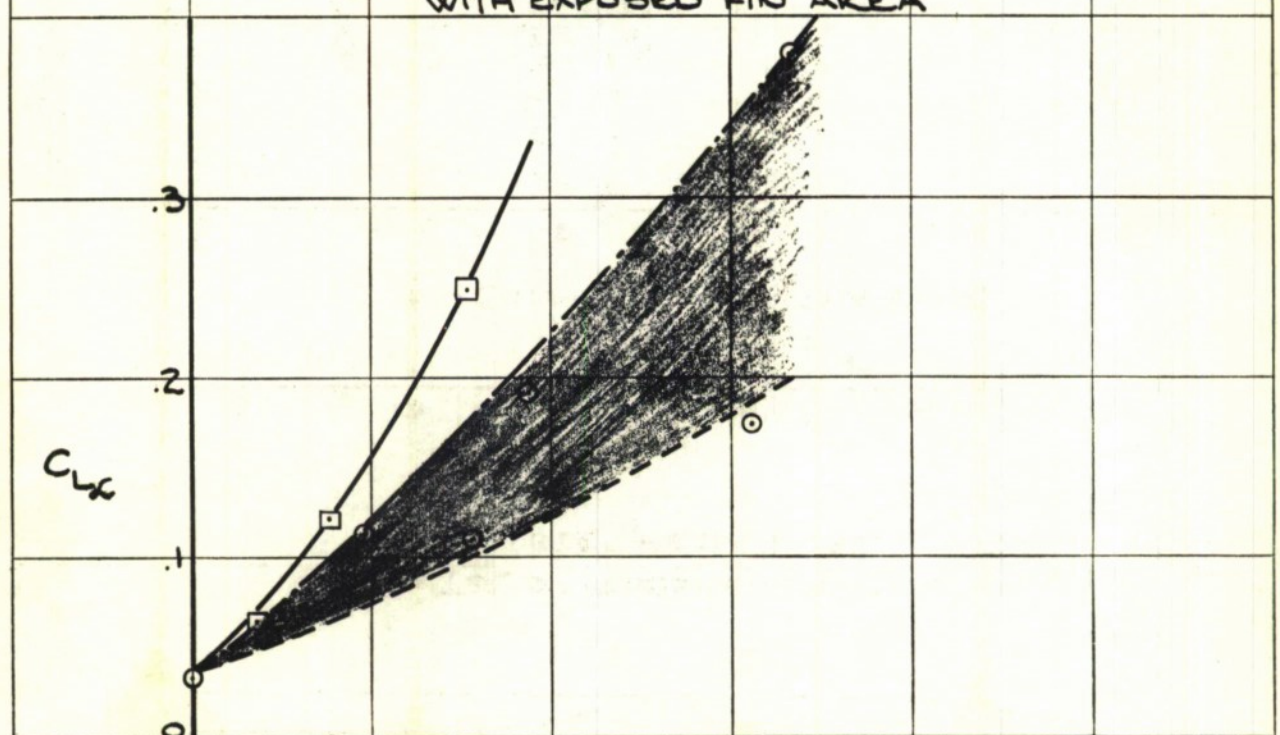

FIG. 3.1-10
LIFT CURVE SLOPE VARIATION WITH FIN ASPECT RATIO

FIG. 3.1-11
CENTER-of-PRESSURE LOCATION FOR POLECAT PROJECTILE

point and marginal center-of-gravity location at M = 1.3. With a center-of-gravity located 4.2 calibers aft of the nose, the POLCAT projectile has a static margin of 0.7 calibers at launch. The maximum static margin of 1.8 calibers occurs at M = 0.9. The pitching moment coefficient given in Figure 3.1-1 is obtained from the static margin variation shown in Figure 3.1-11 and with constant lift curve slope of .095 per degree.

The estimation of the coefficient of damping-in-pitch is based on the experimental data presented in References 21, 22, 26, 27, 28, 29 and 30. The prediction of this coefficient is less reliable than the other aerodynamic characteristics since available experimental data is not directly applicable to the POLCAT configuration. The magnitude of the damping coefficient is assumed to be proportional to Mach number and pitching moment coefficient, even though this assumption is extremely limited and attempts to verify it by correlating available test data were not overly successful. However, for the purposes of the subsequent analysis, this provides a conservative estimate of damping coefficient.

3.1.2 Aerodynamic Loads

In view of the extremely high inertia loads at launch and during control, the aerodynamic loads on the projectile are not critical in the structural design of the projectile. The only aerodynamic loading that can conceivably influence design is the high positive pressure distribution on the nose dome. The importance of this loading is determined in a subsequent section of the report where a stress analysis on the dome is performed. At this point, the pressure distribution on the dome is given in Figure 3.1-12. The distribution is typical for a hemisphere in supersonic flow; this particular distribution was obtained from Reference 31.

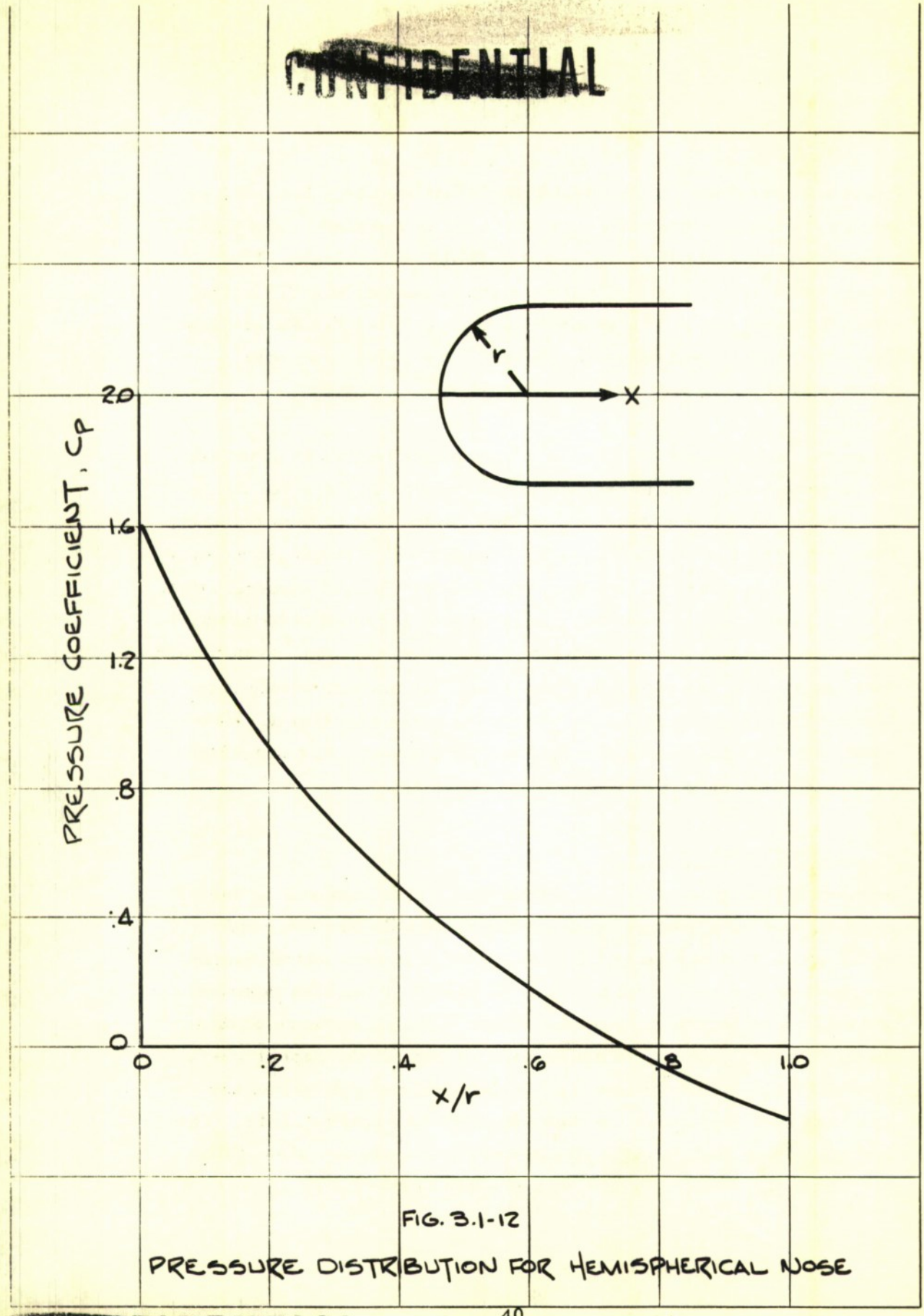

FIG. 3.1-12

PRESSURE DISTRIBUTION FOR HEMISPHERICAL NOSE

3.1.3 Trajectory Characteristics

The drag coefficient variation given in Figure 3.1-1 is used to determine the velocity and time of flight for the design range of 2000 yards. The computations assume angle of attack to be zero and the muzzle velocity to be 1650 ft/sec. For these conditions terminal velocity is slightly less than 1000 ft/sec and time of flight is approximately 5 seconds. The computed velocity and time of flight variation is shown in Figure 3.1-13. In addition to this information the calculations provided the instantaneous relationship between the projectile and the target. These relationships are the most critical aspect of the trajectory characteristics in that they establish the basis for the steering law, the homing seeker requirements, and the impulse control requirements. Since the seeker is an angle sensing device, the relation between the projectile and the target must be established by those angles that are necessary for selecting a steering law and initiating control; namely, the target line of sight angle (λ) and the target polar angle (ϕ_T). Both angles are illustrated in Figure 3.1-13a. Throughout the immediate discussion it is assumed that projectile angle of attack is zero. As a consequence the target line of sight angle (λ) is defined as the angle between the projectile longitudinal axis and the line of sight to the target. Target polar angle (ϕ_T) defines the plane containing the target line of sight angle relative to the vertical. In the case where a projectile is destined to hit the target, LOS angle is zero at impact and a maximum at launch (equal to gun elevation). For trajectories that miss the target, LOS angle increases rapidly as the projectile nears the target. The nature of LOS angle variation for error trajectories is a function of the miss distance, the initial range to target, and the

FIG. 3.1-13
VELOCITY AND TIME OF FLIGHT VS RANGE FOR POLCAT PROJECTILE

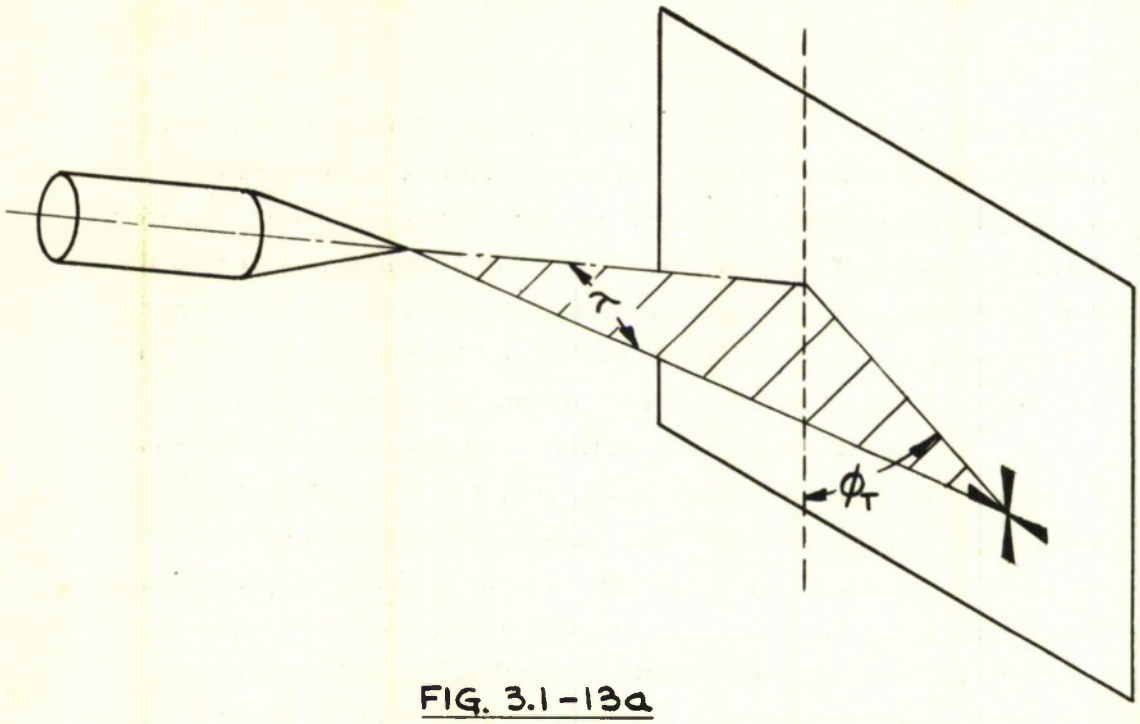

FIG. 3.1-13a

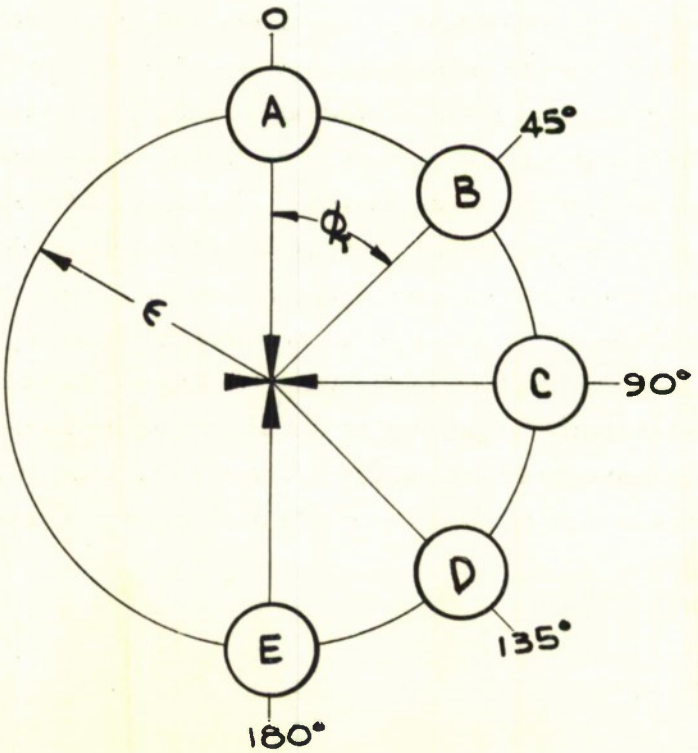

FIG. 3.1-13b

muzzle velocity. Muzzle velocity is assumed to be 1650 ft/sec, miss distance is assumed to be proportional to range and equal to 5 mils, and the initial target range is considered a variable with a maximum value of 2000 yards. The miss distance is selected to represent the expected three standard deviation of impact error for uncontrolled projectile flight based on the known performance of recoilless rifles, the accuracy of simple fire control, and the behavior of fin stabilized ammunition. To fully describe LOS angle variation under the specified conditions, the orientation of the miss distance is varied at each of the considered target ranges. The selected impact pattern in the vertical plane of the target is illustrated in Figure 3.1-13b. Impact "A" and impact "E" represent an overshoot and an undershoot, respectively, with no azimuth error. Impact "C" typifies error in azimuth with no ranging error. This impact pattern based on a constant mil error with range is set at three target ranges, 1200 yards, 1600 yards, and 2000 yards, and then the line of sight angle variation with range determined. The results are given in Figures 3.1-14, 3.1-15, and 3.1-16. While the initial target range (and as a consequence the initial target line of sight angle) is different for the three cases, the overall variations of LOS angle are similar. Initially, LOS angle gradually decreases. Then, at 70% to 80% of target range, LOS angle begins to increase and as range-to-go decreases, LOS angle increases more rapidly approaching a 90 degree value that occurs as the projectile passes the vertical plane of the target. For all initial target ranges, the terminal line of sight angles for all trajectories converge as the projectile approaches the target. The significance of this variation with regard to projectile steering is discussed in Section 3.8 System Analysis.

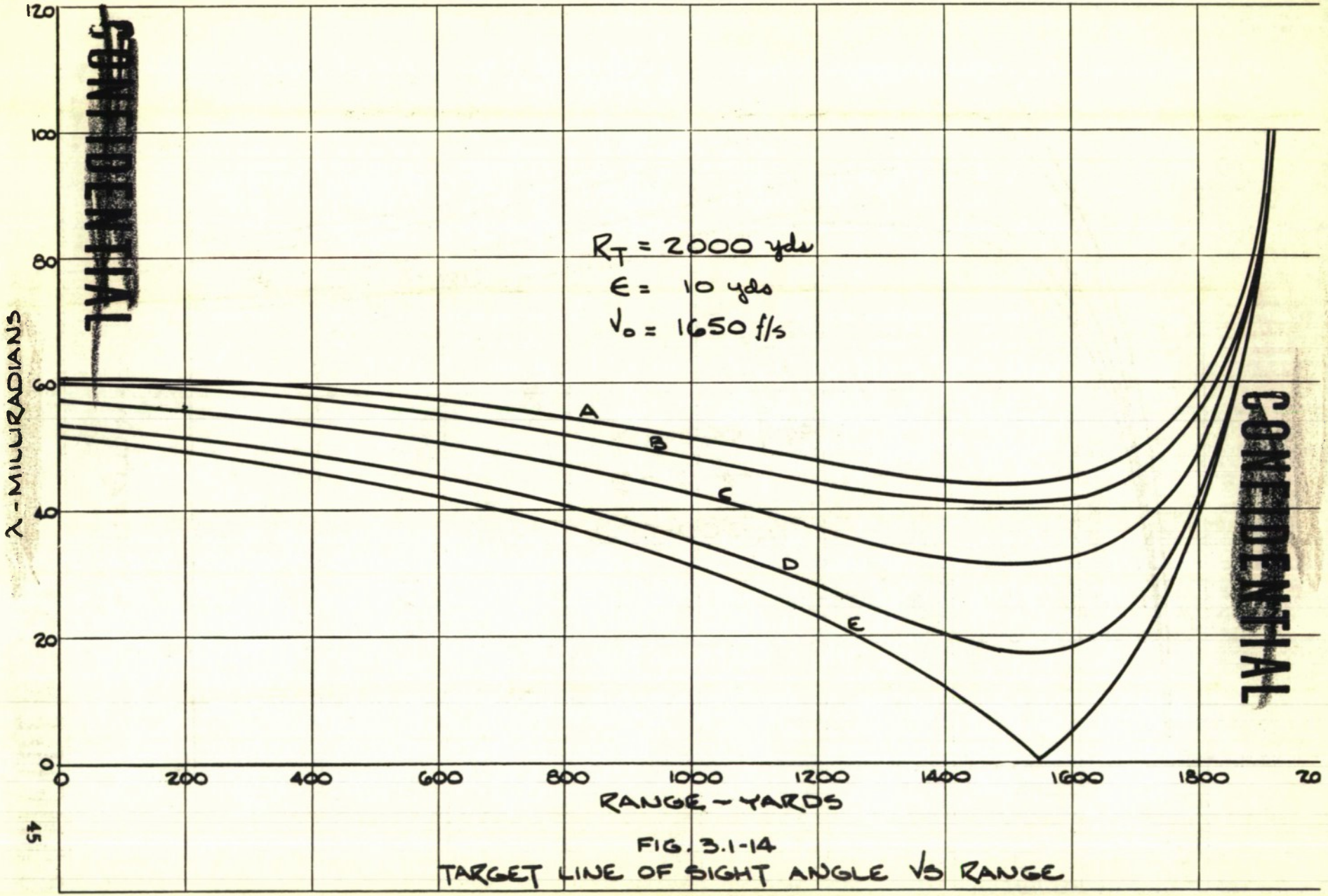

FIG. 3.1-14
TARGET LINE OF SIGHT ANGLE VS RANGE

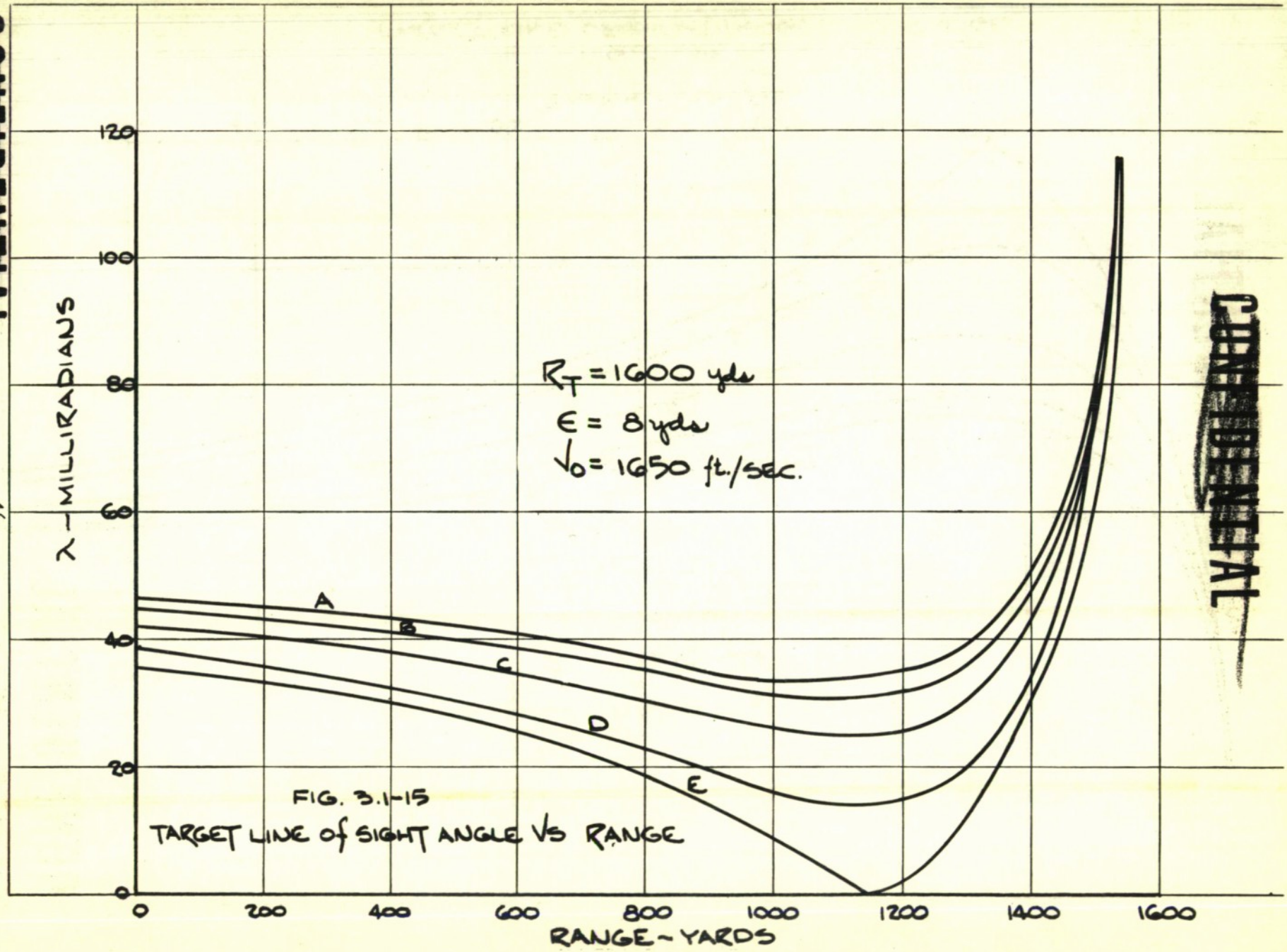

FIG. 3.1-15
TARGET LINE of SIGHT ANGLE VS RANGE

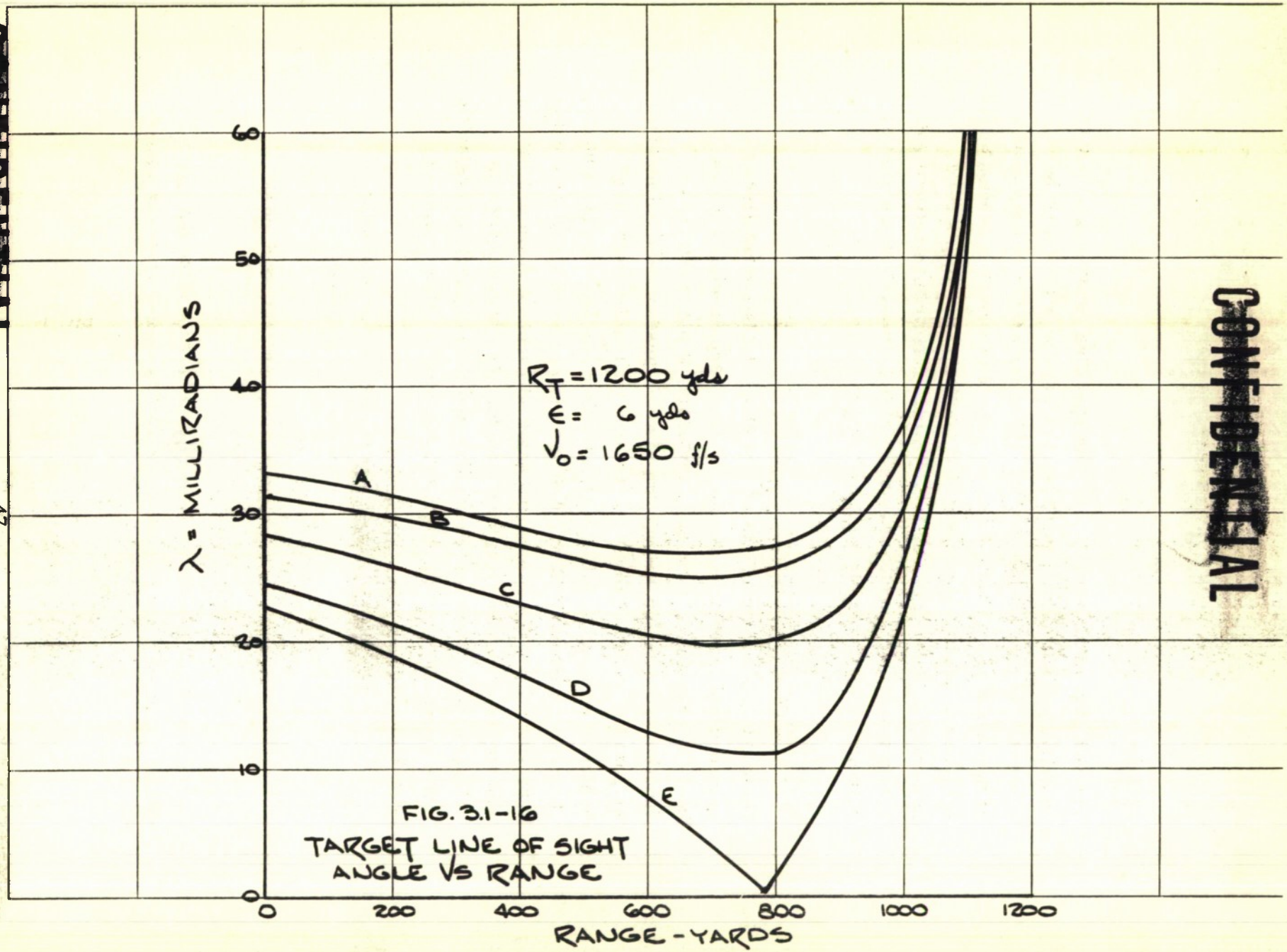

FIG. 3.1-16
TARGET LINE OF SIGHT ANGLE VS RANGE

The variation of target polar for the specified conditions of initial velocity, miss distance, and initial target range is plotted in Figures 3.1-17, 3.1-18, and 3.1-19. Once again the significance of this angle and its variation with regard to seeker operation and initiation of control is presented in Section 3.8. At this point, however, it is noted that in the terminal phase of projectile flight, the magnitude of target polar angle for a given orientation of miss distance is the same for all initial target ranges.

3.1.4 Projectile Dynamics

Up to this point the projectile flight characteristics relative to guidance and control requirements have been developed on the basis of zero angle of attack. Obviously, if the seeker is to function properly the assumption of $\alpha = 0$ must be realized insofar as possible in actual flight. If the projectile possesses large angles of attack it is difficult to formulate any steering law whereby the seeker can initiate control at the desired point along the trajectory since the seeker measured angle will include angle of attack and not the true trajectory error angle. As a consequence an effort is made to analyze the source and the magnitude of projectile angle of attack. The conditions that induce in-flight angles of attack include;

(1) trajectory curvature due to gravity
(2) initial disturbances at launch
(3) winds or gusts
(4) fin or body malalignments and mass asymmetries

Several of these conditions are analyzed to determine the magnitude of the transient angles of attack as well as steady state magnitudes.

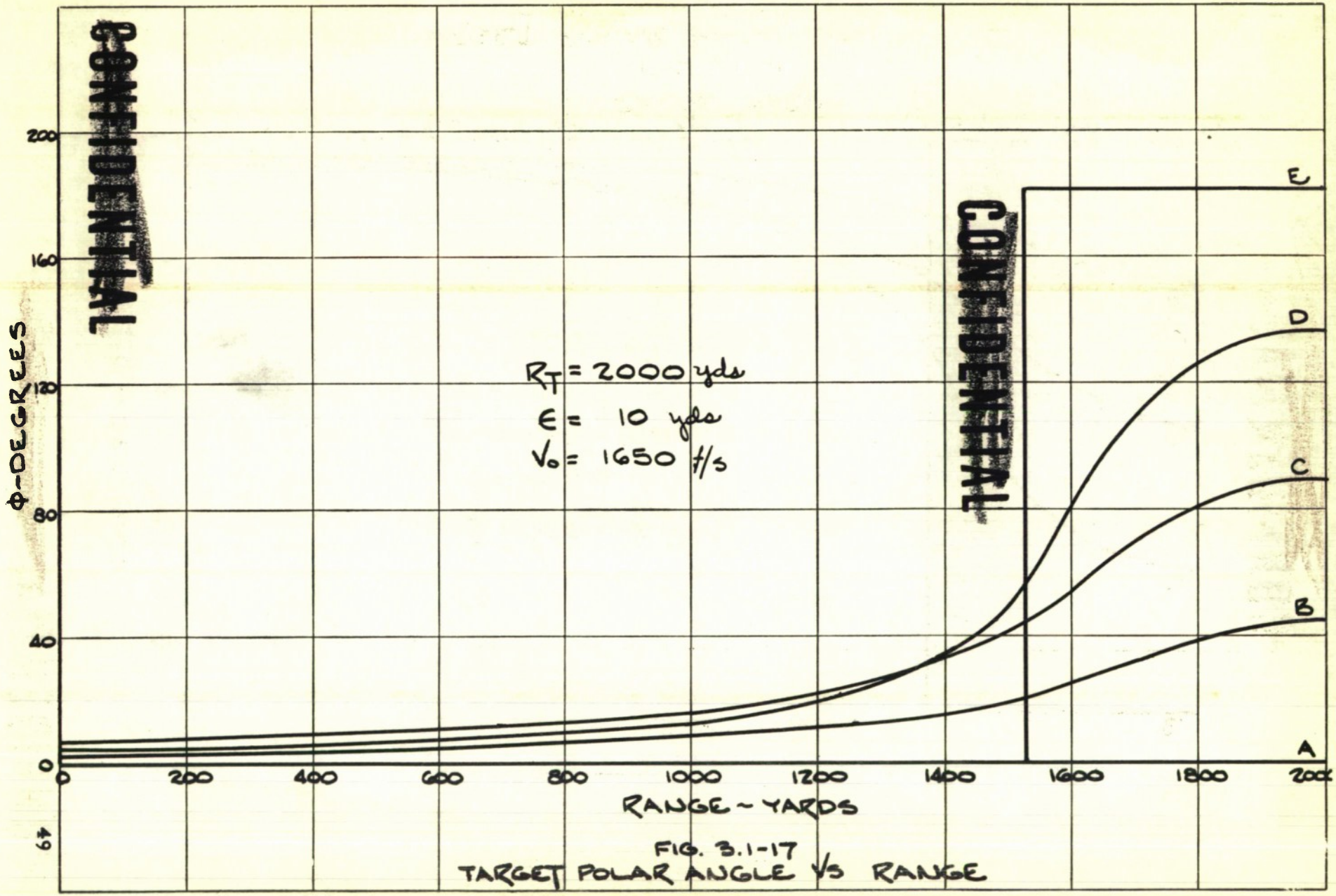

FIG. 3.1-17
TARGET POLAR ANGLE V/S RANGE

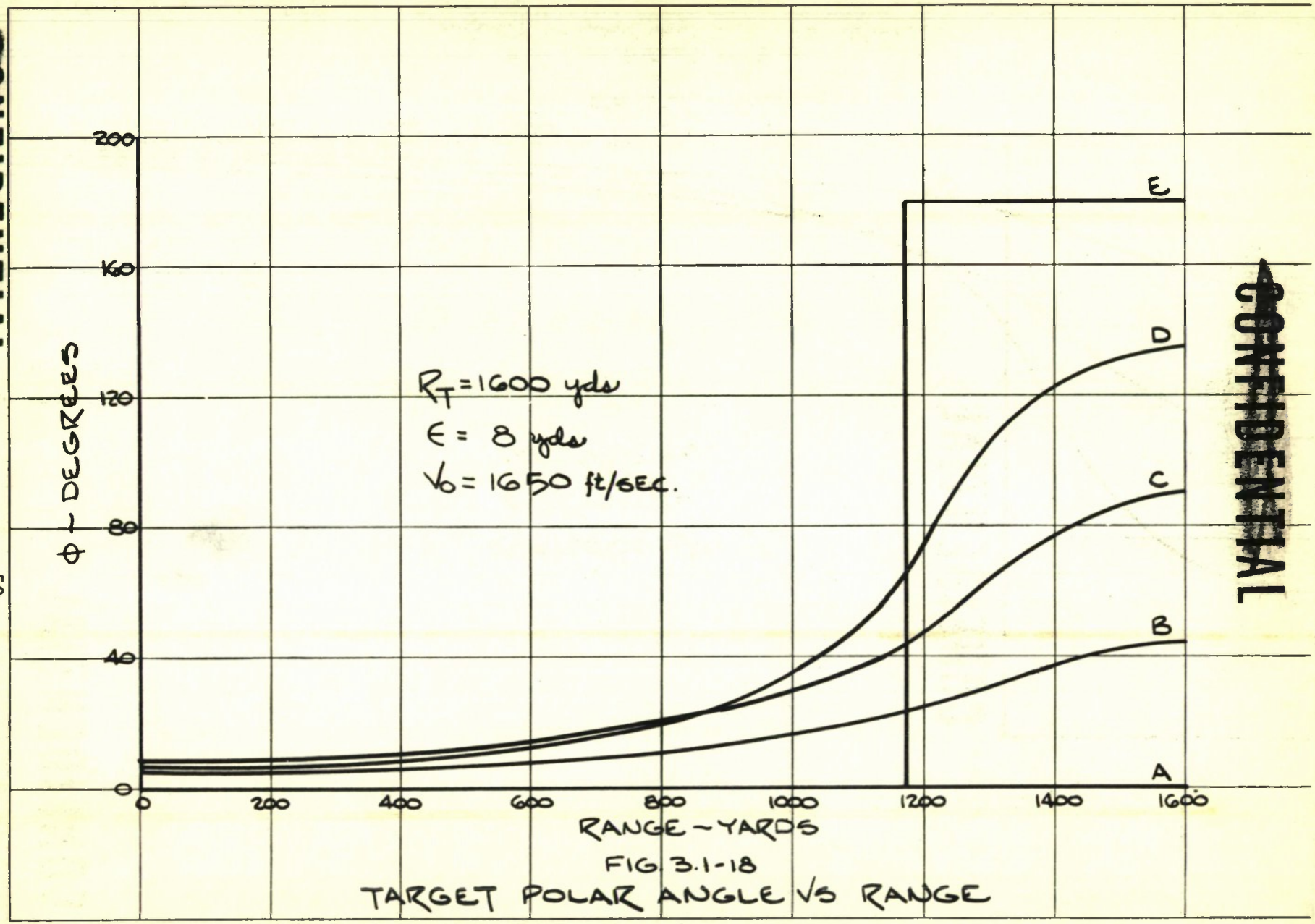

FIG. 3.1-18

TARGET POLAR ANGLE VS RANGE

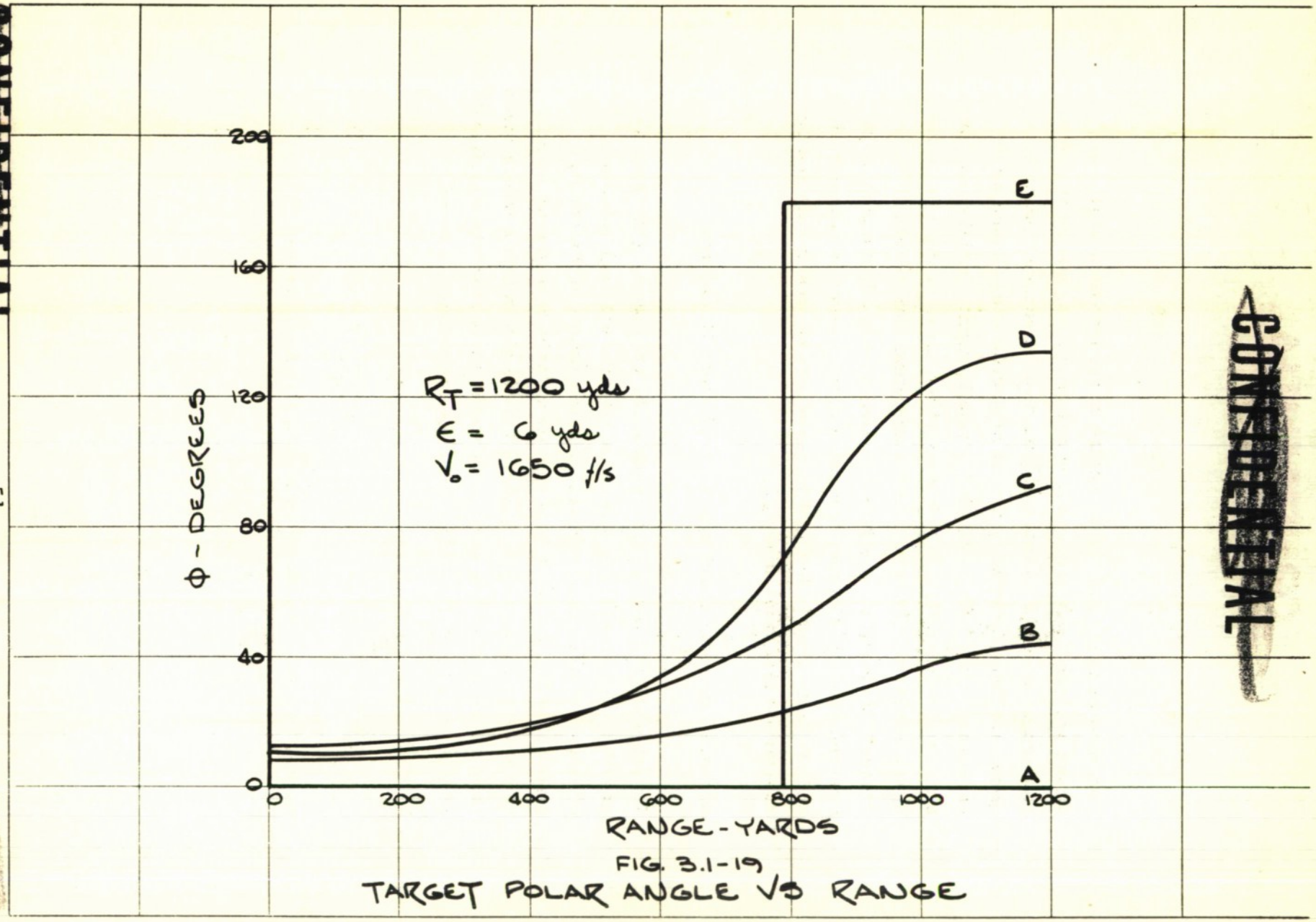

FIG. 3.1-19

TARGET POLAR ANGLE VS RANGE

For conditions (1) and (2) the nature of the transient angles of attack are critical whereas for winds or malalignments the steady state angle of attack is more significant. A second, but no less important consideration is that of projectile cross-coupling or resonance. The effects of wind, malalignment, initial conditions, etc. can be controlled so that a specified limit on angle of attack is not exceeded. However, if the conditions for resonance are present, then angles of attack are subject to such extreme amplifications that satisfactory operation of the seeker is not possible and, in fact, projectile flight in general is adversely affected by substantial increases in drag.

3.1.4.1 Angle of Attack Due to Trajectory Curvature

Trajectory curvature in the vertical is, of course, generated by gravity. This curvature induces a steady state angle of attack often called the yaw of repose. The magnitude of the steady state angle is a function of projectile velocity, projectile stability, and projectile damping-in-pitch. This is shown below where steady state angle of attack is derived approximately from the equations of motion in the vertical plane for the conditions $\alpha = 0$ and $\cos\alpha = 1.0$.

$$I_y\ddot{\theta} = C_{M_\alpha}\, qSd\ \alpha + (C_{M_q} + C_{M_{\dot{\alpha}}})\frac{qSd^2}{2V}\dot{\theta} = 0 \qquad (1)$$

$$mV\dot{\theta} = C_L\, qS - W \qquad (2)$$

Combining and simplifying equations (1) and (2) gives

$$\alpha_{ss} = \left[\frac{C_{M_q} + C_{M_{\dot{\alpha}}}}{C_{M_\alpha}}\right]\frac{gd^2}{2V} \qquad (3)$$

To obtain the transient solution for angle of attack, it is assumed that the projectile leaves the gun with the following initial conditions;

$$\alpha_o = \dot{\alpha}_o = 0$$

$$\theta_o = \dot{\theta}_o = 0$$

$$\gamma_o = 0$$

The effect of gravity is represented, then, as a step function in $\dot{\gamma}$. The solution for α is of the following form;

$$\alpha(t) = \alpha_{ss} \left\{ 1 + Be^{-\mu t} (\sin wt + \beta) \right\} \qquad (4)$$

where $B = 378$

$\mu = 1.92$

$\beta = 1.51$

Based on the aerodynamic coefficients given in Figure 3.1-1, the time history of angle of attack due to gravity is given in Figure 3.1-20. It is apparent that the only significant angles of attack occur during the initial phases of flight where maximum amplitude is somewhat less than 1.0 mil.

Damping is sufficient such that by the time the projectile has traveled 600 yards the transient angle of attack has decayed to 1/10 amplitude. It may be noted that the steady state angle of attack increases with time. However, its maximum value at maximum target range is insignificant; on the order of 0.1 mils.

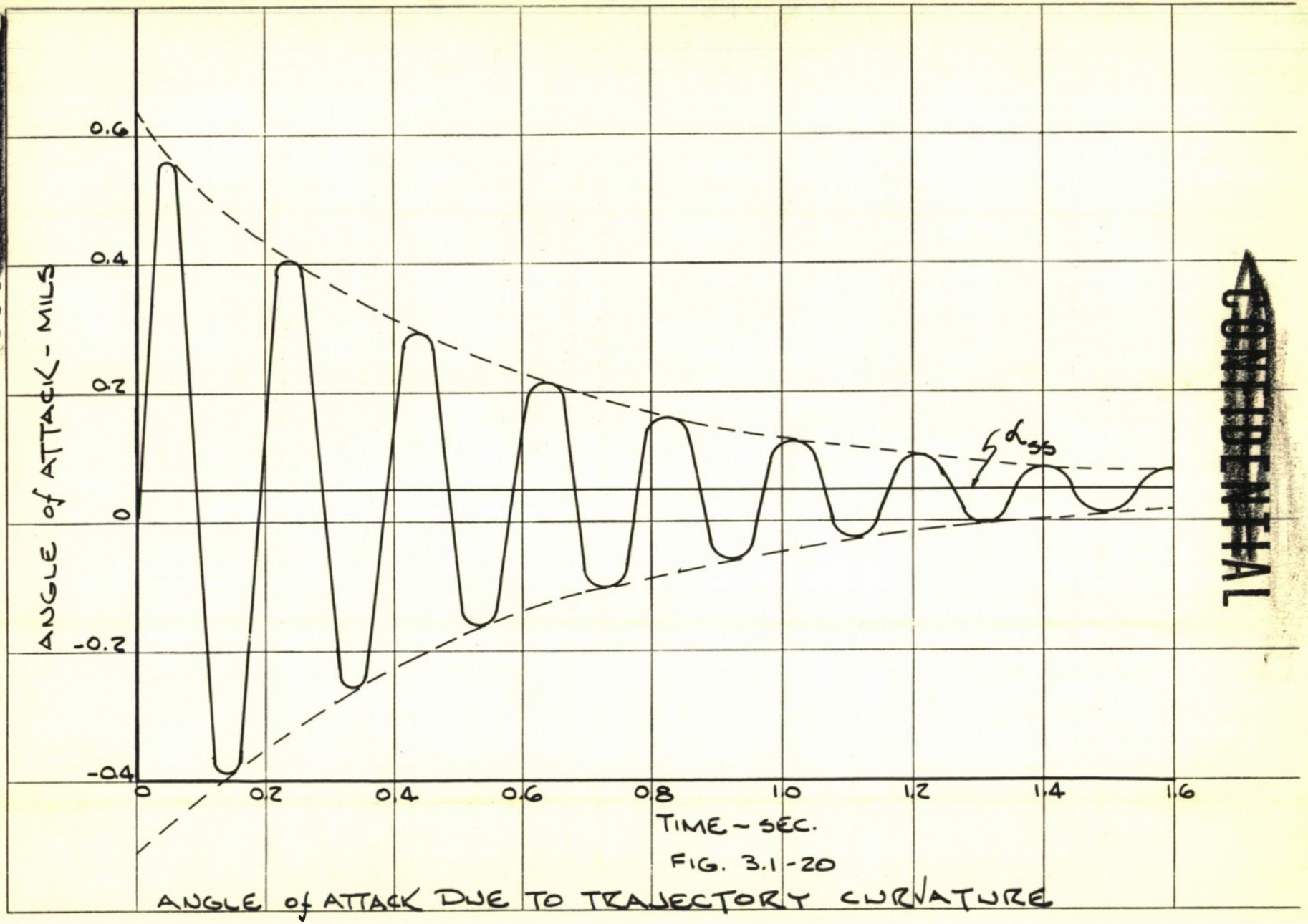

FIG. 3.1-20

ANGLE of ATTACK DUE TO TRAJECTORY CURVATURE

3.1.4.2 Angle of Attack Due to Initial Disturbance

On leaving the gun tube the projectile is subjected to disturbances which generate projectile pitching motion and/or projectile angle of attack. These effects can be attributed to muzzle blast or barrel whip. In either case, the projectile is influenced for only a short time in which case the angular displacement or angular rotation can be treated as an impulse. This was done in a previous analysis presented in Reference 50, wherein the effects of initial pitching rate (θ_o) and initial angle of attack (α_o) on the flight of the test projectile were examined. The same analysis is performed for the POLCAT Configuration using the coefficients given in Figure 3.1-1. The initial disturbance is assumed to be in the form of an initial angle of attack of 1.0 degrees. This estimate is based on the results of the muzzle blast investigations presented in References 32 and 33. Relative to the POLCAT projectile the time history of angle of attack for the specified conditions is expressed by equation (5).

$$\alpha(t) = \alpha_o e^{-1.92\,t} \sin(32.4\,t + 1.51), \text{ deg} \qquad (5)$$

where $\alpha_o = 1^o$

The nature of angle of attack variation is shown in Figure 3.1-21 where it may be noted that maximum angle of attack decreases to .15 degrees or 2.5 mils at a range of 500 yards from the gun.

It is concluded that initial disturbances at launch will not hamper seeker operation provided the seeker is not required to function during the initial phase of projectile flight. The final design of the gun and the projectile must incorporate those means to minimize

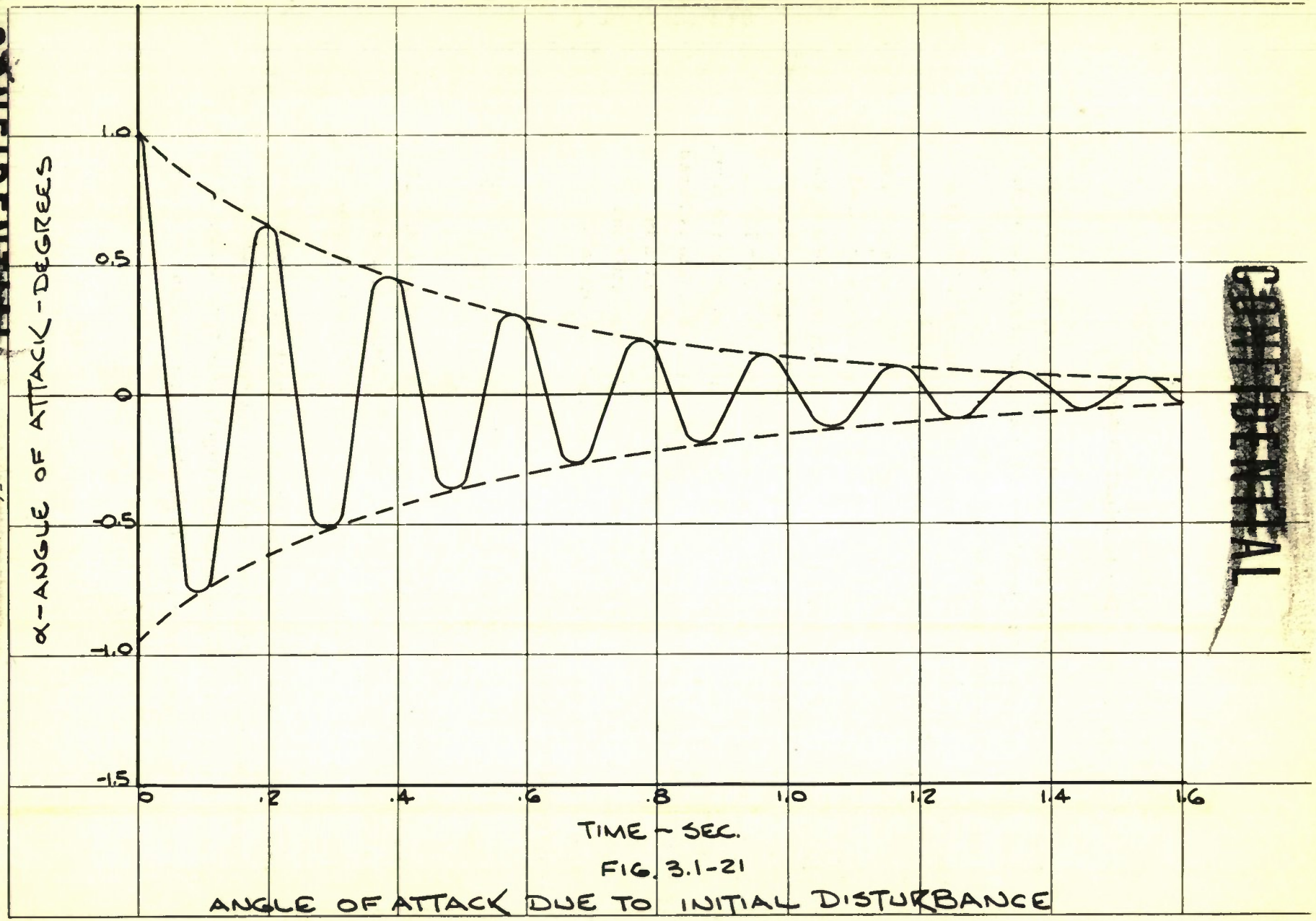

FIG. 3.1-21

ANGLE OF ATTACK DUE TO INITIAL DISTURBANCE

the initial disturbances. Up to this point the POLCAT effort has not included an analysis of sufficient sophistication whereby more specific recommendations could be made.

3.1.4.3 Effect of Wind on Angle of Attack

A detailed analysis of the effect of wind on projectile flight was presented early in the POLCAT effort. See Reference 1. It was shown that a projectile possessing a reasonable static margin (≈ 1.0 caliber) exhibited high flight path stability when subjected to a crosswind. However, as a result of its high flight path stability, the projectile had poor attitude stability. This is typified by a projectile weathercocking into the wind with no change in the direction of center-of-gravity motion. As a consequence a steady state angle of attack is induced and is proportional to the magnitude of the crosswind. Unquestionably a high trim angle of attack could serve to confuse the seeker and preclude intelligent utilization of control. The immediate analysis presents the steady state response of the POLCAT projectile to wind and, then, indicates the means that might be used to reduce steady state angle of pitch. The transient response of the projectile is not discussed here in that the projectile damping characteristics have been established in the preceding discussion.

For the purposes of this discussion it is assumed that the projectile is moving at constant velocity (V) and that flight path angle (γ), pitch angle (θ), and angle of attack are zero at the instant of the application of a crosswind (v). The wind is introduced as a step change in angle of attack where $\alpha_o = v/V$. The equations of motion are;

$$\ddot{\theta} + A\alpha + B\dot{\theta} = 0$$
$$\dot{\gamma} - D\alpha = 0$$
$$\theta = \alpha + \gamma$$

where $A = -\dfrac{C_{M_\alpha}\, qSd}{I_y}$

$$B = -\frac{(C_{M_q} + C_{M_{\dot{\alpha}}})\, qS\, d^2}{2VI_y}$$

$$D = \frac{C_{L_\alpha}\, qS}{m\, V}$$

The steady solution for the initial conditions $\alpha = \theta = \gamma = 0$ at $t = 0$ is given below.

$$\alpha\,(t \longrightarrow \infty) = -\alpha_o \tag{6}$$

$$\theta\,(t \longrightarrow \infty) = -\frac{A\alpha_o}{A+BD} \tag{7}$$

$$\gamma\,(t \longrightarrow \infty) = \frac{BD\alpha_o}{A + BD} \tag{8}$$

To illustrate the wind effect, the following conditions are assumed:

(1) crosswind (v) equals 25 ft/sec.

(2) projectile velocity equals 1650 ft/sec.

(3) projectile stability (C_{M_α}) is varied while damping and lift remain constant.

As a consequence the solutions, given in equation 7 and 8, contain the variable coefficient A. Figure 3.1-22 illustrates the influence of the extremes of projectile stability on flight in wind. In the aerodynamic design of the projectile, there is a choice of providing high flight path stability ($\gamma_{ss} \approx 0$) with a large static margin or providing high attitude stability ($\theta_{ss} \approx 0$) with a low static margin. For the specific initial conditions and with the POLCAT aerodynamic coefficients the magnitude of the steady state quantities are shown in Figure 3.1-23.

This figure also indicates the effect of installing a small rocket sustainer motor in the projectile. Providing the projectile with longitudinal

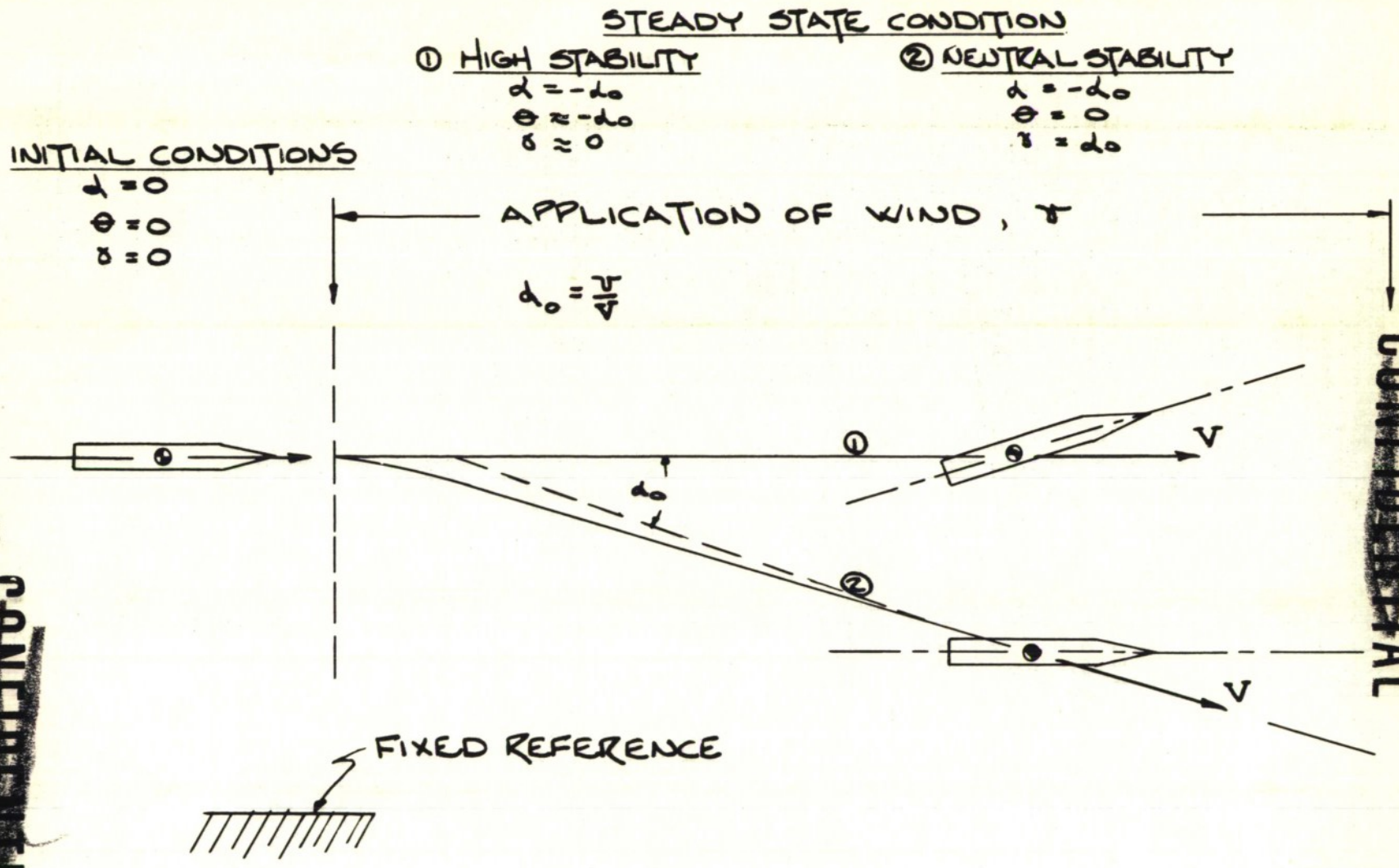

FIG. 3.1-22

EFFECT OF WIND ON PROJECTILE FLIGHT

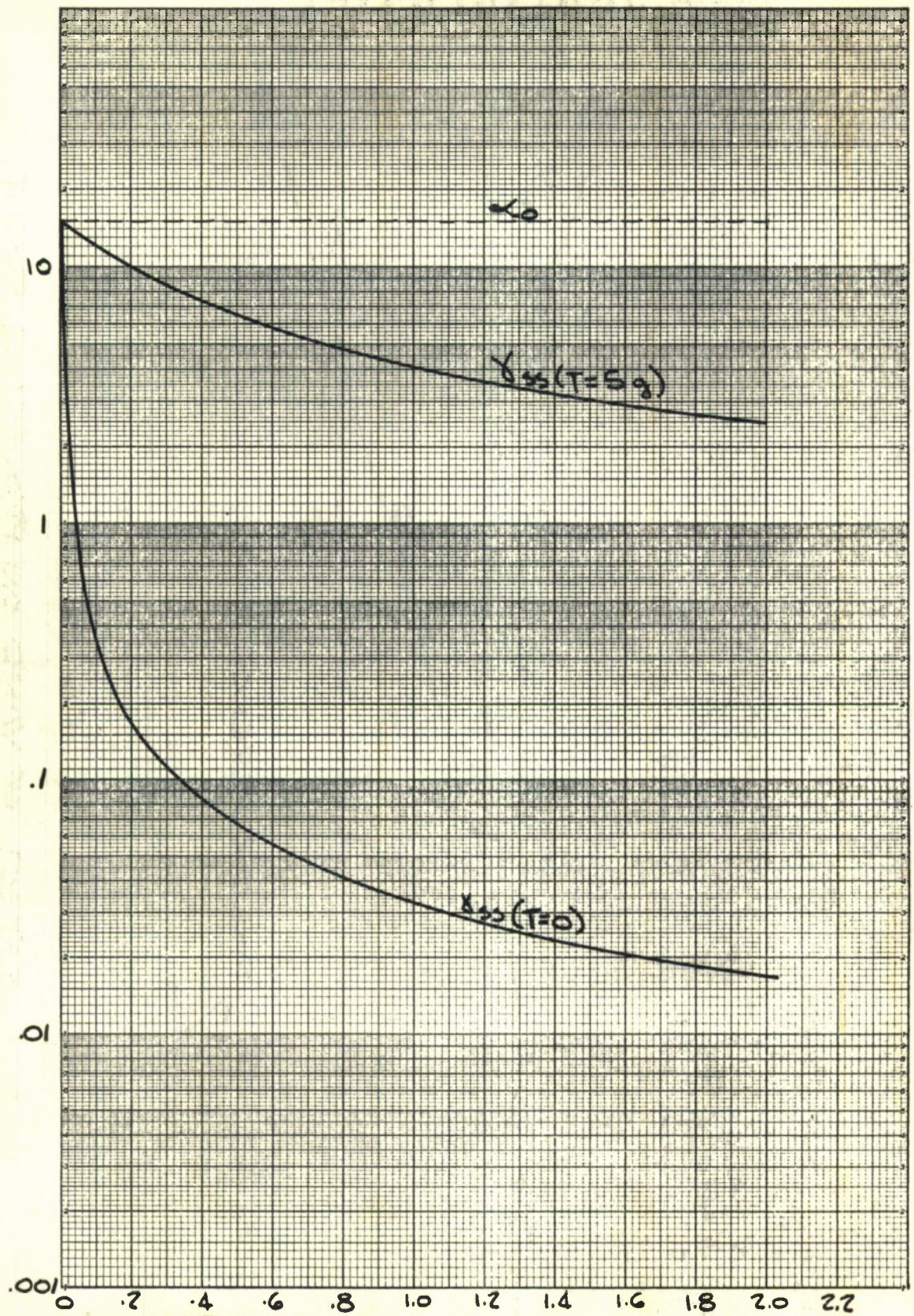

FIG. 3.1-23

EFFECT OF VARIABLE STATIC MARGIN IN WIND CONDITION

thrust is a means for increasing attitude stability at all static margins. Since a trim angle of attack exists in the wind condition it is essential to optimize projectile design for minimum miss distance by establishing the most desirable static margin. This analysis, however, can be conducted only after the magnitude and frequency of crosswinds are established.

3.1.4.4 Effect of Aerodynamic Malalignment and Mass Asymmetry on Angle of Attack

Since malalignments and mass asymmetry are primarily dependent on manufacturing tolerances, it is the objective of the immediate discussion to establish, if possible, reasonable accuracy requirements for projectile fabrication so that satisfactory flight characteristics are assured. Even at this stage of weapon system planning, practical airframe design consists of working with practical manufacturing tolerances. Hence, the requirements on malalignment and asymmetry are guided to some extent by past experience in the fabrication of fin stabilized ammunition. Fortunately, the opportunity was afforded whereby ammunition of this type could be examined. Early in the POLCAT program sixty T184 projectiles were delivered to the Bulova Research and Development Laboratories to be modified for flight test. Before the modification was begun, samples were taken from the shipment and inspected for tail fin and boom malalignment and mass asymmetry. The results of the inspection, presented in Reference 51, indicate both quantities to be exceedingly small. The maximum resultant malalignment of the fins and boom was approximately 0.1 degrees. This result does not agree with the earlier findings of B. G. Karpov of BRL which indicated the malalignments of fin stabilized ammunition to be substantially higher. However, it is believed that the lower malalignments are the result of using better

materials and techniques. In addition to establishing the magnitude of fin malalignments and their effects, the investigations of Reference 37 indicated the extent of fin damage incurred at launch. However this is considered in the structural design of the POLCAT projectile so that this will not be a source of malalignment. Upon consideration of the foregoing and accounting for the aerodynamic characteristics, stability and tail effectiveness, it is estimated that the malalignment will not induce projectile trim angles of attack greater than 10 mils. Since the seriousness of aerodynamic malalignments or mass asymmetries occur in a rolling condition, the remainder of this section is concerned with this condition.

A complete analysis of the roll resonance phenomena is presented in Reference 2. This analysis established a criterion for determining permissible roll rates and, in particular, described the motion of a rolling projectile in the presence of malalignments and asymmetries. At this point, the results are summarized and applied to the POLCAT projectile. In addition to the aerodynamic notation given previously, the following notation is used for the three dimensional analysis.

B	angle of yaw
M'	malalignment moment
ζ	angle between the principal axis and the roll axis which constitutes mass asymmetry

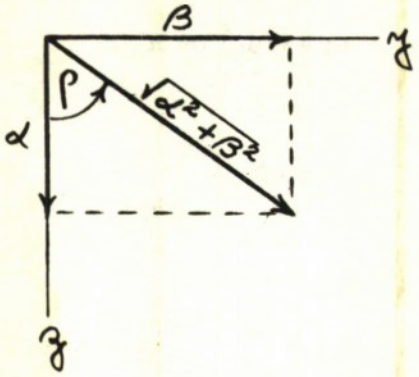

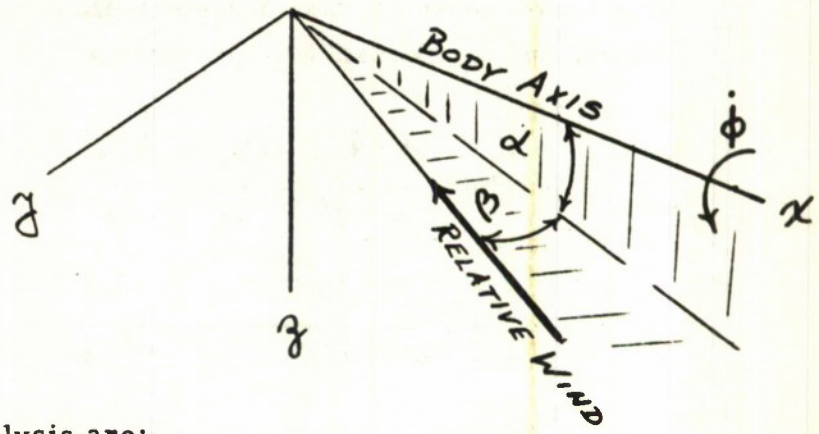

The assumptions of the analysis are;

(1) Velocity and roll rate are constant.

(2) Gravity is neglected.

(3) Mass asymmetry is in the form of a small angle between the principal axis and the roll axis in the pitch plane. The products of inertia $I_{yx} = I_{zy} = 0$, the asymmetry is expressed as $\delta = I_{xz}/I_z$.

(4) With the exception of the malalignment moment (M') in the pitch plane, 90° rotational aerodynamic symmetry exists.

With these assumptions and making use of simplifications such as $I_y = I_z \gg I_x$ and $A + BD \approx A$, the equations of motion are given below.

$$\ddot{\alpha} + (B + D)\,\dot{\alpha} + (A - \dot{\phi}^2)\,\alpha + 2\dot{\phi}\dot{\beta} + (B + D)\dot{\phi}\beta = \frac{M'}{I_y} - \delta\dot{\phi}^2$$

$$\ddot{\beta} + (B + D)\,\dot{\beta} + (A - \dot{\phi}^2)\beta - 2\dot{\phi}\,\dot{\alpha} - (B + D)\,\dot{\phi}\,\alpha = 0$$

$$A = -\frac{C_{M_\alpha}\, qSd}{I_y} \qquad B = -\frac{C_{M_q} + C_{M_{\dot{\alpha}}}\, qSd^2}{2\,V\,I_y} \qquad D = \frac{C_{L_\alpha}\, qS}{mV}$$

The steady state solution of the equations of motion assuming α_o = const. and β_o = const. are given below.

$$\alpha_o = \frac{(A - \dot{\phi}^2)(M'/I_y - \zeta\dot{\phi}^2)}{(A - \dot{\phi}^2)^2 + (B + D)^2\dot{\phi}^2} \tag{9}$$

$$\beta_o = \frac{(B + D)\dot{\phi}(M'/I_y - \zeta\dot{\phi}^2)}{(A - \dot{\phi}^2)^2 + (B + D)^2\dot{\phi}^2} \tag{10}$$

Since $M' = M_\alpha \alpha_m$ where α_m is the steady state, trim angle induced by malalignment for a non-rolling projectile, the resultant angle can be expressed as;

$$\sqrt{\alpha_o^2 + \beta_o^2} = \frac{\frac{\alpha_m}{m}A - \zeta\dot{\phi}^2}{\sqrt{(A - \dot{\phi}^2)^2 + (B + D)^2\dot{\phi}^2}} \tag{11}$$

The direction of the resultant angle relative to missile axes is given in equation 12.

$$\tan\rho_o = \frac{\beta_o}{\alpha_o} = \frac{(B + D)\dot{\phi}}{A - \dot{\phi}^2} \tag{12}$$

By maximizing resultant angles with respect to roll rate in equation 11, an approximation for the roll resonance condition is obtained.

$$\dot{\phi}_{res} = \sqrt{A} = \sqrt{\frac{M_\alpha}{I_y}} \approx w_\theta \tag{13}$$

The amplification of angle of attack with roll rate for aerodynamic malalignment is obtained from equation 11 by setting $\zeta = 0$. The results are plotted in Figure 3.1-24. The effect of mass asymmetry

on resultant angle of attack is derived from equation 11 with $\alpha_m = 0$ and the result is illustrated in Figure 3.1-25. Both cases are examined at M = 1.2 with the aerodynamic coefficients at this speed taken from Figure 3.1-1. The magnitude of resultant angle for malalignment is based on a zero roll rate trim angle of attack equal to 10 mils. For mass asymmetry, resultant angle of attack variation with roll rate is expressed non-dimensionally in terms of the angle δ. In either case it is essential that the projectile roll rate does not approach the projectile pitch frequency. To minimize resultant angle due to aerodynamic malalignment, the projectile would be provided with the highest possible roll rate. Conversely, to minimize angle of attack due to asymmetry, zero roll rate would be selected. However, for the POLCAT application, it is necessary for the projectile to possess a high roll rate in order to provide the seeker with a scanning capability. Therefore, projectile spin rate must be greater than pitch frequency. The upper limit on roll rate is established by requirements of shaped charge penetration which decreases rapidly for roll rates over 20 RPS. As a conseqeunce, the region of desirable projectile roll rate is well defined and illustrated in Figure 3.1-26. By controlling initial spin rate with proper rifling and by limiting spin decay by beveling or canting the tail (see References 36 and 37), the necessary conditions for preventing aerodynamic cross coupling, as shown in Figure 3.1-26, can be realized.

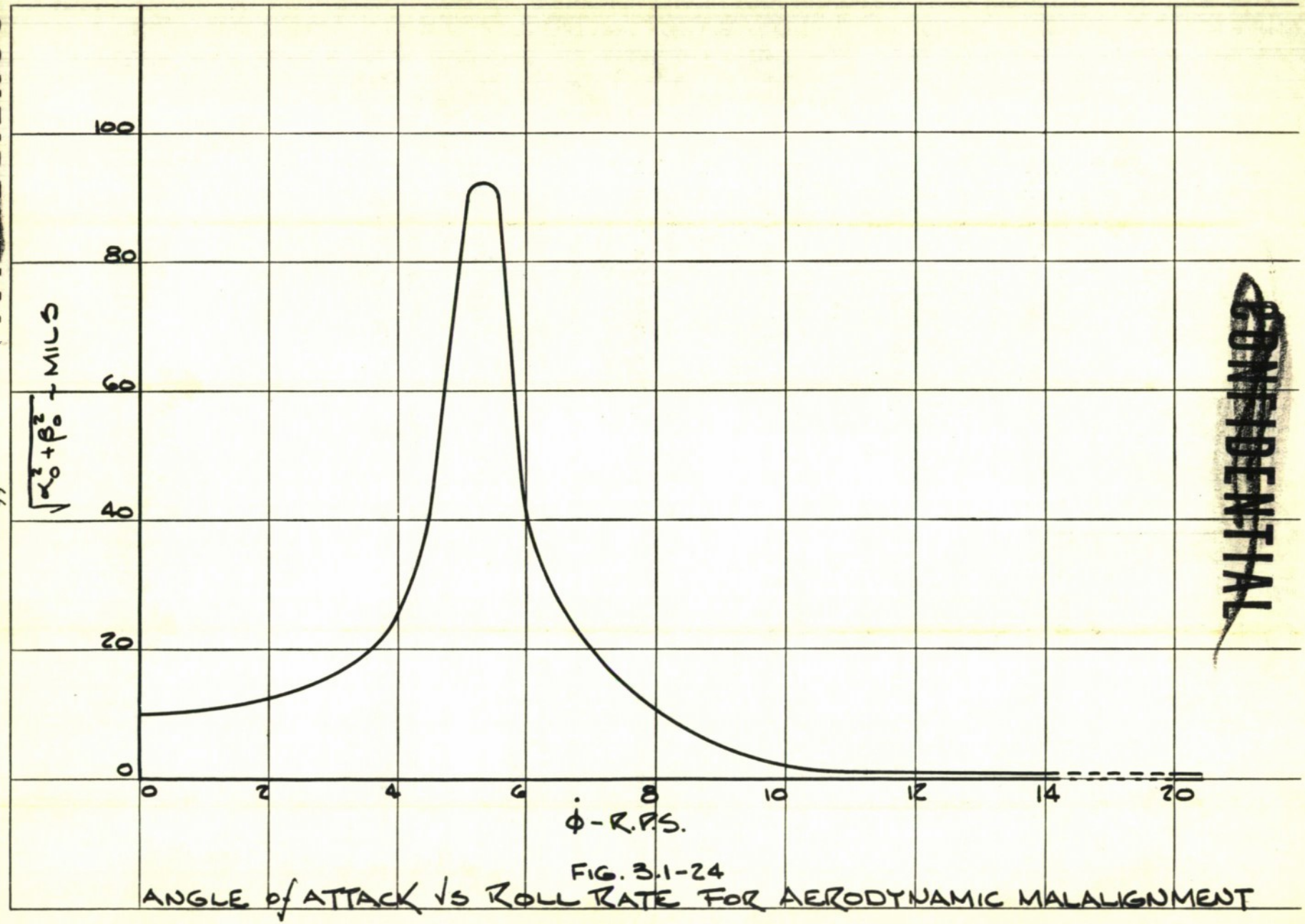

FIG. 3.1-24

ANGLE of ATTACK Vs ROLL RATE FOR AERODYNAMIC MALALIGNMENT

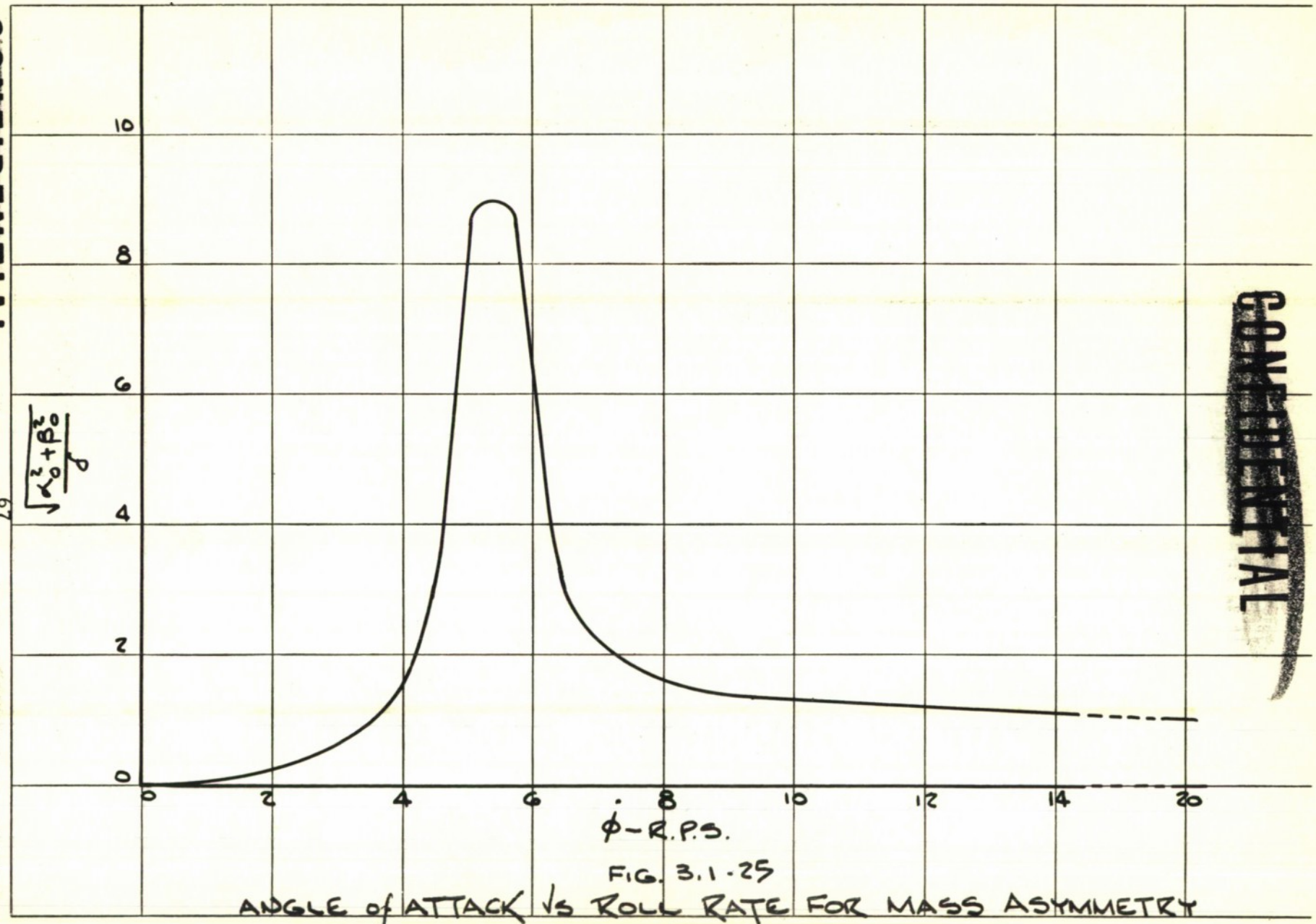

FIG. 3.1-25

ANGLE of ATTACK Vs ROLL RATE FOR MASS ASYMMETRY

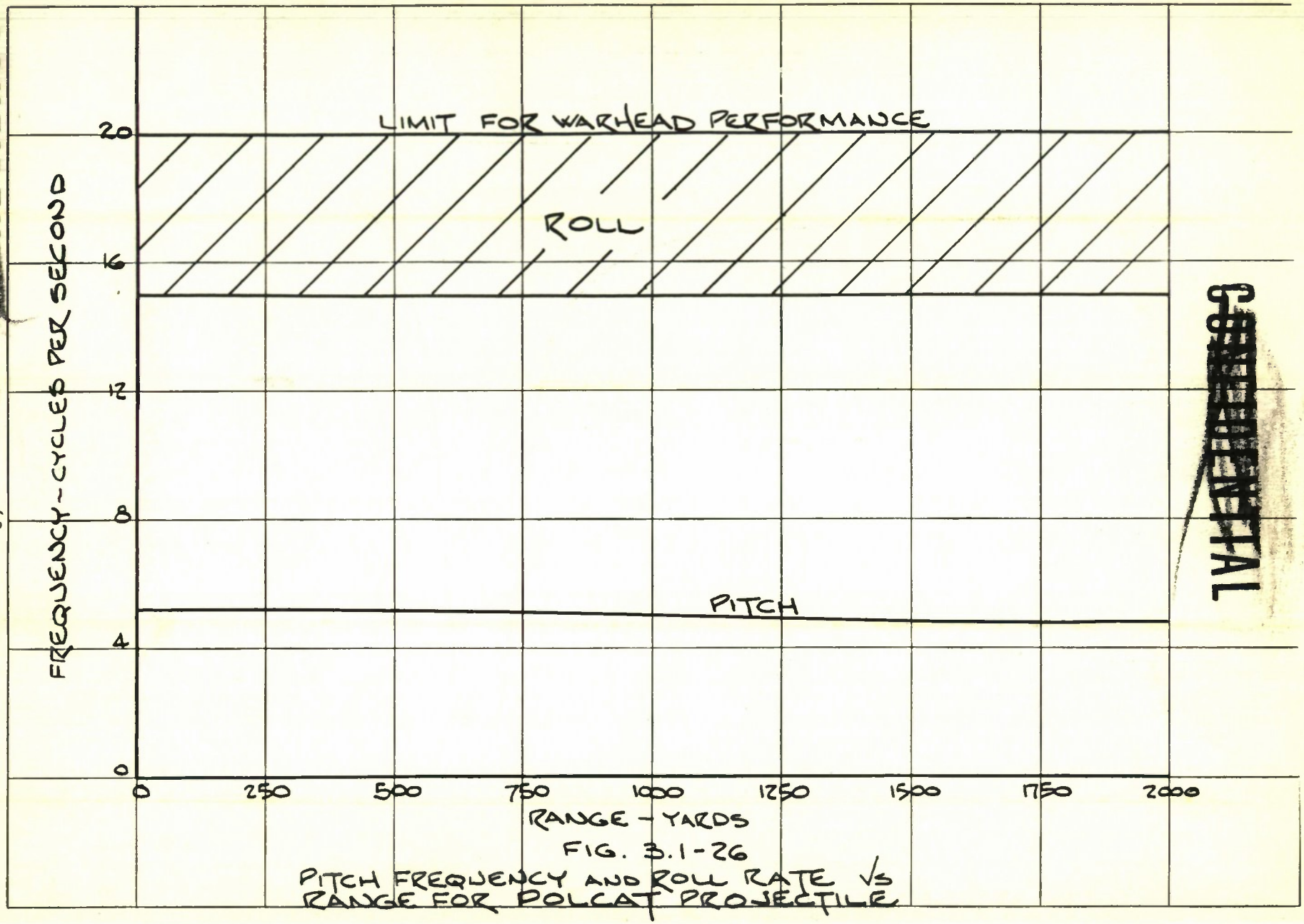

FIG. 3.1-26

PITCH FREQUENCY AND ROLL RATE VS RANGE FOR POLCAT PROJECTILE

3.2 STRUCTURES

This section contains a discussion of the overall structural requirements for the POLCAT projectile. Initially, the loading conditions are presented. Then, the structural configuration of the projectile is given, and the type of construction is discussed. The remainder of the section contains a preliminary load and stress analysis.

The projectile is subjected to three separate types of loads which are considered critical at this time. The first consists of high longitudinal forces which exist during launch. For this condition the projectile must have sufficient structural strength to withstand peak gun pressures and longitudinal set-back effects. In particular the strength of the irdome must be assured during launch. Next, high transverse bending and shearing forces are imposed on the projectile by the c. g. located transverse control impulse.

In addition, the impulse cartridge itself must be capable of withstanding the high local internal pressure to insure delivery of the required impulse to the airframe. Finally, the effect of high aerodynamic pressures on the nose section must be considered.

Dynamic overshoot factors are included in the stress analysis which reflect the dynamic response characteristics of the structural element to the dynamic load condition under analysis.

Sufficient strength must be provided to prevent permanent set which results in body or fin malalignment.

In order to keep weight to a minimum but to insure sufficient strength and rigidity, high strength aluminum and high heat-treat steel are

used wherever feasible. Minimum, but structurally satisfactory wall thickness are utilized to reduce weight.

The basic structural layout of the POLCAT projectile is shown in Figure 3.2-1. The forward portion of the projectile consists of three compact, tubular, sections made of 75 S heat-treated aluminum. These sections house and support the seeker assembly, electronics and power pack assembly, and warhead. The middle portion of the projectile containing the fuze and impulse cartridge sections is made of 4140 steel. The aft section consists of an aluminum conical and cylindrical body section reinforced by four aluminum fins; the fins providing additional stiffness for the tail section.

The results of the stress analysis are given in terms of minimum margins of safety, Table 3.2-1.

Item	Loading Condition	Comments	M.S.
Irdome	Launch	Compression at aft-end of dome	+2.20
Fwd. Body Section	Impulse Control	Bending - Station 15.5	+ 2.87
		Shear - Station 15.5	+ 6.79
	Launch	Compression-Station 15.5	+ 1.78
Tail Section	Impulse Control	Shear - Station 19.5	+11.99
		Bending - Station 19.5	+ 2.36
		Shear - Station 29	+15.01
		Bending-Station 29	+ 1.78
Impulse Cartridge	Impulse Control	Uniform Pressure - Cylinder	+ 0.31
		Uniform Pressure - Flat Plate	+ 0.013

TABLE 3.2-1 : MINIMUM MARGINS OF SAFETY

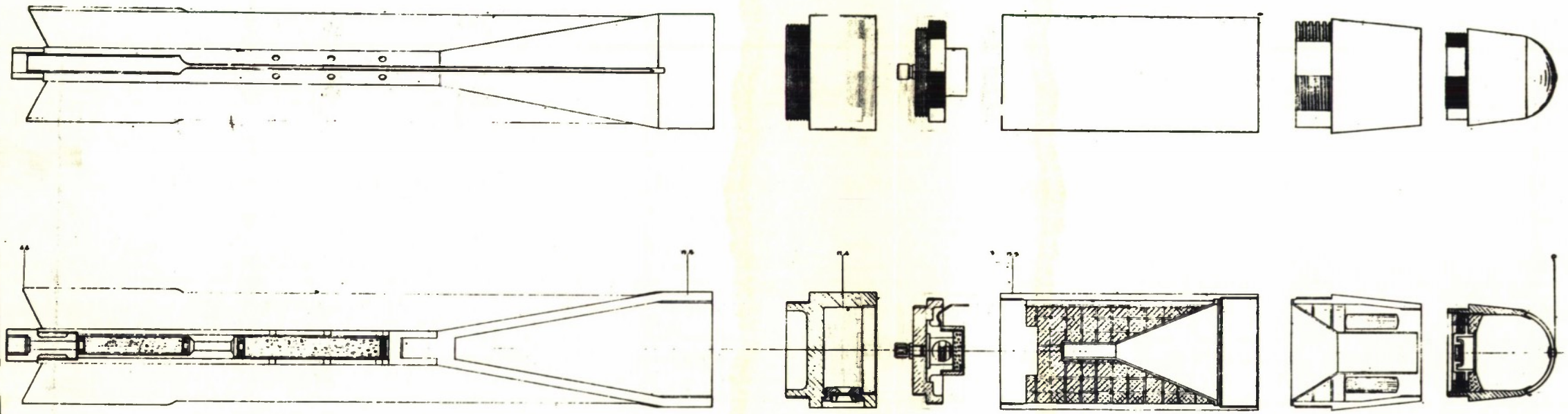

FIGURE 8.2-1
POLCAT MISSILE
SUB-ASSEMBLY BREAKDOWN

3.2.1 Dynamic Overshoot Factor

Since the launching and post-firing transverse impulse loads are applied almost instantaneously, there will be some dynamic overshoot depending on the time duration of the applied load and the period of structural vibration of the projectile. From References (40) and (41) it is seen that the pressure-time variations for the above loading conditions can satisfactorily be approximated by a triangular variation. In Reference (42) the dynamic overshoot factors are determined for a single degree of freedom mass-spring system subjected to a triangular force pulse. The results are summarized in Figure 3.2-2. It is seen that the overshoot is largest when the time duration of the load is equal to the period of vibration of the system. The negative overshoot (rebound after the load is removed) is of interest in the analysis of the seeker dome because of the low allowable stresses.

3.2.2 Load Analysis

The load analysis determines the projectile load distribution for the launching and corrective impulse loading conditions. The loading distribution on the irdome during flight is also determined. The numerical values for the various loading conditions are obtained from References 40, 41 and 43.

Since the loading distribution during launch and after impulse include projectile inertia loads, the weight distribution is determined first. The distribution given in Figure 3.2-3 is based on the projectile weight and balance given in Table 3.2-2. The 1g shear distribution is given in Figure 3.2-4. The shear distribution when multiplied by the appropriate load factor and superimposed with the applied force distribution leads to the determination of the projectile tensions, compressions, shears, and bending moments.

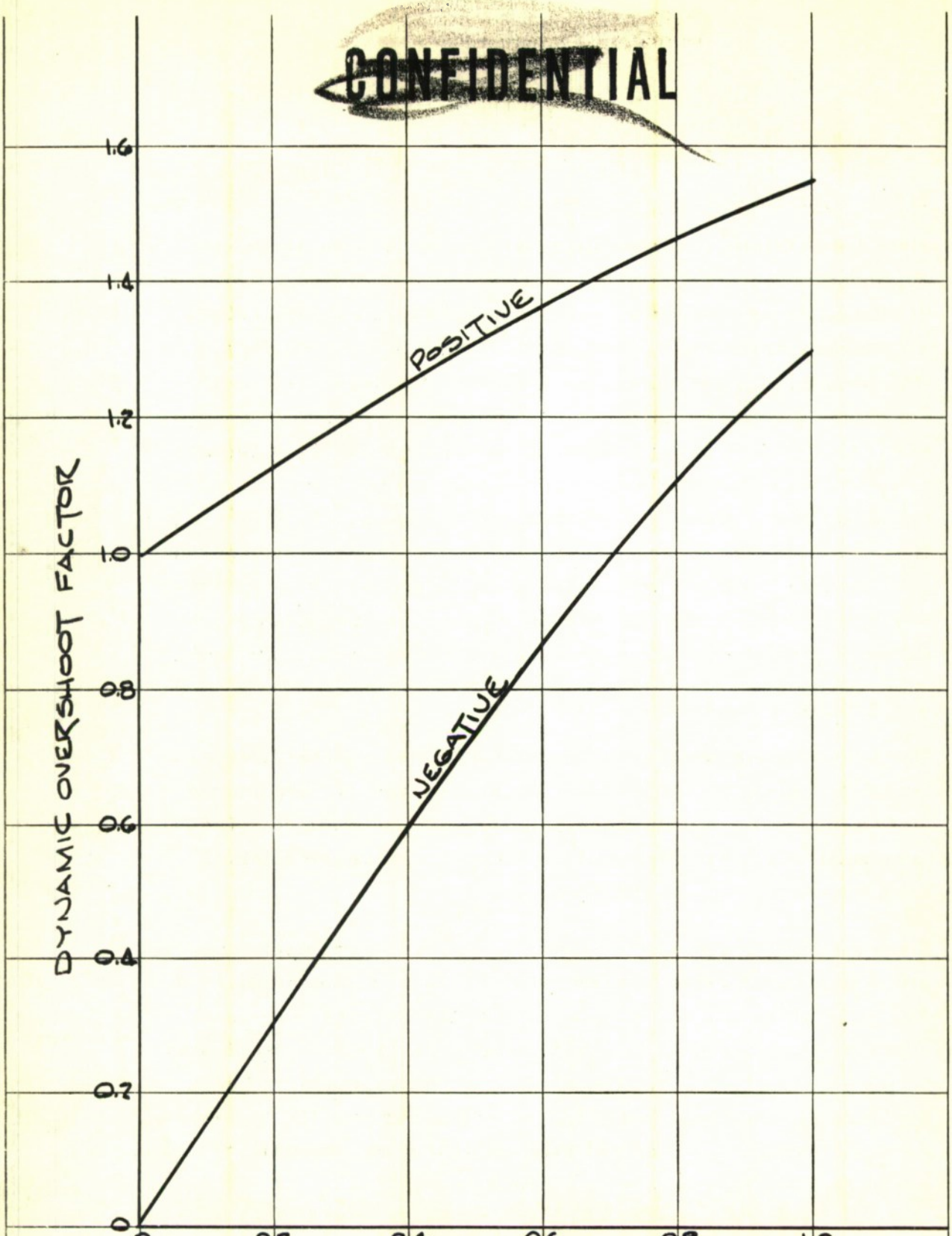

FIG. 3.2-2

DYNAMIC OVERSHOOT FACTORS FOR SINGLE DEGREE of FREEDOM SYSTEM SUBJECTED TO A TRIANGULAR PULSE LOAD

Item	Weight (lb)	Distance from Nose (in)	Moment (in - lb)
1. Dome	.16	.81	.13
2. Nose Section	.30	2.50	.75
3. Mirror Assembly	.23	3.31	.76
4. Batteries	.25	5.0	1.25
5. Potted Electronic Assembly	0.50	6.9	3.45
6. Forward Body Section	2.65	5.9	15.64
7. Shaped Charge Liner	1.11	8.6	9.55
8. Warhead	3.50	12.9	45.15
9. Center Body Section	2.87	11.4	32.72
10. Fuze and Booster	.48	16.0	7.68
11. Rear Conical Body Section	2.06	22.4	46.14
12. Rear Cylindrical Body Section	1.04	36.9	38.38
13. Igniter and Tube	1.45	37.7	54.67
14. Tail Section	1.53	36.94	56.52
15. Cartridge Section	5.18	18.0	93.24
Total	23.40 lbs		406.03 in-lb

C. G. of Round = 17.35 inches from nose

C. G. of Cartridge = 17.43 inches from nose

TABLE 3.2-2 : PROJECTILE WEIGHT AND BALANCE

FIG. 3.2-3
WEIGHT DISTRIBUTION - 18

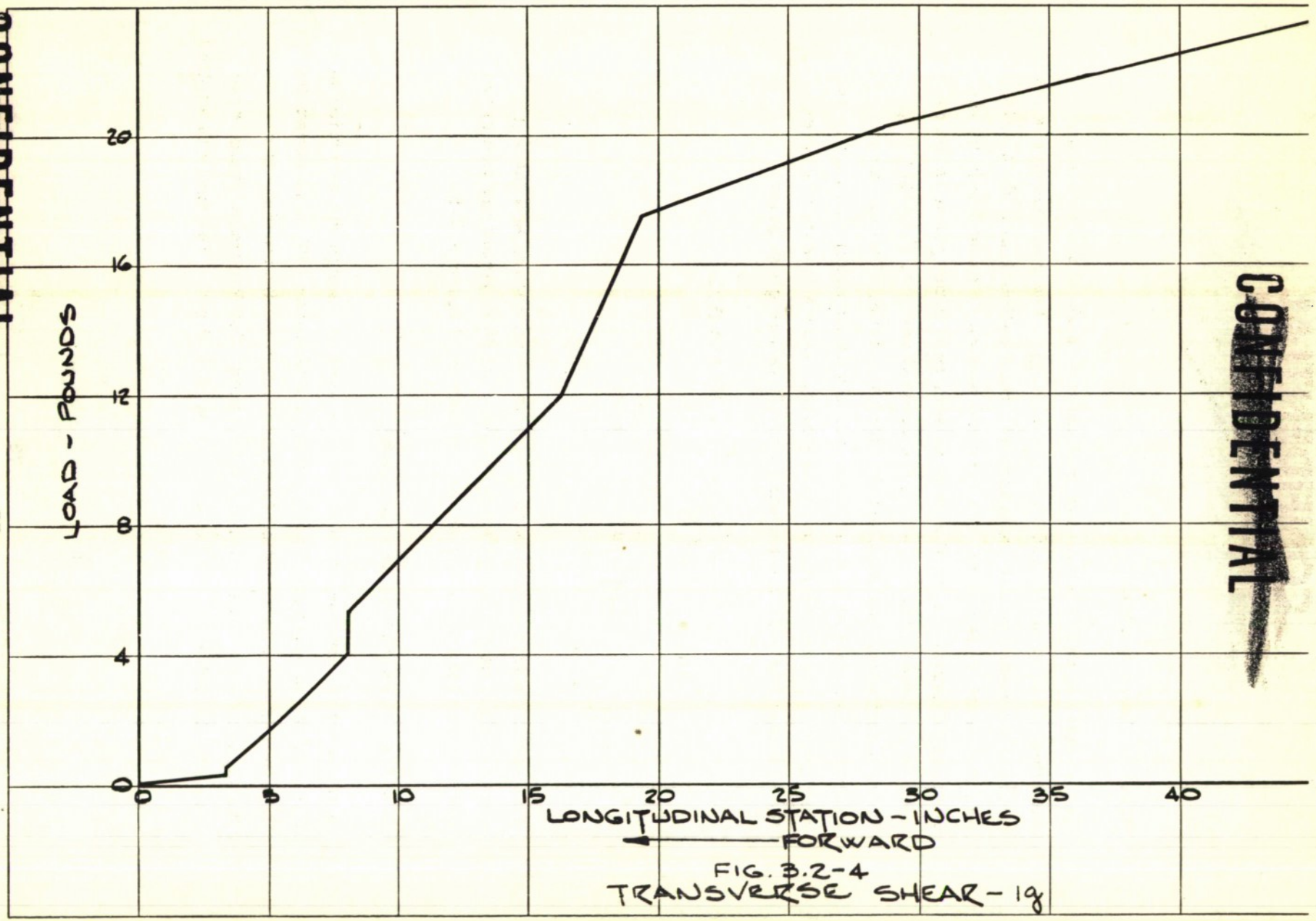

FIG. 3.2-4
TRANSVERSE SHEAR - 1g

3.2.2.1 Launch Loads

The results of the calculations in Section 3.6 show the maximum launching load to be 187,300 lbs (or 8000 g). The gun tube pressure acts on the rear conical body section, rear cylindrical body section, and tail section. However, the forward motion is caused only by the pressure distribution on the conical section. If the gun tube pressure is assumed constant along the conical section, the launching force distribution varies linearly along the cone. The maximum radius of the cone at sta. 19.5 is four times its minimum radius at sta. 29.0. Hence the launch load (lb/in.) varies linearly between the two stations with the forward and aft values given below.

$$q_{\dagger_{19.5}} = \frac{2(187,300)}{(29-19.5)} \times \frac{4}{5} = 31,550 \text{ lb/in}$$

$$q_{\dagger_{29.0}} = \frac{1}{4} q_{\dagger_{19.5}} = 7890 \text{ lb/in}$$

The superposition of the loading system given above, and the 1 g shear distribution multiplied by a factor of 8000 yields the maximum longitudinal load distribution during launch, Figure 3.2-5.

3.2.2.2 Transverse Impulse Loads

A transverse impulse of 35 lb-sec. is used to change the direction of flight of the projectile. Static firings, Reference (40) have shown the duration of force application to be about 3.5 milliseconds. If a triangular force-time relation is assumed, the maximum transverse force is 20,000 lbs., or the equivalent of 850 g's. The force is applied

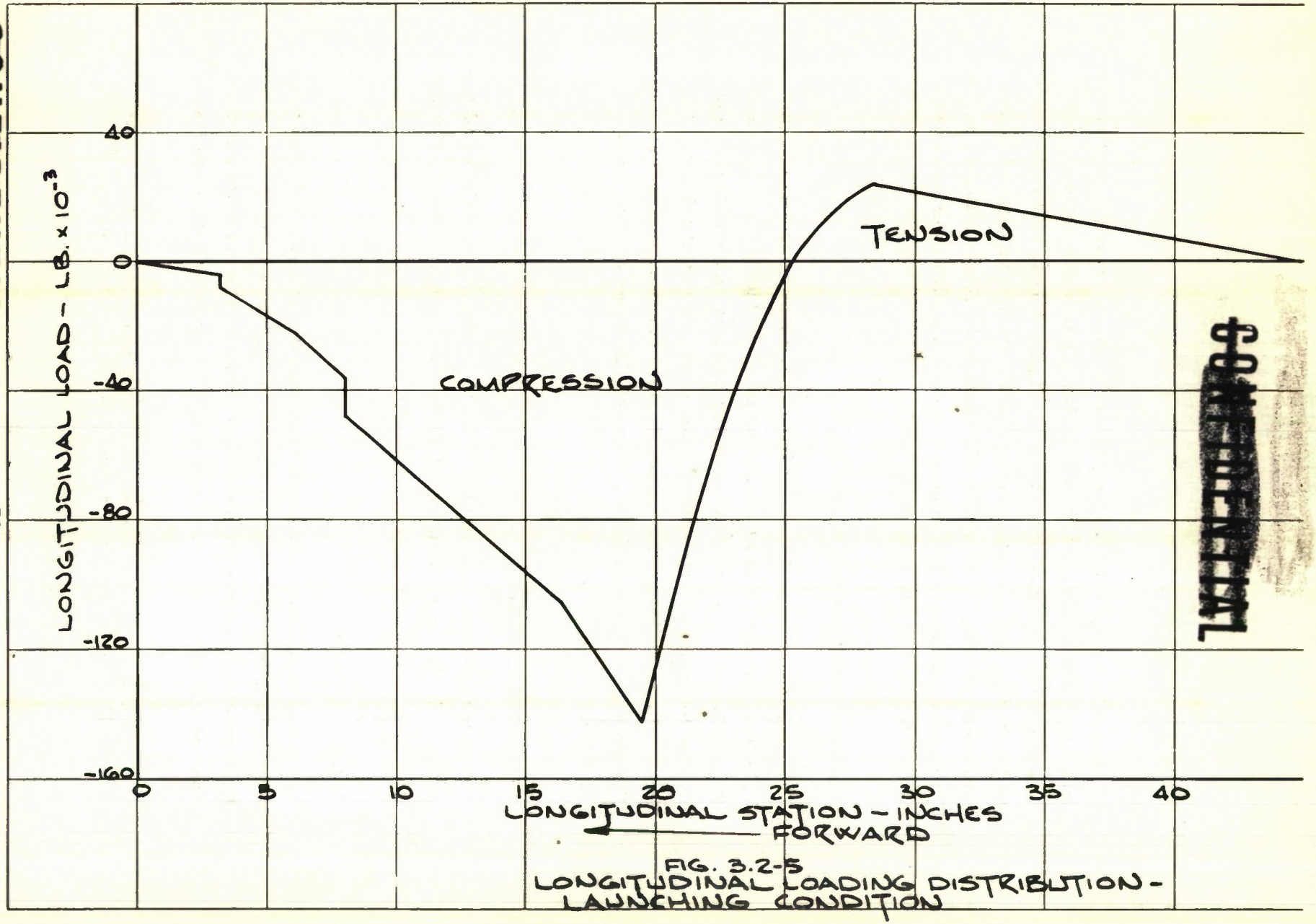

FIG. 3.2-5
LONGITUDINAL LOADING DISTRIBUTION - LAUNCHING CONDITION

at the center-of-gravity of the projectile for reasons of control effectiveness. The transverse shear distribution is computed by superimposing the 1 g shear distribution, Figure 3.2-4, multiplied by a factor of 850 with a constant shear of 20,000 lbs introduced at the center-of-gravity. The shear distribution is given in Figure 3.2-6. The projectile bending moments are computed from the area under the shear curve, see Figure 3.2-7

3.2.2.3 Aerodynamic Loads

The aerodynamic forces on the irdome are computed from Figure 3.1-12. The resulting pressure variation at Mach 1.5 is given in Figure 3.2-8. The drag force on the dome is computed by integrating the longitudinal component of the pressures on the dome. The drag force as a function of dimensionless dome station is shown in Figure 3.2-8. The total drag force on the dome at M = 1.5 is 32.5 lbs.

3.2.3 Stress Analysis

The stress analysis consists of a determination of the ability of the irdome, Center Body Section, Tail Section, and Impulse Cartridge to withstand the critical applied loads.

3.2.3.1 Irdome

The dome is a portion of a sphere assumed to be simply supported. The natural frequency of vibration of the dome is computed in order to determine the dynamic overshoot factor. The deflection at the apex of the dome due to its own weight is given in Reference (44).

$$w = \frac{r^2 q}{Eh}\left[(1+\nu)\left\{\frac{1}{1+\cos\alpha} - \frac{1}{2} + \ln\frac{2}{1+\cos\alpha}\right\} + \frac{1}{2}(1-\nu)\right]$$

FIG. 3.2-6
TRANSVERSE SHEAR -
CORRECTIVE IMPULSE CONDITION

FIG. 3.2-7
BENDING MOMENT-CORRECTIVE IMPULSE CONDITION

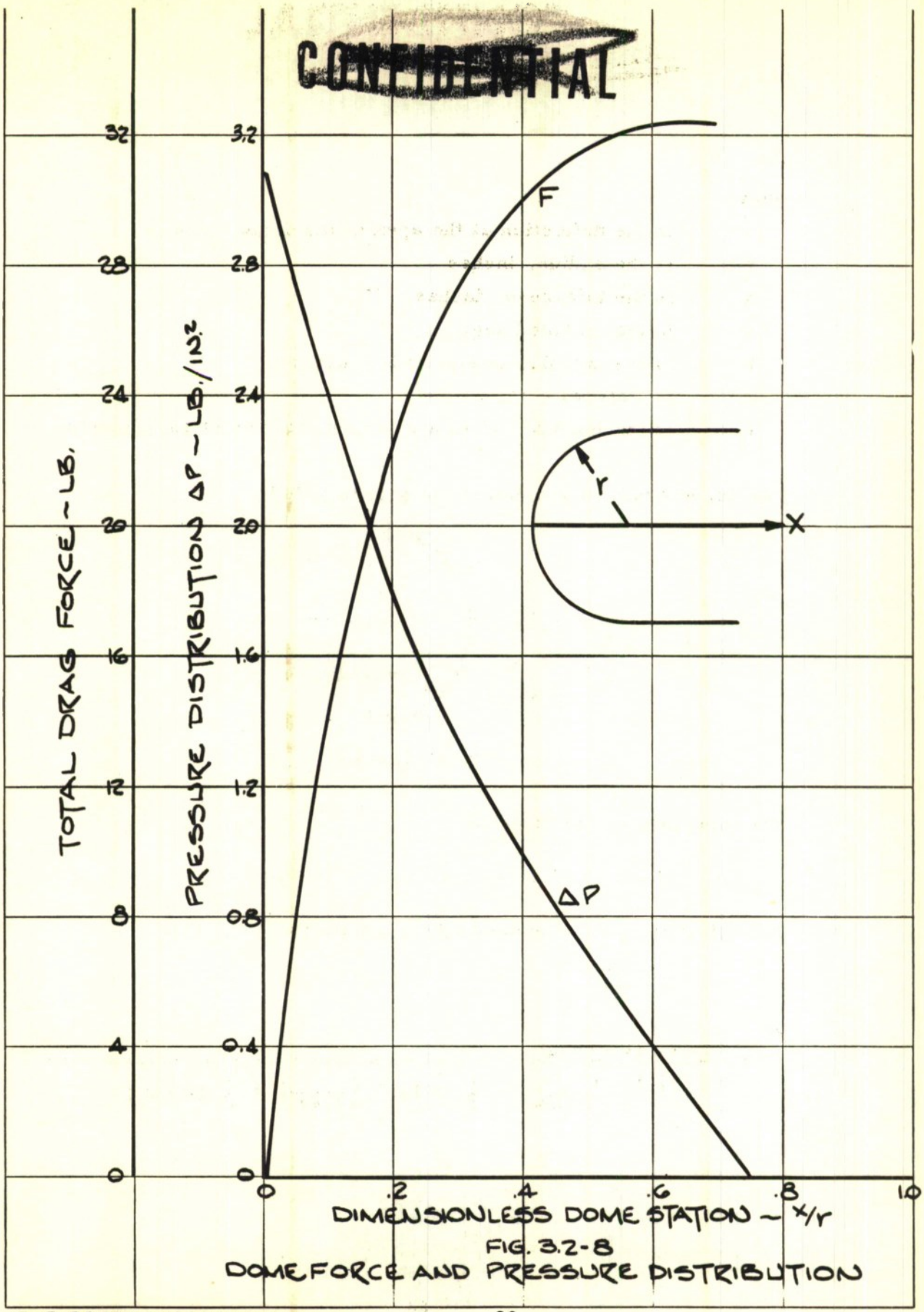

FIG. 3.2-8
DOME FORCE AND PRESSURE DISTRIBUTION

where

w	is the deflection at the apex of the dome, inches
r	is the radius, inches
h	is the thickness, inches
α	is the included angle
E	is the modulus of elasticity, lb/in^2
ν	is Poisson's ratio
q	is the inertia load in lbs per square inch of surface area

The above symbols are defined in Figure 3.2-9.

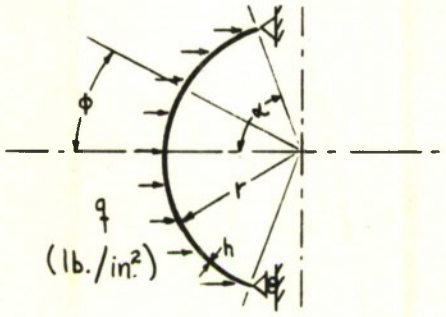

Figure 3.2-9

The total load on the dome is

$$P = 2\pi q r^2 (1 - \cos\alpha)$$

The effective spring constant of the sphere is

$$k = \frac{P}{w}$$

or

$$k = \frac{2\pi Eh (1 - \cos\alpha)}{(1+\nu)\left(\frac{1}{1+\cos\alpha} - \frac{1}{2} + \ln \frac{2}{1+\cos\alpha}\right) + \frac{1}{2}(1-\nu)}$$

The dome is assumed to be made of vicor glass with the following properties:

specific gravity = 2.18

density = 0.079 lb/in^3

modulus of elasticity = 9.6×10^6 lb/in^2

Poisson's ratio = 0.18

modulus of rupture = 10,000 lb/in^2 However, an allowable stress of 2000 lb/in^2 is assumed*

For following quantities which define the geometry of the dome

$r = 1.5$ inches

$\alpha = 70^o$

$h = 0.1$ inch

the spring constant is

$$k = 3.392 \times 10^6 \quad lb/_{in.}$$

A lower bound on the lowest natural frequency can be computed by assuming the dome to be an equivalent spring-mass system of spring constant k. The mass of the dome is

$$m = \frac{2\pi \rho}{g} r^2 h (1 - \cos\alpha) = 0.191 \times 10^{-3} \frac{lb\text{-}sec^2}{in.}$$

The natural frequency for a simple spring - mass system is

$$f = \frac{1}{2\pi}\sqrt{\frac{k}{m}} = 21200 \text{ cycles/sec.}$$

the period of vibration is

$$T = \frac{1}{f} = 0.047 \times 10^{-3} \text{ seconds}$$

The dynamic overshoot factor is determined from Figure 3.2-2 by

*Because of the brittle property of glass, stress concentrations introduced because of slight flaws are not relieved by local yielding.

comparing the period of dome vibration with the period of the gun launch force to provide

$$\text{Ratio} = \frac{0.047 \times 10^{-3}}{0.013} = 0.0036$$

Hence the overshoot factor is approximately equal to unity and the rebound factor is approximately zero. Since the dome is a thin shell ($h/r = 0.15$), the bending stresses are negligible as computed from the following equation, Reference (44).

$$\sigma_b = \frac{q}{2} \frac{2+\nu}{1+\nu} \cos\phi$$

where $q = \eta \rho h$

Here η is the load factor (number of g's)

The maximum bending stress (at $\phi = 0$) is

$$\sigma_b = 84 \text{ lb/in}^2$$

The dome compressive stresses are now computed. The total load on a sector of the dome defined by ϕ is

$$P = 2\pi q r^2 (1 - \cos\phi) = 590 \text{ lb.}$$

The load is resisted over a compressive area of

$$A_c = 2\pi r h$$

The compressive stress is therefore

$$\sigma_c = \frac{P}{A_c} = \frac{r}{h} q (1 - \cos\phi)$$

But since $q = \eta \rho h$,

the compressive stress is

$$\sigma_c = \eta \rho r (1 - \cos\phi)$$

The stress is maximum when $\phi = 70^\circ$, therefore,

$$\sigma_c = 0.658 \eta \rho r = 624 \text{ lb/in}^2$$

The margin of safety is

$$\text{M. S.} = \frac{-2,000}{624} - 1 = +2.20$$

The shearing area is

$$A_s = 2\pi rh \tan \phi$$

The shearing stress is

$$\sigma_s = \frac{P}{A_s} = \eta \rho r \frac{(1 - \cos \phi)}{\tan \phi}$$

Maximum shearing stress occurs when

$$\cos \phi = \frac{-1 + \sqrt{5}}{2} \quad \text{or} \quad \phi = 51.7^\circ$$

Hence

$$\sigma_{s_{max}} = 286 \text{ lbs/in}^2$$

The ultimate shearing stress is assumed as 80% of the modulus of rupture. Therefore the margin of safety is

$$\text{MS} = \frac{8000}{286} = 1 = + 27.0$$

Since the aerodynamic loads on the dome are only 32.5 lbs., this condition is not considered critical.

3.2.3.2 Center Body Section

The center body section consists of a 75S-T6 aluminum cylinder assumed to be simply supported. It is investigated for the launch and corrective impulse conditions.

The maximum compressive launch load on the center body section is 100,000 lbs. at station 15.5, Figure 3.2-5. The external diameter

of the cylinder is 4.25 in., the thickness is 5/16 in. and the unsupported length is assumed as 9 in. The compressive load is resisted over an area of

$$A = \frac{\pi}{4}(4.25^2 - 3.625^2) = 3.86 \text{ in}^2$$

The period of longitudinal vibrations is given in Reference (45).

$$T = 4\sqrt{\frac{\mu l^2}{A E}}$$

where μ is the mass per unit length

l is the length of the cylinder

A is the cross-section area

E is the modulus of elasticity

The values of the constants are

$\mu = 0.826 \times 10^{-3}$ lb-sec^2/in^2

$l = 9$ in

$A = 3.86$ in^2

$E = 10.4 \times 10^6$ lbs/in^2 (75S-T6 Aluminum)

The above constants yield a period of 0.164×10^{-3} sec. Therefore, from Figure 3.2-2 the dynamic overshoot factor is unity.

The compressive stress is

$$\sigma = \frac{100,000}{3.86} = 25,900 \text{ lb/in}^2$$

With a yield stress of 72,000 lbs/in^2 for 75S-T6 aluminum the margin of safety is

$$M.S. = \frac{72000}{25900} - 1 = +1.78$$

The buckling stress is obtained from Reference (46).

$$F_{cr} = 0.3\ E\ \frac{t}{r} = 488{,}000\ \text{lb/in}^2$$

where t is the wall thickness

r is the mean radius of the cylinder

Therefore the cylinder will yield in compression before it buckles axially.

The center section is assumed to vibrate as a cantilever beam. The greatest period of vibration is, Reference (45).

$$T = 1.785 \sqrt{\frac{\mu l^4}{E I}}$$

where I is the area moment of inertia of the cross section.

$$I = \frac{\pi}{64}(4.25^4 - 3.625^4) = 7.54\ \text{in}^4$$

The numerical substitution into the above equation yields a period of 0.469×10^{-3} sec. Since the transverse impulse lasts 3.5×10^{-3} sec., the dynamic overshoot factor is 1.10, Figure 3.2-2.

The transverse shears and bending moments at station 15.5 for the impulse control condition are obtained from Figures 3.2-6 and 3.2-7. The values are

$$V = 9000\ \text{lb}$$

$$M = 60{,}000\ \text{in-lb}$$

The maximum shearing stress occurs at the neutral axis. Its magnitude is given in Reference (46).

$$\tau = \frac{V}{\pi r t} = 5720\ \text{lb/in}^2$$

where V is the applied shear

The dynamic overshoot factor causes the shearing stress to increase to

$$\tau = 5720 \times 1.1 = 6290 \text{ lb/in}^2$$

The allowable shearing stress for 75S-T6 Aluminum is 49,000 lbs/in^2, therefore, the margin of safety is

$$\text{M. S.} = \frac{49000}{6290} - 1 = +6.79$$

The maximum bending stress is

$$\sigma = \frac{Mc}{I} = 16920 \text{ lb/in}^2$$

where M is the applied moment

c is the distance from the neutral axis to the outermost fiber

I is the area moment of inertia about the neutral axis

Numerically

$$c = 2.125 \text{ in.}$$

The dynamic overshoot factor causes the bending stress to increase to

$$\sigma = 16920 \times 1.1 = 18610 \text{ lb/in}^2$$

Since tensile yield stress is 72,000 lb/in^2, the margin of safety is

$$\text{M. S.} = \frac{72000}{18610} - 1 = +2.87$$

3.2.3.3 Tail Section

The tail section consists of a cylinder and a cone reinforced by four fins, Figure 3.2-1. This section is analyzed for the impulse control condition. The maximum shears and bending moments occur at the

forward end of the section. However, the section properties are also maximum at the forward end of the tail section, sta. 19.5, and decrease to a minimum at station 29. Beyond station 29 the section properties are constant. Therefore the analysis includes stations 19.5 and 29. Cross sections of these stations are given in Figure 3.2-10.

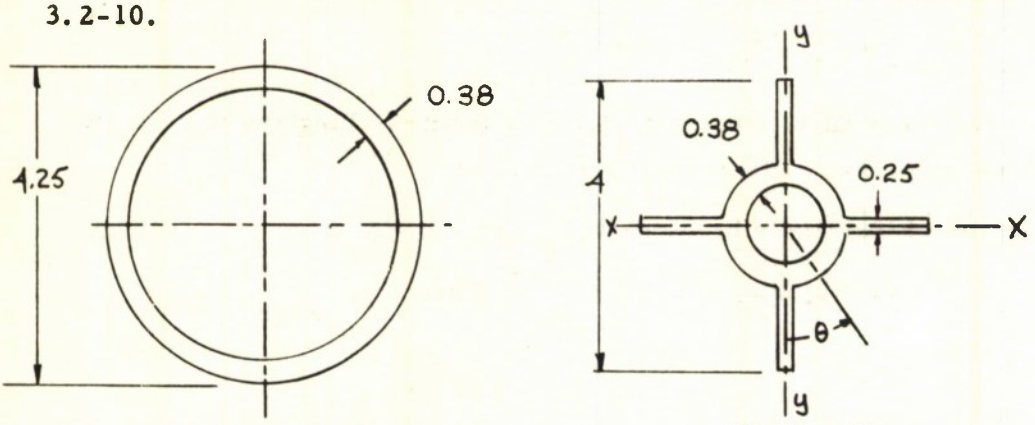

Station 19.5 Station 29

Figure 3.2-10

The area moment of inertia at station 19.5 is

$$I_{19.5} = \frac{\pi}{64} (4.25^4 - 3.50^4) = 8.64 \text{ in}^4$$

The area moment of inertia at station 29 about the x-x and y-y axes are

$$I_{xx} = I_{yy} = 1.48 \text{ in}^4$$

The product of inertia at station 29 is

$$I_{xy} = 0.26 \text{ in}^4$$

The moment of inertia about an axis inclined by an angle θ to the x-x axis is

$$I_\theta = I_{xx} \cos^2\theta + I_{yy} \sin^2\theta + 2 I_{xy} \sin\theta \cos\theta$$

when $I_{xx} = I_{yy}$, the above relation reduces to

$$I_\theta = I_{xx} + 2 I_{xy} \sin\theta \cos\theta$$

The above expression assumes a maximum when $\theta = 45^\circ$. Therefore the maximum moment of inertia is

$$I_{max} = I_{xx} + I_{xy} = 1.74 \text{ in}^4$$

An average moment of inertia of 4.0 is assumed along the tail section for the calculation of the period of vibrations.

The period of bending vibrations is

$$T = 1.785\sqrt{\frac{\mu l^4}{E I}} = 2.78 \times 10^{-3} \text{ sec.}$$

$l = 25$

$E = 10.4 \times 10^6$

$I = 4.0$

Since the force duration is 3.5×10^{-3} sec., it is seen from Figure 3.2-2 that the dynamic overshoot factor is 1.45.

The transverse shear at station 19.5 is 6500 lb. The maximum shearing stress including the dynamic effect is

$$\tau = \frac{6500 \times 1.45}{\pi(2.125)(0.375)} = 3770 \text{ lb/in}^2$$

The margin of safety is

$$M.S. = \frac{49000}{3770} - 1 = +11.99$$

The bending moment at station 19.5 is 60,000 lb-in. The maximum bending stress is

$$\sigma = \frac{60,000 (2.125) (1.45)}{8.64} = 21400 \text{ lb/in}^2$$

The margin of safety is

$$M.S. = \frac{72000}{21400} - 1 = +2.36$$

The transverse shear at station 29 is 3000 lb.

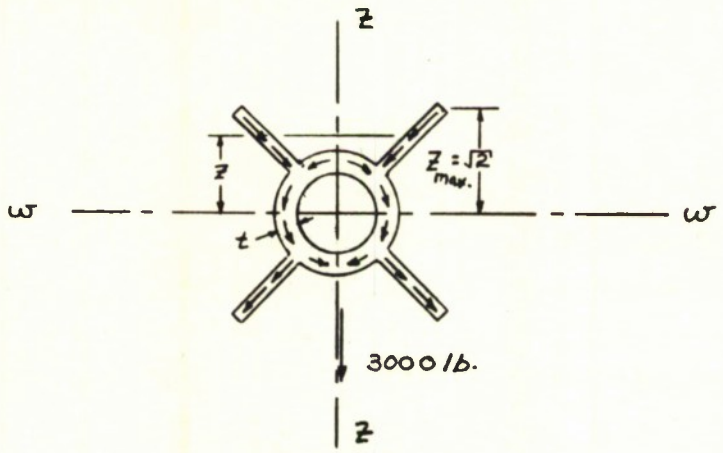

Figure 3.2-11

The direction of shear flow is given in Figure 3.2-11. The maximum shearing stress occurs on the w-w axis. The maximum shearing stress is

$$\tau = \frac{V}{2It} \int_0^{z_{max}} z\,dA$$

The maximum shearing stress including the dynamic factor is

$$\tau = \frac{3000\ (0.918)\ (1.45)}{2(1.74)\ (0.375)} = 3060\ \text{lb/in}^2$$

The tail section consists of 75S-T6 aluminum, therefore, the margin of safety in shear is;

$$M.S. = \frac{49,000}{3060} - 1 = +15.01$$

The bending moment at station 29 is 22,000 lb-in. The bending stress including the dynamic factor is

$$\sigma = \frac{22{,}000\sqrt{2}(1.45)}{1.74} = 25900 \text{ lb/in}^2$$

The margin of safety in bending is critical.

$$\text{M. S. } \frac{72000}{25900} - 1 = +1.78$$

3.2.3.4 Impulse Cartridge

The impulse cartridge is assumed to be a circular cylindrical shell with flat plates at both ends. The material is 4140 steel and the maximum internal pressure is 40,000 psi, Reference (40). The idealized impulse cartridge is shown below in Figure 3.2-12.

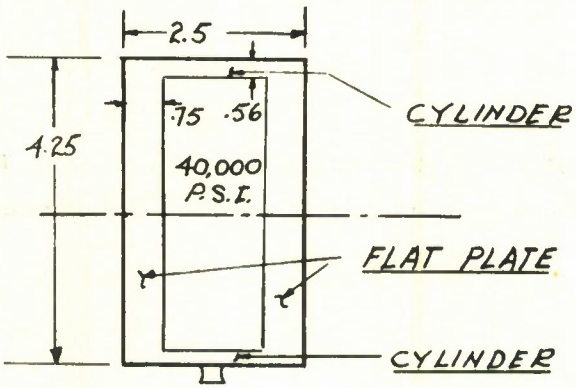

Figure 3.2-12

A dynamic overshoot factor of unity is assumed.

The maximum stress on the cylindrical portion of the cartridge occurs at the inner radius. The radial stress is

$$\sigma_r = 40{,}000 \text{ lb/in}^2$$

The tanengtial stress is Reference (47).

$$\sigma_r = p_1\left[\frac{r_2^2 + r_1^2}{r_2^2 - r_1^2}\right] = 134,000 \text{ lb/in}^2$$

where p_1 is the internal pressure

r_1, r_2 are the internal and external radii.

The yield stress of 4140 steel, Rockwell C41 is 175,000 lb/in^2. The margin of safety in tension is

$$\text{M. S.} = \frac{175000}{134000} - 1 = +0.31$$

The maximum shearing stress is, Reference (47).

$$\tau = p_1\left[\frac{r_2^2}{r_2^2 - r_1^2}\right] = 86,960 \text{ lb/in}^2$$

The allowable shearing stress is assumed as 80% of the tensile yeild stress. Therefore the margin of safety in shear is

$$\text{M. S.} = \frac{8}{10} \times \frac{175000}{86960} - 1 = +0.61$$

The flat plate at the end of the cylinder is assumed rigidly fixed. An average radius of 1.80 in. is assumed. The maximum bending stress is given in Reference (44).

$$\sigma = \frac{3}{4}\frac{qa^2}{h^2} = 172,800 \text{ lb/in}^2$$

where

q is the pressure, lb/in^2

a is the radius, in.

h is the thickness, in.

The margin of safety in bending is

$$\text{M. S.} = \frac{175000}{172800} - 1 = +0.013$$

3.3 CONTROL

A summary of the extensive investigation of impulse type control is presented in this section. The investigation has consisted of detailed analyses to establish the characteristics of impulse control and experimental tests, including flight test, to verify the results of this analytical work and to determine the reliability of this type of control. The following discussion contains;

(1) effect of impulse control on projectile flight with pulse applied at the center of gravity.

(2) results of flight test which substantiate the analysis of (1).

(3) design and static tests of the control unit from which impulse control is generated.

(4) effect of malalignment of control in pitch.

(5) effect of malalignment of control in roll.

(6) effect of roll rate on control effectiveness.

In addition to the aerodynamic notation specified in Section 3.1, the following nomenclature is used.

I_c total impulse delivered to the airframe, lb-sec

F pulse force, lb

τ pulse duration, sec

3.3.1 Effect of Impulse Control on Projectile Flight

By definition, impulse control is a flight path correction technique in which the applied force is of extremely short duration. In the present application the force pulse acts normal to the projectile longitudinal axis and the time duration of total impulse is small compared to the pitch and roll frequencies of the projectile. Based on this fundamental assumption the characteristics of impulse control were established analytically. This effort was quite extensive including two and three dimensional simulation programs. The most complete and detailed description of the analytical studies of impulse control is presented in Reference 2. The basic derivations and the computer diagrams of the simulation programs are given in this reference. In summarizing these results the following conclusions are considered fundamental and hence, the most direct means of presenting the characteristics of impulse control.

(1) Upon application of impulsive control, the projectile velocity vector changes direction instantaneously while the airframe body experiences oscillations at its characteristic frequency. See Figure 3.3-1. The instantaneous, as well as the steady state, angular change in velocity vector is given by;

$$\gamma_c = \frac{I_c}{mV}$$

(2) The steady state magnitudes of flight path angle, angle of attack, and pitch angle subsequent to control application are independent of pulse duration and depend only on the magnitude of total impulse delivered to the airframe.

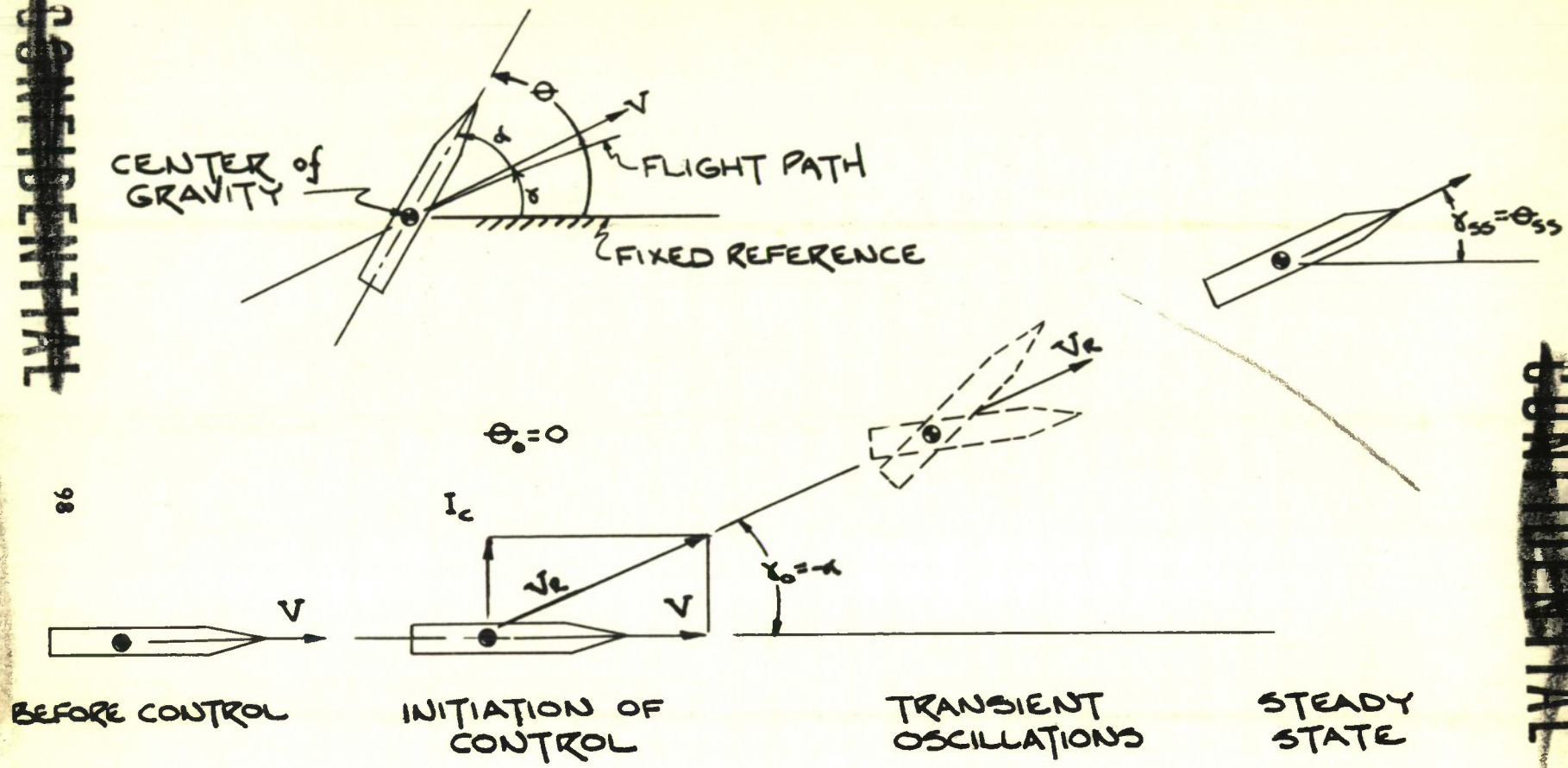

FIG. 3.3-1
EFFECT OF IMPULSE CONTROL ON PROJECTILE FLIGHT

(3) The forward velocity of the projectile is not affected by the application of impulse control.
(4) Transient response subsequent to a pulse of finite duration is not significantly different from the response to the mathematical impulse in zero time provided that the basic definition of impulse control is not violated (τ very small).
(5) The steady state magnitude of flight path angle induced by pulse application varies linearly with respect to pulse location along the body axis. If the projectile is pulsed at its neutral point, the net change in steady state flight path angle is zero.
(6) The magnitude of the transient angle of attack induced by impulse control is minimized by applying the pulse at the projectile center-of-gravity.
(7) When the control force is applied at the projectile center of gravity, the maximum transient flight path angle is insignificant compared to the steady state change.

Since the contemplated pulse duration to be utilized for control of the POLCAT projectile is extremely small ($\approx .003$, sec), projectile motion can be examined by assuming control to be in the form of a pure impulse. Further, since the specific application requires one-shot impulse control, the immediate discussion is concerned primarily with steady state magnitudes of flight path angle, angle of attack, and pitch angle. Finally, the impulse is assumed to act at the center-of-gravity. The equations of motion are:

$$\ddot{\theta} + A\alpha + B\dot{\theta} = 0 \qquad (1)$$

$$\dot{\gamma} - D\alpha = E f(t) \qquad (2)$$

$$\theta = \gamma + \alpha$$

$$A = -\frac{C_{M_\alpha}\, qSd}{I_y} \qquad B = \frac{-\left(C_{M_q} + C_{M_{\dot\alpha}}\right) qSd^2}{2V I_y}$$

$$D = \frac{C_{L_\alpha}\, qS}{mV} \qquad E = \frac{1}{mV}$$

where f(t) is a constant force of magnitude F applied for $0 < t < \tau$, and $I_c = F\tau$. The LaPlace transform of this function is given as:

$$\mathcal{L}[f(t)] = \frac{1}{s}\left(1 - e^{-s\tau}\right)$$

The La Place transforms of the equations of motion are:

$$s(s + B)\,\theta + A\alpha = 0 \tag{3}$$

$$s\gamma - D\alpha = \frac{EF}{s}\left(1 - e^{s\tau}\right) \tag{4}$$

With the assumption that τ is small and control can be represented by a pure impulse; the forcing function becomes:

$$\lim_{\substack{\tau \to 0 \\ F \to \infty}} F\left(1 - e^{s\tau}\right) = sI_c$$

Substituting in equations (4), and solving equations (3) and (4):

$$\alpha(s) = \frac{-(s + B)\, E\, I_c}{s^2 + s(B+D) + A + BD} \tag{5}$$

$$\theta(s) = \frac{A\, E\, I_c}{s\left[s^2 + s(B + D) + A \pm BD\right]} \tag{6}$$

$$\gamma(s) = \frac{(s^2 + Bs + A)\, EI_c}{s\left[s^2 + s(B + D) + A + BD\right]} \tag{7}$$

To obtain the steady state solution, the final value theorem is applied to equations (5), (6), and (7) and the results are:

$$\alpha(t) = 0 \qquad (t \to \infty)$$

$$\theta(t) = \frac{A E I_c}{A + BD} \approx E I_c \qquad (t \to \infty)$$

$$\gamma(t) = \frac{A E I_c}{A + BD} \approx E I_c \qquad (t \to \infty)$$

Applying the initial value theorem gives:

$$\alpha(t) \approx -E I_c \qquad (t \to o)$$

$$\theta(t) = 0 \qquad (t \to o)$$

$$\gamma(t) \approx E I_c \qquad (t \to o)$$

The instantaneous change in flight path angle is indicated. The change in flight path angle resulting from control is henceforth designated as γ_c and expressed as;

$$\gamma_c = \frac{I_c}{mV}$$

Since the control has considered to act as a pure impulse, there is no cross coupling and the three dimensional projectile motion simplifies to the specified two dimensional solution. The effect of displacing the impulse from the center-of-gravity is discussed in Sections 3.3.4 and 3.3.5. The relation between pulse duration and projectile roll is analyzed in Section 3.3.6.

3.3.2 Control Effectiveness Test Program

The unique and desirable characteristics of impulse control as established by the analytical effort described in Section 3.3.1 proved to be extremely appealing in two respects; (1) as a control technique that might be utilized in any number of missile or post firing correction applications and (2) impulse control provided the essential quality whereby post firing correction for the specific antitank weapon system became highly feasible. As a consequence, after formal presentation of the analytical results, personnel of the Pitman-Dunn Laboratories and the Bulova Research and Development Laboratories conferred and decided to explore the possibility of providing some type of experimental verification for this seemingly superior control technique. At the outset, it was established that any suggested experimental effort would not represent a change in the scope or objectives of the overall weapon system study. In November 1956, a proposal for a control effectiveness test program was submitted to the Pitman-Dunn Laboratories. See Reference 3. This proposal described a simple, relatively inexpensive method for realistically demonstrating the kinematic characteristics of impulse control without committing the POLCAT effort to component development program. The proposal was accepted and the subsequent execution of the program is described in the immediate discussion.

3.3.2.1 Concept of Test Program

The method used to determine control effectiveness consists of comparing the impact patterns of uncontrolled projectile flight with the target impact points of impulsively controlled projectile flight. In-flight control will be introduced by a single control cartridge which is designed to deliver sufficient impulse normal to the projectile flight path such that the subsequent change in flight path provides an impact

pattern at the target that can be easily distinguished from the pattern established by the normal dispersion of uncontrolled rounds. Thus, if sufficient uncontrolled rounds are fired to establish a center of impact, the measure of control effectiveness is the displacement of the impact point of a controlled round from the established center of impact. This displacement at the target due to control is a function of the magnitude of impulse delivered by the control cartridge and the distance from the target at which control is initiated. To eliminate, insofar as possible, the latter as a variable in the measure of control effectiveness at the target, the test projectile is fuzed so that upon passing through a yaw card the control system is initiated. By fixing the position of the yaw card relative to the target, it is possible to fire the cartridge at the same distance from the target as well as control the type of firing pattern obtained during the tests.

3.3.2.2 Description of Test Projectile

A standard, 105 mm, long boom T184 projectile modified to incorporate a control cartridge and the required fuzing fulfills the specifications for the test vehicle. An assembly drawing of the test projectile is given in Figure 3.3-2. The projectile weighs 18.1 pounds with a center-of-gravity located 3.3 calibers aft of the nose. The control cartridge is installed in the aft body section so that the transverse impulsive force acts at the center-of-gravity. The cartridge, designed by the personnel at Pitman-Dunn Laboratories, generates 6.9 lb-sec of impulse in 2.5 milliseconds and is initiated by an M52 mechanical primer installed in the side of the cartridge chamber. The fuze system is designed to function the primer after the projectile impacts a yaw card. To permit the projectile to pass through the yaw card before control initiation, a functioning delay is incorporated in the fuze system using a bellows motor. The time delay is obtained from

the time-displacement characteristic of the bellows motor which is initiated by a "lucky" element at the instant of yaw card impact. The bellows motor, then, expands thereby initiating the cartridge primer.

The test projectile weight is low enough to obtain the desired muzzle velocity ($\approx$1650 ft/sec) from the recoilless gun used at the firing range. Other than the placing of ballast in the nose to increase projectile static margin, the modifications to the T184 projectile do not change the basic aerodynamic characteristics of the projectile.

3.3.2.3 Test Results

The experimental data consists of two types;

(1) the target impact pattern of the controlled rounds around the center of impact of the uncontrolled rounds which provide a direct measure of in-flight control capability and (2) high speed motion pictures wherein the nature of projectile motion after control initiation is indicated.

From these data, the two basic characteristics of impulse control are unquestionably substantiated.

(1) The actual in-flight response of a projectile subjected to a transverse impulse is, for all practical purposes, an instantaneous change in flight path angle (δ_c). This change, as established by the previous analytical work, can be expressed as

$$\delta_c = \frac{I_c}{mV}$$

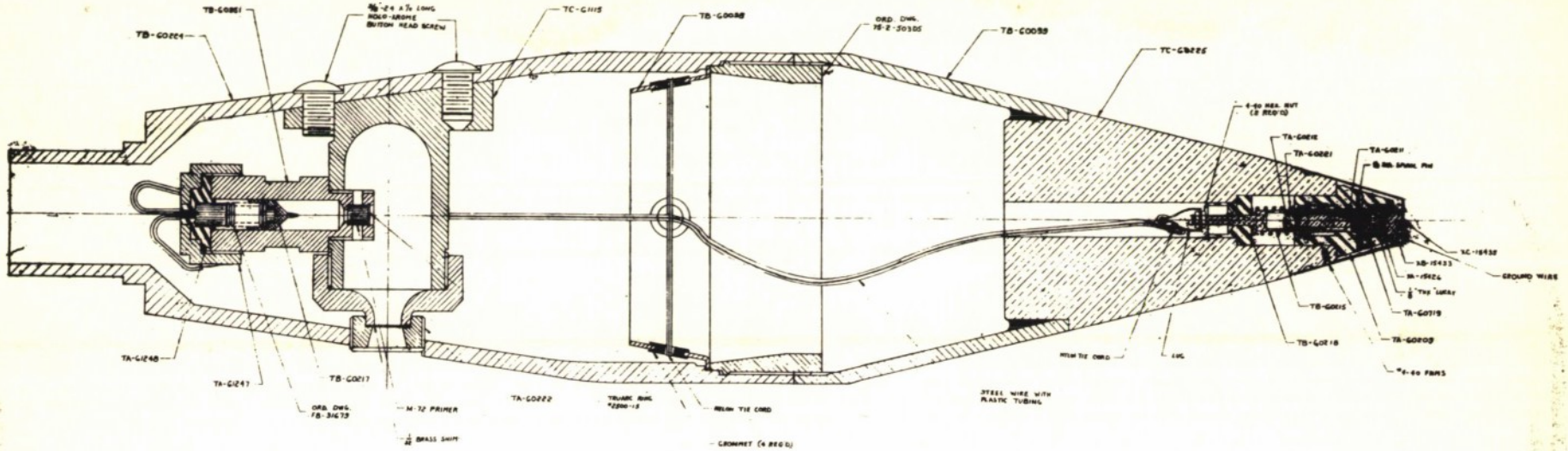

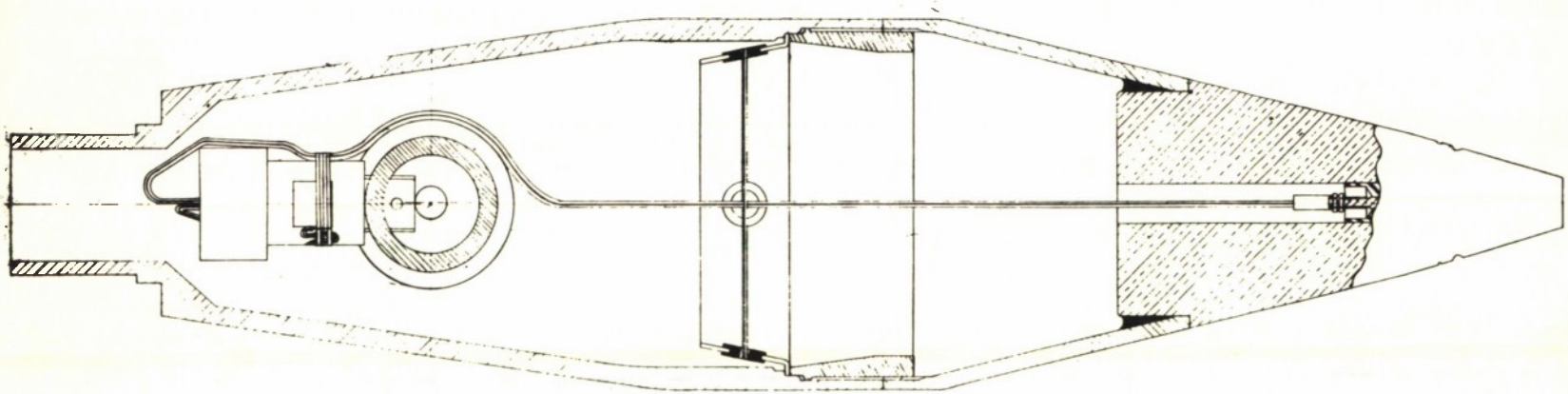

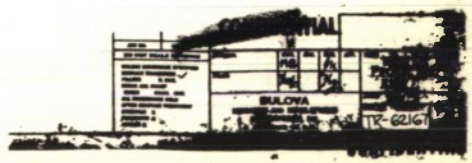

FIGURE 5-5
TEST PROJECTILE ASSEMBLY

(2) If the impulse is directed at the projectile center-of-gravity, the maximum transient in projectile angle of attack due to control is approximately equal to the change in flight path angle. Thus, as long as the impulse acts at the c. g., the perturbations of angle of attack are not substantial and do not influence, other than as desired, the subsequent flight characteristics of the projectile.

The verification of control effectiveness is illustrated in Figure 3.3-3 which presents the impact pattern at the target obtained from the test firings. The ballistic data are given in Table 3.3-1. The impact points are designated by number to indicate the sequence of firing and by the letters "S" and "C" to indicate standard, uncontrolled round and controlled round, respectively. Six rounds, 1S, 2S, 3S, 10S, 11S and 12S, determined the center of impact of the uncontrolled rounds. The displacements of the controlled rounds from this center of impact agree extremely well with the theoretical displacement. Since the projectile was spinning, the angular orientation of the control cartridge at the instant of initiation was random, resulting in the random impact distribution of the controlled rounds about the center of impact. The theoretical displacement is determined from the firing conditions and the known performance of the cartridge. With an average muzzle velocity of 1665 ft/sec and establishing the average point of control (from motion pictures) to be 250 feet from the gun, the average velocity at the instant of control is 1620 ft/sec. Average projectile weight is 18.15 pounds and the cartridge generates 6.85 lb-sec of impulse. The

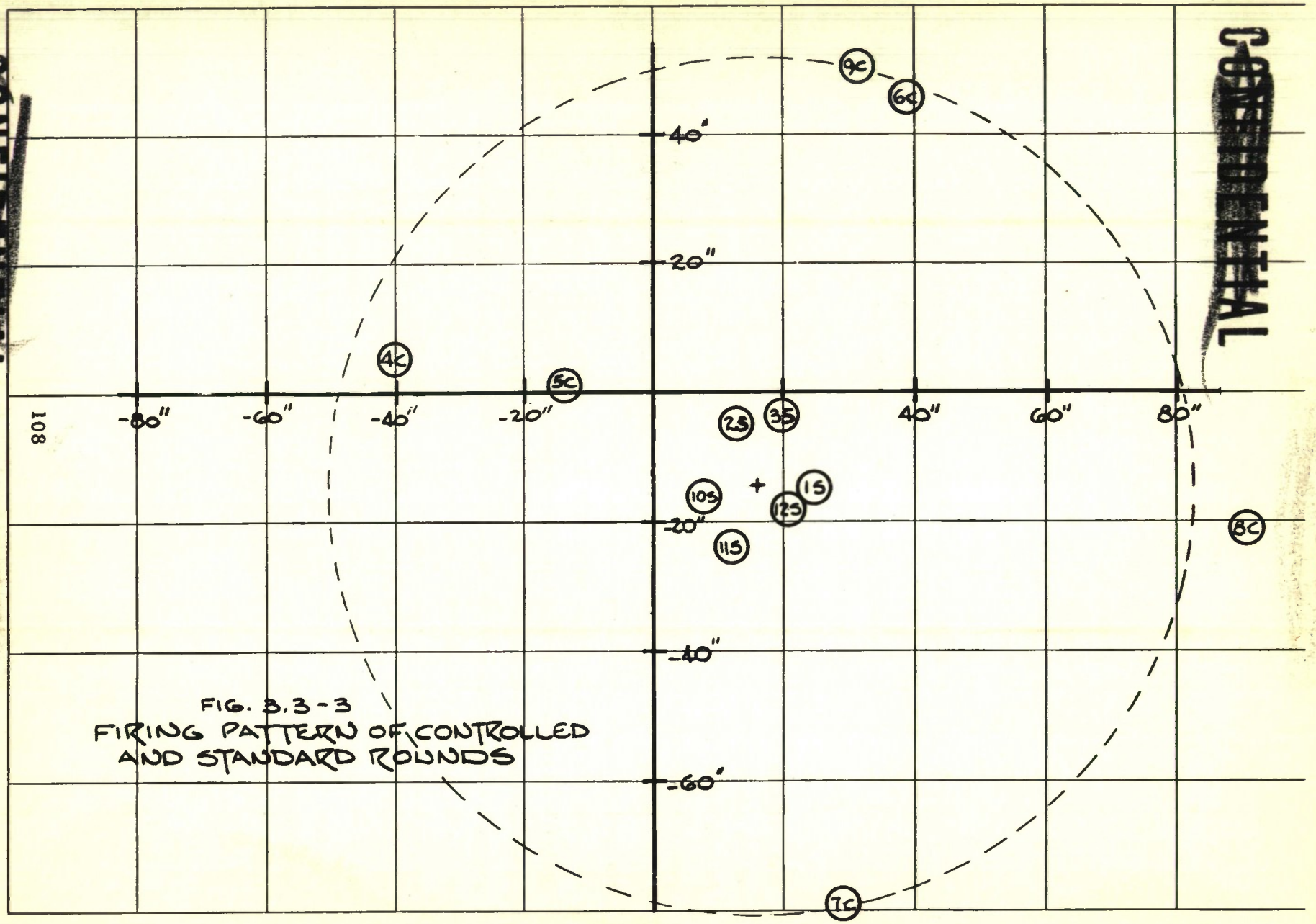

FIG. 3.3-3
FIRING PATTERN OF CONTROLLED AND STANDARD ROUNDS

expected change in flight path angle in mils is;

$$\gamma_c = \frac{(6.85)\ (32.2)\ (1000)}{(18.15)\ (1620)} = 7.5 \text{ mils}$$

Since the target is located 1000 feet from the gun, control is initiated 750 feet from the target giving a control displacement at the target of 67 inches. The impact pattern indicates a small variation from this predicted displacement with the exception of round 5C. From the motion pictures, it is established that the control cartridge in this round failed during burning as evidenced by the flash from the projectile nose as well as from the cartridge nozzle. The variation of control displacement of the other rounds is exceedingly small considering the inherent dispersion of the round itself, and the variations in muzzle velocity, cartridge performance, and delay time after yaw card impact.

During the firings, three high speed cameras stationed normal to the line of firing were used to determine the functioning of the control system and to record any pitching motion after control. Examination of these motion pictures indicates no perceptible angle of attack is induced in any of the controlled rounds. Additional substantiation is provided by the target markings which indicated that all projectiles penetrated at low angles of attack.

While its objectives were limited, the control effectiveness test program was deemed highly successful and furnished particularly essential and qualifying test data for the overall POLCAT effort.

ORDBA Form 25
18 Nov 53

LO 57 - 68
XO 777766-01 105 R 155

TABLE 3.3 -1

BALLISTIC DATA

ELBOW TELESCOPE M 17 - SER 19412
GUNNERS QUADRANT M1 SER 64256

ARMY-FRANKFORD ARSENAL PA

DATE: 12 July 1957

SUBJECT: 1000 FT. ACCURACY STD VS BULOVA RDA

PROGRAM NUMBER:

PROJECT DIRECTOR: WILSON - PISCOPO

WEAPON T17 # 31
CALIBER 106mm
CHAMBER
TUBE
NOZZLE
BARREL TRAVEL
FUZE TYPE

POSITION FT. DIX NJ
RANGE 4
MOUNT: RIGID
PENDULUM #
RIFLE WT.
CASE WT.
WEIGHTS
TOTAL WT.
PERIOD

WEATHER Overcast
REL. HUMD. 31%
BAR. PRES. 29.820"Hg
AMB. TEMP. 80
WIND: VELOCITY 0
DIRECTION N

Weather Report
11:30 HRS McQuire

EL. OF AIM. PT. 3.8 MILS
HT. OF AIM. PT. ABOVE GROUND 84"
SIZE OF TARGET 20'x 20'
CAMERA LOCATIONS see remarks
TERMINAL DISTANCE:
FRAME #1 TO #2
FRAME #2 TO #3

COIL DISTANCES:
GUN TO #1 50.00'
#1 TO #2 49.99'
#2 TO #3 50.00'
#3 TO #4 63.44'

PK = 25186

Tot. Elev. 10.8 mils

PT DATA:
LINE 11
PRE-AMP 2
CALIBRATION iv
GAGE # 305
K 530
C 0.0792
Z 2.5 KC

LOCATION OF YAW CARDS:
4 COIL
213.43 FT FROM MUZZLE
SPIN FRAME LOCATIONS:

TIME OF FLIGHT DISTANCE:
START TO STOP

NOZZLE ROUND NUMBER	PROJECTILE TYPE	PROJECTILE LBS WEIGHT	PROJECTILE COND. PROS XAMINAC	PROJECTILE COND. QUALITY	POWDER LOT NUMBER	POWDER TEMP.	POWDER CHARGE	TIME OF FIRING	TIME OF FLIGHT	VELOCITY CHRONO #1	VELOCITY F/S VELOCITY #1	VELOCITY CHRONO #2	VELOCITY F/S VELOCITY #2	VELOCITY F/S MUZZLE VELOCITY	VELOCITY TERMINAL CHRONO	VELOCITY TERMINAL VELOCITY	RE-TARDATION	PRESSURE CU #1 PSI	PRESSURE PT #2A PSI	PRESSURE #3	PRESSURE #4	M SUP. EL.	ACCURACY IN. VER.	ACCURACY IN. HOR.	RECOIL IN.	RECOIL LB-SEC
262		17.28			R		7.9 LBS IN STD RDS (7.9 LBS and 17 GRAMS HE5428 1 BULOVA RDS)	1210									-	9220	missed			7	-14.5	+24.5		
263	T	17.28			A			1225		1998	1667	3846	1650	1679			.16	9240				"	- 4.5	+12.5		
264	-	17.32			D			1237		3046	1641	1184	-	1653				9520				"	- 3.5	+20		
265	8	18.12	31	*	6			1250		no count	-	no count	-	-			-	9640				"	+6	-40.5		
266	4	18.07	22	*	0		7.0 DEGREES	1305		"	-	3894	1629	1664				9680				"	+1.5	-14		
267	E	18.02	20	*	4			1310		3023	1654	0026	-	1668			.17	10240				"	-79	+38.5		
268	1	18.16	32	*	7			1320		3016	1657	3868 3874	1639	1670			.16	9760				"	-20.5	+90.5		
269	3	18.18	17	*	8			1325		3041	1644	3900	1627	1656			.24	9700				"	+51	+31.5		
270	P	18.14	18	*	(T 28 -			1332		3029	1650	3906	1624	1668			.16	9800				"	-15.5	+ 7.5		
271	R	17.31			/038 WEB)			1340		3000	1660	3848	1649	1679			.16	9800				"	-23.5	+11.5		
272	O	17.32						1345		2977	1679	3816	1662	1692				9840	missed			"	-18	+20.5		
273	TO	17.28						1350		3017	1657	3402	-	1669												
								BULOVA RDS																		
								AV VEL		1665																
								STD RDS																		
								AV VEL		1674																

3.3.3 Design and Test of Impulse Control Unit

The final substantiation regarding the utilization of impulse control techniques is presented herein by describing the means for developing a short duration pulse whereby the idealizations used in analysis are, in practical sense, realizable. The control unit required for the proposed POLCAT projectile is, with the exception of the magnitude of impulse, the same as that designed, built, and fired in the test projectile. The control unit installed in the test projectile consists of a cartridge loaded with rapid burning propellant that generates its total impulse in less than .003 seconds. For purposes of the test program, it was specified that cartridge deliver approximately 7 lb-sec of impulse.

The design and static test of the control cartridge was executed by personnel of the Pitman-Dunn Laboratories. Initially, the cartridge design parameters were investigated in an extensive static firing test program wherein the effect of propellant weight, nozzle shape and size and chamber volume were determined. In all cases pressure and thrust time histories were obtained. These data show conclusively that despite changes in the cartridge configuration and, hence, the magnitude of total impulse delivered, the time variation remained unchanged. This is illustrated in Figure 3.3-4.

The time duration of burning appears to be primarily dependent on the propellant-primer combination. While duration is invariant, peak pressure is not. Obviously, peak pressure is proportional to total impulse but, in addition, it is shown that for a given magnitude of total impulse peak pressure can be varied substantially by changes in nozzle shape. At this point, it may be noted that to generate high

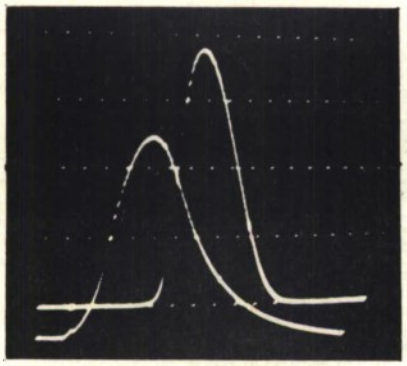

NOZZLE: STANDARD
CHARGE: 15 GRAMS
PEAK PRESSURE: 30,000 PSI
PEAK THRUST: 4500 LBS
IMPULSE: 6.9 LB-SEC

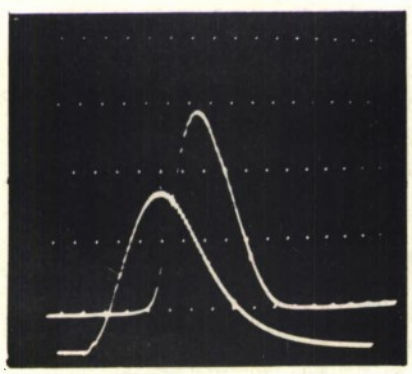

NOZZLE: CONVERGENT
CHARGE: 16 GRAMS
PEAK PRESSURE: 23,000 PSI
PEAK THRUST: 3500 LBS
IMPULSE: 5.2 LB-SEC

UPPER CURVE IS THRUST; LOWER CURVE IS PRESSURE.
INTERVAL BETWEEN TIMING MARKS IS .5 MILLISECONDS.

FIGURE 3.3-4 : PRESSURE AND THRUST TIME HISTORY OF CARTRIDGE FIRING

total impulses (as in the case of the POLCAT design) an extremely efficient nozzle shape is required in order to prevent peak pressure from becoming excessively high.

Following these tests, a series of static firings were conducted with the final cartridge design to establish reliability and to establish that the peak pressure did not exceed 30,000 psi upon which structural design was based. The results of the test as well as the design characteristics of the cartridge are given in Table 3.3-2. The mean of total impulse is 6.85 lb-sec with a standard deviation of .08 lb-sec. (1.2% of total impulse) These data indicate exceedingly reliable performance of the impulse control unit. Although the proposed POLCAT design requires considerably greater impulse than obtained in the tests, the low variation in impulse magnitude can be attained with ease by utilizing the design information obtained in the initial series of firings.

3.3.4 Effect of Impulse Control Malalignment in Pitch

With the same assumptions used in the analysis of Section 3.3.1, projectile flight path change is examined considering the impulse to act along the projectile longitudinal axis but not necessarily at the center-of-gravity is designated as "e" and is positive forward of the c. g., negative, aft. If the equations of motion are solved, including the impulsive moment (e I_c), the steady state magnitude of flight path angle is expressed as;

$$\gamma_c = I_c \left[\frac{\frac{A}{mV} + \frac{eD}{I_y}}{A + BD} \right] \qquad (8)$$

TABLE 3.3-2

CONTROL CARTRIDGE FIRING at FRANKFORD ARSENAL

Round	Peak Pressure (psi)	Peak Thrust (lbs)	Impulse (lb-sec)
1	23,300	5380	6.72
2	22,700	5460	6.81
3	22,500	5540	6.93
4	23,300	5600	6.99
5	22,700	5490	6.86
6	22,200	5450	6.81
7	22,400	5450	6.81
8	22,100	5470	6.84
9	22,600	5540	6.92

Chamber Volume	1.95 cu. in
Primer	M52A4
Blowout Disc	.025 in.
Charge	17 grams

$$A = \frac{-C_{M_a} qSd}{I_y} \qquad B = -\frac{\left(C_{M_q} + C_{M_{\dot{\alpha}}}\right) qSd^2}{2V I_y} \qquad D = \frac{C_{L_a} qS}{mV}$$

If e is assumed to place the impulse at the projectile neutral point, its value in calibers is,

$$e = \frac{C_{M_a}}{C_{L_a}}$$

Substituting this aft displacement of control into equation (8), provides a steady state change equal to zero. Conversely, if e is given positive values (forward of c.g.) γ_c increases. This aspect of impulse control has obvious application to projectile design in that a simple, direct means is available to increase control effectiveness without increasing the magnitude of impulse.

The variation of flight path angle change is given for the POLCAT design in Figure 3.3-5 assuming an impulse magnitude of 35 lb-sec. In addition to varying the point of application of impulse, the effect at two projectile velocities are shown, thus, reflecting the influence of velocity and center-of-pressure movement.

3.3.5 Effect Impulse Control Malalignment in Roll

At this point, the impulse is assumed to be displaced off the longitudinal axis of the projectile. This effect was analyzed in Reference 52 where it was shown that malalignment off the projectile roll induces an instantaneous change in roll rate proportional to the amount of malalignment, the magnitude of impulse, and the projectile moment of inertia in roll. The instantaneous change in roll rate is

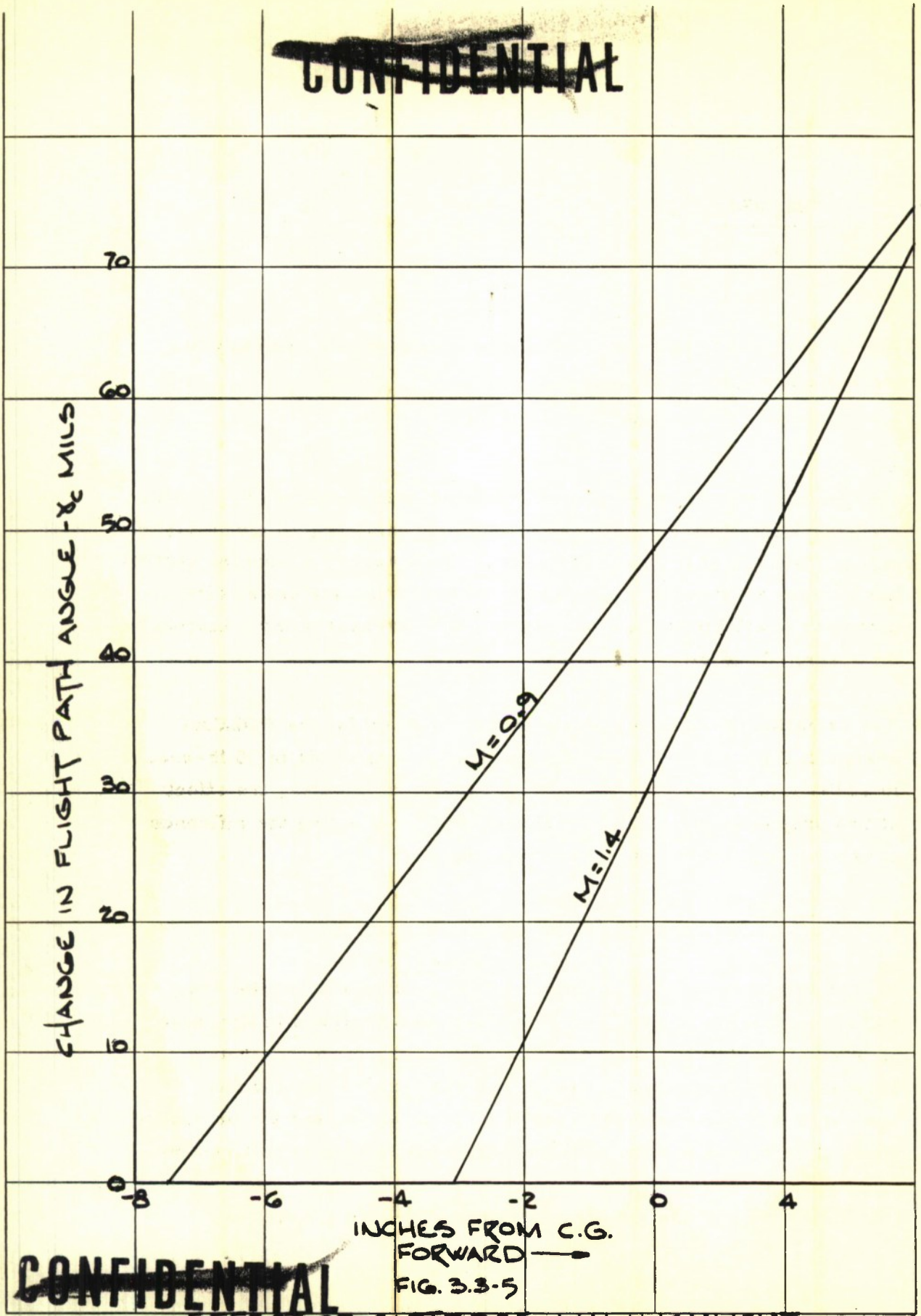

FIG. 3.3-5

EFFECT OF CARTRIDGE MALALIGNMENT IN PITCH ON CONTROL EFFECTIVENESS

expressed as;

$$\Delta\dot{\phi} = \frac{e\, I_c}{I_x}$$

The application of this effect to the POLCAT projectile is illustrated in Figure 3.3-6. This presents a means for assuring that the terminal roll rate of controlled trajectories does not exceed a maximum as dictated by shaped charge performance.

3.3.6 Effect of Roll Rate on Control Effectiveness

Thus far, the discussions of impulse control have assumed pulse duration to be extremely small compared to airframe period in roll or pitch in which case the problem need be considered only two dimensionally. This assumption is valid with respect to the relation between pulse duration and airframe pitching motion, considering the attainable pulse durations and the practical airframe stability and inertia characteristics. However, the relation between pulse duration and projectile roll rate is not as easily predicted. While pulse duration can be specified, roll rate being an externally induced flight condition, independent of projectile aerodynamic or mass characteristics, can assume a sufficiently high magnitude to violate the basic assumption of the impulse control analysis. While this is shown not to be the case in the POLCAT application, this area is examined in an attempt to define where and how impulse control can be utilized. For instance, in the case of high velocity, spin stabilized ammunition, the use of impulse control becomes more difficult since it is conceivable that in this application projectile period of roll can be less than the pulse duration.

The analysis of this condition was initiated early in the POLCAT effort and the results are given in Reference 52. It is concluded that substantial reductions in control effectiveness are realized

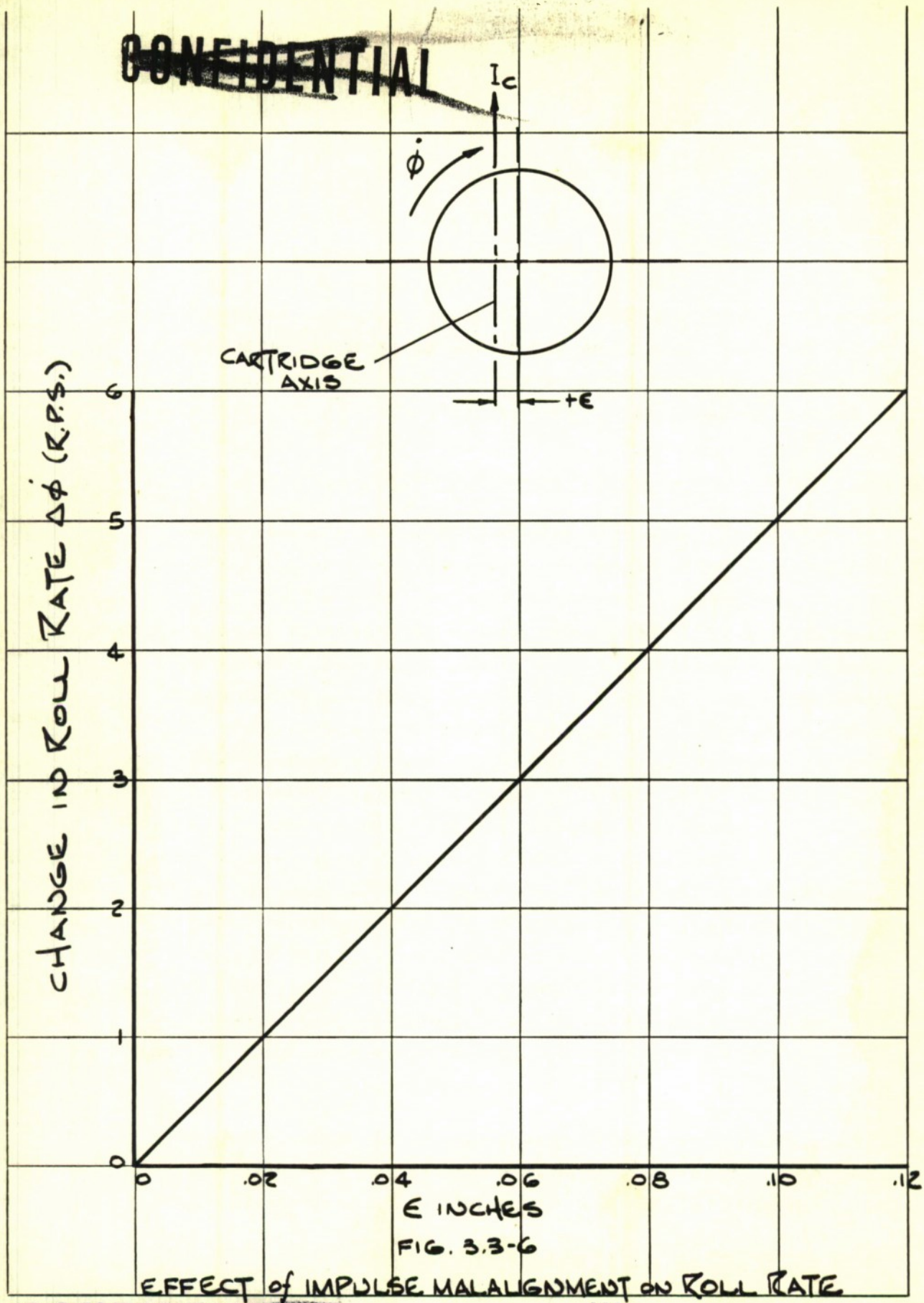

FIG. 3.3-6

EFFECT of IMPULSE MALALIGNMENT ON ROLL RATE

at high roll rate due to the rotation of the control force vector during the control cycle. Further it is shown that the magnitude of this reduction is quite sensitive to pulse shape; the triangular pulse showing the least reduction at a given roll rate. Noting the force-time history obtained experimentally (see Figure 3.3-4) only the triangular pulse is considered. Control effectiveness is defined by a ratio, I_e / I_s, which is determined for the conditions of pulse duration and projectile rolling velocity. I_s is the impulse delivered to the airframe in a non-rolling condition. I_e is the effective impulse realized for control in the rolling condition. Since reduction in control effectiveness results from the rotation of the force vector, the product of pulse time and roll rate determine the magnitude of the reduction. This is expressed for triangular pulses as;

$$(I_e/I_s) = \frac{8}{(\tau\dot{\phi})^2}\left[1 - \cos\frac{\tau\dot{\phi}}{2}\right]$$

For small values of ;

$$(I_e/I_s) = 1 - \frac{(\tau\dot{\phi})^2}{48}$$

The variation of the ratio (I_e/I_s) is plotted in Figure 3.3-7 with the applicable region of $\tau\dot{\phi}$ indicated. Relative to applications other than POLCAT, the control effectiveness ratio is used a criterion for establishing general limits for the utilization of impulse control. Two values of effectiveness ratio, .95 and .80, are selected as being representative of two levels of efficiency that might be apceptable. The maximum pulse durations and projectile spin rates for each of the ratios are given in Figure 3.3-8 for a triangular pulse shape. To indicate possible areas of application, various types of ammunition have been related to roll rate.

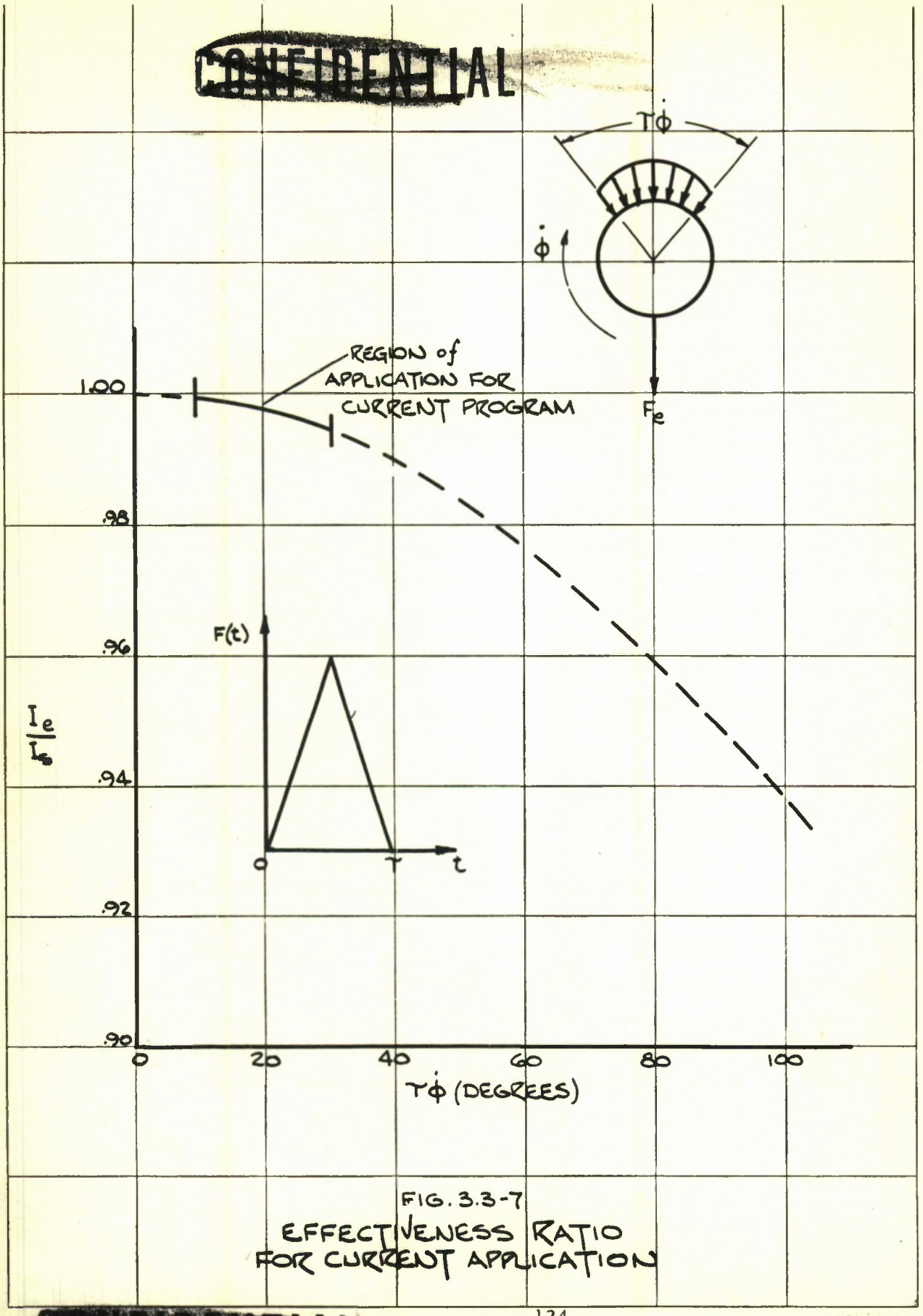

FIG. 3.3-7
EFFECTIVENESS RATIO
FOR CURRENT APPLICATION

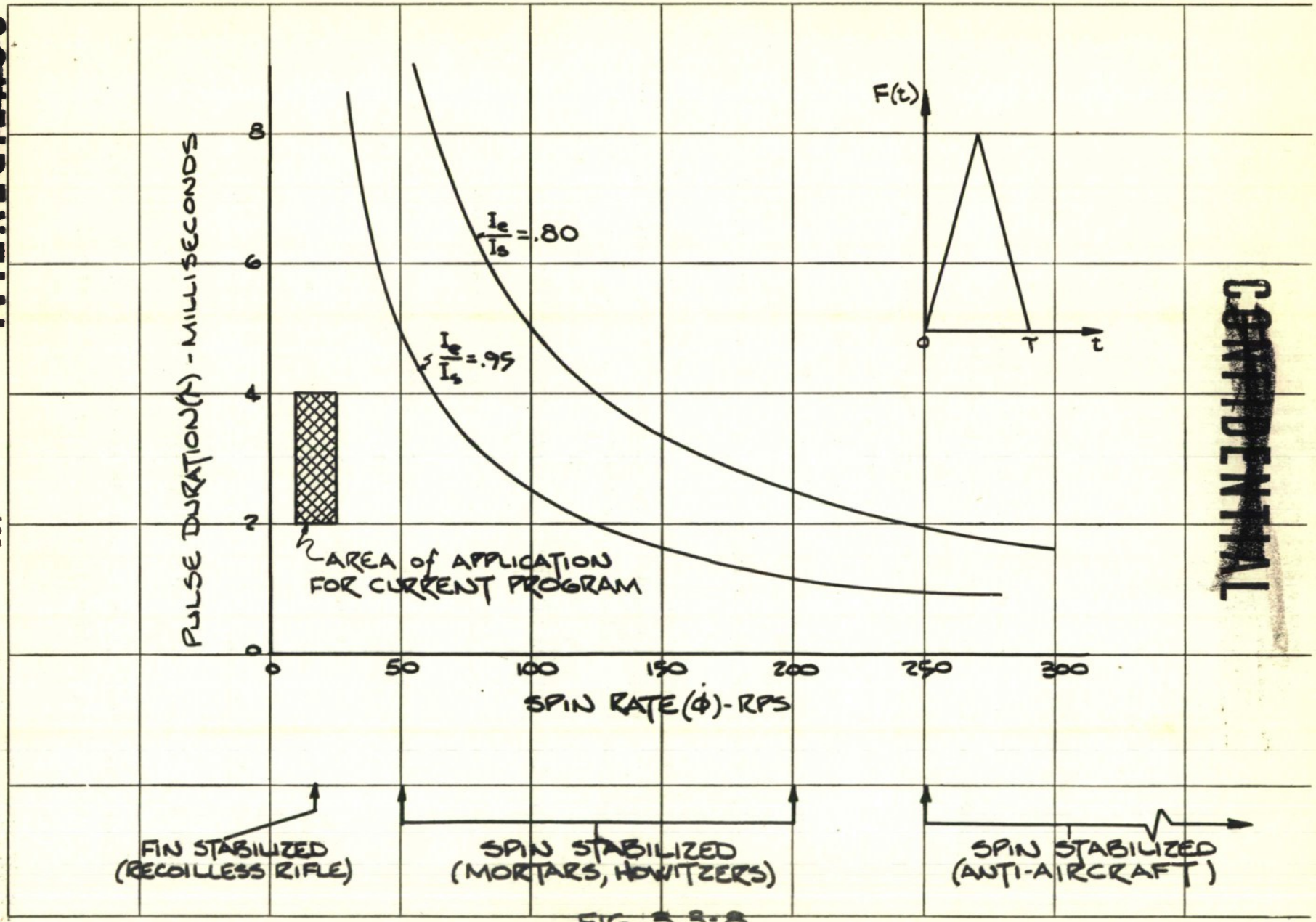

FIG. 5.3-8
LIMITS FOR APPLICATION OF IMPULSE CONTROL

3.4 GUIDANCE

3.4.1 Introduction

The problem of providing guidance for the POLCAT projectile can be approached from several different points of view.

The use of radar for this application has been discarded due to the fact that the complexity of radar systems is incompatible with the space requirements in the recoilless rifle projectile, and due to the deleterious effects of ground on radar directivity.

The use of visible light is discarded due to the need for security.

Of primary interest then is the use of infrared for guidance. Infrared beam riding is discarded due to the capture problem. Infrared command systems are discarded due to the need for two trackers, one being required for the target, the other for the projectile. In addition, the command system has stringent boresight requirements.

Thus only the infrared homing systems remain for discussion.

Active infrared homing is discarded due to the complexity associated with placing an illuminator in the projectile and the difficulty of providing an automatic target illumination capability. The other possible types of infrared homing will now be discussed in greater detail.

3.4.2 The Use of Infrared Techniques for Providing Homing

3.4.2.1 Passive Infrared Homing Guidance

Tanks, as is well known, radiate infrared energy and a considerable amount of work has been done in determining their radiating

characteristics.

The radiation characteristics of the 90mm gun, tank, M-48, for example, are shown in Figure 3.4.1 taken from Reference 53. The results were obtained at a range of 890 feet, and show that under the conditions of this test, operating vehicles present signals above background level. However, when the vehicles are not in operation, the targets are obscured by noise.

In the presence of a decoy target the conditions of Figure 3.4.2 result, the target being obscured by noise. In this case the decoy target was a charcoal heated field stove.

These results show that the application of passive infrared homing to the anti-tank projectile problem is at present marginal. However, since such a technique is very desirable, it is certain that gradual improvements in technique will ultimately enhance this system's capability.

3.4.2.2 Homing Guidance Using Planted Infrared Beacon

Another possible approach to the homing problem is the use of a special spotting round containing a flare and capable of impalement on the target vehicle, with its subsequent combustion providing a homing target. Much preliminary work both theoretical and experimental would be required before its feasibility could be proven.

3.4.2.3 Semi-Active Infrared Homing

As far as is known, very little work has been done in the use of infrared to illuminate a tank by means of a beam of coded energy. If the beam of coded energy is narrow enough so that it only illuminates the target then the coded energy reflected from the target represents a

FIG. 3.4-1

COMPARISON of RADIANCY of M-48 TANK WITH BACKGROUND NOISE

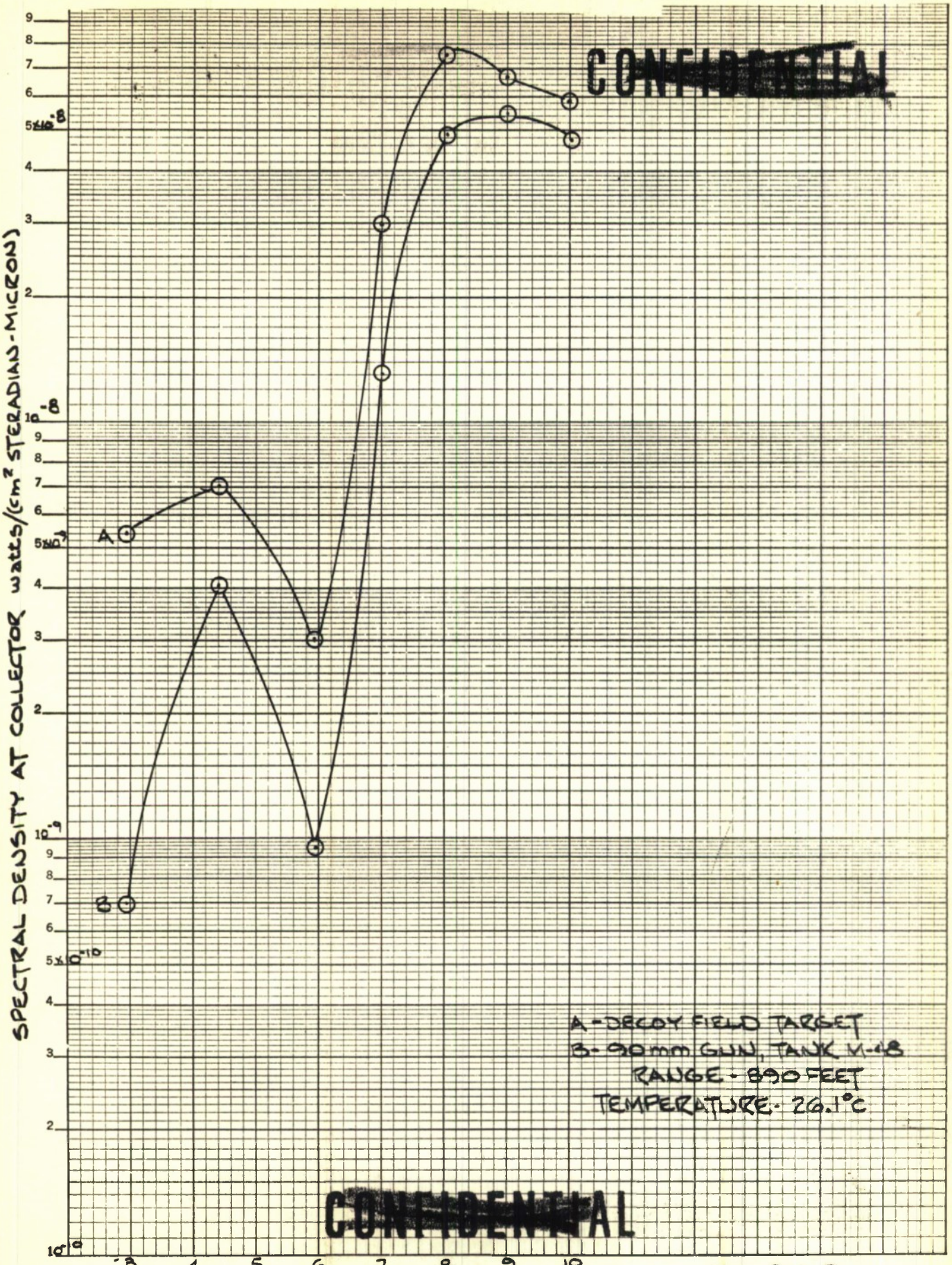

FIG. 3.4-2
COMPARISON of RADIANCY of M-48 TANK WITH DECOY FIELD TARGET

unique method for discriminating the target from background noise. This system would thus entail the use of an illuminator which an operator would train such as to continually illuminate the tank with pulse coded infrared energy. A seeker in the projectile would then obtain target line of sight information utilizing the energy reflected from the tank.

3.4.3 Theoretical Basis for Semi-Active Infrared Homing System

It has been pointed out previously that control of the projectile would be instituted at relatively close range to the target. Thus the seeker does not necessarily have to be capable of acquiring the target at the instant of firing. Calculations have been made for a typical case which indicate that a suitable ratio of signal to noise power will exist. The calculations were made for the following conditions:

illuminator:

carbon arc lamp	3800°K
filtered wavelength	0.8 - 2 μ
reflector diameter	18 inches
beamwidth	1 mil

seeker:

uncooled Pbs cell	NEP 1.5×10^{-11} watts
reflector diameter	105 mm

irdome, reflectors, lenses:

combined transmittance factor	0.7

geometry:

illuminator to target distance	6000 ft.
seeker to target distance	100 ft.

For the above conditions the following signal to noise power ratios

would be obtained for an optimum system.

Temperature (°F)	32		68	
Humidity (%)	40		60	
Target Reflection Coefficient	0.05	0.25	0.05	0.25
Signal/Noise Power Ratio	194	960	143	715
Signal/Noise Ratio (db)	22.9	29.8	21.6	28.5

Now since the inverse square law holds approximately, as the target to seeker distance is doubled the power received is quartered and a 6 db loss in signal results.

Thus the following approximate results are obtained for various values of target to seeker distance.

Signal/Noise Ratio at Seeker (db)

Temperature (°F)		32		68	
Humidity (%)		40		60	
Target Reflection Coefficient		0.05	0.25	0.05	0.25
Target to Seeker Distance (ft.)	100	22.9	29.8	21.6	28.5
	200	16.9	23.8	15.6	22.5
	400	10.9	17.8	9.6	16.5
	800	4.9	11.8	3.6	10.5
	1600		4.8		4.5

It thus appears very likely that adequate signal levels will be available for detection.

3.4.4 Illuminator Design

The primary requirements on the illuminator are: first, that it provide coded infrared energy of sufficient magnitude that the target will reflect

adequate energy and second, that it restrict the coded energy to the target so that effective discrimination from background be obtainable.

The arc lamp is, at present, felt to be most suitable for initial use in the intended application. An arc radiates essentially as a black body and has considerable output in the infrared portion of the spectrum, whereas gas lamps employing xenon, mercury, zirconium, etc. generally have low output in the infrared. Thus it is expected that a carbon arc lamp suitably designed would be adequate for the intended use. A filter such as the Corning type 2550 or 2540 would be suitable for filtering out the visible light while having 90% transmission in the infrared.

Since illumination is to be restricted to the target, the diameter of the illuminated spot must be less than the minimum dimension of the tank. Assuming that the minimum dimension of the tank is 7.5 ft. and the maximum range of interest is 2000 yards, an illuminator beamwidth of the order of 1 mil will be required. Selecting an arc crater diameter of 1.5 mm means that the focal length of the system will have to be 4.92 ft. to obtain the 1 mil beamwdith. If the diameter of the primary reflector is made 18 inches the f number of the system is $4.92 \div 1.5 = 3.3$. The physical length of the illuminator can, of course, be decreased by folding the focal length by means of a secondary reflector.

Modulation of the light beam will most readily be provided by means of mechanical chopping since electrical pulsing of a carbon arc is not possible at high rates.

3.4.5 Medium Considerations

The average clear weather transmittance of atmosphere in the infrared range 0.8 - 2.0 μ is obtained from Reference 54 as

Average Transmittance per Kilometer		
Temperature (°F)	32	68
Humidity (%)	40	60
	0.792	0.672

These figures are not excessive and show the basic utility of the 0.8 - 2.0 μ portion of the spectrum.

3.4.6 Target Characteristics

Only a small percentage of the energy, estimated at from 5 - 25%, can be expected to be reflected from the target. Most of the energy will be either absorbed or scattered. The percentage absorbed will be a function of the type of surface material. The scattering characteristics will be a function of the surface roughness of the material as well as the geometrical shape of the target. Unfortunately, very little experimental data on the infrared reflection characteristics of tanks are available.

3.4.7 Seeker Characteristics

The function of the seeker is the determination of target line-of-sight error angle in order that control of the projectile will be initiated when a target miss is imminent. Since the projectile spins after being fired, it is logical to employ the spin of the projectile for the purposes of scanning. Furthermore, since the projectile will be subjected to high accelerations it appears desirable to utilize a frame-fixed seeker, that is, one which has no parts which move relative to the projectile.

As a result of the work done in investigating the feasibility of such seekers, a number of interesting possibilities have become evident.

The main requirement on such seekers is that they be capable of determining the location of the center of the illuminated spot on the target. Naturally, for a fixed optical receiving system, the size of the spot will increase as the target is approached. The spot size ratio can be shown to be given by the expression

$$S_R = \frac{S_S}{S_D} = \frac{S_I + R_I \theta_I}{R_D \theta_D}$$

S_R = spot size ratio
S_S = diameter of target image on detector
S_D = diameter of detector
S_I = diameter of illuminated spot on target
θ_I = beamwidth of illuminator
R_I = illuminator to target range
R_D = seeker to target range
θ_D = seeker beamwidth

Referring to Figure 3.4-3 it is seen that for a system using a one mil beamwidth illuminator which is 6000 ft from the target, the spot size ratio will be 0.06 (point A) when the seeker is 650 ft. from the target. When the seeker is 80 ft. from the target the spot size ratio is 0.5, (Point B) that is the spot diameter will be equal to one-half that of the detector. The seeker total field of view has been taken as 11 degrees.

For the same one mil beamwidth illuminator 2250 ft. from the target the spot size ratio is 0.03 (Point c) at the maximum control range R_D = 650 ft whereas at the minimum control range R_D = 80 ft. the spot size ratio increases to 0.25 (Point D). Thus, the seeker must accomodate a large range of spot sizes. This requirement means that the seeker must be capable of determining the center of the target image, as distinguished from most other automatic homing systems where the target is essentially a point source.

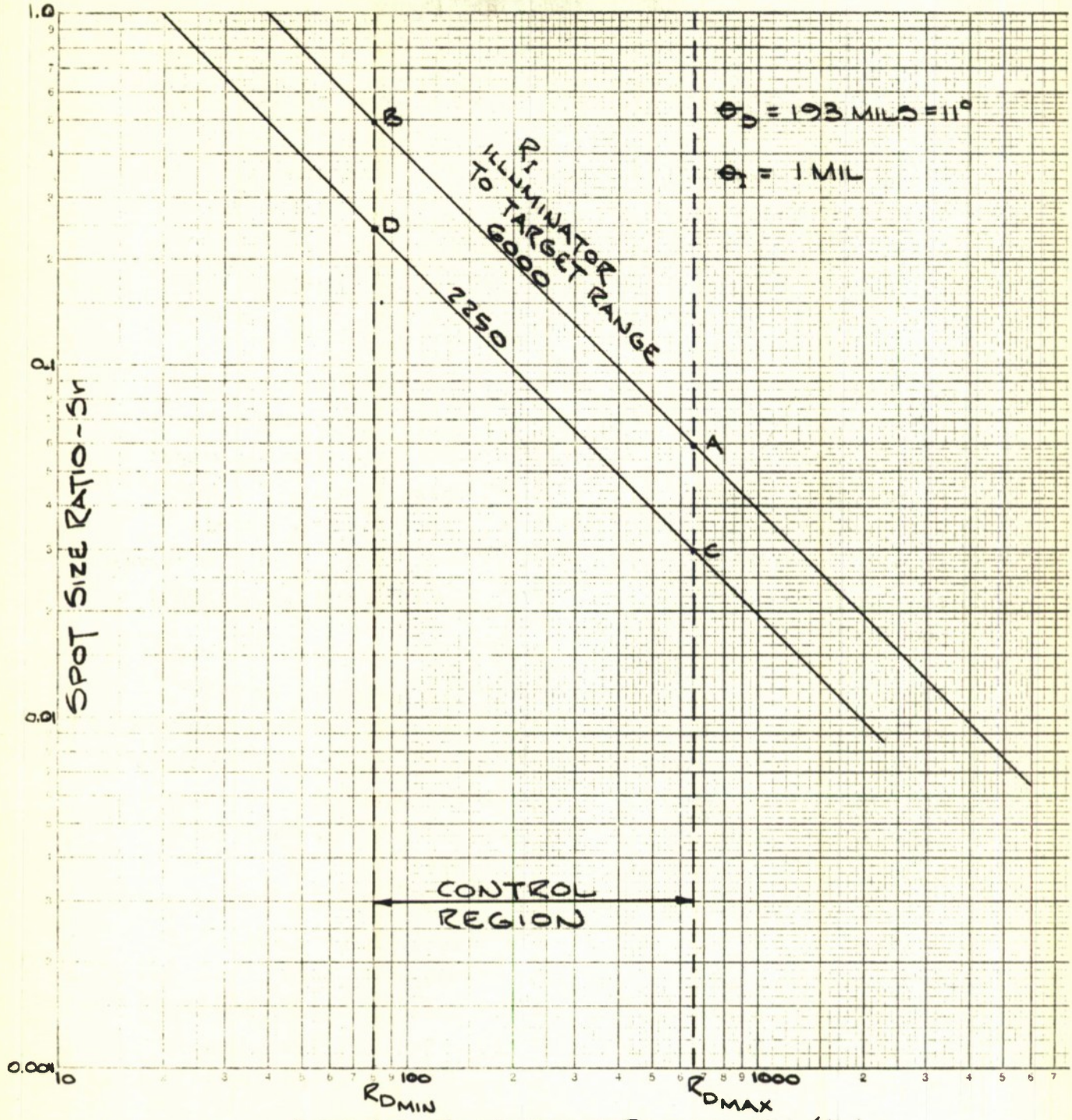

FIG. 3.4-3

SPOT SIZE RATIO VARIATION

3.4.7.1 Seeker Angle Measurement System - Principle of Operation

The seeker recommended for POLCAT will employ spherical coordinate measurement techniques. Referring to Figure 3.4-4. the target is at T, the projectile at P. The axis of the projectile is along PO. Plane XOY contains the target and is assumed to be perpendicular to the axis of the projectile PO. Plane POY is a vertical plane.

The coordinates of the target are given by its polar angle ϕ , its radial angle λ , and its range r. The system does not have to measure polar angle ϕ_T with respect to any space fixed reference; it need only determine the instant at which the polar angle is zero with respect to a reference plane POR which is rotating with the projectile; that is it must know when $\phi_T = \phi_c$. The plane POR represents both the seeker polar reference plane and the impulse control plane.

The key to the seeker operation is its reticle, several forms of which are shown in Figure 3.4-5. There are basically two detectors in each case, respectively marked (1) and (2). The shaded areasa re non-sensitive, the dotted circle represents the target image. Since the projectile spins, the target image traces out a spiral or circular path on the face of the detector.

It will be noted that the detectors are rotationally asymmetric, in fact, each has a principal radius terminating at t_3 and t_3' respectively. The principal radius divides detectors (1) and (2). The function of the principal radius is to provide target polar angle information. When the relative polar angle is zero the position of the control impulse relative to the target is known.

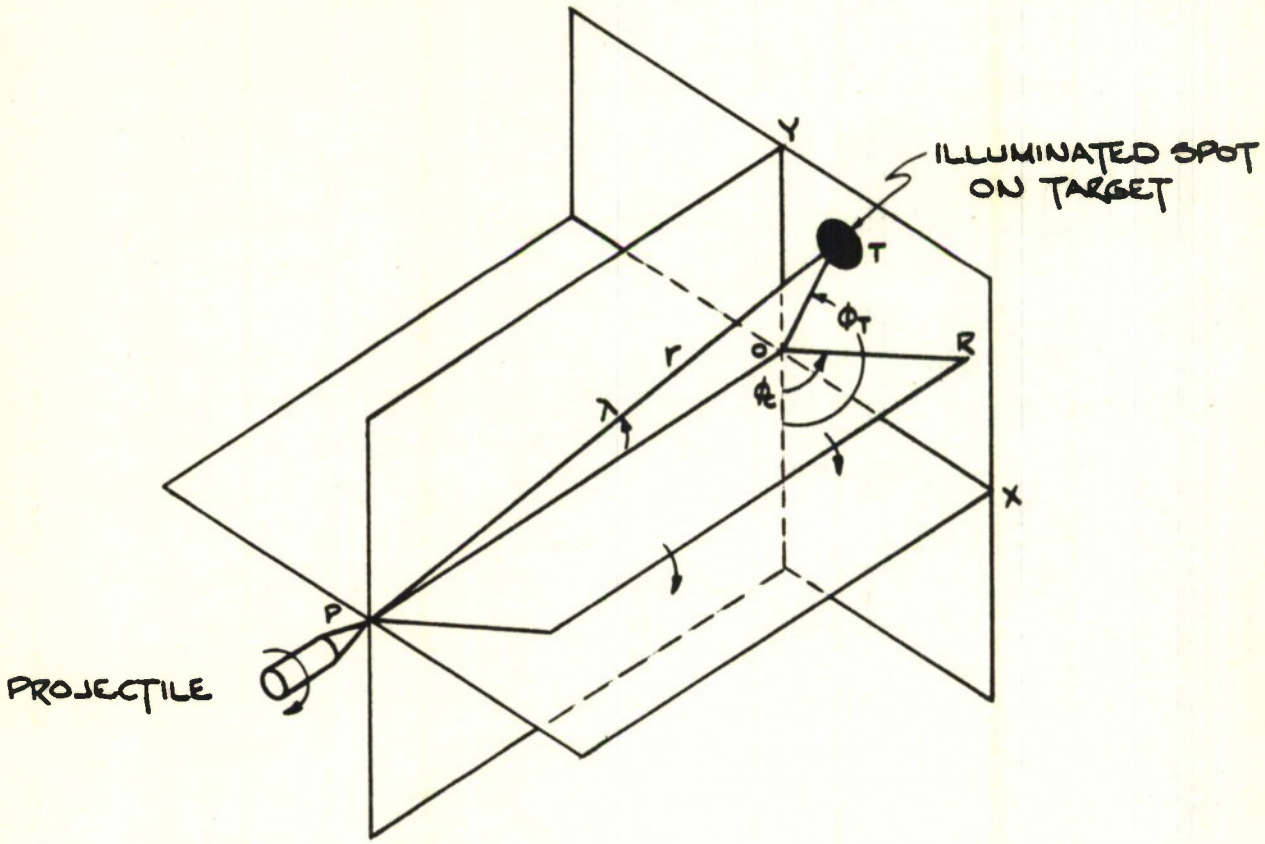

FIG. 3.4·4

COORDINATE GEOMETRY for SEEKER

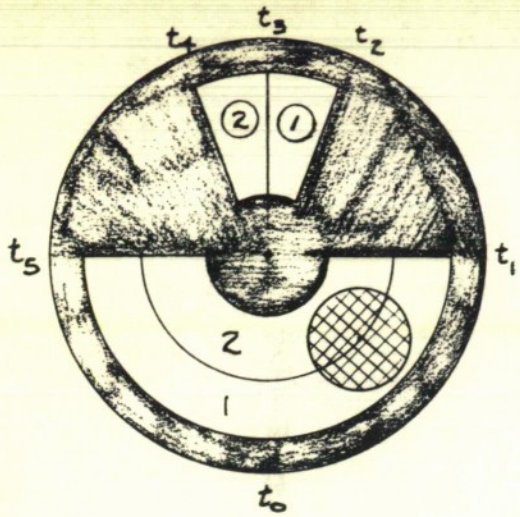

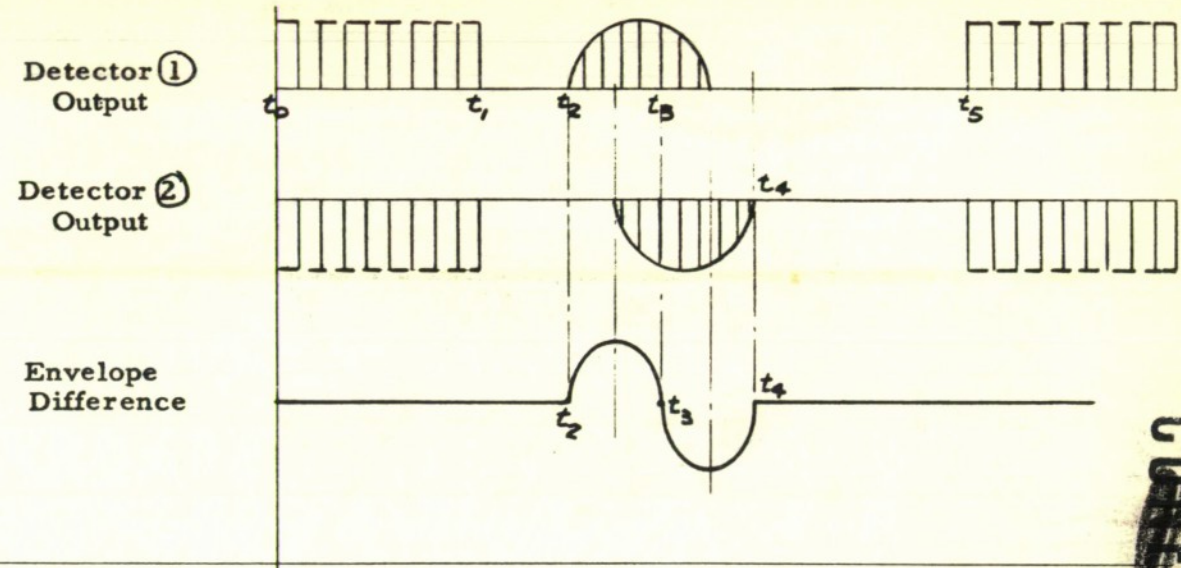

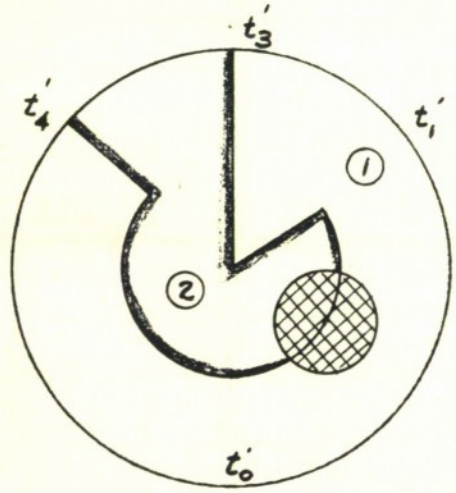

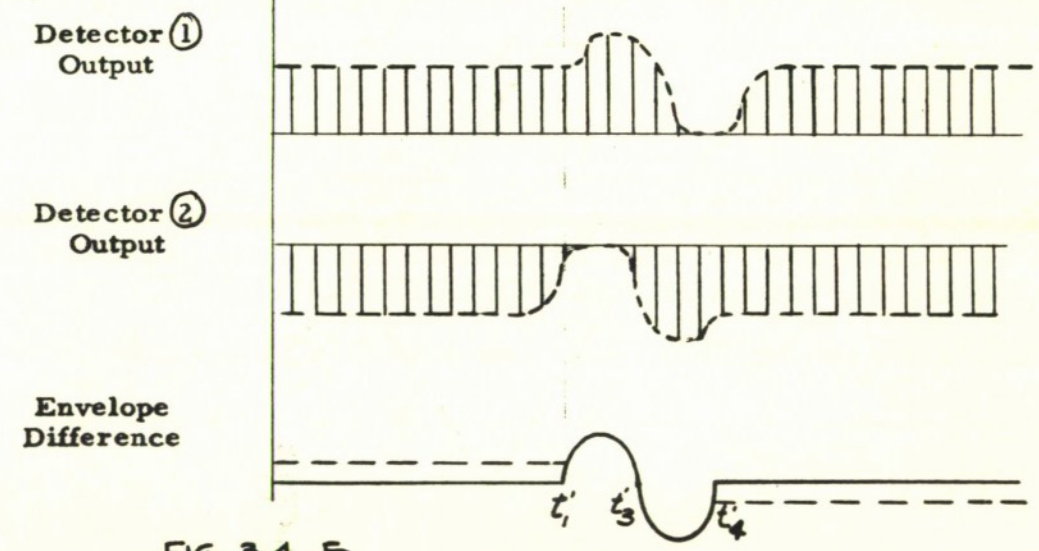

FIG. 3.4-5

RETICLE CONSIDERATIONS

The detectors also have a principal circumference which separates detectors (1) from (2). The function of the principal circumference is to provide target radial angle information. When the relative radial angle is zero the magnitude of the error in the target line-of-sight is known to be the value at which corrective action should be taken. Figure 3.4-6 shows various conditions under which angular measurements can be made.

3.4.7.2 Seeker Design Considerations

As noted in Section 3.2.3.1 Corning Vycor glass No. 7900 shaped into a hemisphere with a thickness of 0.1 inch will satisfy the mechanical requirements of the system. This glass will have a transmittance of 0.9 in the infrared region of interest.

The optical system of the seeker is shown in Figure 3.4-7. A modified cassegrain system is used having a speed of approximately f/1. The primary mirror consists of two Mangin spherical sections which, in effect, remove the aberrations due to the spherical primary mirror as well as those of the hemispherical irdome. The secondary mirror is planar and is placed at the principal focus of the primary mirror. To reduce the size of the image on the detector cell, a field lens is used which has an inverse magnification of 4. Distortion of the target image is not felt to be serious since the system, in effect, determines the centroid of the image, the effect of distortion on determination of the centroid postion being a second order effect.

It should be noted that the foregoing represents only one of the possible combinations of optics, reticles, and detectors which can determine the centroid of a target image.

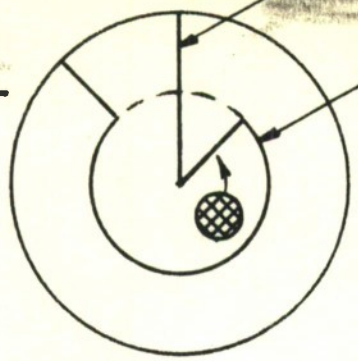

(a) INCORRECT POLAR AND RADIAL ANGLES

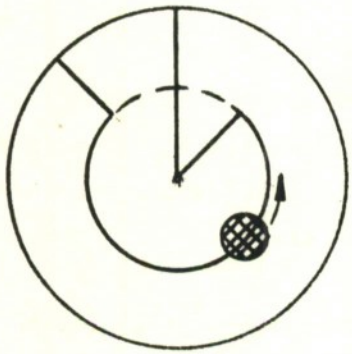

(b) CORRECT RADIAL ANGLE, INCORRECT POLAR ANGLE

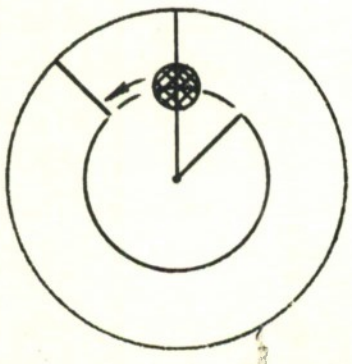

(c) CORRECT RADIAL AND POLAR ANGLE

FIG. 3.4-6

CONDITIONS for ANGULAR MEASUREMENT

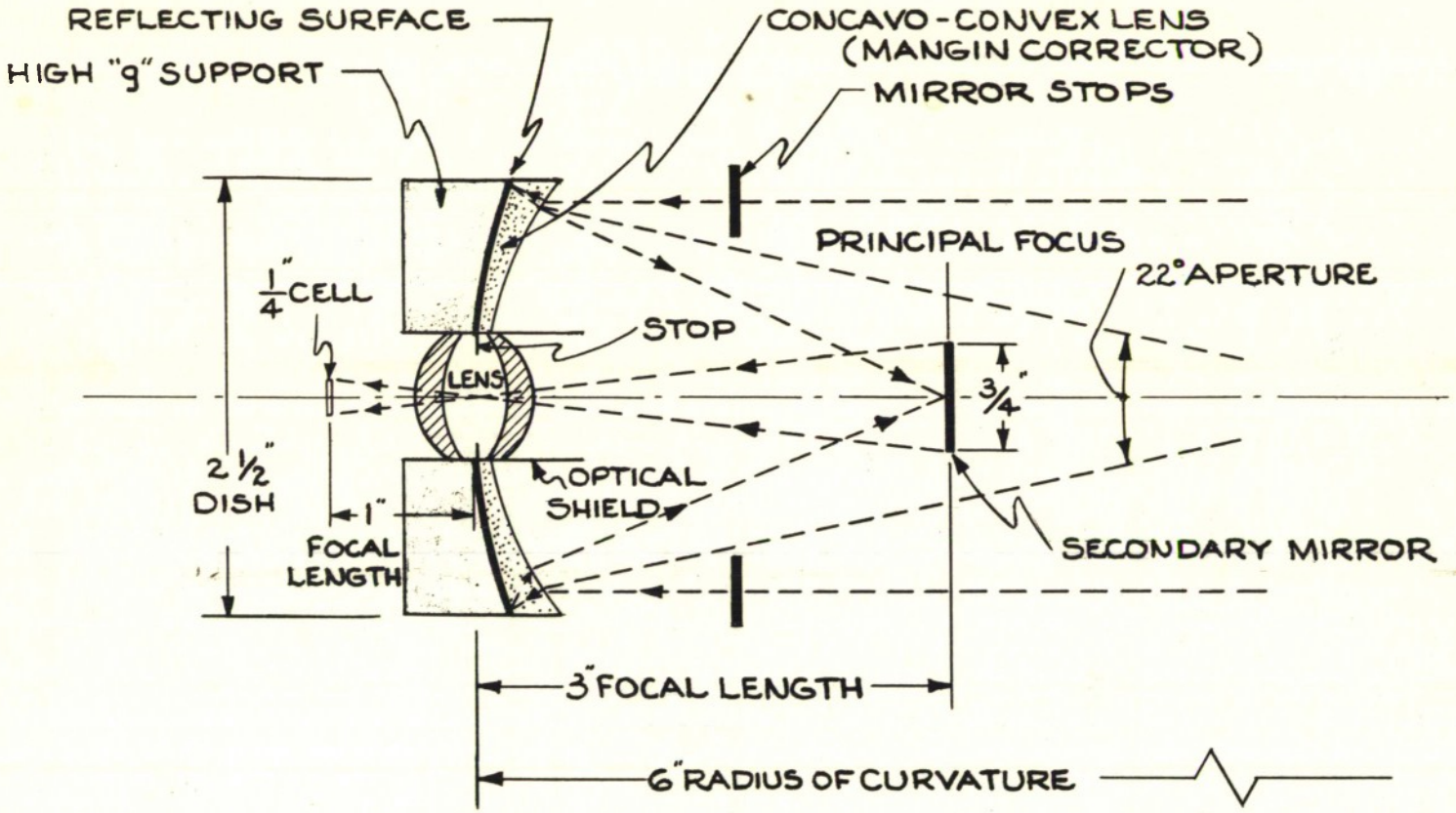

FIG. 3.4-7

LARGE SPOT OPTICAL SYSTEM

The seeker detector selected is the PbS cell which has excellent sensitivity at room temperature over the spectral range 0.8 - 2.0 μ. The noise equivalent power of the receiving system can be shown to be given by

$$NEP = S \sqrt{A\left(\frac{\Delta f}{f}\right)\left[1 + (2\pi f \tau)^2\right]}$$

where the various factors are defined below:

S = Jones' sensitivity factor

Δf = receiver bandwidth

f = chopping frequency

τ = detector cell time constant

A = detector cell area

The area of the detector is given by

$$A = \frac{\pi d^2}{4}$$

$$d = F\,\theta = D\,\theta\,(f/\#)$$

where

d = diameter of detector

F = focal length of seeker optics

θ = field of view of seeker optics

D = diameter of seeker optics

(f/#) = speed of seeker optics

Combining the various equations yields

$$NEP = S \sqrt{\frac{\pi}{4} D^2\,\theta^2\,(f/\#)^2\left[1 + (2\pi f \tau)^2\right]\left(\frac{\Delta f}{f}\right)}$$

As the equation stands, all factors must be minimized for minimum NEP with the exception of the chopping frequency f. The quantities D,

and θ are fixed by other than guidance considerations, the quantities S and τ are a function of the dectector selected. Obviously for low NEP the ratio $\left(\frac{\Delta f}{f}\right)$ must be small which dictates that the receiver bandwidth be considerably less than the chopping frequency. The chopping frequency itself is closely dictated by the spin rate of the projectile, the spot size and the position of the spot on the detector. That is, the target spot only appears on the detector when the illuminator is on, since the illuminator provides the chopping. If the spot size is very small, and the chopping frequency is low the successive target spot images will not overlap and an inaccurate polar measurement will result.

A block diagram of the proposed system is presented in Figure 3.4-8. It is a dual channel system comprising identical logarithmic amplifier channels. The use of logarthmic amplifiers eliminates the need for AGC circuitry. A gated system with a delay period equal to the illuminator lamp pulse interval gates out the lamp frequency and thus provides automatic target discrimination. Both channels feed into a difference detector producing a voltage proportional to the absolute difference in channels A and B. This LOS information is fed to the LOS pulse generator which produces a trigger pulse only when the voltage A-B equals or exceeds the steering law reference voltage.

The output of the difference detector also contains the polar angle information and is fed into a differentiating circuit. This passes only the polar data which in turn is used to trigger the polar gate generator. A polar gate is generated for each revolution of the projectile and thus always appears at the coincidence circuit. The ballistic timer is in series with the cartridge circuit and therefore prevents its operation until a certain period has elapsed. When the LOS angle builds up to its critical value, a pulse will be generated and permitted to pass by the polar gate, thus actuating the cartridge.

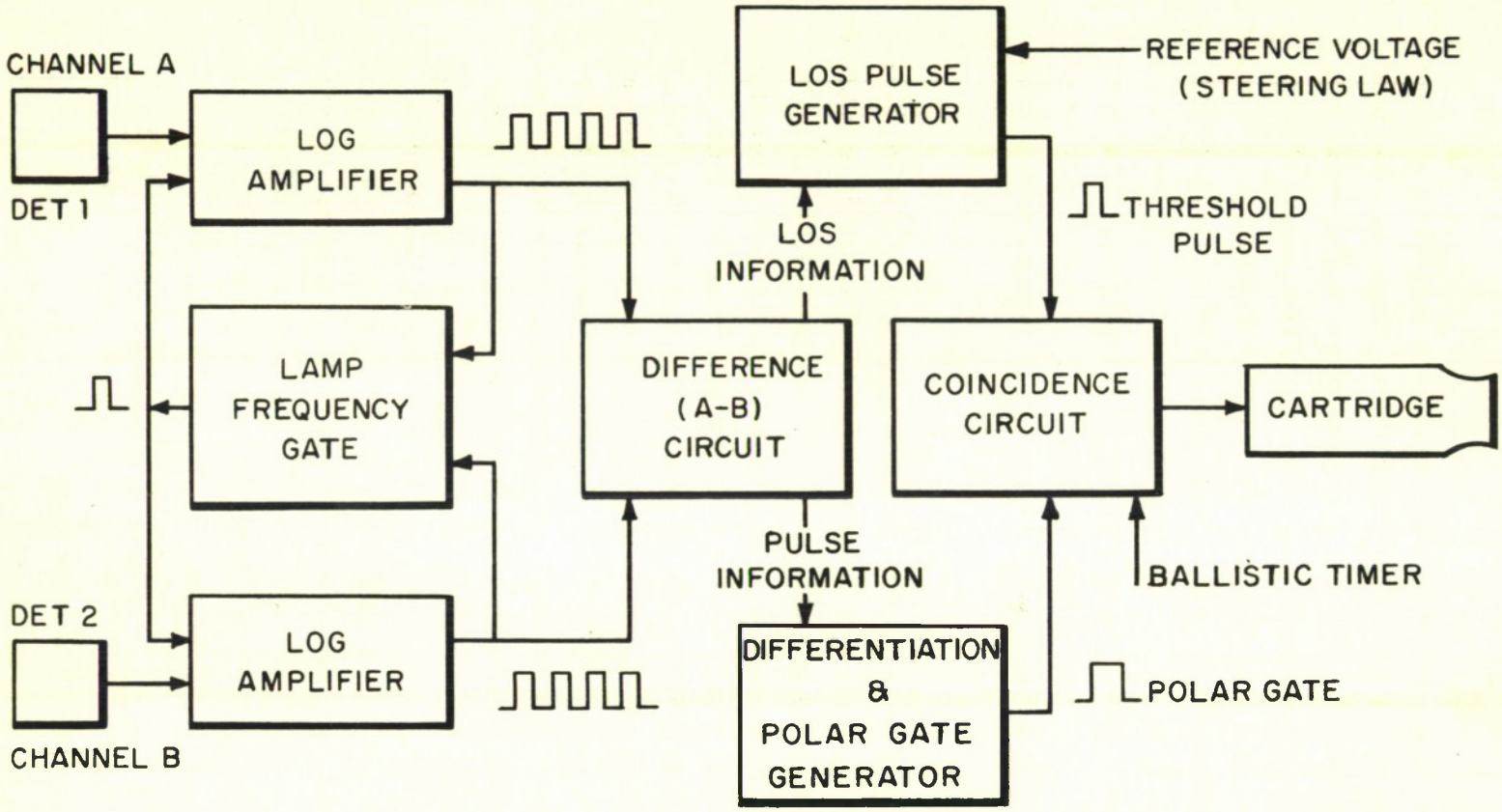

FIG. 3.4-8

SEEKER BLOCK DIAGRAM

3.5 LAUNCHING

The use of the recoilless rifle as the projectile launcher provides a combination of weight and accuracy for launching system that is uniquely compatible with the antitank mission. The logic of recoilless rifle launching is based primarily on the inability of other launching techniques to fulfill both the accuracy and the weight requirement. This is indicated by

(1) comparing gun launching with rail or rocket boosted launching

(2) comparing the two types of guns -- recoil and recoilless.

For the purposes of the immediate discussion, the difference between gun launching and rail launching is defined by the conditions of projectile motion during the period of projectile acceleration. In gun launching, the projectile angular orientation is highly restrained by the gun tube. The only effects that cause initial deviations in projectile flight occur as the projectile leaves the gun tube (muzzle blast and barrel whip). In rocket boosted launching, a considerable portion of the acceleration takes place after the missile has left the rail. Acceleration can be directed away from the desired launching path by any spurious airframe motion. The resulting variation in projectile flight path angle at the end of boost is substantial as indicated in Figure 3.1-23 where σ_{ss} is given for powered and unpowered projectile flight. The only means for decreasing the launching dispersion of this type is to increase acceleration and decrease burning time; the minimum being reached with gun launching. However, in the practical consideration of rail launching, the accelerations are relatively low but the initial dispersion is high (25 to 40 mils). Further, a missile launched in this manner does not attain required velocity until it has traveled a considerable

distance from the gun thereby establishing minimum target engagement ranges. Gun launching permits point blank engagement of targets and minimizes the requirements of post firing correction at long range by virtue of its ability to place the projectile on a relatively accurate trajectory. The latter is particularly significant in that simple control techniques of limited effectiveness can be utilized. Thus, with regard to the specific, short range antitank mission, gun launching is essential in providing unrestricted weapon deployment.

In comparing recoil and recoilless guns for launching, the advantages of the recoilless gun are immediately apparent. While the recoil gun is more accurate, its heavy weight and higher launching accelerations severely handicap its consideration in the specified mission. Unquestionably, the recoilless gun represents the most logical compromise. It is more accurate than rail launchers and much lighter than conventional recoil guns.

At the present time there are several sizes of recoilless rifles that are used operationally. These include 57mm, 75mm, 90mm, and 105mm rifles with development of recoilless rifles 120mm and larger being currently considered by Frankford Arsenal. Of these the 105mm is selected for the POLCAT system based on lethality and weapon development considerations. The 105mm recoilless in the form of the M40 gun system represents an operational gun system that is capable of delivering a relatively large warhead. Preliminary calculations have indicated that with modification this gun fulfills the requirements of launch as given below.

(1) Muzzle velocities of approximately 1650 ft/sec must be imparted to the POLCAT projectile weighing 23.4 pounds.

(2) The standard deviation of muzzle velocity error must be approximately $\pm$ 15 ft/sec.

(3) The gun must be rifled to provide initial projectile spin rates of 19 $\pm$ 2 RPS.

The initial specification appears to require a gun energy in excess of the design performance of the existing gun. However, using the more contemporary techniques for recoilless rifle design (see Reference 55), it is believed that the specified performance can be attained without increasing gun weight. This aspect of the weapon system has not required any extensive attention since the personnel at Frankford Arsenal have continually provided the necessary counsel whenver problems involving the recoilless rifle performance, design, etc. influenced the overall weapon system study.

3.6 FIRE CONTROL

Within the POLCAT application, the basic function of fire control is to provide a simple, yet accurate means for directing the gun launched projectile. Since the projectile is capable of post firing correction, the accuracy requirements of the fire control system are dictated by the capabilities of the projectile guidance and control system and by the performance of the recoilless rifle and the controlled round. The objective of the immediate discussion is (1) to define the relationship between fire control and post firing correction and (2) to select those equipments that fulfill the requirements of fire control for the POLCAT Weapon System.

3.6.1 Use of Fire Control in POLCAT Weapon

In conventional ordnance weapon systems, the hit capability of the weapon is dependent to a great extent upon the accuracy of its fire control. This being the case, the size, weight, and complexity of fire control is often compromised in order to improve weapon accuracy. However, since probability of hit of the conventional ordnance system is not a function of fire control accuracy alone, but is also influenced by aiming error and the inherent dispersion of the ammunition, miss distance approaches an irreducible minimum with "perfect" fire control. To illustrate this basic limitation, the probabilities of hit of the BAT weapon, described in Reference 56, are examined. For a given combination of spotting rifle and fin stabilized ammunition, the probability of first-round hit versus range is shown in Figure 3.6-1. These probabilities were computed assuming the spotting round impacts to be normally distributed on a 7.5' by 7.5' target. For the BAT weapon system, the spotting rifle technique serves as a fire control system.

Considering the round-to-round dispersion of the major caliber round as the only source of error, the proabilities are recomputed and the results, indicated in Figure 3.6-1 by the dashed curve, represent the BAT weapon probability of hit for the same projectile dispersion but with "perfect" fire control. It is to be noted that any contemplated improvement in fire control will yield a relatively small increase in probability of hit. At this point, post firing correction offers the only means for overcoming this basic limitation on hit probability. However, once the weapon system is committed to the utilization of post firing correction both the function and the requirements of fire control are subject to change. In the POLCAT concept, the function of fire control is to merely limit the deviations of projectile flight from target impact trajectories as dictated by the steering capability of the post firing correction system. The accuracy, then, of fire control within the POLCAT system is established by requirements that are compatible with the capabilities of in-flight guidance and control, and consistent with the performance of the gun ammunition. As a consequence, the quality of fire control for POLCAT can be reduced somewhat. This is shown in Figure 3.6-2 where the effect of applying post firing correction to a recoilless system using different types of fire control is given. Probability of first-round hit is indicated for uncontrolled projectile flight as determined by optical fire control and by spotting rifle. Both probabilities are based on the same gun and equal round-to-round dispersions. Despite the superiority of the spotting rifle as a fire control technique, the two systems have equal probabilities of hit when post firing correction is employed. These results, which are given in detail in Section 3.8, provide the basis for removing the spotting rifle from the recoilless gun in the POLCAT system and replacing it with simpler fire control equipment.

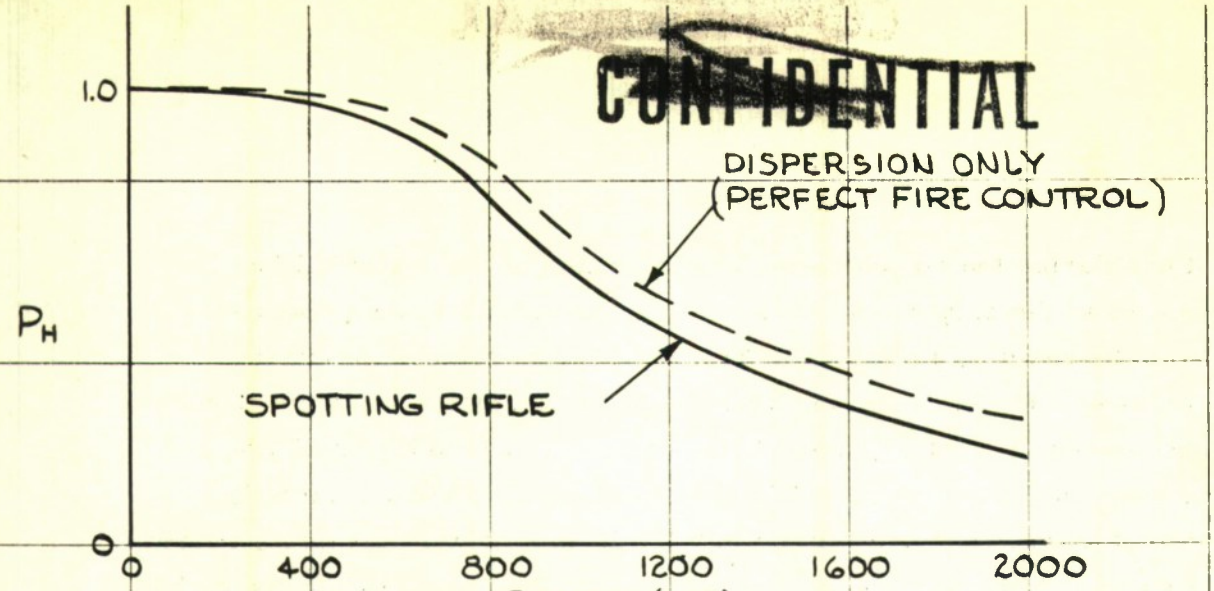

FIG. 3.6-1

BAT SYSTEM HIT PROBABILITIES

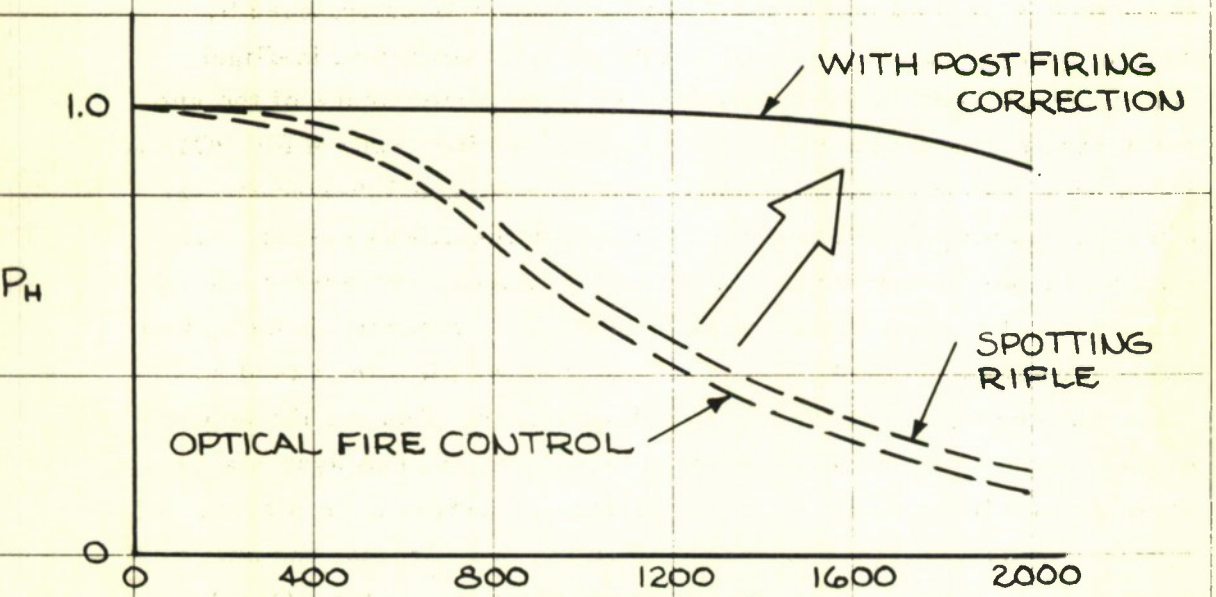

FIG 3.6-2

EFFECT OF POST FIRING CORRECTION
ON HIT PROBABILITY

3.6.2 Recommended Fire Control for POLCAT Weapon

As indicated earlier, the impulse control and infrared seeker requirements are predicated on a three standard deviation of impact error of 5 mils for uncontrolled projectile flight out to 2000 yards. It is required, then, to select fire control equipment capable of this accuracy assuming the round-to-round dispersion of the POLCAT projectile to be equal to the dispersion of standard, fin stabilized recoilless ammunition. This accuracy can be achieved using a standard telescope and an optical range finder. See Table 3.6.1 for performance summary. Since the telescope had been used on the BAT weapon in conjunction with the spotting rifle, the incorporation of the range finder represents the only change in the known conditions of recoilless weapon deployment. The accuracy of this component is given in Figure 3.6-3. These data, obtained from Reference 57, indicate that several existing range finders possess the accuracy assumed for analysis. For the purposes of preliminary system integration, the coincident type range finder is selected. This choice represents a class of existing range finders that fulfill a specific requirement rather than the result of a study wherein a detailed evaluation of range estimation techniques is made. Any future work in this area would include such an evaluation as well as an investigation of techniques to provide the POLCAT system with a night and poor weather capability. This latter effort would require that the lamp be integrated with fire control to provide a secure, broad beam target search capability in addition to providing target illumination.

TABLE 3.6.1

PERFORMANCE of OPTICAL FIRE CONTROL SYSTEM

Function	Characteristics
Target Search and Acquisition	Visual, unaided eye
Target Line of Sight with Telescope	
Type	Elbow
Field of View	12°
Magnification	3x
Accuracy	± 0.1 mils
Optical Range Finding	
Type	Coincident
Field of View	3°
Magnification	14x
Range Accuracy	± 5%

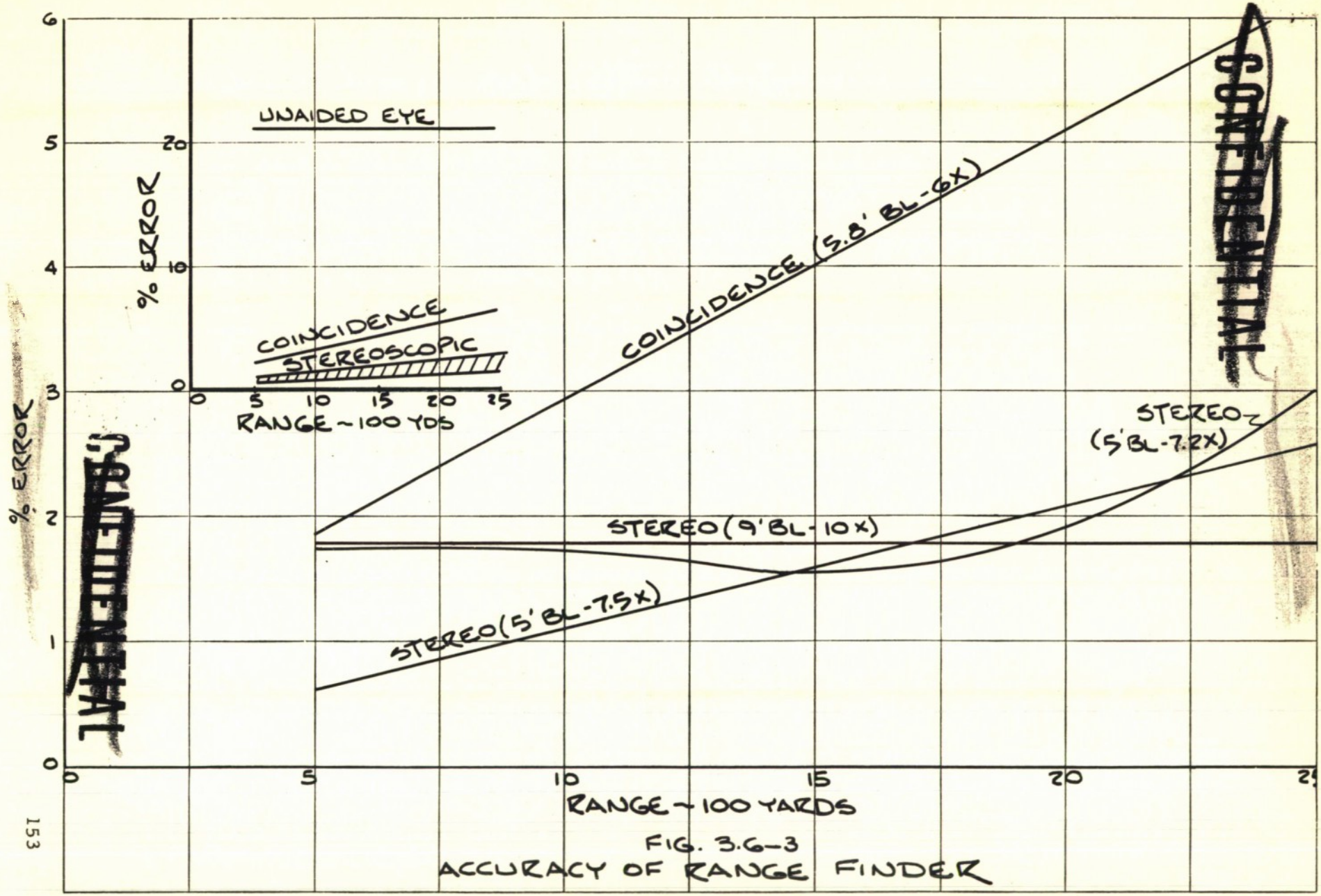

FIG. 3.6-3
ACCURACY OF RANGE FINDER

3.7 WARHEAD AND FUZING

While there are several types of warhead that could suitably be incorporated within the POLCAT projectile, the study has considered only the shaped charge. This selection does not, however, reflect any limitation in the given projectile design since the shaped charge presents the most rigorous design requirements in order to achieve satisfactory warhead performance. Further, the shaped charge provides the most effective means for defeating heavy armor. In view of the sensitivity of shaped charge performance to the geometrical and the dynamic characteristics of the projectile, the design and the installation of the warhead and fuzing system contemplated for POLCAT are, insofar as possible, patterned after current design practices. The following discussion considers, first, warhead performance and, then, the fuzing system.

3.7.1 Warhead Performance

The POLCAT warhead design includes the requirements essential to the penetration of homogenous armor. These requriements are derived from the shaped charge design of the 105mm T119E14 projectile and the warhead studies given in Reference 58.

(1) Projectile spin rate is limited to 20 RPS.
(2) Weight of explosive is 3.5 lbs.
(3) Jet interference in the nose assembly is minimized.
(4) Standoff is greater than two cone diameters.
(5) Cone size, shape, and attachment to the body, are consistent with optimum shaped charge effectiveness.
(6) Projectile body is designed to provide adequate charge confinement.

The effect of spin rate on depth of penetration has received extensive examination and is well known. Figure 3.7.1 gives the decrease in penetration for surface velocity as obtained experimentally. The original data indicate that despite differences in cone diameter, the spin effects on penetration correlated extremely well with the parameter, surface velocity ($\dot{\phi}r$). By limiting the POLCAT projectile spin rate to 20 RPS it is expected that the shaped charge penetration is equivalent to the more effective 105mm, HEAT rounds.

In the design of the nose assembly of the POLCAT projectile, every attempt is made to provide "free" space forward of the shaped charge. While this is accomplished to a considerable extent by careful component layout, it is required that various elements of the seeker be placed forward and along the axis of the shaped charge. However, the nature of these materials to be perforated by the jet is such that no reduction in target penetration is expected. The electronic equipments of larger thickness are placed around the periphery of the nose cone thereby minimizing interference with jet formation.

A critical parameter to shaped charge effectiveness is the standoff distance; the effect on penetration being given in Figure 3.7.2. These data, presented in Reference 58, indicate that the standoff provided by the POLCAT design is short for maximum penetration. However, the selected standoff distance is adequate and considerably more practical for overall projectile design.

3.7.2 Fuzing System

The fuzing system relative to the warhead is similar to those incorporated in existing HEAT rounds. However, the fuze of the POLCAT projectile has the additional functions of providing safety in handling

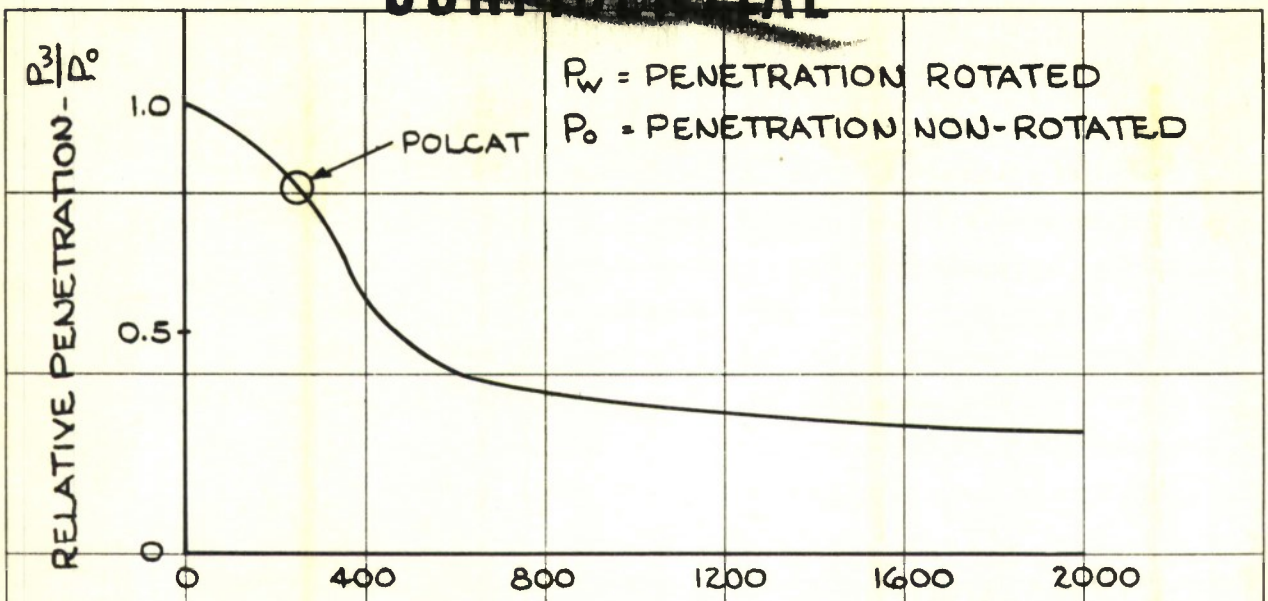

FIG. 3.7-1
RELATIVE PENETRATION VERSUS SURFACE VELOCITY.

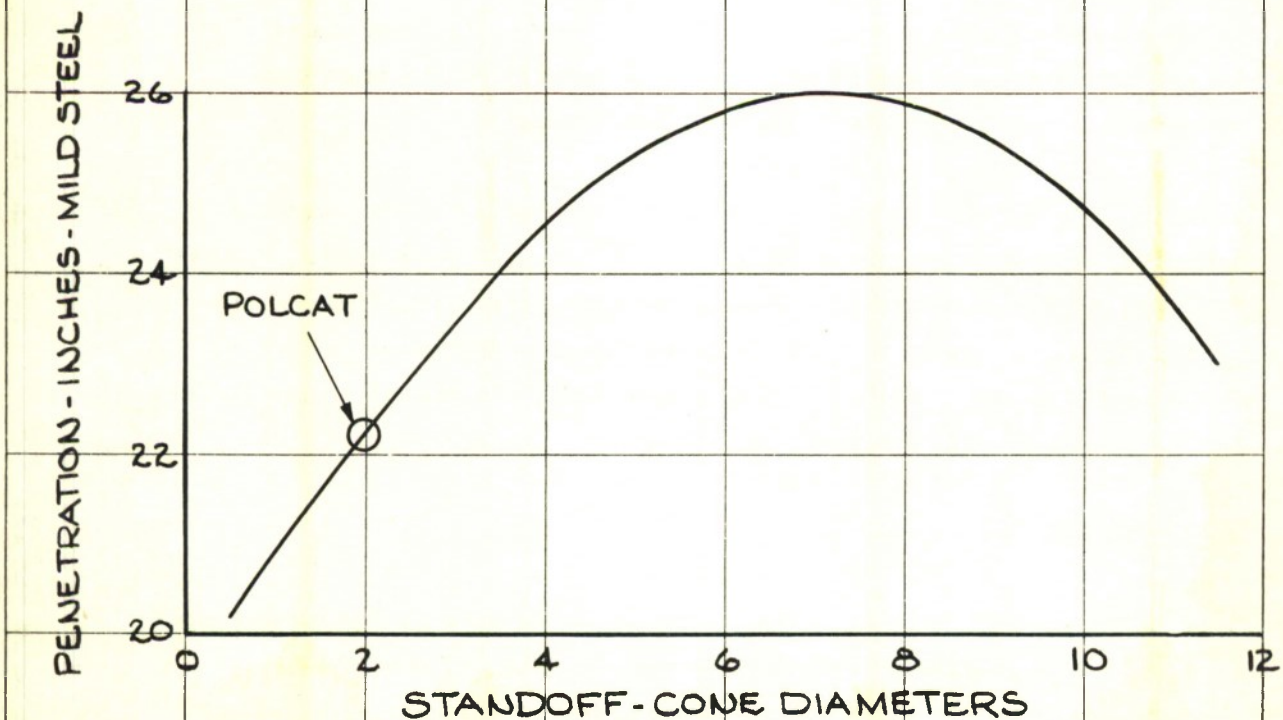

FIG. 3.7-2
PENETRATION VERSUS STANDOFF

with regard to the control cartridge as well as the shaped charge and activating the seeker power supply at launch. The fuze incorporated behind the warhead provides suitable safety and arming after setback by:

(1) Rotating an electrical detonator into line with the warhead booster.

(2) Removing the short circuit between the detonator and the warhead initiator assembly in the projectile nose.

(3) Removing the short circuit between the seeker system and the batteries also located in the projectile nose.

Warhead initiation is provided by five piezoelectric crystal or "Lucky" elements connected in parallel. This arrangement of initiators which assures warhead functioning at the highest angles of obliquity has been tested successfully in the laboratories. Impacting one of the "Luckies" in the parallel assembly produced the required output. The energy losses across the entire load was not detectable.

Since the infrared seeker system initiates the control cartridge, the latter is armed after the battery power is supplied to the seeker and subsequent cartridge initiation is furnished by the seeker power supply.

3.8 SYSTEM ANALYSIS

The final examination of the POLCAT weapon system presented in this section consists of:

(1) Establishing the mutual dependence of the various system components and determining the manner in which each of the sub-systems contributes to fulfilling the over-all system requirements.

(2) Evolving the steering law based on the capabilities of both the guidance and control system, and the assumed trajectory characteristics of the projectile.

(3) Examining the sources of error in the POLCAT system which degrade its performance -- the nature and magnitude of the errors are described.

(4) Estimating the probability of hit for the POLCAT weapon based on the error analysis of (3).

3.8.1 Fundamentals of the POLCAT System

The basis of the POLCAT system operation is primarily determined by the capabilities of the seeker system and the control system, and the flight characteristics of the projectile. The seeker senses both the magnitude of the line of sight angle to the target and the polar position of the target.

The impulse control cartridge is capable of instantaneously changing projectile flight path. Any change in flight path angle is initiated by the seeker which is provided with a pre-determined reference or threshold line of sight angle for control. Further, the target polar angle is perceived only when the control cartridge is oriented to deliver impulse in the target plane. See Figure 3.1-13a. Thus, target polar

angle is measured once every revolution of the projectile. Projectile spin, then, performs the necessary scanning function for the frame fixed seeker; this scanning function being indexed to the control cartridge. The trajectory characteristics of the projectile, discussed in detail in Section 3.1.3, provide the unique quality for post firing correction. With the projectile position relative to the target established by the seeker measured LOS angle, the difference between impact trajectories and miss trajectories is determined by the variation of the LOS angle. The unique characteristic being that the LOS angle of uncontrolled rounds destined to hit approaches zero, whereas the LOS angle of misses, increases rapidly as the round approaches the target.

The manner in which airframe kinematics and seeker operation are combined to initiate control is illustrated in Figures 3.8-1 and 3.8-2. Two conditions must be established prior to functioning the control cartridge. First, the target LOS angle (λ) must equal the pre-selected seeker threshold angle (λ_T). Then, the cartridge polar angle (ϕ_c) must equal the target polar angle (ϕ_T). Figure 3.8-1 shows a typical variation of target LOS angle for a 5 mil undershoot at 2000 yards. When $\lambda = \lambda_T$, the initial requirement for control is reached.

Figure 3.8-2 shows the condition for actual control initiation, $\phi_c = \phi_T$. Since the relation between ϕ_c and ϕ_T is random at the time the LOS angle condition is satisfied, a control delay occurs and is a function of spin rate as well as cartridge orientation at $\lambda = \lambda_T$.

The particular example applies to the POLCAT system design as specified in the previous sections. Considerable variation in the requirements occurs if the performance of any of the system constituents is changed. The interrelationship of system requirements is summarized in Table 3.8-1.

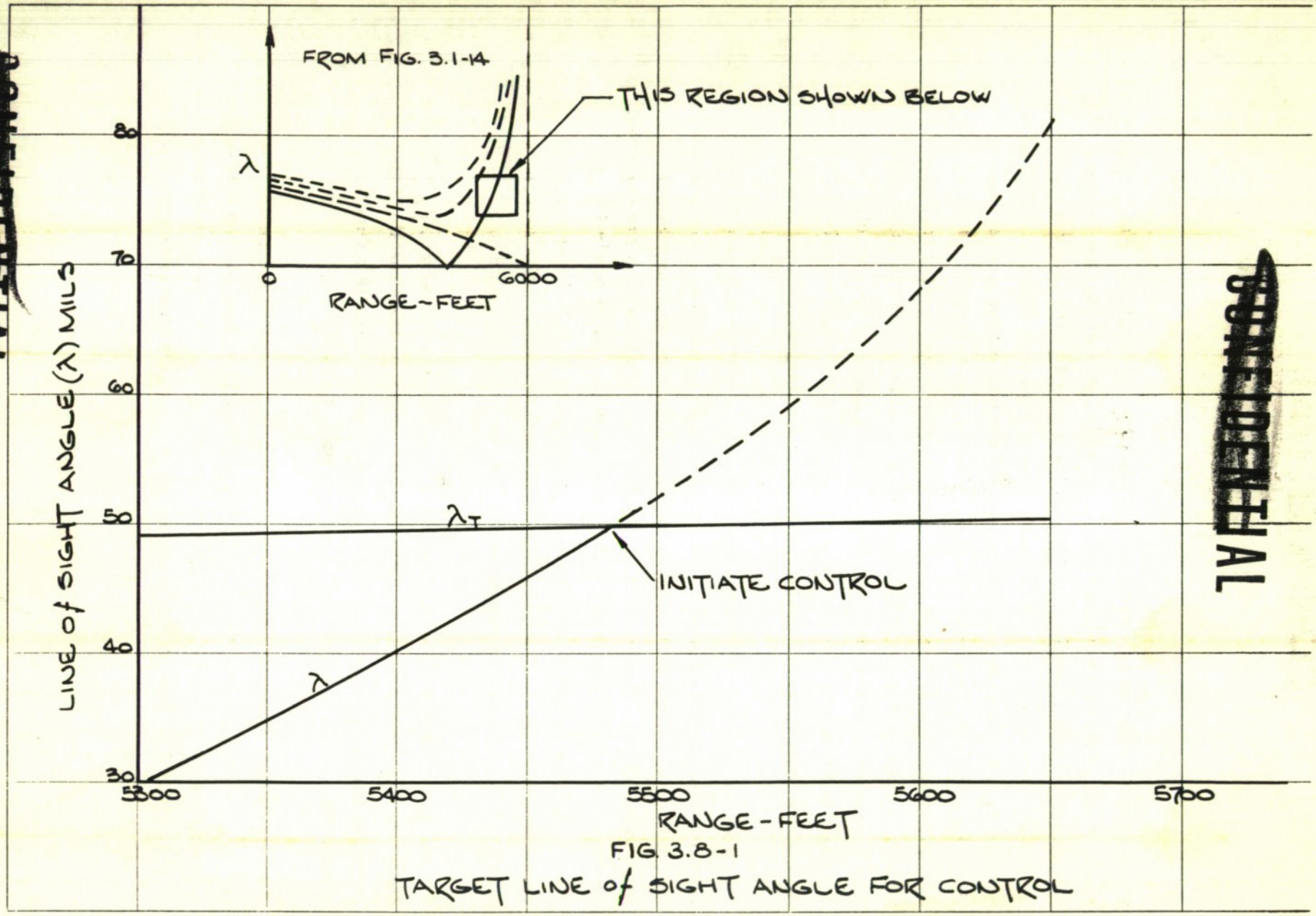

FIG. 3.8-1
TARGET LINE of SIGHT ANGLE FOR CONTROL

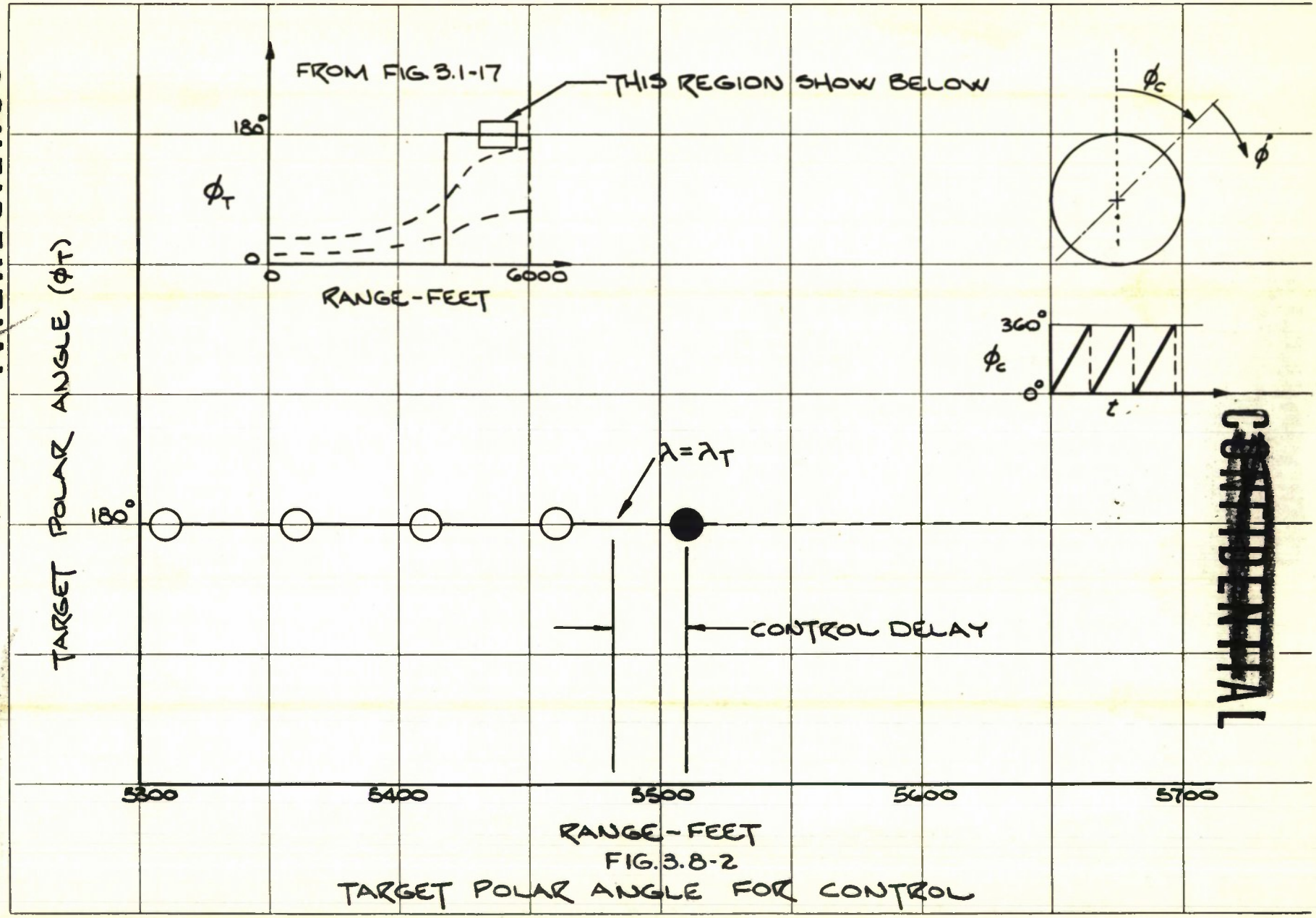

FIG. 3.8-2
TARGET POLAR ANGLE FOR CONTROL

TABLE 3.8-1

SUMMARY OF SYSTEM VARIABLES

System Variable	POLCAT Requirement	Source of System Variation
Miss Distance of Uncontrolled Round	5 mils (approximate)	Fire Control Accuracy Round-to-Round Dispersion
Target LOS Angle	See Figures 3.1-14, 3.1-15, and 3.1-16	Miss Distance of Uncontrolled Rounds Muzzle Velocity Projectile Drag
Impulse Control Magnitude	35 lb/sec	Target LOS Angle Seeker Threshold Angle
Impulse Control Delay	variable, 0 - .05 sec.	Projectile Spin Rate
Seeker Threshold Angle	51 mils @ 2000 yards 45 mils @ 1200 yards	Target LOS Angle Control Magnitude
Seeker Field of View	12^{o}	Seeker Threshold Angle Maximum Target Spot Size (Illuminator Beam Width)

3.8.2 POLCAT Steering Law

The foregoing discussion provides the basis for describing the specific steering law used whenever post firing correction is required. The elements of steering are:

(1) Target LOS angle (λ) has a unique characteristic.

(2) Control is obtained instantaneously and is expressed by $\gamma_c = \frac{I_c}{mV}$.

(3) Target LOS angle is measured by the seeker which possesses a threshold angle (λ_T) that defines the uniqueness of projectile flight relative to hits and misses.

The POLCAT steering law is given by;

$$\gamma_c = \lambda_T$$

for $\lambda = \lambda_T$ and $\phi_c = \phi_T$.

The steering law, then, requires that flight angle be impulsively changed by a magnitude equal to the target line of sight angle at the condition when the target LOS angle equals the threshold angle and when the cartridge has the desired orientation. To establish that the steering law functions in three dimensions in the manner illustrated in Figure 3.8-1, the variation of target LOS angle relative to the seeker image plane prior to control is illustrated in Figure 3.8-3. The various curves represent the different orientations of miss distance at the target as defined in Figure 3.1-13b. This particular case indicates the manner of target LOS variation for a miss distance of 10 yards with the target located at 2000 yards.

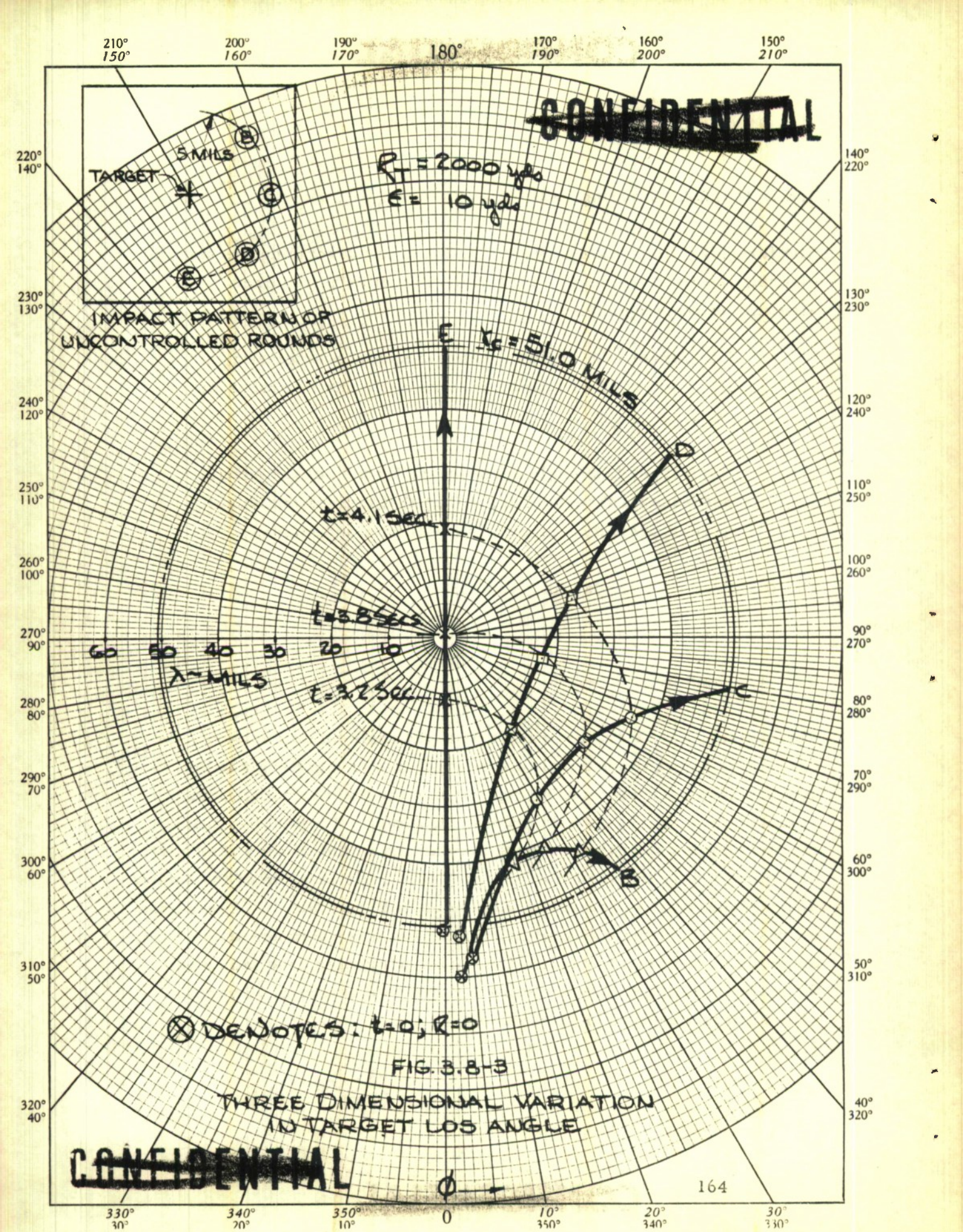

FIG. 3.8-3

THREE DIMENSIONAL VARIATION IN TARGET LOS ANGLE

The limitations of the steering law are associated with the method of generating control, the gravity drop after control, and terrain clearance. Since control is expressed by

$$\gamma_c = \frac{I_c}{mV}$$

it is apparent that for a given magnitude of impulse (I_c), flight path angle change varies with velocity. Varying impulse with velocity is impractical, therefore, the steering law is adjusted to account for the change in control effectiveness with range. See velocity-range curve, Figure 3.1-13. Based on the expected variation of velocity with range, the seeker threshold angle is varied with time so that the initial steering law, $\gamma_c = \lambda_T$, can be applied without a degradation in accuracy with varying initial target ranges.

Inherent to the specified steering technique, are the impact errors subsequent to control resulting from gravity. Since the projectile system does not possess a means for sensing the magnitude of range to the target at the instant of control there is no practical method for compensating for the effect of gravity. However, since gravity effects are proportional to time of flight squared, this error can be reduced substantially by establishing relatively high seeker threshold angles, thereby, requiring control to be initiated very close to the target.

The solution for reducing errors due to gravity, however, introduces the problem of terrain clearance. This aspect of the steering law is critical in that the pre-determined seeker threshold angles can be set at levels that permit the projectile to impact the ground short of the target before control is initiated. This situation is illustrated in Figure 3.8-4 where the impulse control angle (which is equal to threshold angle)

SELECTION of CONTROL ANGLE

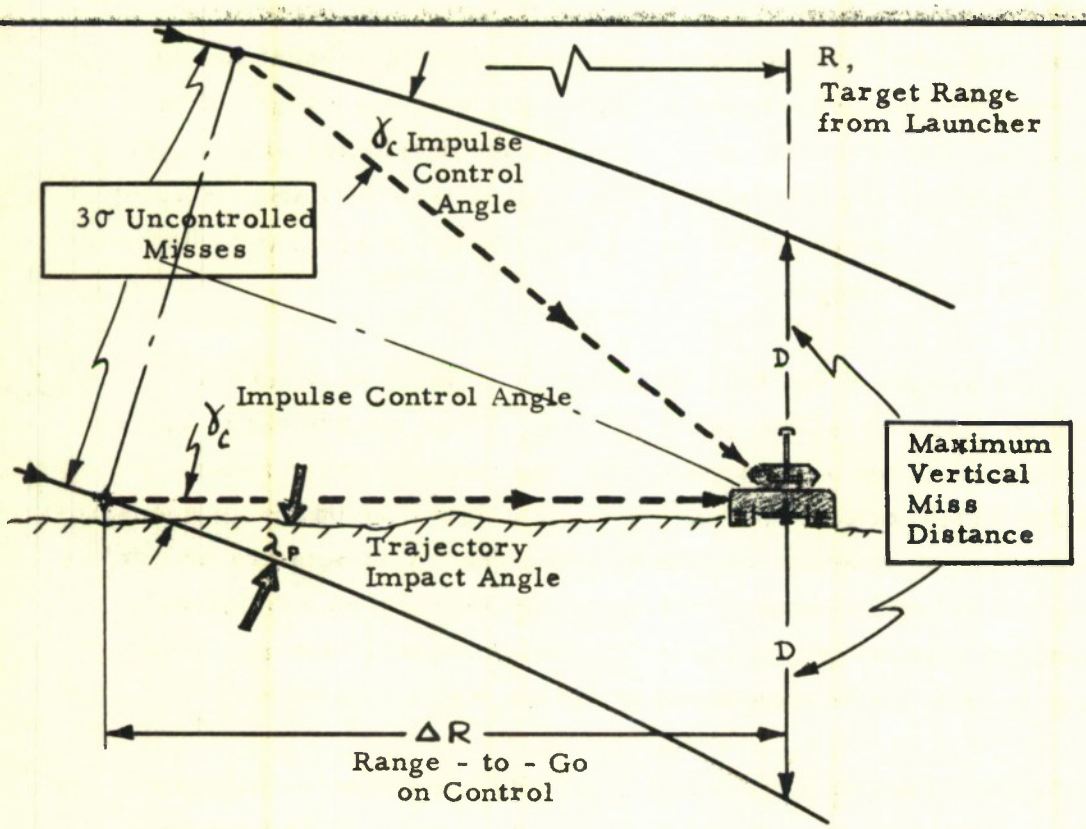

FIG. 3.8-4

is limited by ground impact. This requires the obvious design compromise shown in Figure 3.8-5. At short range, ground effects are critical. At long range, gravity drop is critical; the optimum condition occurring at an intermediate range. The compromise is effected in the POLCAT system by the choice of 35 lb-sec for the magnitude of impulse used in control. The result of this selection is indicated in Figure 3.8-6 where ground impact is shown to be critical at ranges under 1200 yards. The magnitude of these errors as well as the nature and magnitude of the system errors are described in the following section.

3.8.3 POLCAT Error Considerations:

The ability of the POLCAT single-impulse, line-of-sight reference homing system to convert an impending miss into a hit is influenced by a number of factors. Among the most important are the following:

3.8.3.1 Gravity Drop Error:

As shown in Figure 3.8-7a, following impulse control the projectile will not continue in the exact desired course toward the target because of the effect of gravity. Since the simple POLCAT guidance system cannot compensate for such gravity drop errors, it is necessary to design a system which keeps such errors to within tolerable bounds of miss distance by assuring control relatively close to the target. Thus, average ranges to go of several hundred feet assure gravity drop errors of the order of 2 feet or less. For targets represented by a 7.5 ft x 7.5 ft. square, this results in tolerable reductions in hit probability. As is indicated in Figure 3.8-7a, the gravity drop error

$$Z_g = \frac{1}{2} g (\Delta t)^2 = 16.1 (\Delta t)^2 \qquad \ldots\ldots\ldots\ldots \quad (1)$$

- where Δt = time to target impact at the instant of control.

EFFECT of TARGET RANGE on FIXED SINGLE IMPULSE CONTROL

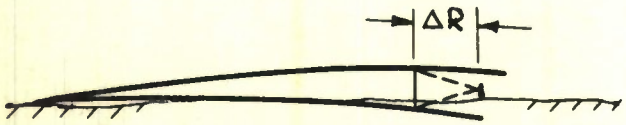

a) R < DESIGN RANGE, $\gamma_c > \lambda_p$
ΔR → smaller; Ground Impact Effects

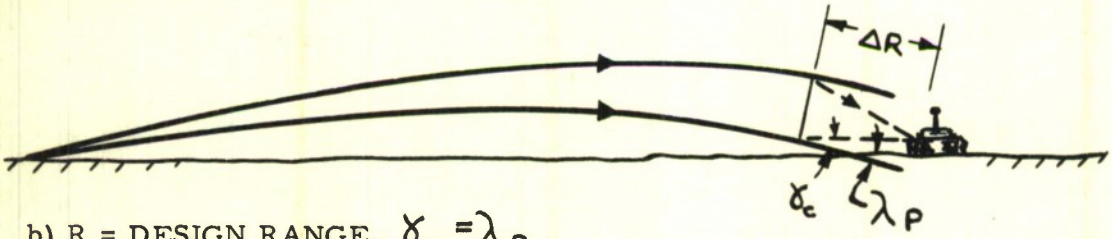

b) R = DESIGN RANGE, $\gamma_c = \lambda_p$

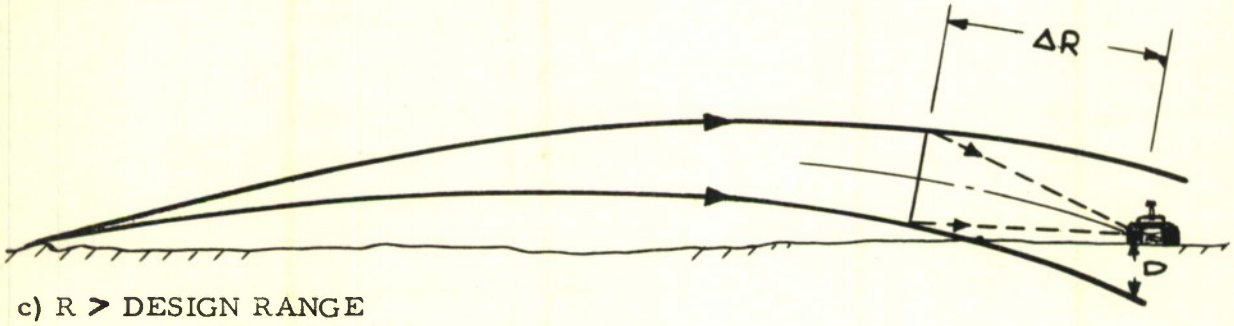

c) R > DESIGN RANGE
(ΔR → Larger)

FIG. 3.8-5

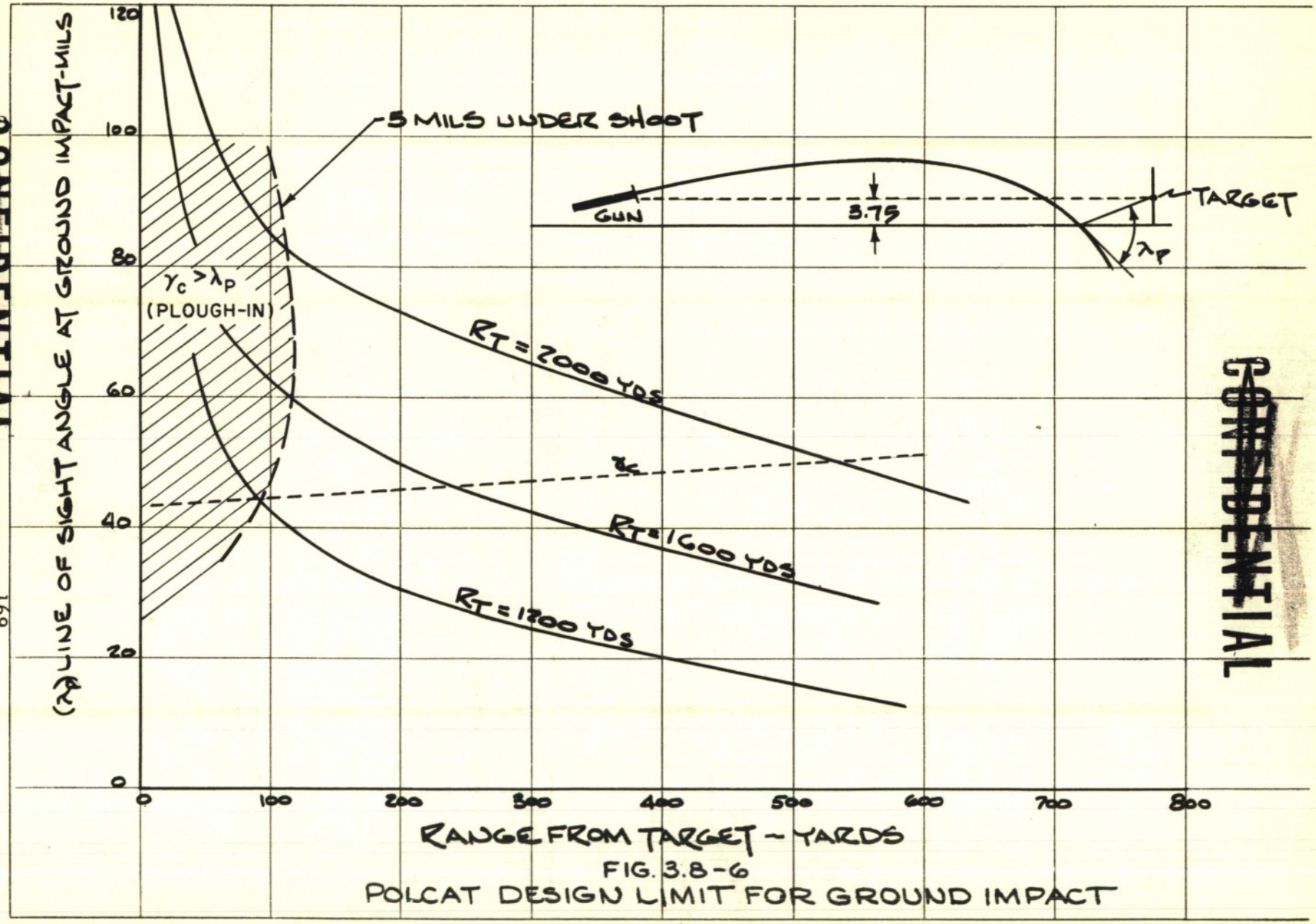

FIG. 3.8-6
POLCAT DESIGN LIMIT FOR GROUND IMPACT

FIGURE 3.8-7

GRAVITY DROP and CONTROL DELAY ERRORS

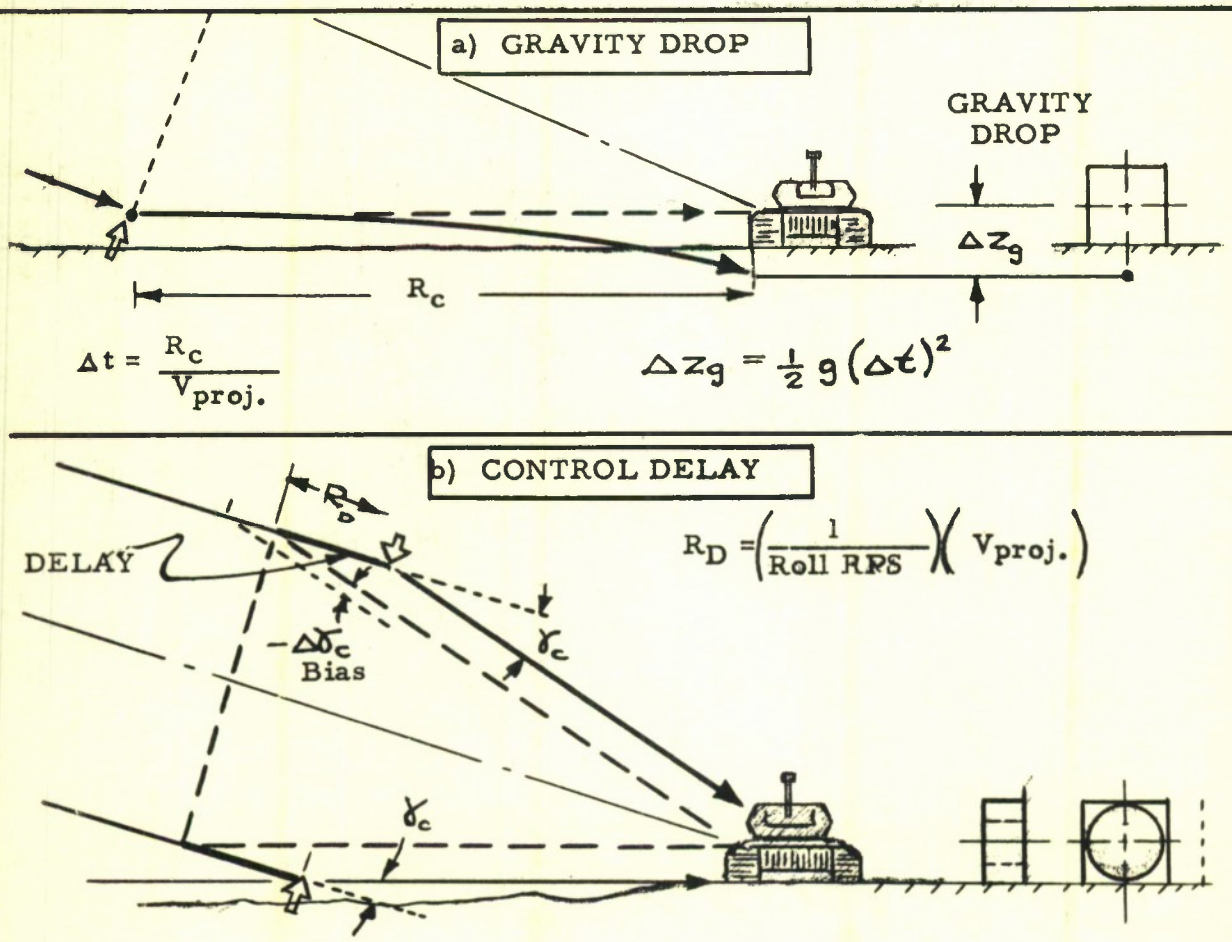

For example, control at a range to go of 300 ft. will result in a vertical drop off of about 1 ft. if we assume a projectile velocity of 900 ft/sec. Figure 3.8-8 shows the specific relationship between gravity drop error, range-to-go at control, and target range (assuming the estimated range-velocity characteristic of the POLCAT projectile).

3.8.3.2 Control Delay Error:

The control delay error, illustrated in Figure 3.8-7b, results from the incorrect orientation in roll of the control cartridge at the instant the critical LOS threshold angle is exceeded. At worst, this control delay may equal the time for one roll revolution of the projectile — assuming a single frame-fixed cartridge nozzle. During this time the projectile will travel a distance

$$R_D = \frac{1}{\text{Roll Rate}} \text{ (Projectile Velocity)} \qquad (2)$$

In turn, the resulting error at the target

$$Z_D = R_D \gamma_c \qquad (3$$

- where γ_c = steering or control angle

As is shown in Figure 3.8-7b, the control delay miss distance is uniformly distributed for all rounds controlled at a given range-to-go, since it is equally likely that the control cartridge will be oriented either fortuitously or unfortuitously the instant the LOS threshold is reached. It is further noted that these miss distances due to control delay tend to be circularly distributed. This is because the points in space where the control impulse is activated are circularly distributed with respect to the target. The maximum miss distance due to control delay can be halved, as shown in dotted lines in the miss distance distribution indicated in Figure 3.8-7b by slightly reducing (i.e. biasing) the LOS

FIGURE 3.8-8

GRAVITY DROP-OFF VS. RANGE-TO-GO at CONTROL for VARIOUS TARGET RANGES

MUZZLE VELOCITY ≅ 1650 ft/sec - 'FOLCAT' Drag Characteristics

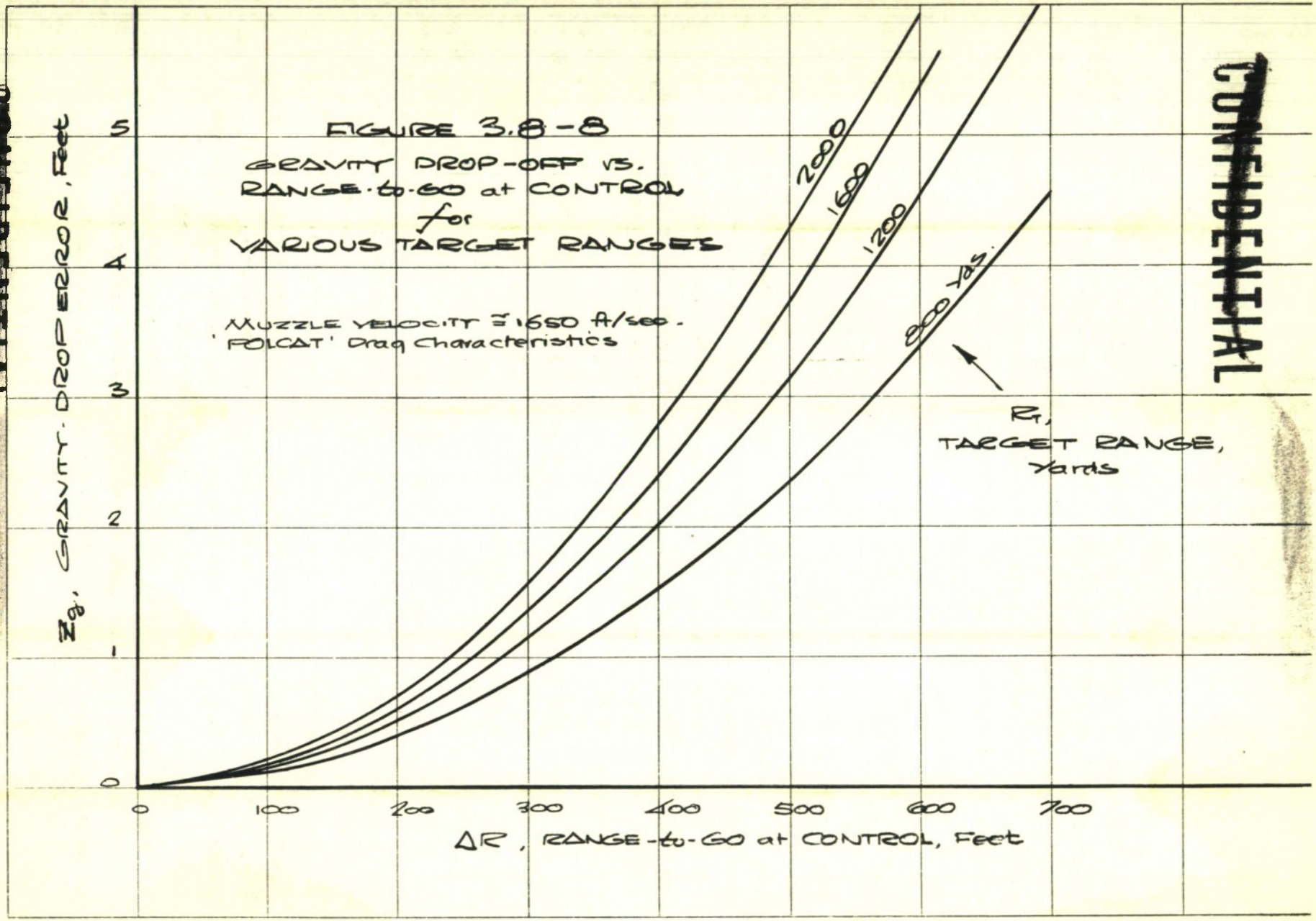

threshold angle by an amount equivalent to half the control delay distance, R_D.

$$\Delta\gamma_{threshold} = -\frac{\frac{R_D}{2}(\gamma_c)}{\Delta R} \qquad (4)$$

- where γ_c = steering or control angle

R_D = max. control delay distance (Eq. 2)

ΔR = Range-to-go at control

In the proposed POLCAT system a roll rate of 20 rps has been selected; it presents a compromise between the high roll rates required for minimizing control delay, and low roll rate required for assuring effectiveness of the shaped charge warhead.

3.8.3.3 Impulse Control Errors

Included in this category are those errors which are due to deviations of the magnitude of the actual steering angle from the desired steering angle, as illustrated in Figure 3.8-9a. Such variability will be caused by round-to-round differences in projectile velocity. Their effect on miss-distance at the target is:

$$\Delta Z_c = \Delta\gamma_c \, \Delta R \qquad (5)$$

- where range-to-go at control = ΔR

and $\Delta\gamma_c = \frac{\Delta \text{Impulse}}{(\text{Proj. Mass})(\text{Proj. Velocity})}$ or $\frac{\text{Impulse}}{(\text{Proj. Mass})(\Delta\text{Proj. Vel.})}$

Cartridge impulse variability has been shown to be of the order of + 3% (3σ) by the POLCAT cartridge ground test program; round-to-round velocity variations are conservatively estimated at $\pm$ 50 ft/sec (3σ). Since both these factors are likely to be normally distributed, the resulting miss distance will, similarly, have a normal (Gaussian) distribution, as illustrated in Figure 3.8-9a. Moreover, since the

FIGURE 3.6-9

CONTROL MAGNITUDE and SEEKER ERRORS

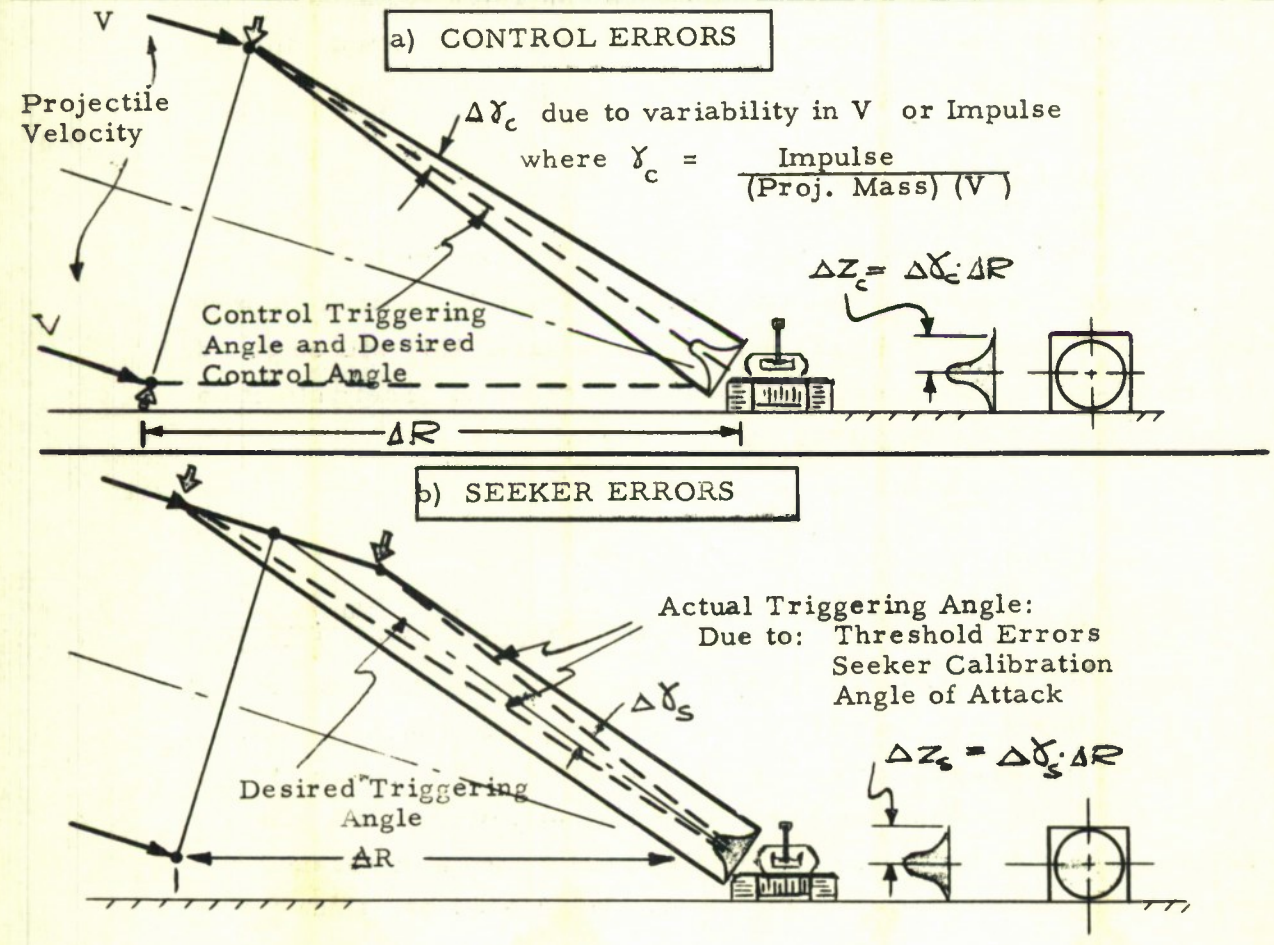

radial direction in which control takes place is equally likely, by virtue of the circular distribution of the uncontrolled trajectories, the distribution of misses due to control errors will, likewise, be circularly distributed.

3.8.3.4 Seeker LOS Errors:

As shown in Figure 3.8-9b, errors at the target will result from actuation of the control impulse at points which correspond to LOS angles which differ from the desired LOS angle (and hence the cartridge steering effect). Such LOS or seeker errors can be caused by a number of factors:

a) Errors in measuring the LOS angle (e.g. seeker calibration errors)

b) Errors in generating the LOS threshold reference for comparison with the seeker-measured LOS angle

c) Angle of attack errors -- ascribable to the fact that the POLCAT seeker is frame-fixed, hence tends to include random and extraneous projectile angles of attack with desired target LOS angles with respect to the projectile instantaneous velocity vector (e.g. flight path).

Figure 3.8-9b illustrates how these various seeker errors are likely to cause either premature or late triggering of the control cartridge. As regards the tolerances on the above factors which are deemed readily obtainable, the following 3σ seeker errors represent what is readily capable of accomplishment by means of the current state-of-the-art.

i) Calibration error $\pm$ 2 mils

ii) Threshold angle $\pm$ 1 mil

iii) Angle-of-attack $\pm$ 5 mils

Items i) and ii) are determined largely by the precision of the seeker optical system and the precision of seeker circuitry. As regards the angle-of-attack error, reasonably small values of angle of attack can, it is believed, be achieved strictly by optimizing the aerodynamics of the projectile and minimizing launching disturbances. Thus, it has been estimated that in the region of potential POLCAT control (ranges $\geq$500 yards), the resultant of all probable projectile pitch oscillation-producing factors (initial gun disturbances such as muzzle blast, and barrel whip; fin malalignments; ballistic drop-off; and fin and mass malalignments) will correspond to a maximum angle of attack of equal to or less than $\pm$ 5 mils.

The effects of seeker LOS measurement (or calibration) errors, threshold (reference) errors, and angle of attack errors on miss distance are all basically similar. Referring to Figures 3.8- 9b, it is seen that all essentially result in triggering the control cartridge (which has a given steering angle capability) at an angle which is either greater or less than the steering capability and its associated LOS threshold angle. All of these error sources are randomly and normally distributed and are causally independent of each other. Their effect on miss distance is:

$$\Delta Z_s = \Delta\gamma_s \, \Delta R \qquad (6)$$

- where $\Delta\gamma_s$ = seeker LOS, threshold or angle-of attack error (radians)

ΔR = range-to-go at control (ft.)

Since, the error sources are normally distributed and since impulse control is equally likely to be initiated in any roll plane, the resulting miss-distance distribution will be circular and normal (i.e. bi-normal) as shown at the bottom right of Figure 3.8-9b.

3.8.3.5 POLCAT Illuminator Errors:

In the proposed POLCAT system the controlled round will be steered toward the center of an illuminated spot on the target. The center of this illuminated spot will be determined by suitably designed reticle in the homing seeker. Under tactical conditions, the operator of the POLCAT illuminator will attempt to direct the 1 mil beam at the center of the target through use of a suitable telescopic sight and illuminator slewing mechanism. It is estimated that rigid construction of the illuminator and its mount together with aided tracking techniques (if necessary), will make it possible to maintain the spot within $\pm$ 1 ft (3σ) of a desired aim point on a moving tank at a range of 2000 yards. This so called "aiming error" of the controlled POLCAT projectile can be assumed to have a circular Gaussian distribution. Since it is causally independent of the other errors it contributes to system error via the square root of the sum of the squares of the component errors.

3.8.3.6 Seeker Roll Reference and Control Errors in Roll:

All of the system errors discussed in the preceding pages, with the exception of the gravity drop error, result in miss distances at the target which are in the LOS plane, i. e. the plane in which the steering effect is required to occur. Two types of error sources, however, produce miss distance effects which are transverse to the required steering plane: i) roll errors on the part of the seeker in accurately sensing the target spot as it passes the roll reference portion of the seeker reticle and ii) roll errors due to inaccuracies in directing the resultant of the control impulse in the correct roll direction -- assuming this has been accurately established by the roll reference element of the seeker. In either case, the steering effect

will not be in the correct, required plane and transverse errors will occur at the target as shown in Figure 3.8-10. The magnitude of the transverse miss distance due to "roll errors" is:

$$r = \Delta\phi \cdot D \tag{7}$$

- where $\Delta\phi$ = roll error in radians
  D = vertical miss distance of uncontrolled trajectory ft.

Seeker roll errors will be caused by the inability of the roll reference element to accurately sense when the target is in the roll reference plane (cf. Figure 3.8-10b), which is also that which to which the impulse cartridge is indexed. Factors likely to cause such inaccuracies are: the basic limitations of reticle and/or cell geometry; variability of target image spot size on the reticle; the intermittency of the signal due to illuminator pulsing; and random calibration errors. In the absence of actual experimental data, it is valid to assume that these errors will have a Gaussian distribution about the intended mean. Based on considerations of the nature of contemplated seeker and illuminator designs, seeker errors in establishing the roll reference plane are preliminarily estimated at approximately $\pm$ 1° (3σ).

Roll errors due to the inaccuracies in directing the control impulse in the correct direction will primarily be caused by variations in projectile spin rate. As is shown in Figure 3.8-10c, the POLCAT impulse cartridge is biased in roll with respect to the roll reference element of the seeker by an angle ϕ_c . This bias angle is selected such that when the projectile is spinning at its standard rate of 20 rps, the cartridge is oriented in the prescribed steering direction (as determined by the seeker roll reference element) 1.5 milliseconds after the seeker

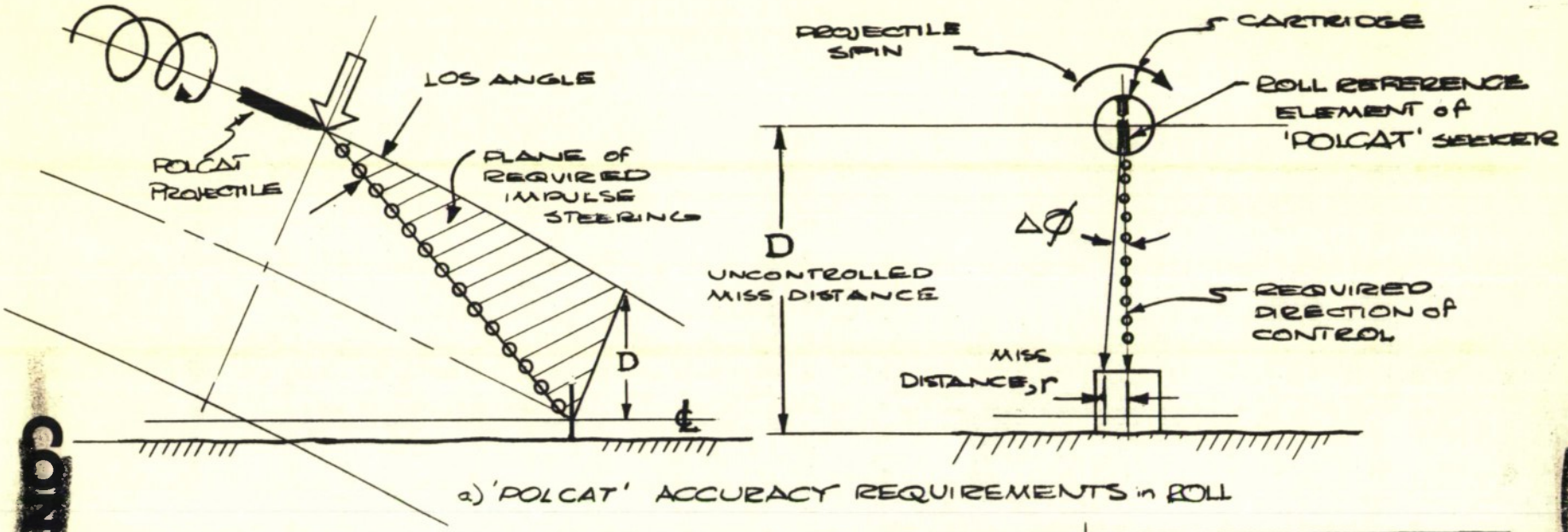

a) 'POLCAT' ACCURACY REQUIREMENTS in ROLL

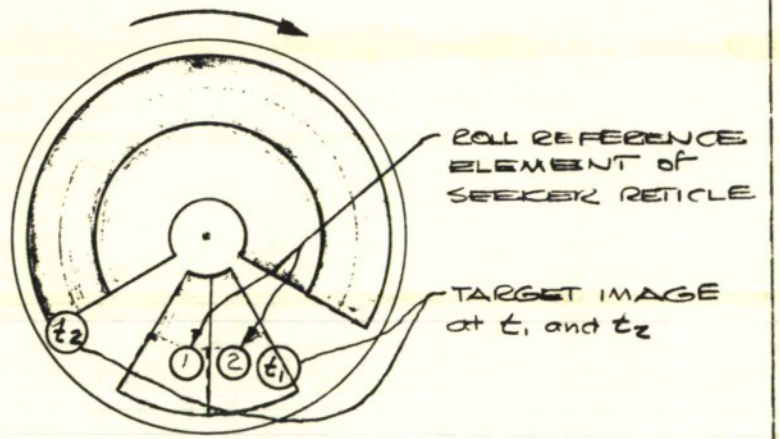

b) SEEKER RETICLE ACCURACY and RESOLUTION CONSIDERATIONS

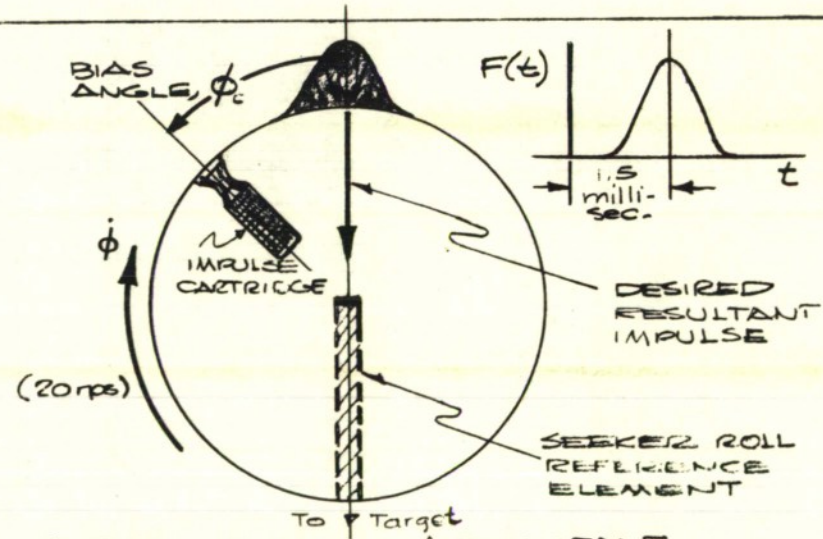

c) DEPENDENCE of RESULTANT IMPULSE DIRECTION on 'POLCAT' ROLL RATE

FIGURE 3.8-10 : 'POLCAT' ROLL ERRORS

has given the command to control. This 1.5 millisecond time interval is the time required for the force function, F(t), of the cartridge (shown in Figure 3.8-10c) to reach its peak. Since the force function is symmetrical the desired resultant impulse will be in the same direction as the peak instantaneous force vector.

Hence, assuming negligible time delays in the seeker circuitry, the POLCAT cartridge must be biased with respect to the seeker roll reference by an amount:

$$\phi_c = \Delta t \ \dot{\phi} \qquad \ldots\ldots\ldots\ldots \qquad (8)$$

$$= (.0015)\ (20 \times 360 \text{ deg/sec})$$

$$= 10.8^{o}$$

It is evident that when the cartridge is biased 10.8^{o} with respect to the roll reference, deviations of projectile spin rate from the design value of 20 rps will cause the resultant control force vector to be in error. This angular error will be in proportion to the spin rate deviation:

$$\Delta\phi = \frac{\Delta\dot{\phi}}{\dot{\phi}}\ \phi_c \qquad (9)$$

- where ϕ_c is as defined in Eq, 7

$\Delta\dot{\phi}$ = error in maintaining standard (constant) spin rate

$\dot{\phi}$ = standard (constant) spin rate

It is estimated that by suitable rifling and projectile rotating band design, the muzzle spin rate can be kept within 20 ± 1 rps; projectile spin can be kept at 20 ± 2 rps by suitable aerodynamic design using canted surfaces to provide rolling moments capable of counteracting the usual roll damping moments. It is accordingly estimated that $\Delta\phi = \frac{2}{20}\ 10.8 = 1$ degree. This is equal in magnitude to the previously estimated "roll error" ascribable to expected inaccuracies of the seeker in establishing the precise roll reference.

Among other possible sources of error affecting the direction of the impulse control force is variability of cartridge ignition delay and thrust build-up time. However, POLCAT cartridge ground tests have shown these to be comparatively negligible.

The above major roll errors due to seeker inaccuracies and variability of projectile spin are likely to be Normally distributed; their corresponding miss distance effects will hence similarly be Normally distributed. Since rounds affected by these errors are assumed to be controlled with equal likelihood in any quadrant with respect to the target, the resultant miss distance distribution will, moreover, have a circular Normal distribution.

3.8.3.7 Wind Errors:

The major effect of cross-winds on the POLCAT system is ascribable to erroneous LOS measurements which result when the projectile assumes a trim angle-of-attack in proportion to the magnitude of the cross-wind. Figure 3.8-11 illustrates how a stable projectile accomodates itself to a steady cross-wind and assumes trim angle-of-attack:

$$\alpha_w = \frac{\text{Velocity of cross-wind}}{\text{Projectile Velocity}} \quad \ldots\ldots\ldots\ldots \quad (10)$$

In the case of the POLCAT system, this trim angle of attack will increase during the flight of a given round due to its decreasing velocity. In its present simple form, the POLCAT system has no way of being able to compensate for wind effects, and, hence, must live with them. System performance degradations due to wind must be viewed from a statistical point of view. Thus, data obtained from the U. S. Weather Bureau have indicated that:

FIGURE 3.8-11

CROSS-WIND EFFECTS on 'POLCAT' SYSTEM

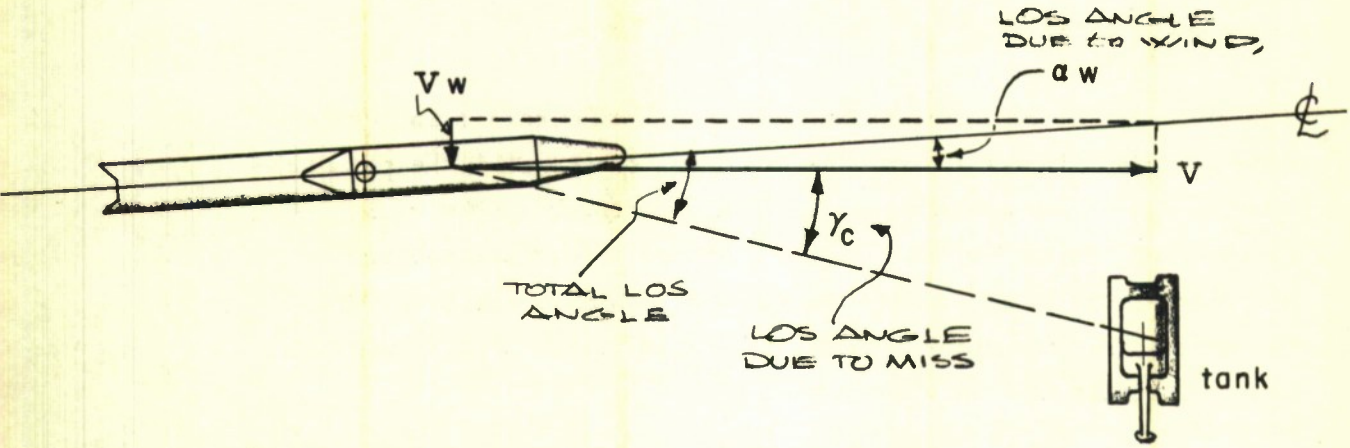

(a) PLAN VIEW OF CROSS-WIND EFFECT
(SHOWING RESULTANT LOS ERROR ($= \alpha_w$) for LATERAL MISSES)

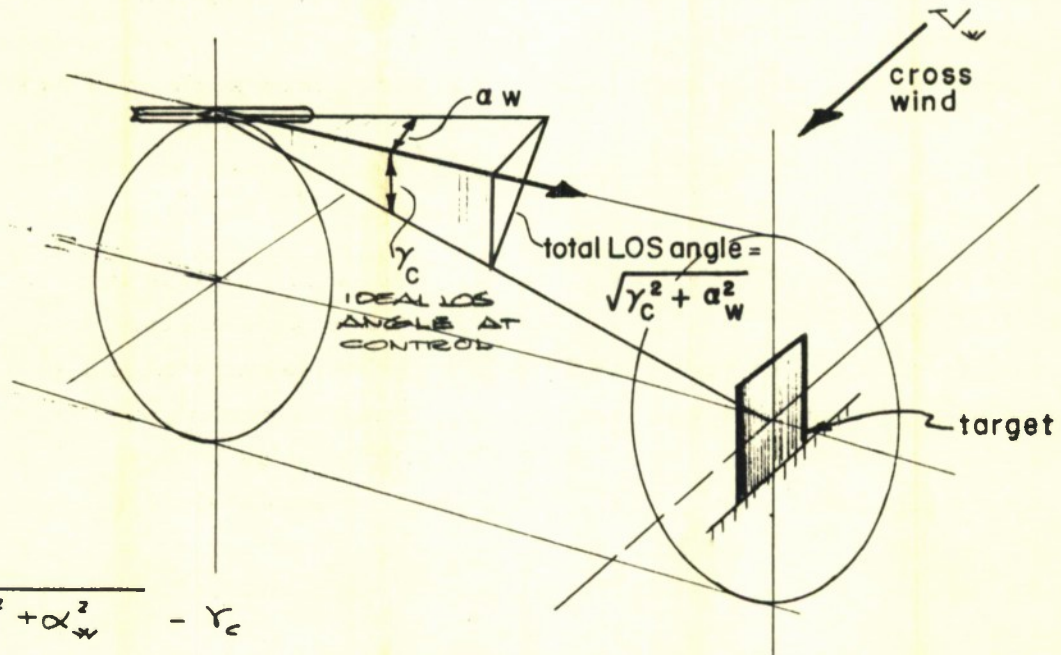

$$\Delta\gamma_v \cong \sqrt{\gamma_c^2 + \alpha_w^2} - \gamma_c$$

(b) SIDE PERSPECTIVE VIEW of CROSS-WIND EFFECT
(SHOWING RESULTANT ERROR $\Delta\gamma_v$ for VERTICAL MISSES)

i) wind velocities $\geq$ 25 mph occur on the average, less than 5% of the time (perhaps less, close to the ground).
ii) <u>average</u> wind velocities over a long period of time are between 5 and 10 mph, depending on location, etc.

The POLCAT system will accordingly be analyzed for situations where wind velocities of 5 and 10 mph (3σ) are assumed to prevail.

Since winds are generally parallel to the ground, seeker LOS errors due to the wind effects will be greatest for rounds which are destined to pass either to the left or right of the target, and least for rounds which are about to miss the target in the vertical plane. Thus, for pure lateral misses, the LOS angle error due to cross-wind:

$$\Delta\gamma_{L_{wind}} \cong (\gamma_c + a_w) - \gamma_c = a_w \quad \ldots\ldots \quad (11)$$

- where $\gamma_c \cong$ steering angle (i.e. LOS angle at control)
a_w = projectile trim angle

For incipient over and undershoots, however:

$$\Delta\gamma_{v_{wind}} \cong \sqrt{\gamma_c^2 + a_w^2} - \gamma_c \quad \ldots. \quad (12)$$

This is because the LOS angle at the instant of control is the resultant of the LOS angle (γ_c) due to over-or undershoot and the incremental LOS angle (a_{wind}) perpendicular to the former due to the projectile's trimming into the wind. (cf. Figure 3.8-11b). In the hit probability calculations which follow, both $\Delta\gamma_{L_{wind}}$ and $\Delta\gamma_{v_{wind}}$ will be calculated.

For ease of analysis, their geometric mean:

$$\overline{\Delta\gamma}_w = \sqrt{\frac{\Delta\gamma_L^2 + \Delta\gamma_v^2}{2}} \quad \ldots\ldots \quad (13)$$

will then be calculated and its miss distance effect Normally and circularly distributed.

3.8.3.8 Summary of POLCAT Error Sources and Their Magnitudes

Table 3.8-2 summarizes the various sources of error discussed in the previous pages, their estimated magnitude, and the nature of their effect as reflected in miss distance in the vertical plane of the target. These data will form the basis for the system hit probability estimates which follow.

TABLE 3.8-2

POLCAT System Errors, Estimated Error Magnitudes, and Corresponding Miss Distance Effects

Type Error	Primarily a Function of:	Estimated Ma gnitude of Error Factor (3σ)	Miss Distance Effect	Miss Distance Distribution
a) Gravity-Drop	Range-to-Go at Control	varies with target range	Eq. 1	Point directly below target center (i.e. vertical bias)
b) Control Delay	Projectile roll rate	.050 sec. max., .025 sec. with biasing	Eqs. 2 and 3	Uniform, circular distribution about target center
c) Impulse Control	i) Impulse variability ii) Velocity variability	± 3% ± 50 ft/sec	Eq. 5	Gaussian circular distribution about target center
d) Seeker LOS Errors	i) Calibration errors ii) Threshold errors iii) Angle-of-attack errors (projectile oscillation)	± 2 mils ± 1 mil ± 5 mils	Eq. 6	Gaussian circular distribution about target center
e) Illumination Errors	Ability to aim illuminator	± 1 ft at target	---	Gaussian circular distribution about target center
f) Roll Errors (Seeker and Control Direction)	i) Roll reference ii) Control direction errors due to roll variability	± 1° ± 1°	Eq. 7	Gaussian circular distribution about target center
g) Wind Errors		Cross Winds = ± 5mph ± 10mph	Eqs. 10 to 13	Gaussian circular distribution about target center

3.8.4 POLCAT Hit Probability Analysis

3.8.4.1 The Mathematical Model for POLCAT Hit Probability

The mathematical model for determining preliminary estimates of POLCAT first-round hit probability are based on the following assumptions:

1) System Composite Hit Probability

The hit probability of POLCAT equals the hit probability of the uncontrolled rounds plus the probability of those rounds requiring impulse-control which are successfully steered to impact the target.

2) Target Characteristics

In accordance with the usual practice in anti-tank hit probability calculations, the target is assumed to be represented by a square area whose dimensions are 7.5 ft x 7.5 ft. and which is perpendicular to the line of fire. As regards target motion, hit probability is determined both for stationary targets and for tanks moving at the typical velocities of 5 and 10 mph.

3) Fire Control

The POLCAT simple fire control system is assumed to provide a ranging accuracy of $\pm 5\%$. For moving targets,

lead estimation is assumed to result in lateral errors in a vertical plane at the target which are no greater than vertical errors due to ranging errors. (This essentially corresponds to a lead prediction accuracy of the order of 2 to 3 mils.)

3.8.4.2 Hit Probability of Uncontrolled POLCAT Projectile

The hit probability of the uncontrolled round is determined at each target range by the relative size of the 7.5' x 7.5' target and the impact pattern of the uncontrolled POLCAT projectile. This impact pattern reflects both vertical and lateral miss distances resulting from the error sources (and their assumed magnitudes) shown in Table 3.8-3.

TABLE 3.8-3

ASSUMED ERRORS of UNCONTROLLED 'POLCAT' PROJECTILE

Type Error	Error Magnitude (3σ)	Remarks
i) Ranging Error	$\pm$5%	Typical of good optical range finders
ii) Boresight Error	$\pm$0.5 mil	---
iii) Dispersion	1.5 to 2.5 mils depending on range	POLCAT pre-control dispersion assumed equal to that of the T-184 projectile (cf. Figure 3.8-13)

The ranging error shows up as a vertical error at the target which is a function of the range error, $\triangle R$, and the ground impact angle γ_i of the uncontrolled trajectory. In this analysis γ_i is equal to λ_p and is computed for various target ranges. The results are given in Figure 3.8-6.

Dispersion characteristics of the uncontrolled POLCAT projectile are similarly assumed equal to those of the T-184 projectile. Figure 3.8-12 shows the best basic experimental data available concerning dispersion of this type of projectile; the POLCAT estimate is represented by a straight line passing between $\sigma \cong 0.55$ mils at 500 yards and $\sigma \cong 0.85$ mils at 2000 yards.

These errors are combined to give maximum lateral and vertical errors (miss distances) of the uncontrolled rounds in Table 3.8-4. Lateral miss distance is caused by Normally distributed dispersion and boresight errors; the total vertical miss distance, on the other hand, includes the effect of the ranging error. Since these errors are causally independent, their combined effects on the total lateral and vertical errors (or miss-distances) are obtained by taking the square root of the sum of the squares of the component errors. Reference to Table 3.8-4 indicates that vertical errors are larger than lateral errors; hence it is concluded that the impact pattern in the plane of the target has an elliptical Normal distribution.

The hit probability versus a square target can be obtained in parts; e.g.,

FIGURE 3-8-12

ESTIMATED DISPERSION CHARACTERISTICS OF UNCONTROLLED "POLCAT" PROJECTILE

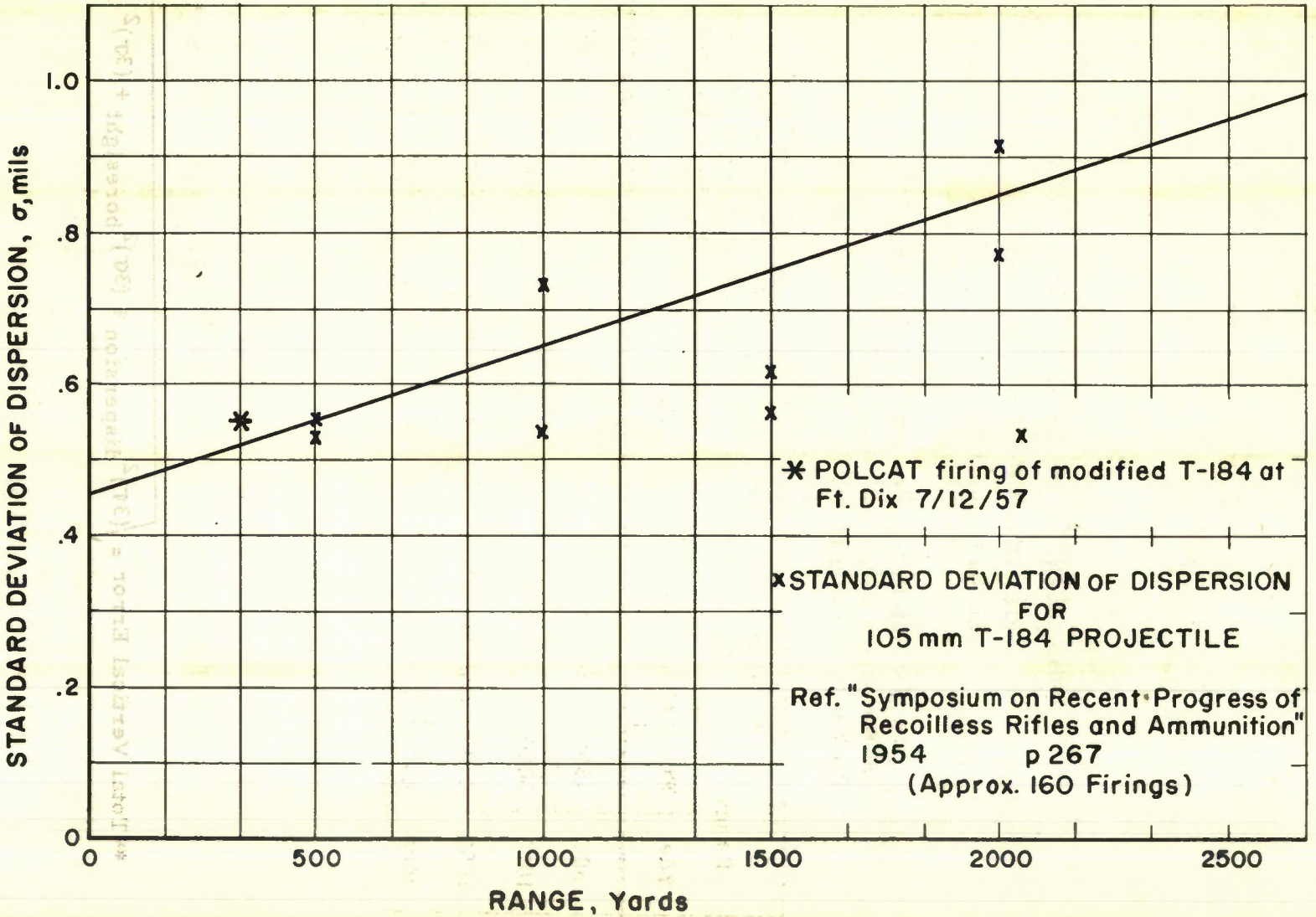

TABLE 3.8-4

CALCULATION of VERTICAL and LATERAL
MISS DISTANCE (3σ) VS. RANGE
(Uncontrolled POLCAT Projectile)

i) Dispersion Error = as shown in Figure 3.8-12
ii) Boresight Error = .5 mils (3σ)
iii) Range Error = $\pm 5\%$ (3σ)

Range		Dispersion 3σ		Boresight 3σ		Total Lateral Error (ft)*	Ranging Horiz. (ft)	Error Vert. Effect (ft)	Total Vertical Error (ft)**
Yds.	Ft.	Mils	ft.	Mils	ft.				
500	1500	1.65	2.48	.75	1.125	2.725	75	.85	2.86
1000	3000	1.95	5.85	.75	2.25	6.26	150	4.5	7.72
1500	4500	2.25	10.2	.75	3.38	10.75	225	12.75	16.7
2000	6000	2.55	15.3	.75	4.5	15.95	300	27	31.4

*Total Lateral Error = $\sqrt{(3\sigma)^2_{\text{dispersion}} + (3\sigma)^2_{\text{boresight}}}$

**Total Vertical Error = $\sqrt{(3\sigma)^2_{\text{dispersion}} + (3\sigma)^2_{\text{boresight}} + (3\sigma)^2_{\text{range}}}$

the probability that a round within the elliptical distribution hits the square target can be expressed as the product of:

i) the probability P_{H_L}, rounds having a lateral normal distribution with σ_x will strike a vertical band lying between $\frac{+x}{2}$ and $-\frac{x}{2}$ and

ii) the probability, P_{H_V}, that rounds having a vertical distribution with σ_y will strike a horizontal band lying between $\frac{+y}{2}$ and $\frac{-y}{2}$.

Hence, $P_{H_u} = (P_{H_L})(P_{H_V})$.

It is noted that a square target lends itself readily to this type of calculation. All that is required is a table of Normal areas,

$$\int_{\delta}^{t} \phi(t)\, dt.$$ (See Reference 59)

Thus, in Table 3.8-5, P_{H_L}, P_{H_V} and the resulting P_{H_u} are calculated for the uncontrolled POLCAT projectile for two values of ranging error: 5% and 1%. The resulting values of P_{H_u} are plotted in Figure 3.8-13.

TABLE 3.8-5

CALCULATION of HIT PROBABILITY of UNCONTROLLED PROJECTILE

7.5 x 7.5 Target

For lateral and vertical miss-distances of Table 3.8-4

(1)	(2)	(3)	(4)	(5)	(6)	(7)	(8)	(9)	(10)	(11)	(12)	(13)
		LATERAL			VERTICAL							
					5% Range Error				1% Range Error			
Range Yds.	Range Ft.	* (1σ) (ft)	$t = \frac{3.75}{1\sigma}$	$P_{H_L} = 2\int_0^t \phi(t)dt$	(1σ) (ft)	$t = \frac{3.75}{(1\sigma)}$	$P_{H_V} = 2\int_0^t \phi(t)dt$	P_{H_u} (5)(9)	(1σ) (ft)	$t = \frac{3.75}{1\sigma}$	P_{H_V}	P_{H_u} (5)(12)
500	1500	.91	4.1	1.0	0.95	3.95	1.0	1.0	.91	4.1	1.0	1.0
1000	3000	2.09	1.79	.926	2.57	1.46	.856	.793	2.11	1.775	.924	.855
1500	4500	3.58	1.05	.706	5.57	.674	.50	.354	3.7	1.013	.689	.486
2000	6000	5.32	.705	.52	10.47	.358	.28	.146	5.61	0.668	.496	.258

* = 1/3 (Total Lateral Error) indicated in Table 3.8-4.

** = 1/3 (Total Vertical Error) indicated in T ble 3.8-4.

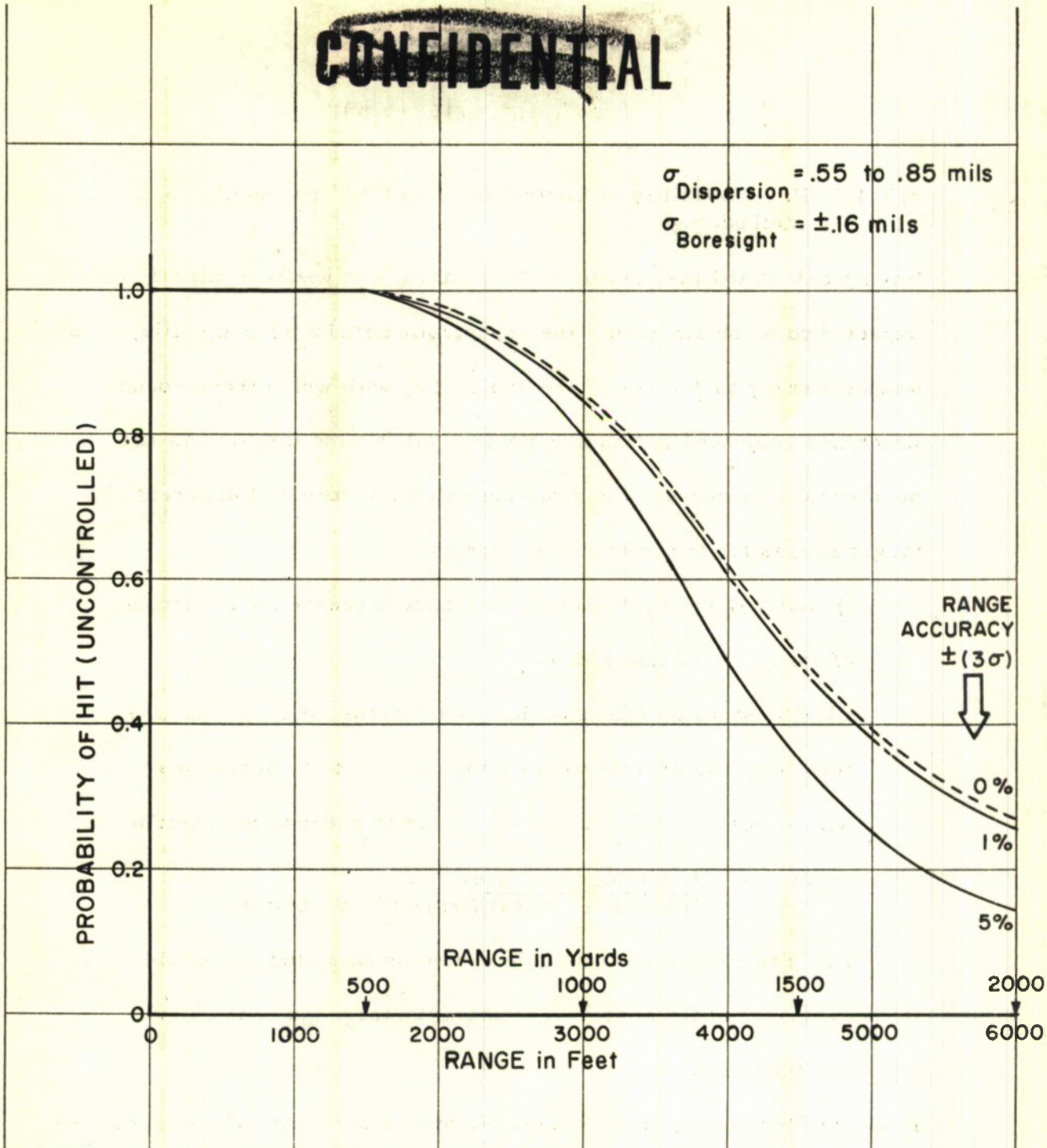

Figure 3.8-13

ESTIMATED FIRST-ROUND HIT PROBABILITY VS. RANGE OF UNCONTROLLED "POLCAT"

(For Various Fire Control Ranging Accuracies)

3.8.4.3 Hit Probability of Controlled 'POLCAT' Projectile; Methodology

Having calculated the maximum (3σ) lateral and vertical miss distances expected to be obtained with the uncontrolled POLCAT projectile, it is now necessary to determine the probability with which those rounds which are subjected to impulse-control will hit the target. As has been shown previously, the situation will be different at different target ranges for the following reasons:

i) Lateral and vertical miss distance increase as a function of range (cf. Table 3.8-4)

ii) The steering effect varies as a function of range for a fixed impulse system where projectile velocity decreases with range (cf. Figure 3.1-13). This is because the control angle $\gamma_c = \frac{\text{(Cartridge Impulse)}}{\text{(Projectile Mass)(Projectile Velocity)}}$

iii) The ground impact angle of the uncontrolled projectile increases with range. This characteristic has been shown in Figure 3.8-6.

In view of the above, it is necessary, once a cartridge of given impulse has been selected, to calculate P_H at a number of target ranges. At each target range of interest, moreover, the probability of controlled hit must be determined for various degrees of uncontrolled misses.

Accordingly, the effect of the various sources of POLCAT errors previously discussed will be calculated at each target range of interest for rounds representative of various "sub-populations" of the population of uncontrolled trajectories. As has already been established, these uncontrolled trajectories are such as to result in a miss distance in the vertical plane of the target (transverse to the line of fire) which are elliptically and normally distributed. For ease of calculation this elliptical distribution of uncontrolled trajectories has been (conservatively) assumed to be circular with a σ equal to the maximum component of the elliptical distribution (i.e. the lateral miss distance has been assumed to be equal to the normally larger vertical miss distance.) Given this circular (and normal) distribution of uncontrolled rounds, it is now possible to investigate more readily the effect of gravity drop, control errors, seeker errors, etc. on rounds representative of 3σ, 2σ, and 1σ uncontrolled miss distances.

As has been previously discussed, a control impulse which corresponds to some intermediate "design range" appears most likely to provide an acceptably high first-round hit probability for the single-impulse POLCAT system preliminarily selected as desirable for reasons of simplicity, low weight, reliability, and low cost. Accordingly, a system optimized for 1500 yards will be investigated.

3.8.4.4 Determination of POLCAT Effectiveness at 1500 Yards

1. Assumptions:

i) The maximum 3σ uncontrolled trajectories provide a miss distance = $\pm$ 16.7 ft (cf. Table 3.8-4).

ii) Impulse cartridge shall be triggered at a LOS angle such that no rounds are likely to suffer ground impact before initiation of control.

iii) Control shall be initiated at points no lower than horizontal plane which passes thru the base of the target, i.e., 3.75 ft. below the midpoint of the target.

iv) The trajectories are linearized in the region of the target, and

v) The post-control behavior of all rounds having a given pre-control dispersion will be identical, and equal to the behavior of rounds representative of 3σ, 2σ, and 1σ miss distances, which are controlled in the vertical plane.

2. Determination of Control Angle, Max. Range-to-Go at Control and Control Impulse:

Figure 3.8-14 illustrates the method used for determining the range-to-go for which 3σ overshoots and undershoots will result in the previously determined miss-diatance at the target ($\pm$ 16.7 ft. @ 1500 yards). Vertical drop-off which occurs between control points (A) and the target plane (B), is computed for various points of impulse control located at various ranges-to-go. The correct range-to-go at control which provides the required vertical miss distance, is obtained by interpolation. In the present instance, Figure 3.8-14 shows this to be 330 ft. short of the target (located at 1500 yds). The corresponding ground impact angle is 45.6 mils; the corresponding projectile velocity 1050 ft/sec. The required design impulse for the control cartridge is determined using the relationship for control angle.

$$\gamma_c = \frac{\text{Impulse}}{(\text{Proj. Mass})\,(\text{Proj. Velocity})}$$

$$\text{Design Impulse} = \frac{45.6}{1000}\ \frac{23.4}{32.2}\ 1050 = 35 \text{ lb-sec.}$$

3. POLCAT Hit Probability Computation (R = 1500 yds)

For the above maximum (3σ) range-to-go, and for the projectile velocity and steering angle capability which exist at the corresponding range, miss distances at the target have been

FIGURE 3.8-14

DETERMINATION of MAXIMUM RANGE-to GO at CONTROL and REQUIRED STEERING ANGLE

R = 1500 Yds.

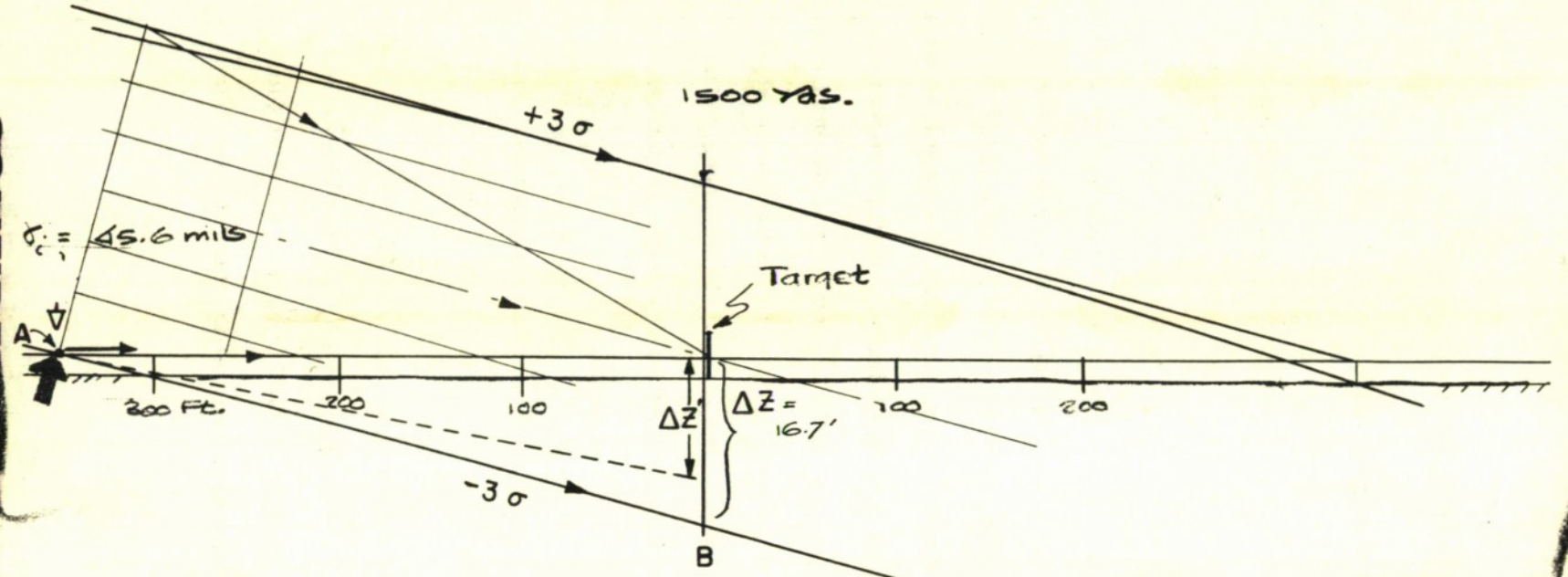

(1) R (ft)	(2) ΔR_c (ft)	(3) γ_i (mils)	(4) $\Delta Z'$ (ft)	(5) V_{ave} (ft/sec)	(6) Δt (sec)	(7) $1/2g(\Delta t)^2$	(4)+(7) ΔZ
4200	300	46.0	13.8	1040	.288	1.33	15.13
4150	350	45.3	15.85	1040	.336	1.82	17.67
4100	400	44.5	17.80	1040	.385	2.38	20.18

R_c = 330 ft.
γ_c = 45.6 mils

calculated for various combinations of expected POLCAT system errors shown in Table 3.8-2. In Table 3.8-6 the miss distances and corresponding P_H produced by these errors are calculated using previously derived relationships. Tables 3.8-7 and 3.8-8 similarly show hit probability calculations for 2σ and 1σ pre-control trajectories. The overall first round hit probability of the POLCAT projectile (at 1500 yds) is then obtained by weighing the values of P_H for 3σ, 2σ, and 1σ errors by the relative number of uncontrolled rounds likely to exist in each such "sub-population." For a bi-normal distribution, these proportions will be as shown below.

Relative Fraction of Rounds in Various Parts of Uncontrolled Distribution

Error of Uncontrolled Shot	Fraction of Shots
$\pm 3\sigma - 2\sigma$	.135
$\pm 2\sigma - 1\sigma$	.472
$\pm 1\sigma - 0$	.393

Using these relationships and the sub-population P_H computed in Tables 3.8-6 thru 3.8-8, Table 3.8-9 derives the overall POLCAT hit probability estimates for R = 1500 yards.

TABLE 3.8-6

Calculation of Probability of Hit of Controlled POLCAT Projectile at R = 1500 yd.

3σ Pre-Control Trajectory (Extreme Miss)
Range-to-Go at Control = 330 ft D = ± 16.7 ft
Control Angle, δ_c = 45.6 mils V = 1040 ft/sec.

Error	Error Elements	Miss Distance (3σ)	$(3\sigma)^2$	Hit Probability
a) Gravity Drop	V_p = 1040 ft/sec $\Delta t = \frac{330}{1040} = .318$ sec.	-1.63 ft =	-	$\bar{y}$ = 1.63 ft. 3σ = 2.38 ft σ = .79 ft
b) Control Delay	.050 sec. max. R_d = 52.5 ft (max.) ΔZ_d = +2.4 ft (max.) ΔZ_d = ± 1.2 ft. by biasing control threshold	± 1.2 ft	1.44	
c) Control Magnitude i) I	± 3% = ± 1.37 mils	± 0.45 ft.	0.20	
ii) V	± 50 ft/sec = 2.19 mils	± 0.72 ft.	0.52	P_{H_L} = 1.0
d) Seeker LOS Errors i) Calibr. ii) Threshold iii) α-Effect	 ± 2 mils ± 1 mil ± 4 mils	 0.66 ft 0.33 ft 1.32 ft	 0.44 0.11 1.74	P_{H_v} = .996 P_H = .996
e) Illuminator	-	± 1 ft	1.0	
f) Roll Errors i) Seeker ii) Control	 ± 1°(17.4 mils) ± 1°(17.4 mils)	 0.29 ft 0.29 ft	 0.09 0.09	$\sum_1^a (3\sigma^2)$ = 5.63; 3σ = 2.38 ft
g) Wind	5mph: $\Delta\gamma_L$ = ± 7 mils, $\Delta\gamma_V$ = ± 0.6 mils	= 5.4 mils ± 1.8 ft	3.24	$\sum_3^a (3\sigma)^2$ = 8.87; 3σ = 2.98 ft, $\bar{y}$ = -1.63 → P_H = .984
	10mph: $\Delta\gamma_L$ = ± 14 mils, $\Delta\gamma_V$ = ± 2.1 mils	= 10 mils ± 3.3 ft	10.9	$\sum_3^a (3\sigma)^2$ = 16.53, 3σ = 4.06 ft, $\bar{y}$ = -1.63 → P_H = .936
h) Target Vel.	5 mph (7.3 ft/sec)	Lateral Bias ± 2.32 ft	-	$\bar{x}$ = 2.32, $\bar{y}$ = -1.63, 3σ = 2.38 → P_H = .961
	10mph (14.6 ft/sec)	4.64 ft	-	$\bar{x}$ = 4.64, $\bar{y}$ = -1.63, 3σ = 2.38 → P_H = .13

TABLE 3.8-7

Calculation of Probability of Hit of Controlled POLCAT Projectile at R = 1500 Yd.

2σ Pre-Control Trajectory
Range-to-Go at Control = 220 ft D = ± 11.1 ft
Control Angle δ_c = 45.6 mils V = 1040 ft/sec

Error	Error Elements	Miss Distance (3σ)	$(3\sigma)^2$	Hit Probability
a) Gravity Drop	V_p = 1040 ft/sec $\Delta t = \frac{220}{1040} = .212$ sec	-0.725 ft	-	$\bar{y}$ = 0.725 ft 3 = 2.23 ft = .74 ft
b) Control Delay	.050 sec. max. plus biasing for 3 ± 1.2 + $\frac{1}{3}$ (1.2)	± 1.6 ft	2.56	
c) Control Magnitude				
i) I	± 3% = ± 1.37 mils	± 0.30 ft.	.09	
ii) V	± 50 ft/sec = ± 2.19 mils	± 0.48 ft	.23	
d) Seeker LOS Errors				
i) Calibr.	± 2 mils	0.44 ft	.19	
ii) Threshhold	± 1 mil	0.22 ft	.05	P_H = 1.0
iii) α-Effect	± 4 mils	0.88 ft	.77	
e) Illuminator Error	-	± 1 ft	1.00	
f) Roll Errors				
i) Seeker	± 1° (17.4 mils)	± 0.193	0.04	
ii) Control	± 1° (17.4 mils)	± 0.193	0.04	$(3\sigma)^2$ = 4.97, 3 = 2.23
g) Wind	5mph = ± 7 mils = ± 0.6 mils = ± 5.45 mils	± 1.2 ft	1.44	$(3\sigma)^2$ = 6.41 3 = 2.54 $\bar{y}$ = -0.725 } P_H = 1.0
	10 mph = ± 14 mils = ± 2.1 mils = ± 10 mils	± 2.2 ft	4.84	$(3\sigma)^2$ = 9.81, 3 = 3.14 $\bar{y}$ = -0.725 } P_H = .998
h) Target Velocity	5 mph (7.3 ft/sec)	Lateral Bias 1.55 ft 3.10 ft	- -	$\bar{x}$ = 1.55, $\bar{y}$ = -.725 } P_H = .999 3σ = 2.23 $\bar{x}$ = 3.10 $\bar{y}$ = .725 } P_H = .81 3σ = 2.23

TABLE 3.8-8

Calculation of Probability of Hit of Controlled POLCAT Projectile

R = 1500 yds
1σ Pre-Control Trajectory

Range-to-go at Control = 110 ft. D = $\pm$ 5.56 ft
Control Angle δ_c = 45.6 mils V = 1040 ft/sec.

Error	Error Elements	Miss Distance (3σ)	$(3\sigma)^2$	Hit Probability
a) Gravity Drop	V_p = 1040 ft/sec $\Delta t = \frac{110}{1040} = .106$ sec	-0.18	-	$\bar{y}$ = -0.18 ft 3σ = 2.32 ft = 0.77 ft
b) Control Delay	.050 sec. max. plus biasing for 3 $1.2 + \frac{2}{3}(1.2)$	$\pm$ 2.0 ft	4.00	
c) Control Magnitude				
i) I	$\pm$ 3% = $\pm$ 1.37 mils	$\pm$ 0.15 ft	0.02	
ii) V	$\pm$ 50 ft/sec = $\pm$ 2.19 mils	$\pm$ 0.24 ft	0.06	
				P_H = 1.0
d) Seeker LOS Errors				
i) Calibr	$\pm$ 2 mils	0.22 ft	.05	
ii) Threshold	$\pm$ 1 mil	0.11 ft	.01	
iii) α-Effect	$\pm$ 4 mils	0.44 ft	.19	
e) Illuminator Error	-	$\pm$ 1 ft	1.00	
f) Roll Errors				
i) Seeker	$\pm$ 1° (17.4 mils)	$\pm$ 0.10	0.01	
ii) Control	$\pm$ 1° (17.4 mils)	$\pm$ 0.10	0.01	$(3\sigma)^2$ = 5.35; 3σ = 2.32
g) Wind	$\frac{5 \text{ mph}}{} = \pm$ 5.45 mils (cf. Table II-5)	$\pm$ 0.6	0.36	$(3\sigma)^2$ = 5.71, 3σ = 2.4, $\bar{y}$ = -.18 } P_H = 1.0
	$\frac{10 \text{ mph}}{} = \pm$ 10 mils (cf. Table II-5)	$\pm$ 1.1	1.21	$(3\sigma)^2$ = 6.56; 3σ = 2.56, $\bar{y}$ = -.18 } P_H = 1.0
		Lateral Bias		
h) Target Velocity	5 mph (7.3 ft/sec.)	0.77 ft	-	$\bar{x}$ = 0.77, $\bar{y}$ = -.18, 3σ = 2.32, P_H = 1.0
	10 mph (14.6 ft/sec)	1.55 ft	-	$\bar{x}$ = 1.55, $\bar{y}$ = -.18, 3σ = 2.32, P_H = .997

TABLE 3.8-9

Determination of Overall POLCAT Hit Probability : R = 1500 Yards.

	Condition	(1) Pre-Control Trajectory	(2) P_H	(3) $P_{H_{ave}}$	(4) Relative Number	(5) (3) x (4)	Hit Probability
Stationary Target	No Wind	3	0.996	.998	.135	.1348	
		2	1.00	1.00	.472	.472	P_H=.9998
		1	1.00	1.00	.393	.393	Total
		0	1.000			.9998	
	5 mph Wind	3	0.984	.992	.135	.134	
		2	1.00	1.00	.472	.472	P_H=.998
		1	1.00	1.00	.393	.392	Total
		0	1.00			.998	
	10 mph Wind	3	0.936	.967	.135	.1305	
		2	.998	.999	.472	.471	P_H=.995
		1	1.00	1.00	.393	.393	
		0	1.00			.9945	
Moving Target (no wind)	5 mph Target	3	0.961	.980	.135	.132	
		2	0.999	.9995	.472	.472	P_H=.997
		1	1.00	1.000	.393	.393	
		0	1.00			.997	
	10 mph Target	3	0.13	0.47	.135	.064	
		2	0.81	0.90	.472	.425	P_H=.881
		1	0.997	0.999	.393	.392	
		0	1.00			.881	

3.8.4.5 Determination of POLCAT Effectiveness at 2000 Yards

1) Assumptions:

(i) The maximum 3σ uncontrolled trajectories have a vertical miss distance of $\pm$ 31.4 ft. (Table 3.8-4)

(ii) Control impulse, optimized for 1500 yds = 35 lb-secs.

2) Control Angle and Maximum Range-to-Go

$$\text{Projectile Velocity} = \frac{\text{Impulse}}{mV} = \frac{35}{(.726)(990)} = 48.4 \text{ mils}$$

Max. Range-to-Go at Control

$$(\Delta R)\frac{48.4}{1000} = 31.4$$

$$\Delta R = 650 \text{ ft.}$$

POLCAT Probability Computation (R = 2000 Yds)

Tables 3.8-10 through 3.8-12 include hit probability calculations R = 2000 yds for the errors previously listed in Table 3.8-2 and for a variety of operational conditions. The sub-population hit probabilities are plotted in Figure 3.8-15; overall system hit probabilities at 2000 yards are computed in Table 3.8-13.

TABLE 3.8-10

Calculation of Probability of Hit of Controlled POLCAT Projectile at R = 2000 yds

3σ Pre-Control Trajectory
Range-to-Go at Control = 650 ft.; D = ± 31.4 ft
Control Angle = 48.4 mils; V = 980 ft/sec

Error	Error Elements	Miss Distance (3σ)	$(3\sigma)^2$	Hit Probability
a) Gravity Drop	V_p = 980 ft/sec $\Delta t = \frac{650}{980}$ = .663 sec	-7.1 ft	-	
b) Control Delay	.050 sec. max. = 2.4 ft max. = ± 1.2 ft by biasing control threshold	± 1.2 ft	1.44	
c) Control Magnitude				P_{H_H} = .996
i) I	± 3% = ± 1.45	±0.89	0.79	
ii) V	± 50 ft/sec. ±2.52	± 1.60	2.56	P_{H_v} = .004
d) Seeker LOS Errors				P_H = .004
i) Calibr.	± 2 mils	± 1.3 ft	1.69	
ii) Threshold	± 1 mil	± 0.65 ft	0.42	
iii) α=Effect	± 4 mils	± 2.60 ft	6.76	
e) Illuminator	-	± 1 ft	1.00	
f) Roll Errors				
i) Seeker	± 1° (17.4 mils)	0.55 ft	0.30	
ii) Control	± 1° (17.4 mils)	0.55 ft	0.30	$\Sigma(3\sigma)^2$ = 15.26; 3σ = 3.91
g) Wind	5mph = ± 7.45 mils = ± 0.6 mils = ± 5.3 mils	3.44 ft	11.82	$\Sigma(3\sigma)^2$ = 27.08, 3σ = 5.2 P_{H_H} = .97 P_{h_v} = 0.3 P_H = 0.3
	10 mph = ± 14.9 mils = ± 2.2 mils = ± 10.6 mils	6.89 ft	47.4	$\Sigma(3\sigma)^2$ = 62.66; 3σ = 7.9 P_{H_H} = .84 P_{H_u} = .10 P_H = .08
h) Target Velocity		Lateral Bias:		
	5 mph (7.3 ft/sec)	4.84 ft	-	$\bar{x}$ = 4.84 $\bar{y}$ = 7.1 3σ = 3.91
	10 mph (14.6 ft/sec)	9.7 ft	-	$\bar{x}$ = 9.7 $\bar{y}$ = 7.1, 3σ = 3.91 P_H = .001

TABLE 3.8-11
Calculation of Probability of Hit of Controlled POLCAT Projectile
at R = 2000 Yds.

2σ Pre-Control Trajectory
Range-to-Go at Control = 4.33 ft. D = ± 20.9 ft
Control Angle = 48.4 mils, V = 980 ft/sec

Error	Error Elements	Miss Distance (3σ)	$(3\sigma)^2$	Hit Probability
a) Gravity Drop	V_p = 980 ft/sec. $\Delta t = \frac{433}{980} = .442$	-3.14 ft	-	$\bar{y} = 3.14$ 3 = 3.32 = 1.11
b) Control Delay	.050 sec. max. = 2.4 ft. max. = ± 1.2 + $\frac{1}{3}$(1.2) with biasing	± 1.6 ft	2.56	
c) Control Magnitude				
i) I	± 3% = ± 1.45 mils	± .620 ft	0.39	
ii) V	± 50 ft/sec = ± 2.52 mils.	± 1.09 ft	1.19	
d) Seeker LOS Errors				
i) Calibr.	± 2 mils	± .866	0.75	
ii) Threshold	± 1 mil	± .433	0.19	
iii) α-Effect	± 5 mils	± 2.16	4.66	
e) Illuminator	-	± 1 ft	1.00	
f) Roll Errors				
i) Seeker	± 1°	0.36 ft	.13	
ii) Control	± 1°	0.36 ft	.13	$(3\sigma)^2 = 11.0$; $3\sigma = 3.32$
g) Wind	5 mph = ± 7.45 = ± 0.6 = ± 5.3 mils	2.3 ft.	5.30	$(3\sigma)^2 = 16.3$, $3\sigma = 4.04$ $P_{H_H} = .994$; $P_{H_V} = .675$ $P_H = 0.67$
	10 mph = ± 14.9 mils = ± 2.2 mils = ± 10.6 mils	4.6 ft	21.20	$(3\sigma)^2 = 32.2$, $3\sigma = 5.68$ $\bar{y} = -3.14$ $P_{H_H} = 0.95$, $P_{H_V} = 0.625$ $P_H = 0.59$
		Lateral Bias		
h) Target Velocity	5mph (7.3 ft/sec)	3.22 ft	P_H = .48	$\bar{x} = 3.22$, $\bar{y} = 3.14$; $3\sigma = 3.32$
	10mph (14.6 ft/sec)	6.44 ft		$\bar{x} = 6.44$, $\bar{y} = 3.14$; $3\sigma = 3.32$ $P_H = .006$

TABLE 3.8-12

Calculation of Probability of Hit of Controlled POLCAT Projectile

at R = 2000 Yds

1σ Pre-Control Trajectory
Range-to-Go at Control = 216 ft; D = $\pm$ 10.5 ft
Control Angle = 48.4 mils; V = 980 ft/sec

Error	Error Elements	Miss Distance (3σ)	$(3\sigma)^2$	Hit Probability
a) Gravity Drop	V_p = 980 ft/sec $\Delta t = \frac{216}{980} = .22$ sec	-0.78	-	$\bar{y}$ = -0.78 ft 3σ = 2.62 σ = 0.87
b) Control Delay	.050 sec. max. with biasing; $\pm 1.2 + \frac{2}{3}(1.2)$	$\pm$ 2.0 ft	4.0	
c) Control Magnitude				
i) J	$\pm$ 3% = $\pm$ 1.45 mils	$\pm$ .313 ft	0.10	
ii) V	$\pm$ 50 ft/sec = $\pm$ 2.52 mils	$\pm$ .544 ft	0.30	
d) Seeker LOS Errors				
i) Calibr.	$\pm$ 2 mils	$\pm$ .432 ft.	0.19	
ii) Threshold	$\pm$ 1 mil	$\pm$ .216 ft.	0.05	
iii) a-Effect	$\pm$ 5 mils	$\pm$ 1.08 ft.	1.17	
e) Illuminator Error	-	$\pm$ 1 ft	1.00	
f) Roll Errors				
i) Seeker	$\pm$ 1°0	$\pm$ 0.18	.03	
ii) Control	$\pm$ 1°	$\pm$ 0.18	.03	$(3\sigma)^2$ = 6.87, 3σ = 2.62
g) Wind	5 mph = $\pm$ 5.3 mils (Table ~~H-10~~)	$\pm$ 1.15 ft	1.32	$(3\sigma)^2$ = 8.19, 3σ = 2.86 $\bar{y}$ = -0.78 P_{H_H} = 1.0, P_{H_V} = .999, P_H = .99
	10 mph = $\pm$ 10.6 mils (Table ~~H-10~~)	$\pm$ 2.29 ft	5.25	$(3\sigma)^2$ = 12.12, 3σ = 3.48 $\bar{y}$ = -0.78 P_{H_H} = 1.0, P_{H_V} = .995 P_H = .995
		Lateral Bias		
h) Target Velocity	5mph(7.3 ft/sec)	1.61 ft	-	$\bar{x}$ = 1.61, $\bar{y}$ = -.78, 3σ = 2.62 P_H = .993
	10mph(14.6 ft/sec)	3.21 ft	-	$\bar{x}$ = 3.21, $\bar{y}$ = -.78; 3σ = 2.62 P_H = .903

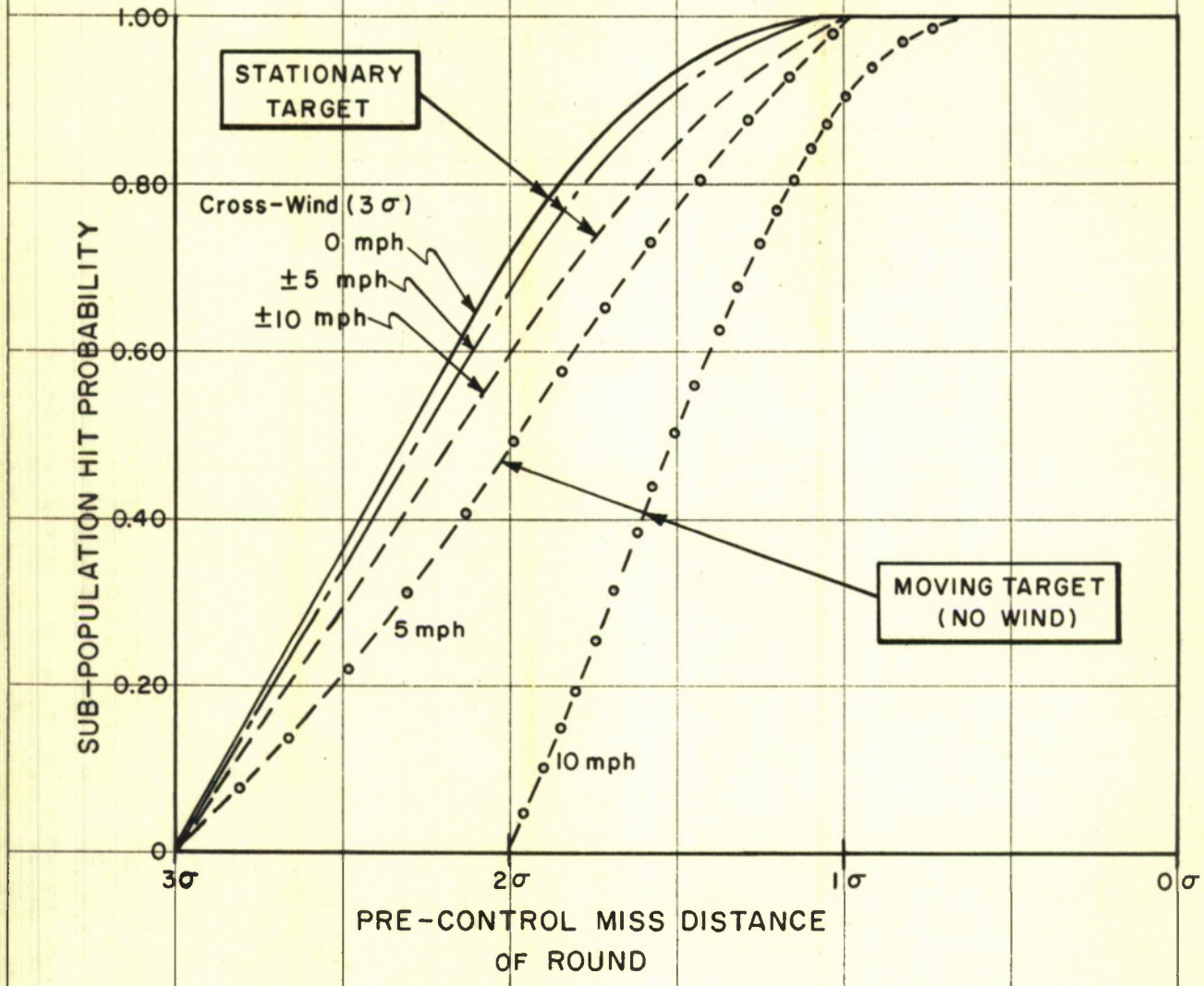

Figure 3.8_15

SUB-POPULATION HIT PROBABILITIES
VS
PRE-CONTROL MISS DISTANCE
R = 2000 Yards
(± 3σ = ± 31.4 Feet)

TABLE 3.8-13

Determination of Overall POLCAT Hit Probability at R = 2000 Yards.

	Condition	(1) Pre-Control Trajectory	(2) $P_{H_{ave}}$ (Fig. 3.8-14)	(3) Relative Number	(4) (2)x(3)	(5) (4)
Stationary Target	No wind	3	.36	.135	.049	P_H=.876
		2	.92	.472	.434	
		1	1.00	.393	.393	
		0				
	0-5 mph(max) Cross-wind Condition	3	.34	.135	.046	
		2	.90	.472	.425	P_H=.864
		1	1.00	.393	.393	
		0				
	0-10 mph(max) Cross-wind Condition	3	.30	.135	.041	
		2	.86	.472	.406	P_H=.84
		1	1.00	.393	.393	
		0				
Moving Target	5 mph Target Velocity (Transverse)	3	.23	.135	.031	
		2	.78	.472	.368	P_H=.792
		1	1.00	.393	.393	
		0				
	10 mph Target Velocity (Transverse)	3	0	.135	0	
		2	.50	.472	.236	P_H=.629
		1	1.00	.393	.393	
		0				

3.8.4.6 Summary of Estimated Hit Probabilities of the POLCAT System

Tables 3.8-9 and 3.8-13 list estimated POLCAT first round hit probabilities for a preliminary near-optimum single-impulse system. This system has been optimized for 1500 yards and utilizes a single impulse cartridge having an impulse of 35 lb/secs. Figure 3.8-16 shows some of the related performance characteristics of this system (date which were obtained during the course of hit probability calculations of the sort included in the preceding pages.

Finally, Figures 3.8-17 and 3.8-18 summarize the estimated first round hit probability characteristics (including an estimated reliability factor of 0.98) of the POLCAT system for the anticipated errors deemed inherent in the system and for several likely operational cross-wind and moving-target conditions.

It is noted that under ideal non-moving target, non-wind conditions the POLCAT system clearly fulfills the objectives initially set in the Feasibility Study: first round hit probability 0.85 at ranges out to 2000 yards. It is also noted that the system is only moderately affected by typical cross-winds and moving target conditions at extreme range (2000 yards) and only to a negligible extent at the "design range" of 1500 yards. In conclusion, it is to be noted that improved performance under cross-wind and moving target conditions is deemed attainable at

extreme range with this type of system by moderate increases in control impulse; i.e., by selecting a design range in the region of 1750 to 2000 yards.

FIGURE 3.8 - 16

PERFORMANCE of SINGLE - IMPULSE SYSTEM

Cartridge Impulse ≅ 35 lb-secs.
Design Range = 1500 yds

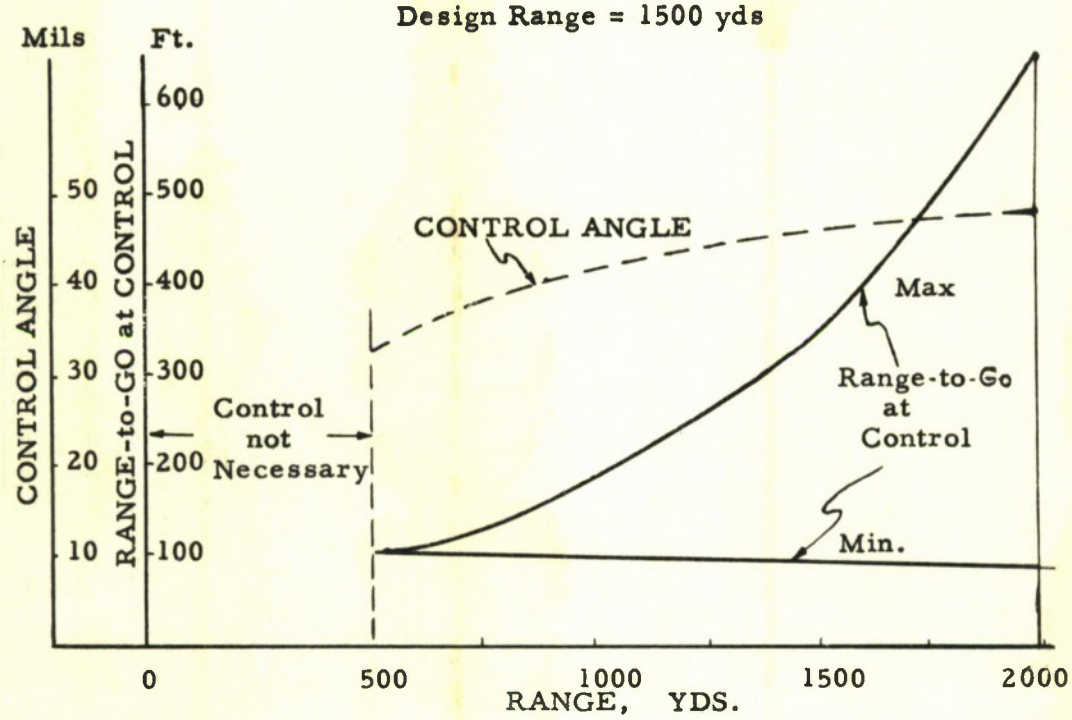

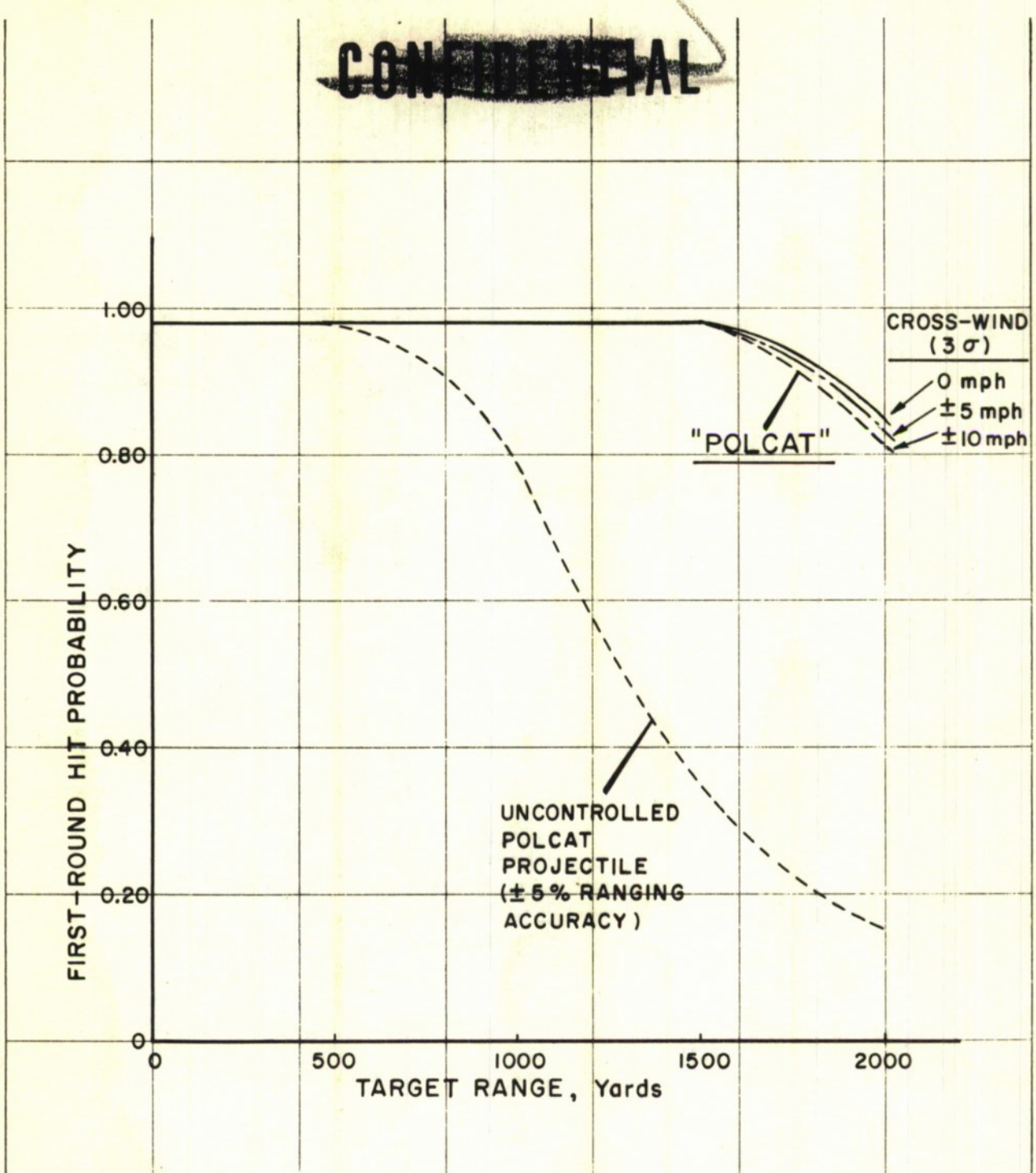

Figure 3.8-17

ESTIMATED FIRST-ROUND HIT PROBABILITY
OF "POLCAT" PROJECTILE
FOR SEVERAL CROSS-WIND CONDITIONS
(STATIONARY TARGET)
Includes Reliability Factor = 0.98

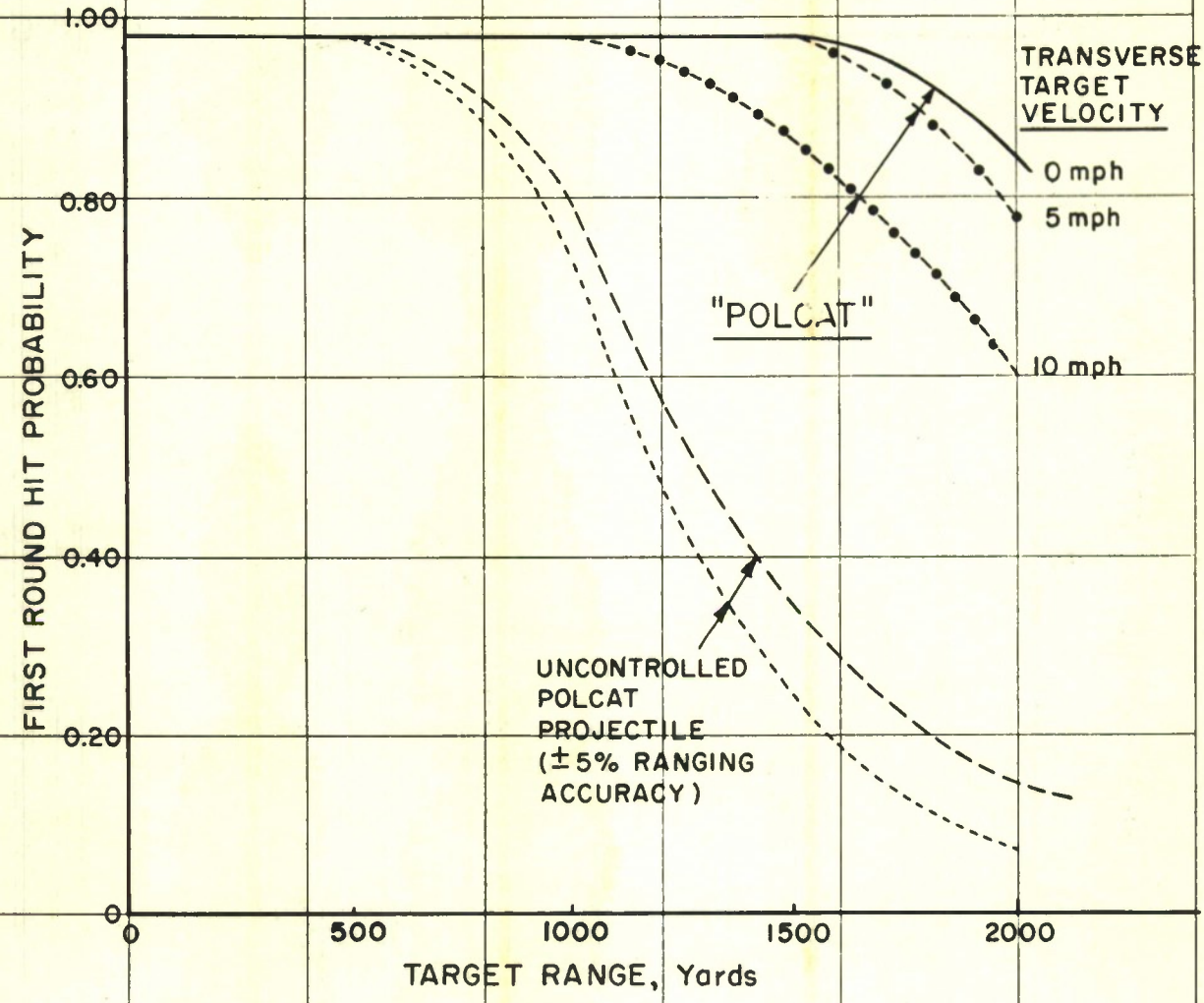

Figure 3.8-18

ESTIMATED FIRST-ROUND HIT PROBABILITY OF "POLCAT" PROJECTILE FOR SEVERAL TARGET VELOCITIES (NO CROSS-WIND)
Includes Reliability Factor = 0.98

4.0 Conclusions and Recommendations

Based on the technical effort summarized in this report, it is concluded that:

(1) The suggested anti-tank weapon system which utilizes post firing correction in the form of a projectile incorporating a frame-fixed infrared seeker and impulse-type control, fulfills the primary objective of the study program--providing high probabilities of hit at long range for recoilless weapons.

(2) The weapon system concept, whereby the capabilities of both fire control and post firing are utilized to minimize miss distance, has application to other weapon systems in addition to recoilless anti-tank weapons.

(3) In addition to fulfilling the accuracy requirement, the suggested weapon system possesses the primary characteristics, simplicity, ruggedness, and mobility, to permit its deployment in forward combat areas. By virtue of these characteristics, the suggested weapon system retains the required flexibility for use in the more advanced concepts of warfare: air drop missions, Sky-Cav, etc.

(4) The impulse control technique, as developed during the program, proves to be a highly effective means for obtaining projectile control. This technique is particularly compatible with missile referenced or homing type guidance systems.

(5) The aspects of the suggested weapon system which appear less critical with regard to an engineering development program include:

(a) use of the recoilless rifle for launch.

(b) use of optical fire control to obtain required accuracy for uncontrolled rounds.

(c) use of an explosive cartridge for impulse control

These conclusions are based on the performance of presently operating components or systems and on experimental work conducted during the program.

(6) The aspects of the suggested weapon which has proven to be feasible but appear to require a substantial engineering effort for development include:

(a) use of a frame-fixed seeker for guidance.

(b) use of airframe motion for seeker scanning.

(c) use of semi-active target illumination

In view of the foregoing, it is recommended that a technical effort be initiated to fully qualify the suggested weapon system. This effort in the form of a development program or a series of component testing programs, should have the objective of producing an engineering prototype POLCAT weapon system prior to 1960.

REFERENCES

(1) Weapons System Feasibility Study of a Controlled Recoilless Rifle Projectile. Status Report for period 4/1/56 to 7/1/56. Fenton, S., Kaswen, M. and Reismann, H.

(2) Weapons System Feasibility Study of a Controlled Recoilless Rifle Projectile. Progress Letters Nos. 6 and 7 for period 10/1/56 to 12/12/56. Reismann, H.

(3) Weapons System Feasibility Study of a Controlled Recoilless Rifle Projectile. Control Effectiveness Test Program dated 10/22/56. Fenton, S.

(4) NACA RM L55J13 Preliminary Free-Flight Study of the Drag and Stability of a Series of Short Span Missiles at Mach Numbers from 0.9 to 1.3. Hall, James Rudyard.

(5) NACA RM L51E25 Flight Investigation of the Drag of Round Nosed Bodies of Revolution at Mach Numbers from 0.6 to 1.5 Using Rocket Propelled Test Vehicles. Hart, Roger G.

(6) NACA RM A52B13 The Effect of Bluntness on the Drag of Spherical Tipped Truncated Cones of Cones of Fineness Ratio 3 at Mach Numbers 1.2 to 7.4. Sommer, Simon C. and Stark, James A.

(7) NACA RM L53D14a Investigation of the Drag of Blunt Nosed Bodies of Revolution in Free Flight at Mach Numbers From 0.6 to 2.3. Wallskog, Harvey A. and Hart, Roger G.

(8) NACA RM L57F25 Effect of Nose Shape on Subsonic Aerodynamic Characteristics of a Body of Revolution Having a Fineness Ratio of 10.94. Polhamus, Edward C.

(9) NACA RM L52F23 Preliminary Free Flight Investigation of the Zero Lift Drag Penalties of Several Missile Nose Shapes For Infrared Seeking Devices. Piland, Robert O.

(10) NACA RM L57D19 Aerodynamic Characteristics of Missile Configurations with Wings of Low Aspect Ratio for Various Combinations of Forebodies, Afterbodies, and Nose Shapes for Combined Angles of Attack and Sideslip at a Mach Number of 2.01. Robinson, Ross B.

(11) NACA RM A51J25 Aerodynamic Characteristics of Bodies at Supersonic Speeds. A Collection of Three Papers.

(12) NACA RML56D16 Zero Lift Drag of a Series of Boml Shapes at Mach Numbers from 0.60 to 1.10. Stoney, William E. and Royall, John F.

(13) NACA RM A53G08 A Method for Calculating the Lift and Center of Pressure of Wing-Body-Tail Combinations at Subsonic Transonic, and Supersonic Speeds, Neilson, Jack N., Kaattari, George E. and Anastasio, Robert F.

(14) NACA TN 3283 Aerodynamic Forces, Moments, and Stability Derivatives for Slender Bodies of General Cross Section. Sacks, Alvin H.

(15) NACA RM L55G06a Some Research on the Lift and Stability of Wing-Body Combinations. Pwiser, Paul E. and Fields, E. M.

(16) BRL TN 565 Wind Tunnel Tests of the T131 105mm Heat Projectile

(17) BRL TN 724 Wind Tunnel Tests of the T153 120mm Heat Projectile. Krieger, R. H.

(18) BRL MR 838 Some Aerodynamic Effects of Head Shape Variation at Mach Number 2.44. Dickinson, Elizabeth R.

(19) NACA TR 835 Properties of Low Aspect Ratio Pointed Wings at Speeds Below and Above the Speed of Sound. Jones, Robert T.

(20) NACA TM 971 The Elliptic Wing Based on the Potential Theory. Krienes, Klaus

(21) BRL MR 696 Aerodynamic and Flight Characteristics of the 90 mm Fin Stabilized Shell, Heat, T108. Karpoo, R. G.

(22) NACA RM L53E22 Flight Investigation of the Aerodynamic Derivatives and Performance of Control Systems of Two Full-Scale Guided Bombs. Seaberg, Ernest C. and Geller, Edward S.

(23) Aerodynamic Test Data and Notes. (Unpublished) Fenton, S.

(24) NACA RM A56G16 Wing Body Combinations with Wings of Very Low Aspect Ratio at Supersonic Speeds. Jorgensen, Leland H. and Katzen, Elliott D.

(25) NACA RM L53J09a Wind Tunnel Investigation at Low Speed of the Effect of Varying the Ratio of Body Diameter to Wing Span From 0.1 to 0.8 on the Aerodynamic Characteristics in Pitch of a 45° Sweptback Wing-Body Combination. Johnson, Harold S.

(26) NACA RM L57G10a Experimental Determination of Damping In Pitch of Swept and Delta Wings at Supersonic Mach Numbers. Moore, John A.

(27) NACA RM A50J26 Experimental Damping in Pitch of 45° Triangular Wings. Tobak, Murray, Reese, Jr., David E, Beam, Benjamin H.

(28) NACA RM L55K16 Flight Investigation at Low Angles of Attack to Determine the Longitudinal Stability and Control Characteristics of a Cruciform Canard Missile Configuration with a Low-Aspect-Ratio Wing and Blunt Nose at Mach Numbers from 1.2 to 2.1. Brown, Jr., Clarence A.

(29) NACA RM L50I27 The Longitudinal Stability, Control Effectiveness, and Control Hinge-Moment Characteristics Obtained from a Flight Investigation of a Canard Missile Configuration at Transonic and Supersonic Speeds. Niewald, Roy J. and Moul, Martin T.

(30) NACA RM L55H31 A Theoretical Analysis of a Simple Aerodynamic Device to Improve the Longitudinal Damping of a Cruciform Missile Configuration at Supersonic Speeds. Clements, James E.

(31) NACA RM L52K06 Pressure Distribution and Pressure Drag for a Hemispherical Nose at Mach Numbers 2.05, 2.54, and 3.04. Chauvin, Leo T.

(32) NAVORD 2861 Semi Annual Progress Report for Angled Arrow Projectile Program. Period ending 11/30/52

(33) BRL MR 649 Effect of Muzzle Blast on Maximum Yaw. Hitchcock, H. P.

(34) JAS Preprint No. 543 Some Recent Aerodynamic Techniques in Design of Fin-Stabilized Free-Flight Missiles for Minimum Dispersion. Hunter, M. W., Shef, A., Black, D. V.

(35) BRL TN 590 Spin and Aerodynamic Characteristics of the 105mm Shell T-131, Heat.

(36) BRL MR 697 A Method of Determining the Spin Characteristics from Yaw Card Firings as Applied to the 105mm Shell T131E31. McAllister, Leonard C.

(37) BRL MR 879 Effectiveness of Several Simple Methods of Aerodynamic Control of Spin of the 90MM, Heat, T108E40 Shell. Karpov, B. G., Simon, W. E.

(38) NACA RM L57E09a An Investigation at Low Speed of the Spin Instability of Mortar-Shell Tails. Bird, John D., Lichenstein, Jacob H.

(39) NACA RM L56G20a An Investigation of a Source of Short Round Behavior of Mortar Shells. Bird, John D., Lichenstein, Jacob H.

(40) "Weapons System Feasibility Study of a Controlled Recoilless Rifle Projectile" Progress Report No. 11, Contract No. DA-30-069-ORD-1766, covering period 4/18/57 to 5/15/57.

(41) Frankford Arsenal Report No. R-1404 The Application of a Magnetic Recoding-Analog Computer System to the Reduction of Interior Ballistic Data Obtained from Recoilless Rifle Firings. Levine, A.

(42) Research Paper 2138 Response of Accelerometers to Transient Accelerations. Levy, Samuel and Kroll, Wilhelmina D.

(43) AD34245 Symposium on Recent Progress of Recoilless Rifles and Ammunition, 11-13 January 1954. Held at Midwest Research Institute, Kansas City, Missouri.

(44) Theory of Plates and Shells. Timoshenko, S.

(45) Mechanical Vibrations. Den Hartog, J. P.

(46) Aircraft Structures. Peery, David J., Ph. D.

(47) Resistance of Materials. Seely, Fred B., M.S.

(48) Formulas for Stress and Strain. Roark, Raymond J.

(49) Bulova Research and Development Report. Weapons System Feasibility Study for a Controlled Recoilless Rifle Projectile. Progress Report No. 12. Fenton, S.

(50) Bulova Research and Development Report. Weapons System Feasibility Study for a Controlled Recoilless Rifle Projectile. Progress Report Nos. 8 and 9. Fenton, S.

(51) Bulova Research and Development Report. Inspection of T 184 Projectile. Gordon, A.

(52) Bulova Research and Development Report, Weapons System Feasibility Study for a Controlled Recoilless Rifle Projectile. Progress Report No. 11. Fenton, S.

(53) Proceedings of the I.R.M.P. Symposium: Infrared Measuring Program 1956. Aerial Reconnaissance Lab., Wright A.D.C. 24-25 April 1957.
Report No. 57WCLR-2647 (Secret) P. 491 ff.

(54) Fundamentals of Infrared for Military Applications. S. S. Ballard, etc. Rand Report R-297 March 31, 1956. (Confidential).

(55) Harvey Machine Co., Inc. Status Reports. Design and Application of Light Metals to Large Caliber Recoilless Rifles and Mount.

(56) Symposium on Recent Progress of Recoilless Rifles and Ammunition, Dept. of Army. 11-13 January 1954, held at Midwest Research Institute.

(57) BRL TN 493 Probabilities of a First Round Hit For Various Antitank Projectiles.

(58) Firestone Tire and Rubber Company. Summary Report on Recoilless Rifles, Accessories, and Ammunition. January, 1957.

(59) Introduction to Mathematical Statistics, Hall, P. Wiley, 1947.

Distribution

3 - Office, Chief of Ordnance
Department Army
Washington 25, D. C.
Attn: ORDTS

3 --Attn: ORDTU

3 - Attn: ORDTW

1 - Attn: ORDTB-Bal

1 - Attn: ORDTN

1 - Attn: ORDTX

1 - Commanding General
Aberdeen Proving Ground
Maryland
Attn: Dr. B. Karpov
Exterior Ballistics Lab

1 - Attn: D. Hardison
Weapons Systems Lab

1 - Attn: Project Mauler

1 - Attn: Goodwin Morrow
D & PS

1 - Commanding General
Ordnance Ammunition Command
Joliet, Illinois

1 - Commanding General
Ordnance Tank and Automotive Command
1501 Beard Street
Detroit 9, Michigan

1 - Commanding General
Ordnance Weapons Command
Rock Island, Illinois
Attn: F. D. Grossman

1 - Commanding General
Army Ballistic Missile Agency
Redstone Arsenal
Huntsville, Alabama

4 - Commanding General
Redstone Arsenal
Huntsville, Alabama
Attn: Ordnance Missile Lab

1 - Attn: Rocket Development Lab

1 - Commanding Officer
Picatinny Arsenal
Dover, New Jersey
Attn: Samuel Feltman Ammn Lab

1 - Attn: Tactical Atomic Warheads Lab

1 - Commanding Officer
Rock Island Arsenal
Rock Island, Illinois
Attn: Laboratory

1 - Commanding Officer
Springfield Armory
Springfield 1, Mass.
Attn: Engineering Dept

1 - Commanding Officer
Watertown Arsenal
Watertown 72, Mass.

1 - Commanding Officer
Watervliet Arsenal
Watervliet, New York

1 - Commanding Officer
Diamond Ordnance Fuze Lab
Washington 25, D. C.
Attn: Technical Reference Sec
ORDTL 06.33

1 - Commanding General
White Sands Proving Ground
New Mexico
Attn: Technical Staff

1 - Deputy Chief of
Staff Operations
Department of the Army
Washington 25, D. C.
Attn: Director, Guided Missiles

1 - Chief of Staff, R&D
Department of the Army
Washington 25, D. C.
Attn: Maj. W. Parker

1 - Attn: Col Carlson
Operations Research Office
(Pentagon)

1 - Chief of Staff, R&D
Department of the Navy
Washington 25, D. C.
Attn: Director
Special Weapons Branch

1 - Deputy Chief of Staff for
Military Operations
Department of the Army
Washington 25, D. C.
Attn: Lt Col R. H. Oslich

1 - Commanding General
Continental Army Command
Fort Monroe, Virginia
Attn: Dr. F. C. Brooks
Director, CORG

1 - Attn: Director
Combat Development (Special)

1 - Attn: Material Development

1 - President
U. S. Army Artillery Board
Fort Sill, Oklahoma

1 - President
U. S. Army Armor Board
Fort Knox, Kentucky

1 - President
U. S. Army Infantry Board
Fort Benning, Georgia

1 - President
U. S. Air Defense Board
Fort Bliss, Texas

1 - Commandant
U. S. Army Artillery & Missile School
Fort Sill, Oklahoma
Attn: Col Casady
Director, Dept of Combat Dev

1 - Commandant
The Armored School
Fort Knox, Kentucky

1 - Commandant
The Infantry School
Fort Benning, Georgia

1 - President
U. S. Army Airborne &
Electronics Board
Fort Bragg, North Carolina

1 - Commanding Officer
Ordnance Guided Missile School
OTC
Redstone Arsenal
Huntsville, Alabama
Attn: Maj. Marvin D. Parker

3 - Commandant
Command & General Staff College
Fort Leavenworth, Kansas

1 - Commanding General
Combat Development Experimentation Center
Fort Ord, California

1 - Johns-Hopkins University
Operations Research Office
7100 Connecticut Avenue, N. W.
Chevy Chase,
Washington 15, D. C.
Attn: Document Control Office

1 - Attn: Dr. W. Pettijohn

1 - Attn: Dr. J. Young

1 - Assistant Secretary of Defense (R&D)
Department of the Army
Washington 25, D. C.
Attn: Director, Ordnance

1 - Attn: Director, Guided Missiles

2 - Director
Weapon Systems Evaluation Group
Office, Secretary of Defense
Washington 25, D. C.

1 - Director
Office, Special Weapons Dev
CONARC
Fort Bliss, Texas

1 - Ordnance Liaison Officer
Field Command
Armed Forces Special Weapons Project
P. O. Box 5100
Albuquerque, New Mexico

1 - Chief
Armed Forces Special Weapons Project
P. O. Box 2610
Washington 25, D. C.

1 - Commandant
Hq, U. S. Marine Corps
Washington 25, D. C.

1 - Director
Marine Corps Landing Force
Development Center
Marine Corps Schools
Quantico, Virginia

1 - Chief, Bureau of Ordnance
Department of the Navy
Washington 25, D. C.
Attn: ReO

1 - Commanding Officer & Director
David W. Taylor Model Basin
Washington 7, D. C.
Attn: Aerodynamics Laboratory

1 - Commanding Officer
Naval Air Rocket Test Station
Lake Denmark
Dover, New Jersey

1 - Commander
Naval Proving Ground
Dahlgren, Virginia

1 - Commander
Naval Air Missile Test Center
Point Mugu, California

1 - Commander
Naval Ordnance Test Station
Inyokern, China Lake, Calif.
Attn: Technical Library

1 - Commander
Naval Ordnance Laboratory
White Oak, Silver Spring, Md.

1 - Chief of Staff
United States Air Force
The Pentagon
Washington 25, D. C.
Attn: Operations Analysis Div

1 - Commander
Air Research and Development
Command
P. O. Box 1395
Baltimore 3, Maryland

1 - Commander
Air Force Special Weapons Center
Kirtland Air Force Base
New Mexico
Attn: Technical Inf Intell

1 - Commander
Air Force Cambridge Research Center
Air Research & Development Command
L. G. Hanscom Field
Bedford, Mass.

1 - Commander
Wright Air Development Center
Wright-Patterson Air Force Base
Dayton, Ohio
Attn: WCSP

1 - NACA Langley Memorial Aeronautical
Laboratory
Langley Field, Virginia

1 - NACA Lewis Flight Propulsion Lab.
Cleveland Airport
Cleveland, Ohio

1 - Director
Nat'l Advisory Commitee for
Aeronautics
1512 H Street, N. W.,
Washington 25, D. C.

1 - Director, Jet Propulsion Lab.
Ordnance Corps Installation
4800 Oak Road Drive
Pasadena, California

1 - U. S. Atomic Energy Commission
Sandia Corporation
P. O. Box 5400
Albuquerque, New Mexico
Attn: Dr. W. O. MacNair

1 - U. S. Atomic Energy Commission
Sandia Corporation
Livermore Branch
P. O. Box 969
Livermore, California
Attn: W. J. Howard

1 - U. S. Atomic Energy Commission
Los Alamos Scientific Laboratory
P. O. Box 1663
Los Alamos, New Mexico

1 - U. S. Atomic Energy Commission
1901 Constitution Avenue
Washington 25, D. C.
Attn: Classified Technical Library

5 - Armed Services Technical Information Agency
Document Service Center
Arlington Hall Station
Arlington 12, Virginia
Attn: DSC-SD